Universitat Autònoma de Barcelona

BOOSTING ENDOGENOUS MECHANISMS FOR NEURONAL PROTECTION AND REPAIR AFTER INJURY IN CENTRAL NERVOUS SYSTEM

DAVID ROMEO GUITART

Universitat Autònoma de Barcelona

BOOSTING ENDOGENOUS MECHANISMS FOR NEURONAL PROTECTION AND REPAIR AFTER INJURY IN CENTRAL NERVOUS SYSTEM

Presented by

DAVID ROMEO GUITART

ACADEMIC DISSERTATION

To obtain the degree of PhD in Neuroscience of the Universitat Autònoma de Barcelona, September 2017

Supervised by	**PhD Student**
Dra. Caty Casas Louzao	**David Romeo Guitart**

Group of Neuroplasticity and Regeneration (UAB)

NeuroPlasticity & Regeneration

Fundació La Marató de TV3

GOBIERNO DE ESPAÑA MINISTERIO DE ECONOMÍA Y COMPETITIVIDAD

BCFI

INc Institut de Neurociències

The research described in this thesis is performed at the “Departament de Biologia Cel·lular, Fisiologia I Immunologia, Institutut de Neurociencies, of the Universitat Autònoma de Barcelona” in the Group of Neuroplasticity and Regeneration.

Financial funding:

David Romeo Guitart was supported by a PIF grant of Universitat Autònoma de BARCELONA (2014). The research funding was from La Marató, MINECO and CIBERNED.

Table of Contents

Summary

Neurons have endogenous mechanisms of neuroprotection that are capable to activate against those insults that will lead to their death. Motoneurons (MNs) can activate these mechanisms when they suffer a distal axotomy (DA) of the sciatic nerve. However, when the injury is more proximal to their soma, such as root avulsion (RA), these mechanisms are not activated and the MNs undergo degeneration. Therefore, both injuries cause a separation of the MNs from their target organs, but with different results, since in the DA, MNs survive and regenerate, whereas in the RA, they die. By elucidating the mechanisms that MNs activate endogenously after DA, we can induce them in the RA model to support their survival and promote their regeneration.

Recent studies have shown that systems biology can be useful in discovering new drug therapies to treat complex pathologies. At the same time, the repurposing of drugs that are currently used in the human clinic for other purposes generates advantages, as their clinical translation is faster. The TPMS bioinformatics tool combines the point of view of systems biology and the concept of drug repurposing. This thesis was initiated using TPMS to discover new neuroprotective therapies that disturb the pro-death phenotype of MNs after avulsion towards the pro-regenerative triggered after DA.

Initially, we tested the neuroprotective power of these combinations in models of death *in vitro* and *in vivo*. The combination with a larger protective effect was named NeuroHeal. Using immunohistochemical techniques, we validated the molecular mechanisms predicted *in silico* for NH, which included the activity of Sirtuin 1 (SIRT1) and other neuroprotective proteins. Moreover, we demonstrated that the oral treatment with NH increased the functional recovery after a sciatic nerve injury.

Regarding the second and third episodes, we confirmed that the activity of SIRT1 has neuroprotective effects on other models of MN death after a nerve injury produced during different stages of growth. Surprisingly, although the activity of SIRT2 is considered as the antithesis of SIRT1, it prevents the death of MNs blocking an exacerbated microglial response. We also discerned that NH can avoid the

apoptotic death of MNs during early stages of development by the autophagy induction.

Since the NH can sustain the survival of MNs and increase their regenerative capacity on adult stages, we decided to test it in a model more similar to the human clinic of the nerve root injuries. In this pre-clinical model, we injured the nerve roots and re-introduced them surgically two weeks later into the spinal cord. The NH maintained the survival of MNs for six months, increased its regeneration, reduced muscular atrophy and favored the formation of functional neuromuscular junctions. Overall, these findings suggest that NH may be an effective pharmacological therapy to increase the survival of MNs and accelerate the recovery of motor function after nerve injuries.

Articles produced from the work of this thesis:

Peer reviewed publication:

- Romeo-Guitart D, Fores J, Navarro X, Casas C. **Boosted Regeneration and Reduced Denervated Muscle Atrophy by NeuroHeal in a Pre-clinical Model of Lumbar Root Avulsion with Delayed Reimplantation**. Scientific Reports, 2017.

Under revision:

- Romeo-Guitart D, Forés J, Herrando-Grabulosa M, Valls R, Leiva-Rodríguez T, Galea E, et al. **Neuroprotective Drug for Nerve Trauma Revealed Using Artificial Intelligence**. Scientific Reports, 2017.

In preparation:

- Romeo-Guitart D, Leiva-Rodríguez T, Sima N, Vaquero A, Domínguez-Martín H, Ruano D, Casas C. **Neuroprotection of Disconnected Motoneurons requires Sirtuin 1 activation but Sirtuin 2 depletion or inhibition with AK-7 is detrimental**
- Romeo-Guitart D, Navarro X, Caty Casas. **NeuroHeal Confers Neonatal Neuroprotection Inducing SIRT1-Dependent Autophagy**

Abbreviations

AD, Alzheimer's disease

AIF1, Apoptosis inducing factor 1

AIS, Axon initial segment

AKT, Protein Kinase B

ALS, Amyotrophic lateral sclerosis

ANN, Artificial neuronal network

ATF4, activating transcription factor 4

ATF6, activating transcription factor 4

ATG, Autophagy-related gene

BDNF, brain-derived neurotrophic factor

BiP, Binding immunoglobulin Protein

CD86, Cluster of Differentiation-86

CHOP, C/EBP-Homologous Protein

ChAT, Choline acetyltransferase

CMA, chaperon-mediated autophagy

CMAP, compound muscle action potential

CNS, central nervous system

CREB, cAMP response element-binding

CSPG, chondroitin sulfate proteoglycans

DA, distal axotomy

DCTN1, dynactin subunit 1

ECM, extracellular matrix

Eif2α, eukaryotic translation initiation factor 2α

ER, endoplasmic reticulum

ERAD, ER-associated degradation

ERK, extracellular signal-regulated kinases

ERO, ER-overload response

FOXO, Forkhead box protein O

GAP43, Growth associated protein 43

GDNF, glial-derived neurotrophic factor

GSK, glycogen synthase kinase

HAT, histone aceyltransferases

HD, Huntington's Disease

HDAC, histone deacetylase

IAP, inhibitor of apotosis

IF, Intermediate filaments

IGF, insulin-like growth factor

IL-1β, Interleukin 1β

IL4, Interleukin 4

IRE1α, inositol-requiring protein-1 α

JNK, JUN amino-terminal kinase 3

Kif5c, Kinesin heavy chain isoform 5C

LC3, microtubule-associated protein 1 light chains 3

MN, motoneuron

mTOR, mammalian target of rapamicyn

MT, microtubules

NF, neurofilament

NGF, nerve growth factor

NF-Kβ, nuclear factor kappa-light-chain-enhancer of activated B cells

NMJ, neuromuscular junction

P62, Sequestosome 1

P70S6K, 70-kDa ribosomal protein S6 kinase

PAR, poly(ADP-ribose) polymer

PARP1, poly(ADP-ribose) polymerase 1

PCD, programmed cell death

PD, Parkinson's disease

PERK, RNA-activated protein kinase-like ER kinase

PI3K, Phosphatidylinositol 3-kinase

PN, peripheral neuropatías

PNL, peripheral nerve lesion

PNS, peripheral nervous system

PPI, protein-protein interaction

PTEN, phosphatase and tensin homologue

RA, root avulsiom

RAG, Regeneration-Associated gene

ROS, reactive oxygen species

SC, spinal cord

SCI, spinal cord injury

SIRT, Silent Information Regulator 2

STAC, sirtuin-activating compounds

STAT, signal transducer and activator of transcription

TBI, traumatic brain injury

TF, transcription factor

TNFα, tumor necrosis factor-a

TPMS, therapeutic performance mapping system

TRAF2, TNF-a receptor-associated factor 2

Ulk1, unc-51-like kinase 1

UPR, Unfolded protein response

UPS, ubiquitine-proteasome system

Xbp1, X-box binding protein 1

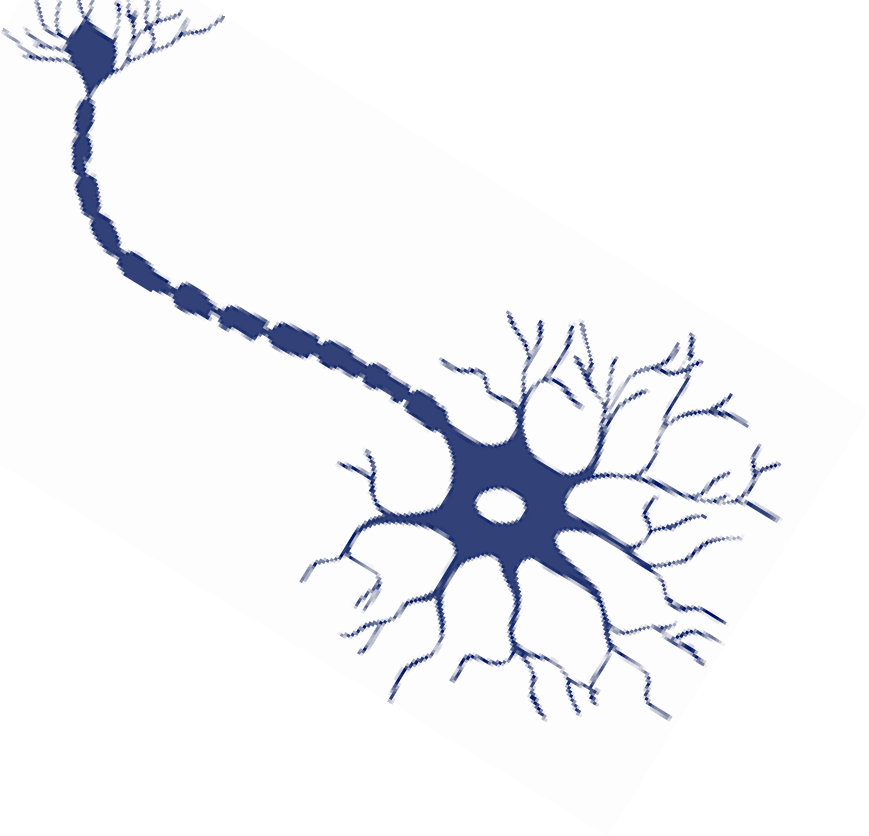

INTRODUCTION

Introduction

1. Motor Nervous system

Motor system is an ensemble of organs that is responsible for the movement of animals. It is formed by neuronal, muscular and other elements that act coordinately to perform an action. The part of motor system present within the nervous system is composed by primary motor cortex (Penfield homunculi), basal ganglia, brainstem (cerebellum), spinal cord, motor axons and neuromuscular junctions (NMJ).

1.1 Lower Motoneurons

The directors of motor system actions are the motoneurons (MNs), which are located within the central nervous system (CNS) at brain, brainstem and spinal cord (SC). They carry signals from CNS to the muscles, skin and glands. MNs can be described as upper MNs or lower MNs. The upper are present in the brain, and they are responsible of the initiation of voluntary and postural movements. The lower, which are present in the brainstem and SC, are governed by the superior ones and they integrate the autonomic reflexes and perform voluntary movements. The lower MNs located at the anterior grey column of the spinal cord are classified as α, β and γ MNs. The α-MNs innervate extrafusal muscle fibers and are the main responsible of muscle contraction initiation. The γ-MNs innervate intrafusal muscle fibers of muscle spindles and modulate the muscle contraction. The β-MNs innervate the intrafusal muscle fibers of muscle spindles.

1.1.1 Types and Biochemical characteristics of Motoneurons

MNs are a subtype of cholinergic neurons. These neurons are classified as cholinergic because they express the Choline acetyltransferase (ChAT) enzyme, so they can release Acetyl choline vesicles at the synapsis. This neurotransmitter is related with development and plasticity. Cholinergic neurons are located at the brain, brainstem and spinal cord (interneurons and MNs). They can be immunohistochemically discerned by molecular markers (i.e interneurons and pyramidal neurons) (Consonni et al., 2009). Recently, it has been described that a

variant of ChAT is also expressed in those neurons present at the DRGs (Naser and Kuner, 2017). MNs are also classified regarding its location, excitability, target organ and vulnerability to death, and therefore on their physiological function (Haenggeli and Kato, 2002a; Tadros et al., 2016). MN ability to orchestrate the motor response depends on its membrane potential and its ability to trigger action potentials. In this way, MNs from different zones of the CNS have slight differences in their excitability. The MNs present in the hypoglossal nuclei need to discharge more action potentials at high frequencies, otherwise, those from the SC need lower movement velocities and therefore less action potentials production (Tadros et al., 2016). Although not fully understood, these differences can be related with differences on the ionic channels conformation of their membrane. Spinals MNs also differs from the others in the distance of their axons, since they need a longer distance to reach all the muscles of the body.

MNs are surrounded and supported by different cellular types: microglia, astroglia, oligodendrocytes and ependymal cells. Although they have different functions, their main role is to sustain, feed and ensure a correct health of neurons allowing an optimal performance of the nervous system. They also protect MNs from external or internal insults. Indeed, microglia expresses receptors for some neurotransmitters and neuropeptides to monitor the state of the neurons (Pocock and Kettenmann, 2007) and the astrocytes reuptake neurotransmitter excess to maintain the CNS homeostasis (Perdan et al., 2009). Microglia also secrets trophic factors as nerve growth factor (NGF), brain-derived neurotrophic factor (BDNF) and glial-derived neurotrophic factor (GDNF) to sustain neuronal survival (Colonna and Butovsky, 2017) or support new-born neurons favoring functional recovery after injury (Song et al., 2016). Therefore, microglia have an active role on neuroplasticity. On the same way, the central nervous system is protected by the blood-brain barrier, which helps to maintain a correct homeostatic environment and isolates neurons from damaging compounds.

1.1.2 Target requirement

During development, neurons are overproduced and some of them should die by programmed cell death (PCD) to obtain an optimal nervous system with a

proper neuronal circuits formation. PCD is essential to ensure a correct neuron-target networking within the CNS. This process is mainly mediated by caspases, and under normal conditions is apoptotic. When this apoptosis is blocked by genetic modulation, neurons bypass this inhibition and normally die by non-apoptotic and unknown processes (Miura, 2011; Yamaguchi and Miura, 2015).

Rita Levi-Montalcini was the first in describe this death in DRG neurons (Hamburger and Levi-Montalcin 1949) and she observed that the use of anti-NGF antibody promoted the death of these neurons (Levi-Montalcini and Booker, 1960). Therefore, during development, neurons need the support of trophic factors to stay alive. This hypothesis is widely observed in the PNS, because MNs and DRG neurons are overproduced and their survival depends on pro-survival factors produced by target tissues. Other studies suggest that neurons die by PCD when they establish some incorrect or inappropriate connections with target tissues. Thus, PCD also eliminates error-prone neurons in those nervous system zones with a precise spatial topographic map (Yamaguchi and Miura, 2015).

1.1.2.1 Target requirement during development and program cell death.

Several *in vitro* studies describe a natural death of spinal MNs during late embryonic states on mice, chicken or frog. This death is mainly caused by the deprivation of target-produced neurotrophic factors, although other type of compounds can avoid MNs demise such as the cardiotrophin-1. Different compounds are able to sustain the MNs during development, and it has been proposed that they need a cocktail of different substances to stay alive (Oppenheim, 1996). NGF is retrogradely transported until the MN in neonatal rats, but it does not avoid its death after axotomy (Yan 1998). This indicates that MNs need a combination of neurotrophic factors to survive. This study also demonstrated that muscle produces some of the compounds that MN needs to stay alive. Regarding the molecular process, MNs that control leg-movement on *Drosophila* die by apoptosis, and the blockage of this death is correlated with defects in axon targeting and errors in dendritic pattering (Baek et al., 2013). Apoptosis is also responsible for MN death during metamorphosis of *Drosophila* (Winbush and Weeks, 2011).

Regarding the development of MNs after birth *in vivo*, only it has been demonstrated that the MNs of the hypoglossal nuclei die through an apoptotic way and that the spinal ones does not die by PCD after birth (Lance-Jones, 1982; Michaelidis et al., 1996; Lowry et al., 2001). So, PCD in spinal MNs occurs only during embryonic states.

1.1.2.1 Target requirements in adult MNs and neurodegeneration

After target deprivation during adult-hood, MNs activate intrinsic machinery to survive. Several programs are engaged to counteract the lack of neurotrophic factors. Adult MNs express the protein family known as inhibitor of apoptosis (explained below, 4.2). So, although they initiate apoptosis as neonatal ones, they express proteins that block this PCD (Perrelet et al., 2004; Kole et al., 2013; Casas et al., 2015). In fact, the sciatic axotomy did not cause a significant MN loss. Therefore, only embryonic or neonatal MNs need trophic support for survive.

1.2 Peripheral motor compounds

Once the central nervous system initiates actions potentials, they must be transported until the target organ, to perform the programmed action. . This signal will be transported through the PNS. PNS is composed by cranial and spinal nerves, ganglia, plexus, sensory receptors and neuromuscular junctions (NMJ).

1.2.1 Nerves and motor axons

The axons that extend from central neurons will bundle to form the nerve of the PNS. MNs are located at the ventral horn of the spinal cord, and their axons emerge through the ventral roots to the PNS. Nerves are composed by those axons, fibroblasts, blood vessels that supply the tissue, and Schwann cells that are the responsible to myelinate axons to increase their conduction velocity. Nerves are composed by 3 different layers: epineurium, perineurium and endoneurium. Axons present in the nerve, hereinafter called as fibers, can be classified by its diameter, myelination (myelinated or unmyelinated) and the propagation speed of action potential (Erlanger and Gasser, 1930). Motor system is composed by those

myelinated efferent fibers that are throwed out by α, β and γ MNs. Fibers are classified in A, B and C type. Fibers are classified in A, B and C types. Axons of α type (Aα fiber) will innervate the extrafusal muscle fiber, meanwhile the γ type (Aγ fiber) will innervate the muscle spindle. B-type fibers innervate both type of muscle fibers. The motor fibers from α-MNs have the higher conduction velocity and higher diameter than other types. Recent studies discern two separable part of the axons that share protein composition: the axon initial segment (AIS) and the nodes of Ranvier. The first one is the proximal region of the axon and serves as the site where action potentials are triggered. The nodes of Ranvier are the gaps between myelin sheaths and allow the propagation of the action potential. They differ in their mechanisms of assembly. AID formation depends only of the neuron, meanwhile nodes of Ranvier structuration is influenced by extrinsic factors (Nelson and Jenkins, 2017).

1.2.2. Neuromuscular junctions

Once the MN initiates the AP and this is conveyed throughout the axon, it will provoke the release of acetyl choline at the neuromuscular junction (NMJ) provoking a muscular action potential. When several MNs trigger jointly, they will provoke a compound muscle action potential (CMAP) at the muscle. This action needs the active role of the ionic channels that are present throughout the axon, and are also present within the NMJ and muscle fiber. Indeed, mutations or changes on its expression have been related with neuromuscular pathologies (Cooper and Jan, 1999) and with the neuropathic pain apparition after nerve injuries (Seltzer et al., 1991). Therefore, the generation of action potentials and the presence of ionic channels yielded to the use of electrophysiological techniques to monitor the state of the nervous system during disease or after injury. Besides, these techniques were useful to study the state of MNs in neurodegenerative disease (Morales et al., 1987), or the grade of axon regeneration and muscle recovery after nerve injury (Navarro, 2016).

NMJ is formed by the pre-synaptic and post-synaptic components, that are separated by a 50-80nm-wide gap. This gap is known as synaptic cleft. Regarding the pre-synaptic, the motor nerve terminal has Schwann cells and contains the

synaptic vesicles with the acetylcholine. Several proteins should act coordinately to release these vesicles once the action potential arrives at the end-up of the axon. The synaptic crest is a basal lamina formed by Schwann cells and compounds secreted by skeletal muscle. In muscle, the post-synaptic membrane is highly folded with crests that contain the acetylcholine receptors and troughs that have the voltage-gated sodium channels. NMJ is covered by the secreted material of Schwann cells until the muscle fiber and by kranocytes cells (Tintignac et al., 2015). After muscle denervation, is essential a correct rebuilding of the NMJs to recover the motor function at clinical level (Sakuma et al., 2016).

2. Traumatic lesions to motor nervous system

Although the part of motor nervous system present in the CNS is protected by cranium and spinal column, several factors can damage brain and spinal cord. Traumatic brain injury (TBI) and spinal cord injury (SCI) are provoked when an external physical insult causes damage to them. This can be from mild to severe, and will provoke functional disabilities. TBI leads to motor deficits such as loss of ambulation, coordination and fine motor skills. Meanwhile the SCI promotes loss of movement, autonomic functions, sensations and the neuropathic pain apparition. The mechanical insult will disrupt the tissue and will directly kill neurons by disruptive forces. Just after the impact, molecular responses like excitotoxicity, inflammation and others are triggered, and they will determine the future functional impairment (Shoichet et al., 2008).

2.1 Brachial and Lumbar plexus injury

The mechanical injuries that affect the interface between CNS and PNS and provoke a dramatic motor function loss, are termed as root avulsion (RA). RA can be considered as a peripheral nerve lesion (PNL), which is a disruption of the neuron-muscle connection. RA can be produced to a single or some nerve roots from brachial, lumbar and facial zones, or can affect a complete plexus. RA can be the most serious type of injury to the peripheral nerve, causing aa grave impairment of the quality of life of the patient (Htut et al., 2007). RA of one or more roots is presented at clinical in 70% of thus traumatic accidents with an affectation to brachial plexus

(Kachramanoglou et al., 2017) RA is often caused by high-energy traffic accidents (mainly motor vehicle), sportive (i.e. American football), iatrogenic injuries and during obstetric interventions (Pondaag et al., 2004; Buitenhuis et al., 2012; Daly et al., 2016; Kachramanoglou et al., 2017). Brachial plexus injury (BPI) is present in 1.2% of the multi-trauma admission patients in Canada and 450-500 supraclavicular injuries occur every year in UK (Goldie and Coates, 1992). Neonatal BPI affects 2-3 of 1000 births (Pondaag et al., 2004). Nowadays, the only treatment for new-born and adult patients is the root reimplantation, but the recovery after this reparation is sometimes incipient (Htut et al., 2007). At the same time, RA injuries are characterized by a strong neuropathic pain that is correlated with a maintained inflammatory response (To et al., 2013) (see below), which will affect the patient life.

2.2 Types of PNL

PNL can appear as the result of mechanical traumatic lesions (traffic, laboral and obstetric interventions), compression, stretch or ischemia, and it will interrupt the connection between the neuron and its target organ. Thus, patients with this type of lesions will suffer paralysis, sensory disturbances, anesthesia and lack of autonomics functions on the affected body areas. Therefore, quality of life of the subjects will be drastically reduced by the functional deficits and by the apparition of neuropathic pain. This pain appears when the somatosensory system, which includes fibers and central neurons, suffer some lesion or disease. This phenomenon is characterized by an uncontrolled inflammatory response and by a central sensitization. The second one is based on the reduction of the inhibitory synapses present at the spinal cord combined with an increase on the inputs that arrive from fibers (Andrade et al., 2011; Baron et al., 2013; Luchting et al., 2015). Although the PNLs are characterized by the apparition of this pain, those that directly affect the interface between CNS and PNS like RA are characterized by one that is unbearable and long-lasting (Cohen and Mao, 2014a). Although several experimental therapies based on drugs, physical exercise or deep brain stimulation have been postulated to reduce partially or totally the apparition of this pain (Cobianchi et al., 2017; Colloca et al., 2017), no effective treatments are present in clinical level nowadays.

Hereinafter, we will focus on PNLs that annually affect about 13-23 people per 100,000 in developing countries (i.e. 300,000 in Europe) and cause a substantial economic and social burden in a global perspective (i.e. 150$ Billion in USA health care) (Noble et al., 1998; Taylor et al., 2008a; Grinsell and Keating, 2014). PNLs are classified in different subtypes depending on the severity of the injury and the distance between the nerve stumps. The prognosis and functional recovery after PNL will be determined by both, and by the time needed by the nerve to regenerate and reconnect with the target. Initially, Seddon classified the mechanical lesions in three types: neurapraxia, axonotmesis and neurotmesis (Seddon, 1943). At 1951, Sunderland divided more deeply the PNL in five different injury grades (Sunderland, 1951) and at 1988 Mackinnon added a new grade named 6 (S. E. Mackinnon and A. L. Dellon, 1988). Nowadays, this classification is still used (Chhabra et al., 2014) (**Fig. 1 and Table 1**). The Grade 1 (Neuropraxia of Seddon), is usually related with a blockage of nerve conduction without anatomical interruption. The Grades 2, 3 and 4 (Axonotmesis of Seddon) imply the anatomical affectation of the axon, axon-endoneurium or axon-endoneurium-perineurium, respectively. The Grade 5 (Neurotmesis of Seddon) is a complete transection of the nerve. The Grade 6 or Mixed is a mixture between grades 2 and 4 involving a more common clinical scenario of the PNL. After a PNL of grade 1 or 2, the re-growth of the axon occurs spontaneously and a complete functional recovery will be obtained. After grade 3, the partial recovery without surgical repair can emerge, but for grade 4 and 5 surgical repair is mandatory to warranty some grade of recovery.

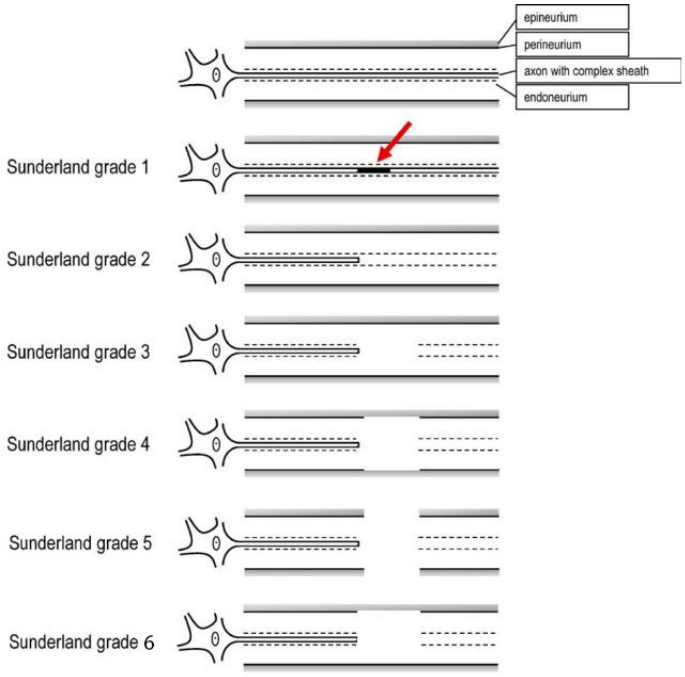

Figure 1. Classification of the different PNL. Schematic representation of the 6 degrees of nerve injury according to Sunderland and Mackinnon. Red arrow indicates a conduction blockage. The other grades are classified depending of the affected layer, that can be the axon, endoneurium, perineurium and epineurium (Adapted from Deumens et al. 2010).

Table 1: Actual classification of nerve injuries (Extracted from Seddon 1943, Sunderland 1951 and S. E. Mackinnon and A. L. Dellon 1988,)

Seddon	Sunderland and Mackinnon	Description
Neuropraxia	Grade 1	Only myelin is affected. Temporal blockage of transmission
Axonotmesis	Grade 2	Only the axons are disrupted
Axonotmesis	Grade 3	Axon and endoneurium are broken
Axonotmesis	Grade 4	Only epineural tissue is maintained
Neurotmesis	Grade 5	Complete nerve transection
Mixed	Grade 6	Nerve injury with features of type 2 and 4

It is important to mark that not all the dysfunctions of the PNS are related with a direct traumatic injury. Some peripheral neuropathies (PN) will block the connection between MNs and muscle, favoring the apparition of neuropathic pain and of neuromuscular disorders that can provoke paralysis in extreme cases (Laing, 2012). PN can be from genetic origin such as Charcot-Marie-Tooth disease, acquired during lifetime such as those induced by diabetes mellitus, caused by adverse effects of drugs treatments or provoked by inflammatory responses (England and Asbury, 2004). Neurodegenerative pathologies can also disrupt the neuron-muscle connection. The amyotrophic lateral sclerosis (ALS) is characterized by an axonopathy that affects MNs and that will cause its death. Independently of the ALS etiology (familiar or sporadic), one of its hallmark is the retraction of the axon of

MN, which will lead to the muscle denervation (Robberecht and Philips, 2013). Although unclear, this disturbance has been related with an unbalance of the axonal transport (Taylor et al., 2016), that it is also present in other CNS or PNS neurodegenerative diseases where axonal integrity is endangered (Millecamps and Julien, 2013).

3 Murine models of lesions to motor system

Experimental models are useful to elucidate information about which are the underlying mechanisms that provoke neuron death or its regeneration and to obtain new drug therapies to increase functional recovery after PNL. The approximations can be performed *in vivo* or *in vitro*.

3.1 In vivo murine models

Several *in vivo* models are widely used to mimic the clinical scenario of PNL, and to discern which factors modulate nerve regeneration. The used species go from mammal models (rat and mice) or other vertebrates (*Danio rerio*), until invertebrates as *C. elegans*. Some differences arise from its anatomy and its molecular features. Among all the animals used for PNL studies, the rat/mice (murine) species are the most commonly used, taking advantage of its big size to perform precise microsurgeries. Several murine models are used for the study the survival and regeneration of MNs after PNL.

When MNs suffer the disconnection from their target organ after PNL they will suffer several changes, which in some cases, can promote their death. The death of MN after PNL depends of the crosstalk and the convergence of different molecular mechanisms that are triggered after MN disconnection, and that will be further explained below (Section 4 of Introduction). On the other hand, for the study of the mechanisms that underlie PNL and orchestrate the nerve regeneration, different models have been described. The murine specie are the mainly used for this studies (Tos et al., 2009). The difference between these models reside on the difficulties and barriers presented to the MNs to effectively regenerate until the target organ. These depend on the severity of the injury, the distance from the soma and the age of the

animals. Crush injury of the nerve (axonotmesis), which is the breakdown of the axons continuity by compression, allows to a good recovery because each axon reconnects with its anterior target. Otherwise, the neurotmesis is a complete transection of the nerve and it can be repaired by a suture, an autograft or with a conductive tube, and this injury recapitulates accurately the clinical of the PNL. Neurotmesis causes a completely disorganization the anatomical structure of the nerve (Lago and Navarro, 2006), leading to a poor functional recovery of the animals. Other used models are those based on the ligation or partial compression of sciatic nerve or the spinal roots. They present a mixture of axon degeneration and neuropathic pain apparition, but they do not allow a correct quantification of nerve re-growth and functional recovery after injury.

Aiming to obtain a more realistic model of death of MNs combined with axonal regeneration which fits better with human PNL and its clinical impact, some authors performed the avulsion of ventral or brachial roots in combination with an immediate reparative surgery (Eggers et al., 2010; Pintér et al., 2010; Torres-Espín et al., 2013). Few studies have been conducted with a delayed reparation of avulsed roots and all them are focus on the roots present at brachial level (Gu et al., 2005). Nowadays, no articles describe a study where the avulsion of the roots that conform lumbar plexus is combined with a delay of its reparative surgery

3.2 *In vitro* models: cell lines, primary and Organotypic cultures

To reduce animal use but obtaining reliable results, several specific factors that neuroprotect the MNs against insults or modify its axonal regeneration can be analyzed through *in vitro* approximations. These studies give information about the molecular pathways that underlie MN death or axonal elongation.

Cell lines such as PC12 or NSC34, to obtain neurons or MNs respectively, or JS-1 to obtain Schwann cells can be used, and they are useful to reveal new neuroprotectants, to study material biocompatibility or to depict molecular mechanisms (Geuna et al., 2016). The large number of cells and experiments carried out with low costs make this approach more attractive. Furthermore, the results obtained through this cell lines should be interpreted with caution due to the

neoplastic origin of the cells and the high variability that arises from the susceptibility of the cells to the culture conditions (Tos et al., 2009).

Other *in vitro* approximation is the obtaining of primary cell cultures from animals. Depending on the aim of the study, different sub-cellular populations can be purified (motoneurons, DRGs neurons or Schwann cells) and be cultured (Haastert et al., 2007; Tos et al., 2009; Severini et al., 2017). This approach reduces the animal use, but its preparation is labor-extensive and the cells only can be maintained during few weeks in culture. For nerve injury, recently has been published a new protocol that mimics the nerve axotomy in cultured neurons (Zhou et al., 2016). Adding some complexity, the co-culture of MNs with Schwann cells is an useful model to study the behavior of nerve during regeneration *in vitro* (Haastert et al., 2005). Besides, the co-culture of neurons with glial cells in separate scaffolds mimics the connections that arise within the nerve between neurons and Schwann cells or fibroblasts (Gingras et al. 2009).

The most representative *in vitro* approximation is the organotypic culture of the entire tissue. The culture of a whole piece of tissue is named organotypic culture. Curiously, after processing the spinal cord to obtain the explants, its cytoarchitecture is maintained and the motoneurons are able to interact between them. This makes its culture a reliable model (Crain and Peter, 1967). For neurite growth studies, it is needed the design of a 3D environment that mimics the nerve tissue. The organotypic culture of the entire tissue in combination with a matrix of a material that allows axon regeneration (i.e. collagen) (Allodi et al., 2011), will permit to the neurons to remain on its natural environment. This allows to maintain the interactions between neurons and glia, and will allow them neurons to extend their axons. This model can also yield information about the role of glia on the axonal growth of MNs. It is important to figure out that depending on the aim of the study, the cultured tissue must be different (for example for motor axons growth, the used tissue is the spinal cord). Spinal cord slices can also be cultured to discern or to elucidate modulators of the molecular pathways that provoke MNs demise. This *in vitro* model can reproduce some hallmarks of the death of MNs after trauma or in neurodegenerative diseases, such as ecotoxicity or inflammatory reaction. These cultures can be maintained during several weeks (Guzmán-Lenis et al., 2009b. These

models are also useful to found neuroprotectants for death of MNs or spinal cord injuries (Guzmán-Lenis et al., 2009a, 2009b). Recently, 3D printing technique has been used to culture DRG and to analyses its growth (Badea et al., 2017).

Although *in vitro* models can be useful, *in vivo* models are still needed as the main goal of nerve regeneration is to replace the distal part of the nerve and correct reconnect with denervated organ. Therefore, functional studies in whole organism are still mandatory.

4. Molecular mechanisms in neurodegeneration and regeneration after nerve injury

Nerve injuries are characterized by a rapid retrograde response that will recruit the needed molecular machinery at the neuron soma to induce the axonal regrowth. After axotomy, neurons dedifferentiate its phenotype to face up with the injury (González-Forero and Moreno-López, 2014), shifting from neurotransmission state to the pro-regenerative one. This process is triggered quickly after PNL and implies phenotypic and morphological changes, which are named chromatolysis and neuronal reaction. Chromatolysis is linked with the disorganization of the Nissl bodies, that provokes the release the polyribosomes and ribonucleotides into the cytoplasm. With this, neurons try to counteract the insult decreasing the neurotransmission-related compounds and raising the synthesis of structural proteins and growth associated effectors.

Axon-soma connections are essential for a correct neuronal response, and for this, the retrograde transportation of information through long distances is essential. Neurons need to detect axonal injury to face up the insults and activate its pro-regenerative machinery. The events that are initiated can be classified in early or late events (Rishal and Fainzilber, 2014). The breakdown of the axon membrane is accompanied by the disruption in the ionic balance, which leads to the propagation of a calcium wave (Ziv and Spira, 1995) and the firing of action potentials (Mandolesi et al., 2004). Both events are propagated towards the neuronal soma. This Ca^{2+} will activate endogenous molecular programs like the induction of a set of pro-regeneration genes (Michaelevski et al., 2010), and the

epigenetic modification of the genome by histone acetyltransferases at CNS or histone deacetyltransferases at the PNS (Cho et al., 2013; Puttagunta et al., 2014). Those are needed for axonal membrane resealing and cytoskeletal rearrangement (Cho and Cavalli, 2012), which are essential events to induce an efficient initiation of the growth cone (Ghosh-Roy et al., 2010; Bradke et al., 2012). Genes that are upregulated after PNL and that are directly linked with axonal regrowth are termed as Regeneration-Associated Genes (RAGs) (Chandran et al., 2016). Among them, the growth-associated protein-43 (GAP43) is a widely described RAG that is strongly triggered within the peripheral axons after injury, and that is well correlated with a successful nerve regeneration (Afshari et al., 2009). Neurons present in the CNS are incapable to regenerate after injury, and this is partially caused by its low-intrinsic ability ty trigger an efficient RAGs response. The expression of RAGs is a tightly regulated process that needs specific activation of determined TFs and the coordinated modulation of gene expression by them. This RAGs programs can be also modulated by epigenetic processes, so the modulation of those enzymes that orchestrates epigenetics marks are a feasible approach to enhance axonal regeneration within the CNS (Fagoe et al., 2014). The late events are directed by signaling macromolecular networks that include molecular axis of the JUN amino-terminal kinase 3 (JNK3), the signal transducer and activator of transcription 3 (STAT3) and the extracellular signal-regulated kinases (ERKs).

4.1 Retrograde degenerative and endogenous neuroprotective mechanisms

Depending on the animal species, the maturation state of, the distance to the soma (pre- or postganglionic) and the subpopulation, neurons, and specifically the MNs, undergo a massive death after PNL. The proximity between the injury and the neuronal soma is directly correlated with a higher cell death of dorsal root neurons (Ygge, 1989). Spinal MNs from rat are extremely susceptible to the avulsion or preganglionic transection of the roots that form brachial or lumbosacral plexus (Penas et al., 2009a), but when the injury is at postganglionic level, no significant death of MNs is detected (Vanden Noven et al. 1993; Karalija et al. 2016;). Parallelly, only those MNs from hypoglossal nuclei of mice, are susceptible to the transection of the hypoglossal nerve at distal level from the soma (Kiryu-Seo et al., 2005).

Besides, only immature MNs are susceptible to the postganglionic injury of the sciatic nerve in both species (Lowrie et al., 1994; Sun and Oppenheim, 2003).

MNs have endogenous mechanisms to counteract the insult and survive. During early days post RA, it has been described that several pro-death or pro-survival molecular actors participate, and their imbalance leads MNs towards its death (Casas et al., 2015) (Fig. 2). The pro-death mechanisms that are related with the demise of MNs are: apoptosis, necrosis, anoikis, ER stress, nucleolar stress cytoskeleon rearaggements, selective autophagy and mithocondrial dysfunction. The endogenous mechanisms of neuroprotection engaged by MNs are: anti-apoptosis, anti-anoikis, anti-necrosis, autophagy, UPR, reactive oxidant species hormesis and mitochondrial well function. The programs initiated within the MNs after axotomy, especially those that are a hallmark of its death, and those that are activated by the MN-environment, will be disclosed hereinafter.

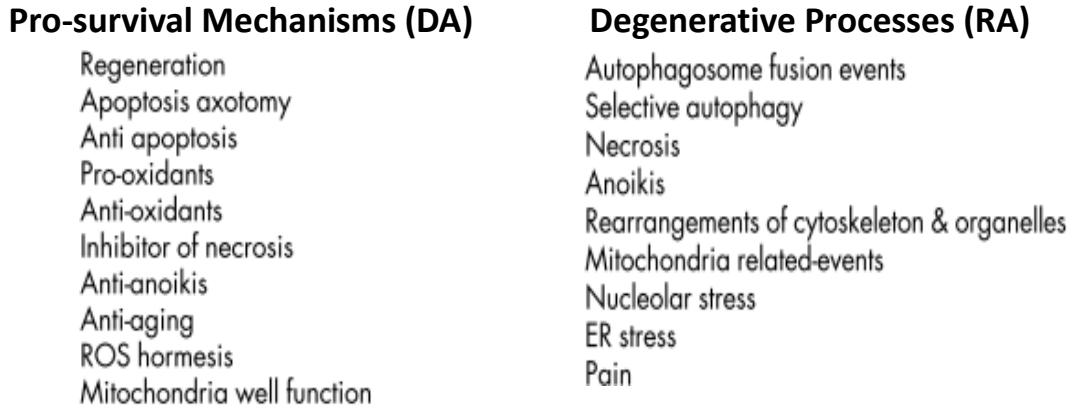

Figure 2. **Endogenous mechanisms of neuroprotection or death engaged by the MNs after different PNL**. The molecular mechanisms that are triggered by the MNs in two slightly different rat models of PNL, that have an opposite outcome on MN survival. In the DA, a nerve injury where MNs activate endogenous mechanisms to face up the insult and they regenerate their axon until the target organ, its survival is not compromised. In the RA, a nerve injury that activates those mechanisms within the MNs that will lead to their death (Extracted from Casas et al. 2015).

4.1.1 Apoptosis

Not all the cells can decide when they die, and the apoptotic death is a subtype of PCD that can be chosen or forced after some insults. Neuronal PCD is essential for a correct nervous system development (Raff et al. 1993; Miura 2011). PCD was initially described as a controlled intrinsic process that remove the unwanted cells from the pluricellular organisms. The aim of this cellular function is to refurnish the

tissues, reducing the non-functional cells and favoring the renewal of them (Taylor et al., 2008b). Apoptosis is a subtype of PCD that was discovered in developing, normal or insult-affected tissues (J. F. R. Kerr 1972). Apoptosis is defined as an active cell death that maintains the integrity of cell plasma membrane and of organelles, and it is mediated by the activation of caspases (Fan et al., 2017). In fact, apoptosis death shares similarities with those processes that are initiated by cells during differentiation (Bell and Megeney, 2017). Apoptosis dysregulation is the cause of several neurodegenerative or inflammatory pathologies, and of some kinds of cancer. Recent studies suggest that adult neurons differ from neonatal ones in their specific intrinsic machinery to avoid cell death. They point that during neurodegeneration mature neurons become more susceptible because they convert to the neonatal-phenotype, and this can be related with their death (Kole et al., 2013).

PCD and some kinds of apoptotic deaths are driven by the proteolytic type of enzymes termed caspases, which are zymogen proteins that require a proteolytic processing to be active. Caspases induced death is a highly controlled process which needs several players to act coordinately to cause the final cell death. Apoptosis can be triggered by two different pathways. The extrinsic, that depends of extracellular ligands, or the intrinsic, that depends of mitochondrial compounds (**Fig. 3**). Once initiated by the activation of pro-death receptors such as FASR, or by the liberation of the cytochrome c from mitochondria to the cytosolic space, the initiator caspases (Caspase 1, 2, 4, 6, 9, 10, 12 and 14) will become active (Ichim, Gabriel; Tait, 2016). These active caspases will unleash the cleavage of the effector caspases (3, 6 and 7), which will execute apoptosis. Although humans and mice have a different set of caspases, the underling mechanisms are very similar (Man and Kanneganti, 2016).

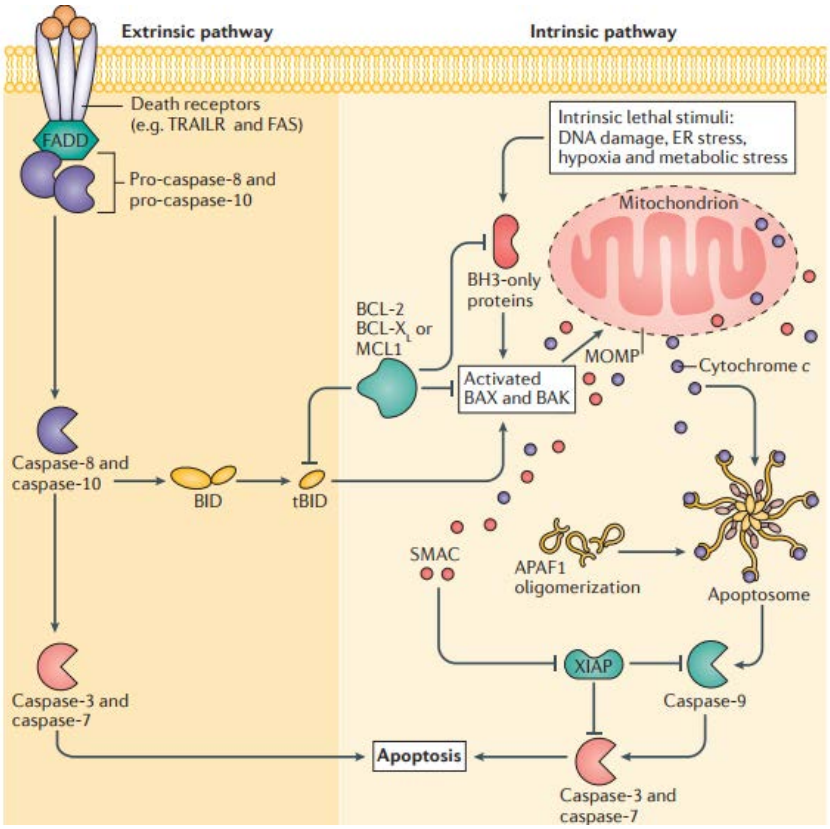

Figure 3: Extrinsic and intrinsic apoptotic pathways. The extrinsic pathway is initiated when the death receptors (TRAILR or FAS) are activated. Once active, they will activate caspase 8 or 10, which will process caspase 3 or 7 and they will lead to apoptosis. On the other hand, the intrinsic pathway is triggered after the mitochondrial outer membrane permeabilization and the consequent release of cytochrome c. This can be triggered after an internal stimulus or by the inhibition of Bcl-2 proteins. This permeabilization is mediated by BH3-only proteins. Cytochrome c allows the polymerization of the apoptotic protease activating factor 1 (APAF1) to form the apoptosome. This will activate caspase-9, which will cleavages the caspase 3 and 7, those that will drive cell to apoptosis. Intrinsic and extrinsic pathways can crosstalk by the caspase-8 mediated cleavage of BHD3-interacting death domain agonist (BID) (Extracted from Ichim, Gabriel; Tait 2016)

The proximal disconnection of MNs from their target organs by root transection or by RA will compromise their survival (Koliatsos et al., 1994; Martin et al., 1999; Penas et al., 2009a). These type of injuries will lead to a massive retrograde death of the 80% of MN within 3-4 weeks after injury (Penas et al., 2009a). So far as we know, the molecular pathways that characterize this death are controversial and remain unclear. Initially, the program was classified as apoptotic (Martin et al., 1999) or necrotic (Li et al., 1998), but some authors did not found caspase activation (Penas et al., 2011a) or necrotic markers (Casas et al., 2015). In contrast, when the MNs are disconnected from their target at neonatal stage, independently of the distance from the soma, its death is characterized by apoptotic

hallmarks such as cleaved caspase 3 or TUNEL labelling (Oliveira et al., 1997; Sun and Oppenheim, 2003). In the neonatal stage, the deletion of the pro-apoptotic gene BAX or the inhibition of apoptosis reduced drastically the percentage of death of MN after RA or nerve injury (Deckwerth et al., 1996; Chan et al., 2001; Sun and Oppenheim, 2003). Therefore, the survival or death of MNs after nerve injury is determined by the type of injury and its developmental stage. To sum up, the RA is a severe type of PNL that may occur during adulthood after the detachment between nerve and spinal cord. This injury will initiate molecular programs that will lead to a non-apoptotic death of MNs. However, the distal axotomy of the nerve initially triggers molecular programs that share similarities with RA (Penas et al., 2009a, 2011a). This indicates that after PNL the MNs have a similar early response.

Although some hallmarks of apoptosis like the nuclear presence of the apoptosis inducing factor 1(AIF1) orcaspase-3 cleaved, and C/EBP-Homologous Protein (CHOP) are found in ALS mice model, it is unclear if the MNs suffer apoptotic death in this pathology (Ghavami et al., 2014). Caspase 3 cleavage is also found *in vitro* in a model of Charcot Marie Tooth with MN death (Jacquier et al., 2017), but these MNs are more resistant to apoptosis (Rizzo et al., 2016). Therefore, although apoptotic machinery is active and recruited on the soma of MNs, apoptosis is not the executive program of their death. Similar results are found in MNs after RA injury. RA induces apoptotic pathways but also anti-apoptotic ones, and this balance leads these neurons to an alternative and unknown death.

Finally, although caspase activation have been widely related with cell death, recent evidences shown that they can also act remodeling the nervous systems without promote cell death (Williams and Mukherjee, 2017), and that its activity depends on its subcellular position. Therefore, maybe the active forms of caspases found in neurodegenerative tissues had a non-death related role, and the final neuron death is through other fatal mechanisms.

4.1.2 Anti-apoptosis

During evolution, cells have developed several mechanisms to prevent its death when it is unneeded or to avoid a premature PCD. Cells only trigger an efficient apoptotic death when the balance between pro- or anti-apoptosis machineries

pushes towards death. The anti-apoptosis is driven by three family protein: FLICE-inhibitory proteins, Bcl-2 and Inhibitors of Apoptosis Proteins (IAPs). Alterations on those gatekeepers are related with some kinds of cancer (Portt et al., 2011). IAPs exert neuroprotection in ischemia models (Rami et al., 2008) or avoid death of MNs after nerve injury during neonatal stages. In fact, IAPs are proposed to be the responsible of the blockage of MN death after axotomy during adulthood (Perrelet et al., 2004). A post translational modification of the X-linked–IAP (XIAP) blocks its anti-caspase 3 function, and it has been described as a contributor to the Parkinson's disease (PD) pathogenesis (Tsang et al., 2009). Ischemic preconditioning, which partially reduces ischemia detrimental effects, acts through IAPs and enables cells to survive although caspase cascade is active (Tanaka et al., 2004). IAPs also mediate the GDNF-induced pro-survival effect on MNs after neonatal axotomy (Perrelet et al., 2002). The MNs activate XIAP after RA, which indicates that their intrinsic mechanisms to avoid apoptosis are triggered, and this justifies their non-apoptotic death.

Other protein pathways can avoid cell death by the modulation of pro-apoptotic proteins. In this sense, the protein kinase B (AKT) has been described as a pro-survival player by the blockage of apoptosis (Kennedy et al., 1997). p53 is a tumor-suppressor protein that can induce apoptosis by different ways (Yonish-Rouach et al., 1991; Fridman and Lowe, 2003). AKT inhibits p53 by its degradation, blocking its pro-apoptotic effects (Gottlieb et al., 2002). Otherwise, caspases are able to inhibit AKT by cleavage, indicating a fine-tune modulation of cell survival and death within cells (Rokudai et al., 2000). On the other hand, AKT activity is also able to phosphorylate the Forkhead box protein O (FOXO) TFs, which are related with apoptosis (Dijkers et al., 2000) and this turns on cell survival (Brunet et al. 1999). AKT-dependent phosphorylation avoids FOXO entrance to nucleus averting its induction of pro-apoptotic genes such as the Bcl-2 interacting mediator of cell death (BIM) or Bcl-2 nineteen-kilodalton interacting protein 3 (Bnip3) (Dijkers et al., 2000; Tran et al., 2002). Specifically, AKT-dependent phosphorylation of FOXO3a has been related with cell survival (Brunet et al., 2001).

4.1.3. Parthanatos

The poly(ADP-ribose) polymerase (PARP) family is composed by 18 different proteins (Ame et al., 2004), which are nuclear under normal conditions. Among them, PARP1 is the most widely described and it is needed to face up to different types of DNA damage (Ray Chaudhuri and Nussenzweig, 2017). Parallelly to its activity as DNA gatekeeper, it has an active role on cell death. The death phenomenon that is triggered by PARP1-activity is termed as Parthanatos (PAR, from the enzyme + Thanatos, *death* in Greek). PARP1 can promote direct or indirect cell death. PARPs are considered the major NAD^+ consumers, so its hyperactivation can lead to the depletion of NAD^+ levels. This will lead to cell death by energy failure (Houtkooper et al., 2012). Nevertheless, this hypothesis is currently being revised (Fossati et al. 2007; Fan, Dawson, and Dawson 2017).

For the direct death, PARP1 activity produces the PAR polymer (Andrabi et al., 2006), which is a tag-signal of cell death (Fan et al., 2017).It has been implied in the neuronal death present in Alzheimer disease (AD) (Strosznajder et al., 2012). The treatment with PARP1 inhibitors reduces the neurological damages after ischemia or traumatic brain injury (TBI) in humans (Gerace et al., 2015).The PAR polymers are needed within the nuclei for DNA repair. When the PAR polymers are translocated to the cytosol and mitochondria, they will induce the translocation of AIF1. AIF1 enters to nucleus and induces large-scale DNA fragmentation. Its active participation is essential to induce the PCD (Joza et al., 2001). The mice termed as "harlequin" have a mutation on AIF1. Neurons from this mice are more susceptible to stress, indicating that AIF1 has some beneficial role in cellular homeostasis (Klein et al., 2002). A recent study shown that hypoxia induced neuronal death is related with PAR polymer formation and it is directly linked with the nuclear translocation of AIF1 (Lu et al., 2014). AIF1 nuclear function on apoptosis has been linked with neonatal or adult ischemia, and with neurodegenerative diseases (Thal et al., 2011; Ghavami et al., 2014; Fan et al., 2017; Yang et al., 2017). Mutations on AIF1 gene are also linked with infantile motor neuron disease (Diodato et al., 2016).

Although parthanatos has been defined as a caspase-independent death, PARP1 can also be cleaved by suicidal proteases such as caspase, cathepsins,

calpains and granzymes. This different processing drives the way through which cells die (Chaitanya et al., 2010b; Fan et al., 2017). Depending on its processing, the formed fragments of PARP1 will be active or inactive. When PARP1 cleavage results in an active fragment, the cell death will be apoptotic, necrotic or autophagic (Chaitanya et al., 2010b). Caspase-3 can cleavage PARP1 giving two fragments of 24 and 89 kDa. The second one forms a protein complex that has a different transcriptomic program and will lead to apoptotic death (Castri et al., 2014). The cleavage of PARP1 onto its active form has been described in neurodegenerative diseases (Chaitanya et al., 2010b) and in ischemic brains (Chaitanya and Babu, 2009). The 89 kDa active form of PARP1 also has the ability to release AIF1 from the mitochondria, and this induces AIF1-dependent neuronal death (Hong et al., 2006; Qiao et al., 2016). When PARP1 is processed onto other type of fragments, it will became inactive or will act as a molecular switch between apoptotic, necrotic or autophagic cell death (Zhu et al., 2009). This autophagy triggering can help cell to overwhelms the stress and stay alive (Chaitanya et al., 2010b). Otherwise, when PARP1 is cleaved by lysosomal proteins will promote necrotic cell death (Gobeil et al., 2001). Therefore, PARP1 activity and its processing is a tightly regulated mechanism that can promote DNA repair or cell death. Currently it is unknown whether parthanatos is present in the death of MN after RA.

4.1.4. Anoikis

Interactions between cell and extracellular matrix (ECM) are essential for a correct cell function within tissue. When this crosstalk is averted, cells die through a PCD named anoikis, which shares common pathways with apoptosis. Interestingly, the breakdown of the intrinsic program of anoikis confers malignancy to tumor cells, giving them the eventual ability to scape and reattach onto other tissues (Frisch and Screaton, 2001). The major effectors of these interactions are the integrin proteins. Integrins are formed by the combination of α and β subunits, which will determine their ligand specificity and their intracellular signaling. On the other hand, signals from ECM are transmitted to neurons through integrins, being them essential for cell functions like shape, survival, motility and proliferation. Integrins are also important for the intracellular signaling of the growth factors (Stupack and Cheresh, 2002).

Specially, the β1 subunit of the integrins is an essential protein for cell-ECM interaction, and anoikis response is induced when their interactions are blocked (Bouchard et al., 2007). When its activity is antagonized in neuron culture, cells will trigger apoptotic mechanisms and will die (Bonfoco et al., 2000). Furthermore, the intracellular signaling of this subunit is related with the survival of the neurons from DRGs (Santos et al., 2012). Moreover, for a correct function of β1 subunit and although its expression has not been disrupted, its correct transport and anchorage to cell membrane are essential for its correct performance. Recently, it has been described that the blockage on its transport is present in the death of MNs after RA (Casas et al., 2015). Therefore, when the axotomized neurons are unable to properly interact with ECM, they trigger molecular mechanisms that drive them to fatal outcome.

4.1.5 Anti-anoikis

Although the disconnection from their environment triggers anoikis programs, cells have developed anti-anoikis subroutines to counteract anoikis-promoted death. Many metastatic cells activate this program to detach itself from the ECM without initiate apoptosis. This leads them to spread within the organism without die (Buchheit et al., 2014). MNs trigger anti-anoikis programs to survive after DA, meanwhile after RA injury it is not detected. This maybe a possible promoter of its cellular demise (Casas et al., 2015). Anti-anoikis can be initiated by tyrosine kinases, small GTPases (Buchheit et al., 2014), NF-κB (Toruner et al., 2006), the Phosphatidylinositol 3-kinase (PI3K)/AKT or ERK axes, and by autophagy (Lock and Debnath, 2008). NF-κB modulates anti-anoikis by the triggering of anti-apoptotic proteins such as Bcl-2 and IAP-1 (Lock and Debnath, 2008), meanwhile PI3K/AKT role in cell survival is widely documented and it contributes to the survival of differentiated cells (Song et al., 2005; Bouchard et al., 2007). ECM detachment also induces autophagy (see below), which is a self-protective mechanism (Lock and Debnath, 2008).

4.1.6 Autophagy

Autophagy, literally self-eating from Greek, is a group of mechanisms highly controlled by the eukaryotic cells that are activated to degrade its cytoplasmic

content through lysosomal degradation. The main function of this process is the maintaining of the cellular homeostasis. The way through the cytosolic content is delivered to lysosomes classifies three different modalities of autophagy (**Fig. 4**). One is the microautophagy, which involves the direct invagination of the lysosomal membrane and the degradation of the engulfed material. The second is the chaperon-mediated autophagy (CMA), which main role is to degrade the soluble protein aggregates with the help of chaperones. The other is the macroautophagy, hereinafter called as autophagy, which is a cell process that leads to the transport of cytoplasmic content through the autophagosome formation and the aggregation of lysosomes (Galluzzi et al., 2017). This process culminates with the autolysosome formation and the lysosomal degradation of the transported cargo. Although autophagy was initially observed only in cells under starvation, recent studies showed that cells have a basal level of autophagy to regulate protein homeostasis. Importantly, these basal levels are needed for neuron maintenance under normal conditions (Komatsu et al., 2006). The autophagy can also be activated as a self-protective mechanism to fight an insult, thus helping the cell to adapt to the new conditions.

Autophagic flux, which is a term used to determine the efficiency of the autophagic response, is defined as the rate at which lysosomes degrade the substrates of autophagy (Loos et al., 2014). A functional autophagic flux is a process highly coordinated by different Autophagy-related (Atg) genes, kinases and other regulatory proteins. All them working together will be the responsible for the initiation, nucleation, elongation, closure and correct fusion of the autophagosomes with the lysosomes to degrade the cytosolic load (Galluzzi et al., 2016). Neuron will upregulate genes related with autophagy to degrade axonal material after target disconnection (Penas et al. 2011a).

Mammalian target of Rapamycin (mTOR), Beclin-1 and the unc-51-like kinase 1 (Ulk1) are essential for a correct initiation and nucleation of autophagy (Russell et al., 2013; Galluzzi et al., 2016), and therefore to correctly form the double-membrane autophagosomes. This initiation can be triggered by Phosphatidylinositol 3-kinase/Protein Kinase B (PI3K/AKT) kinases, and its inhibition by 3-methyladenine or LY294 compounds block the autophagic response

(Galluzzi et al., 2016). Several studies aimed to depicter which is the origin of the membranes that form the autophagosomes. Published studies suggest that they come from ER, mitochondria, plasma membrane, endosomes or other subcellular sites (Kaur and Debnath, 2015). The process of nucleation ends once the autophagosomes have enclosed with the autophagic substrates inside.

Besides this, the elongation phase will be initiated and the autophagosomes will engulf more cytosolic content. The Atg7 and 10 cooperate to form the Atg5-Atg12 complex, which supports the autophagosome elongation. This process recruits to the autophagosomal membranes the microtubule-associated protein 1 light chains 3 (LC3) and facilitates its lipidation (Kaur and Debnath, 2015). Atg5 protein is specific of macroautophagy, so it is a good readout of macroautophagic flux (Galluzzi et al., 2016). To detect which are the cytosolic contents to be engulfed by the autophagosomes, cells have developed degradative signals to earmark this cargo. The most common is the ubiquitin-binding domain, which can be detected by LC3-binding domains or other receptors such as the Sequestosome 1 (p62). LC3 is also essential for the expansion of the autophagosome. During the elongation, the resulting autophagosome will be trafficked to the cell periphery by the dyneins, where it will fuse with endocytic and lysosomal vesicles leading to the formation of an autolysosome (Ravikumar et al., 2005). This fusion will provoke the degradation of the cargo material releasing autophagy-derived metabolites such as amino acids, glucose and others (Kaur and Debnath, 2015).

Alterations on the proteins related with the initial phases of autophagy have been observed in ALS (Menzies et al., 2015). Autophagy inductors such as rapamycin exerted neuroprotection after cerebral ischemia, TBI and AD (Spilman et al., 2010; Wang et al., 2012a; Galluzzi et al., 2016). Mutations on the p62 protein, which is responsible for the autophagosome elongation, have been observed in sporadic and familiar ALS (Teyssou et al., 2013). In fact, p62 activity has a neuroprotective role in those fly models that are characterized by protein aggregates, which are a hallmark of neurodegenerative diseases (Saitoh et al., 2015). The blockage or disruption of a correct autophagosomes and lysosomes maturation have been observed on Charcot–Marie–Tooth disease type 2 and ALS, (Menzies et al., 2015). This will lead to an aberrant accumulation of autophagic processes within the cytoplasm. This

accumulation can also be provoked by a lysosomal dysfunction. During the first days after TBI, autophagy is correctly initiated but the autophagosomes are not cleared, which indicates that autophagy is not resolved. This is caused by lysosomal dysfunctions, and it finally provokes neuronal death (Sarkar et al., 2014). This blockage in the autophagosomes clearance is also observed in human brains of AD (Boland et al., 2008)

The MNs trigger this protective mechanism after RA to face up the injury, but the flux is impaired at somewhere. This defect averts averting the pro-survival effect of autophagy (Penas et al., 2011a). Recent studies showed that this blockage can be partially provoked by cytoskeletal disarrangements, which avoid a correct fusion of the autophagosomes with lysosomes (Casas et al., 2015). After SCI in mice, the autophagy induction avoided the retraction of the axons and enhanced their regrowth, which leads to an increased recovery of motor function (He et al., 2016b). Those effects were mediated by the degradation of a MT-destabilizing component, which turns on a better intraneuronal axonal transport and an improvement of axonal behavior (He et al., 2016b). A blockage on the endolysosomal pathway causes defects on the remyelination and axonal regeneration in the Charcot-Marie-Tooth type 4J neuropathy and after nerve injury (Vaccari et al., 2015). Autophagic increase on Schwann cells reduces neuropathic pain after nerve injury (Marinelli et al., 2014). Therefore, autophagy has neuroprotective effects after injuries to the nervous system.

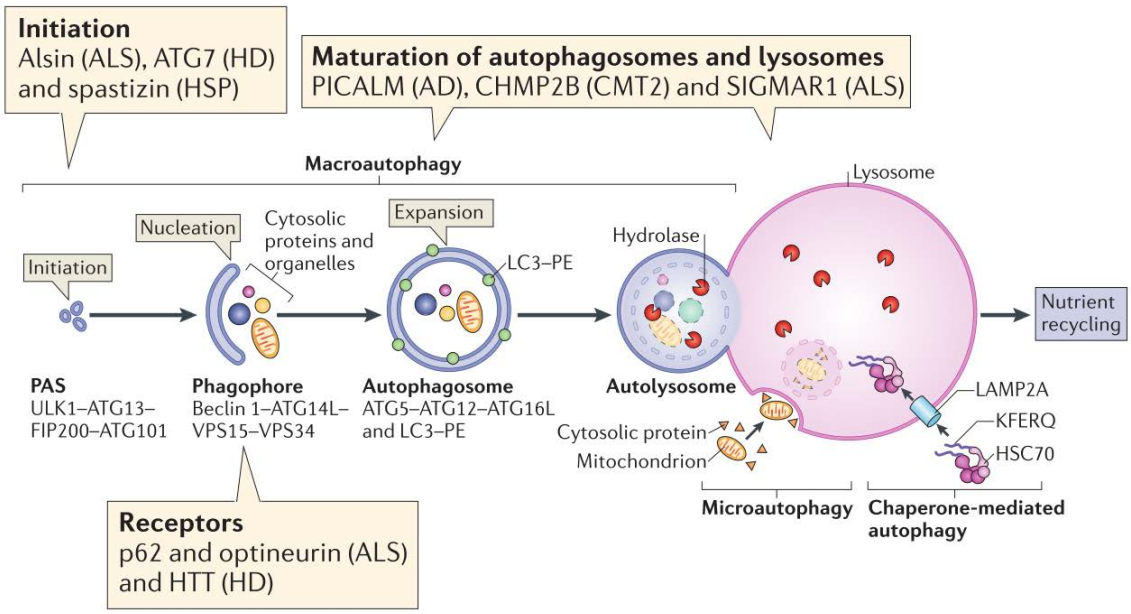

Figure 4: Types of autophagy and molecular processes of the macroautophagy. For the macroautophagy, the initiation and nucleation of autophagosomes needs the activity of the unc-51-like kinase 1 (Ulk1), Beclin1 and VPS34. For its expansion and maturation, autophagy-related protein (Atg)5-Atg12 and the microtubule-associated protein 1 light chain 3 (LC3) are needed in the autophagosome membrane. They will recognize autophagic substrates and will help with the lysosomal fusion. The resulting autophagosome fuses with endocytic and lysosomal vesicles, leading to the autolysosome formation and degrading the cargo. Neurodegenerative diseases are associated with impairments in initiation, nucleation, expansion and fusion, leading to an incorrect autophagosomes formation and blocking the autophagic flux (Modified from Kaur and Debnath 2015 and Menzies, Fleming, and Rubinsztein 2015).

Although is a cell protective mechanism, it has been reported that an overactivation of autophagy can leads to cell death (Joshi and Ryan, 2014; Marino et al., 2014). Although the type of death is fine different, the inhibition of autophagy after ischemia promoted pyramidal neuron survival on neonatal and adult mice (Koike et al., 2008). Surprisingly, the blockage of the initiation of autophagy promotes functional recovery after spinal cord hemisection and avoids apoptotic cell death (Bisicchia et al., 2017; Luo et al., 2017). If we focus on axotomized neurons, the blockage of autophagy is also neuroprotective for the rubrospinal neurons (Bisicchia et al., 2017). The inhibition of the autophagy that is induced after the exposure to human prions reduced the neuronal death provoked by these proteins. This indicates that autophagy induction has some role in neurodegeneration (Moon et al., 2016). Adding controversy, some chemotherapeutic-treated cancer cells activate autophagy to overpass the induced apoptotic death after the treatment.

Atg5 can be cleaved losing its pro-autophagic role and shifting its activity towards cell death induction (Maiuri et al., 2007). Although, Beclin1 has been related with anti-apoptotic effects, when it is cleaved by caspases, its C-terminal enters to mitochondria and sensitize cells to apoptotic signals (Kang et al., 2011b). Therefore, some crosstalk between both cellular processes exists, and cells can modify them to increase its survival possibilities to face up the insult (Maiuri et al., 2007).

4.1.7. Cytoskeleton rearrangement after nerve and during death of MNs

Neuronal cytoskeleton consists in three main polymers: microtubules (MTs), intermediate filaments (IF) and actin microfilaments. They interact forming the cytoskeleton network, which is extended through all the axon and it is an essential structure to connect the central nervous system with the periphery. Cytoskeleton network allows the exchange of information between soma and the end-tip of the axon.

MTs are formed by heterodimers of α- and β-tubulin, and they extend throughout the cell forming a dynamic network. They are essential for neuronal migration, neurite outgrowth, dendritic spine dynamics and for a correct axonal behavior (Kapitein and Hoogenraad, 2015). MTs stability decreases after nerve injury or in some neurodegenerative pathologies such as ALS or Charcot-Marie-Tooth (Almeida-Souza et al., 2011; Dubey et al., 2015). Actin cytoskeleton is constructed by actin monomers (G-actin) and its main function in neurons is to manage the intracellular restructuration to regulate its cell morphology and the internal or external movement (Luo, 2002). IF, from now neurofilaments (NFs), are formed by the polymerization of three polypeptides: NF light (NF-L), medium (NF-M) and heavy (NF-H) subunits (Lee et al., 1993) and they confer mechanical resistance and stability to the cytoskeleton structure.

After axon breakdown MNs undergo cytoskeletal rearrangements (Penas et al., 2011a; Casas et al., 2015). It is described that after MNs suffer a blockage of cytoskeletal transport after RA. This defect can impair a correct organelle distribution and promote MN final death. In this model, the amount of acetylated-tubulin is dramatically reduced, pointing out that MT dynamics are also altered

when the survival of MNs is endangered (Almeida-Souza et al., 2011). Disturbances of actin and MTs are described in different neurodegenerative diseases (Eira et al., 2016). The axonopathy present in AD, Friedreich's Ataxia or ALS is characterized by a "dying back" phenomena and by the loss of MTs (Baas et al., 2016). This phenomenon is based on a progressive axonal degeneration that end-up on the neuronal cell body. Although the underling mechanism is not clearly defined, cytoskeleton rearrangements like disturbance of the dynamics of MTs are described (Dubey et al., 2015). Mutations on tubulin interaction sites are also present in those mouse models characterized by the degeneration of motor axons (Compagnucci et al., 2016) or in postmortem brains from AD patients (Zhang et al., 2015). This event is related with synaptic dysfunction and loss of mature spines (Zempel and Mandelkow, 2015). The stabilization of MTs has proven to block neuronal death (Nahm et al., 2013). Therefore, the dynamic of MTs is a highly controlled process and its imbalance can carry out devastating consequences for neuron survival or its axonal performance (Almeida-Souza et al., 2011). Modulation of MTs stability has also been successful to accelerate axonal growth in the CNS (Ruschel et al., 2015). Therefore, MNs suffer changes on their cytoskeletal dynamics, and these can play a key role to face up with the insult and for axonal regrowth.

Cytoskeletal structures are the railways, meanwhile, the kinesin and dynein motor proteins are the trains that transfer the cargo by anterograde or retrograde transport, respectively (Pareyson et al., 2015). Therefore, motor complexes are also essential for the survival of MNs. The kinesin family is formed by the kinesin-1 (historically named kif5) and the kinesin-3 (KIF1A, KIF1Bα and KIF1Bβ) members (De Vos and Hafezparast, 2017). KIF5c is enriched in MNs (Kanai et al., 2000) and its genetic ablation or spontaneous mutation have been linked with MN diseases and paralysis (Xia et al., 2003; De Vos and Hafezparast, 2017). Moreover, KIF1 aberrations have not been directly linked with any MN disease. Indeed, KIF1Bβ is overrepresented on motoneurons and it is not modified during disease progression (Conforti et al., 2003). Dyneins are a multiprotein-complexes formed by different proteins, being the p150glue (dynactin1-DCNT1) the most present. A dysfunctional dynein/DCTN1 has been used as an ALS mice model. Its mutation causes a defective axonal transport that leads to an ALS-like phenotype and to MNs death (LaMonte et al., 2002; Heiman-Patterson et al., 2015).

4.1.8 Unfolded protein response

Axonal injuries provoke a disruption of the endoplasmic reticulum (ER) homeostasis (Penas et al., 2011a). ER is an organelle present in the eukaryotic cells that forms an interconnected network and it is responsible for protein transduction, folding, post-translation modifications and transport of nascent proteins to different cellular localizations. It also acts as a gatekeeper maintaining the quality of the cell proteins by checking all the newly synthesized proteins. Therefore, ER senses the cell state and any disturbance on its behavior can compromise its functionality and will lead to the accumulation of misfolded proteins. These perturbations will induce ER stress and will activate the ER-overload response (ERO), the ER-associated degradation (ERAD) pathways, or the unfolded protein response (UPR), which is a highly conserved cellular response. ERO is activated when an excessive transport of proteins is detected throughout the membrane of the ER (Kuang et al., 2005), and ERAD marks misfolded proteins and drives their degradation through the ubiquitin–proteasome system (Meusser et al., 2005). Thus, an imbalance between ER capacity to fold proteins and the protein load will induce a coordinated UPR. The Binding immunoglobulin Protein (BiP) is an ER-resident chaperone that is the main sensor of the UPR. In normal conditions, BiP remains bounded to the three major effectors of the UPR: the RNA-activated protein kinase-like ER kinase (PERK), the inositol-requiring protein-1 alpha (IRE1a) and the activating transcription factor-6 alpha (ATF6) (Bertolotti et al., 2000; Sommer and Jarosch, 2002).

One of the UPR branches is the PERK-eIF2α-ATF4 pathway. When BiP unbounds from PERK, it autophosphorylates, homodimerizes and transphosphorylates itself (pPERK) to become active. pPERK directly phosphorylates the alpha subunit of the eukaryotic translation initiation factor 2 α (eIF2α) at Ser51 inhibiting the protein synthesis (Harding et al., 2000b) to reduce the protein load to ER. Although the translation of common proteins is inhibited, some stress-response TFs like the activating transcription factor-4 (ATF4) are increased (Harding et al., 2003) because its mRNA escapes from the translation inhibition (Harding et al., 2000a; Ma and Hendershot, 2003).

The second arm and the most conserved of the UPR is the Ire1α-X-box binding protein 1 (Xbp1) (**Fig. 2**). Ire1 is a highly conserved type I ER transmembrane protein, with a kinase and endoribonuclease domain on its structure. After any disturbance of ER, BiP releases Ire1α, which facilitates the dimerization of its cytosolic portion and leads it to its autophosphorylation (Shamu and Walter, 1996). This turns on the activation of its cytosolic RNase subdomain, conferring RNase activity to IRE1. Its substrate is the mRNA of the X-box binding protein 1 (Xbp-1) transcription factor (TF). After pIRE1a-dependent splicing, Xbp1 mRNA turns active and becomes a strong TF (Sidrauski and Walter, 1997; Yoshida et al., 2001). If the Ire1α branch is chronically active, pIre1α will lead to the phosphorylation of the tumor necrosis factor-a (TNF-α) receptor-associated factor 2 (TRAF2). After this, the JUN N-terminal kinase (JNK) pathway is activated and it will trigger apoptotic cell death (Nishitoh et al., 2002) by different ways: inducing Fas ligand and therefore the extrinsic pathway of caspase 8, inhibiting the anti-apoptotic proteins Bcl-2 and Bcl-xL, or promoting the release of the cytochrome c from mitochondria, which will activate the intrinsic apoptotic pathway (Kharbanda et al. 2000; Tournier et al. 2000; Hite et al. 2009; Faris et al. 2016).

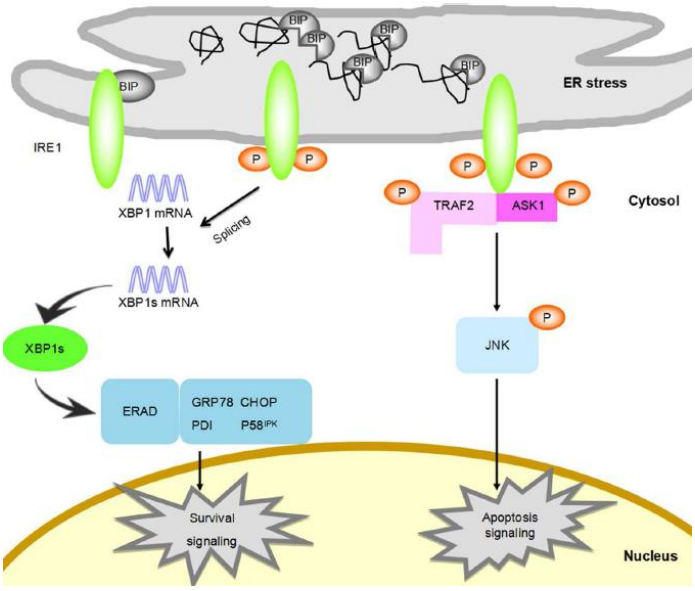

Figure 5: Schematic diagram of the Ire1α branch of the UPR. When BiP detects a high load of unfolded proteins, it dissociates from Ire1α and allows it complete activation. Once active, it acquires endoribonuclease activity. Xbp1 mRNA is cleaved by Ire1, releasing the processed form of Xbp1 (Xbp1s), that will enter to the nucleus and will induce the expression of GRP78, CHOP and other genes. In parallel, the kinase activity of Ire1 will phosphorylates TRAF2-ASK1 complex to finally induce the JNK dependent apoptosis (Xiang et al., 2016).

The third branch of UPR is activated through the ATF6 effector, an unusual basic leucine zipper (bZIP) TF. Under ER-stress, ATF6 is released from BiP and it is translocated to the Golgi apparatus (Chen et al., 2002), where it is cleaved by the

proteases site-1 protease (S1P) and S2P. This process results in the release of a functional and soluble fragment of 50Kd of ATF6 into the cytosol, which migrates to nucleus and induces those genes with an ER stress response element in their promoter (Schröder and Kaufman, 2005).

Those signaling pathways, englobed as UPR, will lead to changes in the gene expression profiles of specific proteins (i.e. chaperones, transcriptional factors) aiming to increase the capacity of cell to correctly fold proteins, enhance misfolded protein clearance or inhibit the protein synthesis (Lindholm et al., 2006). ATF4 induces the expression of genes involved in the response to different stresses like the amino acid deprivation, hypoxia, mitogens, redox alterations and apoptosis (Fels and Koumenis, 2006) and also upregulates the expression of CHOP/GADD153, which is required for the ER-stress mediated apoptosis (Wang et al., 1996). ATF6 will upregulate genes such as BiP, Protein Disulfide Isomerase, GRP94 and Xbp1 (Yoshida et al., 2000; Chen et al., 2016), enhancing cell ability to correctly fold proteins. This Xbp1 upregulation will increase the UPR response, acting as a positive feed-back. Once in the nucleus, Xbp1 protein upregulates a set of core genes involved in protein transportation, ERAD and other cell functions. Thus, Xbp1 increases gene expression in a condition-specific way forming a transcriptional regulatory network that is expanded in response to ER stress (Acosta-Alvear et al., 2007).

Neurons are one of the most sensitive type of cells to misfolded proteins. The UPR signaling has been involved in several neurodegenerative diseases such as ALS, AD or AD (Taylor et al., 2002) and it is triggered after nerve injury (Hu et al., 2012) (**Fig. 6**). An alteration on the ER distribution and morphology in the axonal compartment has been also observed in neurodegenerative diseases (Shaohua Li et al. 2013). Although unknown, an unresolved stress of ER can be the responsible of neuronal death progression during neurodegeneration. UPR has been described as an endogenous protective mechanism of cell but its activation can also promote cell apoptotic death (Liu et al., 2013b). I.e., the PERK axis has pro or anti-apoptotic abilities (Li et al., 2013a). Although initially was thought that any disturbance on the ER will trigger a complete UPR response, recent evidences shown that the coordinate co-activation of the three branches is not mandatory. In fact, CHOP blockage or Xbp1 s overexpression increased neuron survival after nerve injury,

which indicates that the UPR branches had different roles on neuron destiny (Hu et al., 2012). When the survival of MN is compromised after RA, Xbp1s and ATF4 are also present (Penas et al., 2011a).

The way through which the neurons trigger UPR after injury remains unelucidated. In fact, misfolded proteins are not detected in the axonal ER after injury (Hu, 2016). It is plausible that ER stress present in the neuronal soma is either induced by a retrograde signal from the axon, or that it is triggered at axonal level and subsequently translocated to the neuronal soma. ER is the major Ca^{2+} storage of the cell, and the injury provokes a wave of increased levels of axoplasmic Ca^{2+} towards the soma. This Ca^{2+} will provoke ER disturbance and the consequent UPR response, which can be linked with neuronal death (Li et al., 2013a). Indeed, Ca^{2+} can activate PERK, and therefore triggering UPR at axon or at soma after nerve injury (Bollo et al., 2010). Another developed hypothesis is that UPR is independently triggered on axon and soma. Xbp1 mRNA is present at the neurites and its spliced form is retrogradely translocated to the soma (Hayashi et al., 2007). BiP and CHOP are upregulated at axon and retrogradely transported after nerve injury (Valenzuela et al., 2016). The distal axotomy of the sciatic nerve increases Xbp1 splicing and the expression of BiP and ATF4 within the soma of MNs (Penas et al., 2011a). Therefore, the UPR is present after axonal injury. Hetz and colleagues also showed that Xbp1 splicing is increased after nerve injury, and that it is essential for nerve regeneration after nerve crush (Oñate et al., 2016). Moreover, ATF6 has a pro-regenerative role on axonal growth, meanwhile ATF4 has no function on it (Valenzuela et al., 2016).

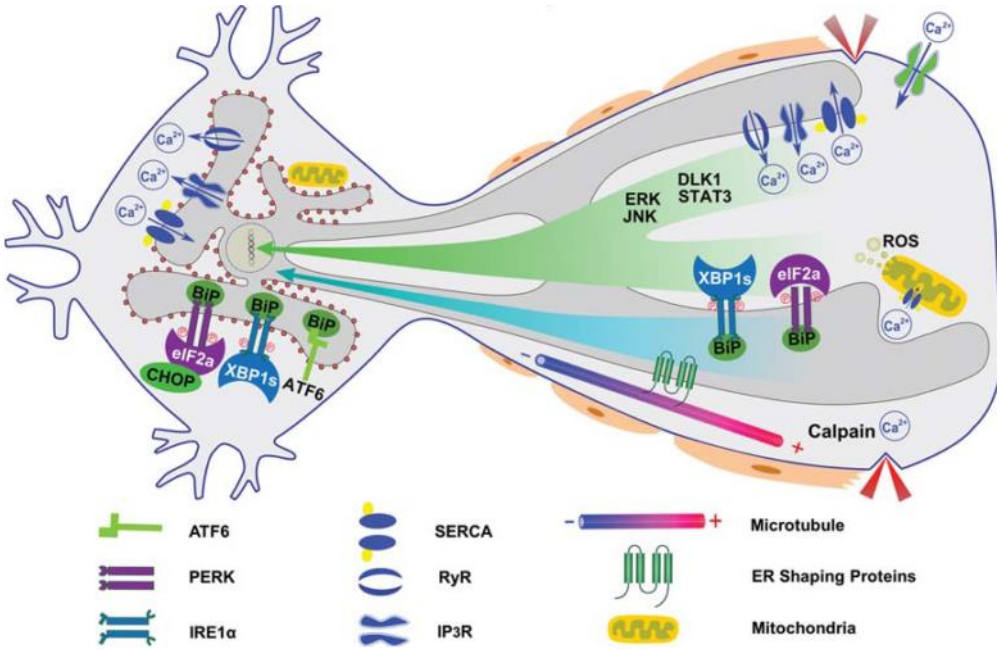

Figure 6: UPR initiation and its propagation after axonal injury. ER is localized within the neuronal soma, and it continues throughout the axon. ER stress can be induced directly after the disruption of the ER network by the axonal injury. ER stress can also be induced by retrogradely-transported signals such as: i) the entrance of Ca2+ at the axoplasm after injury, which will disrupt the ER Ca2+ homeostasis and will induce UPR at soma, ii) those signaling associated with the injury such as ERK, JNK and STAT3, or iii) the ER stress mediators that are induced at axonal level such as the splicing of Xbp1, phosphorylation of Eif2α or BiP (Extracted from Li et al., 2013a).

4.2 Glial reaction

The non-neuronal cells that surround the MNs in ALS are able to modify the animal outcome, indicating that neuron behavior in the CNS can be altered by external inputs (Clement et al., 2003). After axonal damage, the environment that surrounds the axotomized neurons suffers morphological changes to remodel the scenario favoring the formation of new circuitries. These changes, that are the displacement of presynaptic terminals and neurite retraction, are driven by glial cells (astroglia and microglia) (Aldskogius et al., 1999). Several compounds like free radicals, cytokines (i.e. Interleukins (IL)), chemokines and amino acids are released, and they will trigger an inflammatory response (Olsson et al., 2005). Moreover, some caspases can cleavage interleukins such as IL-1β and induced the inflammatory response (Man and Kanneganti, 2016).

Consequent with the insult, microglia modifies its morphology and its gene expression, adopts an amoeboid morphology, proliferates and increases its phagocytic activity (Greenhalgh and David, 2014). The inflammatory reaction mediated by microglia has a beneficial roles, which are clear the debris to set the stage for future remodeling (Mueller et al., 2016), sustain neuron survival (Colonna and Butovsky, 2017) or support the new-born neurons (Song et al., 2016). On the other side, microglia can trigger neuron death by phagocytosis of the vulnerable neurons or by the release of pro-inflammatory molecules (nitric oxide, glutamate, IL-1β or TNFα), which will avert any functional recovery (Qu et al., 2012; Brown and Vilalta, 2015).

Although not correctly, microglia phenotypes are classified as M1 or M2 (**Fig. 7**), being pro- or anti-inflammatory, respectively (Martinez and Gordon, 2014). This classification is based on their surface receptors and their specialized functions, and it depends on its interactions with environment and with neighbor cells (neurons, astrocytes, oligodendrocytes and external macrophages) (Lan et al., 2017). The M1 is linked with proinflammatory, oxidative and cytotoxic cascades that cause the progression of neurodegenerative diseases, neuron death and functional impairment. M1 microglia is characterized by the secretion of interleukins such as IL-1β and TNFα, or by surface receptors like the major histocompatibility complex II or the Cluster of Differentiation-86 (CD86). The microglial-mediated release of compounds promote a decline of MNs after trauma on in ALS, and it is also related with the neuronal death after viral infection (Loane and Byrnes, 2010; Frakes et al., 2014; Verma et al., 2016). The inhibition of its pro-cytotoxic activity slows the progression of neurodegenerative diseases (Olmos-Alonso et al., 2016; Tang and Le, 2016). IL-1β directly activates apoptotic pathways on neurons to promote their death *in vitro* (Fankhauser et al., 2000) or after SCI (Wang et al., 2005). Although microglial activation can be driven by several modulators, a master protein of it is the nuclear factor kappa-light-chain-enhancer of activated B cells (NF-κB) (Lan et al., 2017). Specific microglial activation by NF-κB has been directly linked with its neurotoxic effects towards MNs in ALS disease (Frakes et al., 2014; Wachholz et al., 2016).

M2 phenotype, which is related with tissue remodulation and debris clearance, is characterized by IL4 secretion or by the surface receptor CD206 (Lan et al., 2017). The promotion of a M2 environment by the external treatment of IL4 reduced the harmful effect of inflammation after spinal cord injury and reduced the consequent functional impairment (Francos-Quijorna et al., 2016). In accordance, a more anti-inflammatory phenotype rescues neurons from death *in vitro* (Zhao et al., 2006) and after nerve injury (Villacampa et al., 2015). M2 microglia also releases neurotrophic factors to sustain neuron viability (Tang and Le, 2016).

Axotomy-induced microglial response is an extrinsic factor than raises neuronal death (Kobayashi et al., 2015) and that has an important role on neuropathic pain apparition (Guan et al., 2015) and maintenance after nerve injury (To et al., 2013).

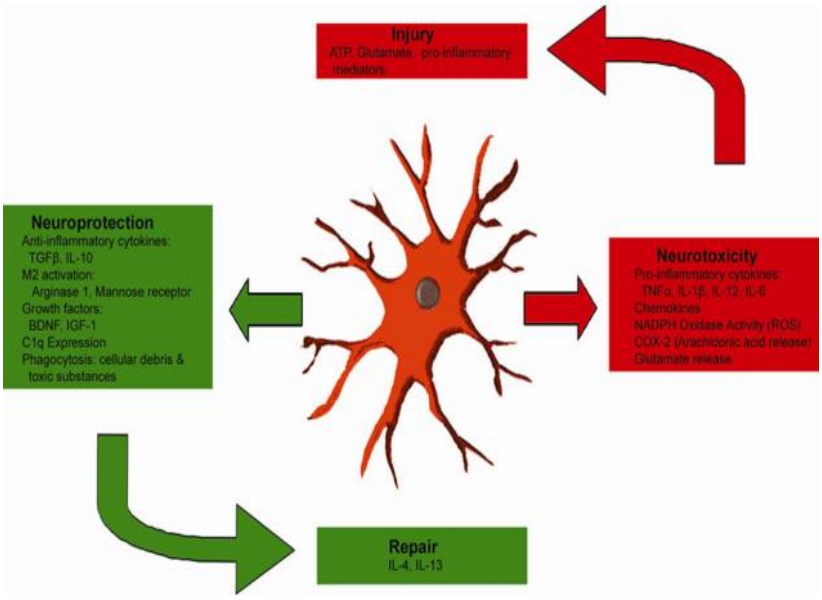

Figure 7: Microglial phenotypes. M1 is characterized by the release of pro-inflammatory cytokines such as TNFα and IL-1β, and it is related with an exacerbation of the injury and neurotoxicity. M2 releases anti-inflammatory compounds such as IL-10, exerts neuroprotection and favors neuronal repair (Extracted from Loane and Byrnes 2010).

Astrocytes migrate toward the affected zone within days post injury. They form the glial scar and encapsulate the affected zone by the release of ECM compounds to avoid the flux of pro-death or inflammatory compounds (Silver and Miller, 2004; Silver et al., 2014). Among the released compounds, the chondroitin sulfate proteoglycans (CSPGs) are a well-described inhibitor of the spontaneous axonal regrowth. Astrocytes can be activated by reactive microglia, becoming pro-cytotoxic astrocytes (termed as A1-like). When they become reactive, they can release factors that will promote neuron death (Bi et al., 2013). Recently, it was

described that they can provoke the death of axotomized neurons (Liddelow et al., 2017). Reactive astrocytes can also acquire a more pro-survival phenotype for the neurons (termed as A2-like by Liddelow et al. 2017), which can exerts neuroprotection after spinal cord injury (Faulkner, 2004; Okada et al., 2006).

4.3. Sirtuins in the nervous system

Cell metabolism contains a high amount of functions related with cell behavior that are directed by enzymatic processes. Some of these functions are modulated by the level acetylation state of proteins (McCarty and McCarty Kenneth S., 1974). This enzymatic process manages several cellular functions, from the activity of a specific protein to the epigenetic program of the whole cell. The acetylation balance is a dynamic and highly controlled process directed by two enzymatic families: the histone deacetylases (HDACs) and the histone aceyltransferases (HATs).HDACs family is composed by four classical subfamilies: class I, IIa, IIb, III and IV. (Haberland et al., 2009). Regarding the class III family, the Silent Information Regulator 2 (Sir2) was its first discovered member, and it was found out in the yeast *Saccharomyces cerevisae* (Klar et al., 1979). After this, the family was re-named as Sirtuin and it was described in several species such as bacteria, yeast, plants and humans. This figures out the conservation of this family during evolution (Ramadori and Coppari, 2010). Seven SIR2's orthologues have been described in mammals (SIRT1-7) (**Fig. 8**). They vary in their tissue expression, subcellular localization and enzymatic activity, but they share a conserved catalytic core. Although they were initially described only as deacetylase enzymes, few years ago was discovered that some of them are also able to modify proteins by ADP-ribosyltransferase activity (Frye, 1999; Tanny et al., 1999).

Sirtuin	Activity	Localization	Substrates and/or targets	Function
SIRT1	Deacetylase	Nucleus	H3K9, H3K56, H4K16, H1K26, SUV39H1, p300 and PCAF	Chromatin regulation and transcription
			HDAC1, PARP1, p53, KU70, NBS1, E2F1, RB, XPA, WRN, survivin, β-catenin, MYC, NF-κB and TOPBP1	DNA repair and cell survival
			PGC1α, FOXO1, FOXO3A, FOXA2, CRCT1, CRCT2, PPARα, PPARγ, LXR, FXR, RARβ, SREBP1C, SREBP2, HNF4α, HIF1α, HIF2α, CREB, NKX2-1, STAT3, TFAM, MYOD, NHLH2, UCP2, TSC2, eNOS, LKB1, SMAD7, AKT, ATG5, ATG7, ATG8, 14-3-3ζ, PGAM1, ACECS1, PTP1B and S6K1	Metabolism
SIRT2	Deacetylase	Cytoplasm	Tubulin, keratin 8, PAR3 and PRLR	Differentiation
			G6PD, LDH, PEPCK1, ACLY, MEK1, ITPK1, S6K1 and PGAM	Metabolism
		Nucleus	H4K16, H3K56, H3K18, CDC20, APC/C, CDK9 and BUBR1	Cell cycle
			FOXO1, FOXO3A, p300, NF-κB and HIF1α	Metabolism
SIRT3	Deacetylase	Mitochondria	LCAD, VLCAD, HMGCS2, NDUFA9, SKP2, SDHA, ACECS2, GDH, IDH2, MRPL10, PDP1, SOD2, OTC, CYPD, OPA1, PDH, FOXO3 and GOT2	Metabolism
SIRT4	• ADP-ribosylase • Lipoamidase • Deacetylase	Mitochondria	GDH, IDE, SLC25A5, PDH and MCD	Metabolism
SIRT5	• Deacylase • Deacetylase	Mitochondria	CPS1, HMGCS2, PDH, SDH, SOD1 and GAPDH	Metabolism
SIRT6	• Deacylase • Deacetylase • ADP-ribosylase	Nucleus	H3K9, H3K56, CtIP, GCN5, SNF2H, G3BP, FOXO3 and PARP1	Chromatin and DNA repair
			MYC, HIF1α, NF-κB, TNF, SREBP1, SREBP2 and USP10	Metabolism
SIRT7	Deacetylase	Nucleus	MYC, H3K18, PAF53, HIF1α, HIF2α, ELK4, RNA Pol I, MYBBP1A, TFIIIC2 and p53	Transcription
			mTOR, DCAF1, DDB1, CUL4B and GABPβ1	Metabolism

Figure 8: Table summing up of the different SIRTs (1-7), its cellular sub-localization (cytoplasm, nucleus and mitochondria), its different activities and their targets (Extracted from Chalkiadaki and Guarente 2015).

Besides the direct modulation of several proteins through deacetylation processes, the acetylation state of histones can determine other cellular processes by epigenetic changes. Transcriptional dysfunction, a common hallmark of neurodegenerative diseases, is characterized by aberrations on the molecular machinery that orchestrates gene expression through epigenetic marks (Lazo-Gómez et al., 2013). The epigenetic mechanisms of methylation and acetylation regulate the chromatin stability, and therefore, the repair, replication and transcription of DNA. These modifications are important for chromosome integrity, cellular differentiation, development and aging. During last years, this genome editing has been detected in post-mortem samples from ALS and Huntington's disease patients (HD) (Figueroa-Romero et al., 2012; Francelle et al., 2017). The

enforced methylation of DNA has been linked with MN death in ALS and the hyperacetylation of histone with the death of dopaminergic neurons (Chestnut et al., 2011; Jin et al., 2014).

4.3.1 Role of Sirtuin 1 in neurodegeneration

Sirtuin 1 (SIRT1), due to its ability to extend lifespan in several models and for being the closest homolog of Sir2 protein of yeast, is the most widely described. Although it was initially described as a nuclear protein (Michishita et al., 2005), a few years ago it was found at cytoplasm instead of at nucleus, indicating that it has different substrates depending on its subcellular localization (Stünkel et al., 2007). Nowadays, SIRT1 is pointed to have some role on energy expenditure and therefore on mitochondrial-genes expression (Canto et al., 2009). It is the most widely studied due its role in caloric restriction, lifespan expansion, metabolic homeostasis, genomic stability and prevention of aging-related diseases (Vaquero, 2009; Houtkooper et al., 2012). Accumulating evidence shows that SIRT1 orchestrates several functions at neuron level through its deacetylase activity towards histones (Histone3) (Imai et al., 2000), p53 (Luo et al., 2001a), and other like NF-κB, cAMP response element binging (CREB), PARP1, and FOXOs (Houtkooper et al., 2012) (**Fig. 9**).

SIRT1 activity induces p53 deacetylation to avoid apoptotic cell death (Luo et al., 2001a; Vaziri et al., 2001) and neurodegeneration (Hasegawa and Yoshikawa, 2008). Moreover, SIRT1 activity directly represses FOXO1, 3 and 4 (Motta et al., 2004), which are highly related with metabolism of lipids and glucose, and also with cell response to stress (Houtkooper et al., 2012). There is some controversy about the biological significance of FOXOs regulation by SIRT1. Published studies showed that SIRT1 activity towards FOXOs inhibits them, which leads the cell towards cycle arrest and survival, getting it away from apoptosis initiation (Maria E. Giannakou and Linda Partridge, 2004). On the other side, in the *C. Elegans in vivo* model, SIRT1 promoted FOXO activation and extended its lifespan through an improved mitochondrial function (Mouchiroud et al., 2013). So, depending on the cell state, SIRT1 selectively deacetylates FOXOs and drives its activity, giving other layer to their transcriptional activity (Brunet et al., 2004).

Other key target of SIRT1 activity is the CREB TF, which is highly related with glucose homeostasis, learning, memory and growth-factors mediated cell survival (Mayr and Montminy, 2001). CREB is activated by phosphorylation on the residue Ser-133, and then exerts neuronal survival through specific gene expression (Finkbeiner, 2000). Recently, SIRT1 activity has been related with the activation of the transcriptional axis of CREB and this promoted neuroprotection in Huntington disease (HD) model (Jeong et al., 2012).

SIRT1 Gain-of-Function, using transgenic mice or the sirtuin-activating compounds (STACs), demonstrated protection in different neurodegenerative diseases such as ALS, AD and HD (Kim et al., 2007; Jiang et al., 2012; Watanabe et al., 2014). Regarding the cellular response after axonal injury, SIRT1 activity demonstrated a positive neurite-growth effect through the inhibition of mTOR pathway in cell culture (Guo et al., 2011). Specifically, axonal and cytosolic presence of SIRT1 has been related with neurite elongation (Sugino et al., 2010; Li et al., 2013c).

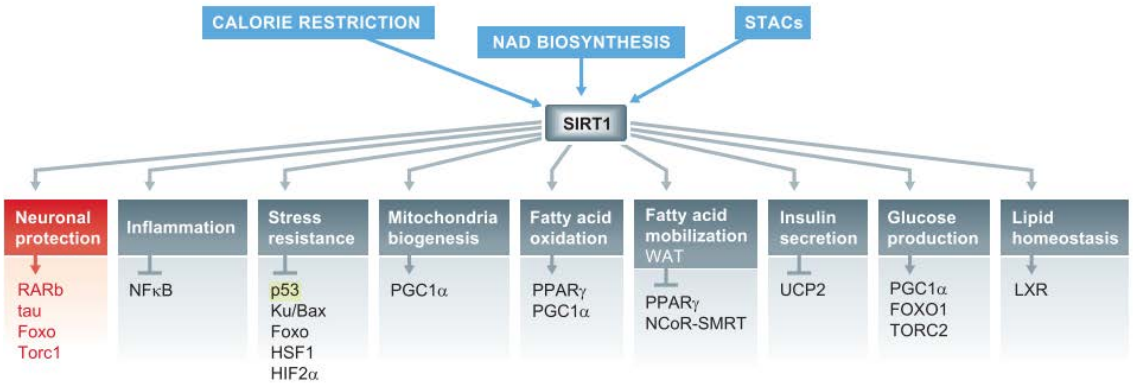

Figure 9: SIRT1 deacetylates several proteins and it can exert different functions. SIRT1 can be active through different ways and it will exert neuroprotection, will reduce inflammation or will promote other important functions for cell behavior (Extracted from Donmez and Outeiro 2013).

4.3.2 Sirtuin 2 in neurodegeneration

After SIRT1, the SIRT2 has recently emerged as a new player in the cancer and neurodegeneration fields. SIRT2 is ubiquitously expressed throughout all the tissues, being higher in brain regions such as cortex, spinal cord and others (Gomes

et al., 2015). Moreover, it is the mainly sirtuin of the cytoplasm, and it normally interacts with microtubules, being the α-tubulin the main target of its deacetylase activity (North et al., 2003). Furthermore, SIRT2 is translocated to the nucleus during mitosis and it actively deacetylates the Histone H4 (Vaquero et al., 2006). The SIRT2 activity is also related with the modulation of FOXOs and NF-κB, which points out that there is interplay between SIRT2 and SIRT1 (Donmez and Outeiro, 2013).

A recent report suggested the role of SIRT2 in inflammation. SIRT2 regulates the pro-inflammatory gene expression that is mediated by NF-κB. SIRT2deacetylates the p65 subunit of NF-κB at Lys-310, gathering its activity and reducing the inflammatory response (Rothgiesser et al., 2010) (**Fig. 10**). The SIRT2 ablation is also linked with NF-κB hyperacetylation, exacerbated microglial activation, increased pro-inflammatory cytokines and the collagen-induced arthritis (Lin et al., 2013; Pais et al., 2013). The inhibition of SIRT2 also increases the cerebral edema formation after traumatic brain injury by an overactivation of NF-κB (Yuan et al., 2016). When SIRT2 is overexpressed in those *in vitro* or *in vivo* models that characterized by a marked inflammatory reaction, the production of reactive oxidant species (ROS) and pro-inflammatory cytokines is reduced, which indicates its anti-inflammatory role (Kim et al., 2013).

SIRT2 is accumulated in brains and spinal cords from old mice (Maxwell et al., 2011) and its overexpression in neuron culture induces apoptotic death (Pfister et al., 2008). Results until now figure out that SIRT1 and SIRT2 have opposite roles in neuron death (Donmez and Outeiro, 2013), although their role in neurodegenerative diseases remains poorly understood. The ablation of SIRT2 activity by a specific inhibitors yielded neuroprotection *in vitro* and *in vivo* in PD models (Outeiro et al., 2007; Chen et al., 2015b) or in a HD mouse model (Chopra et al., 2012). Controversially, the same inhibitor was not able to expand the lifespan of the ALS mice (Chen et al., 2015b), although SIRT2 is upregulated in the spinal cord of SOD1 mutant mouse during the progression of the pathology (Valle et al., 2014). Moreover, the treatment with the SIRT2 inhibitor AK7 impaired the hippocampal functions (Jung et al., 2016), indicating a positive role of SIRT2 in neuronal behavior. SIRT2 activity is also important for a correct myelin sheath formation and it concedes resistance to the axonal degeneration that characterizes the WldS mice

(Suzuki and Koike, 2007; Beirowski et al., 2011). Thus, the exact role of SIRT2 in neuronal and axonal behavior after injury remains elusive.

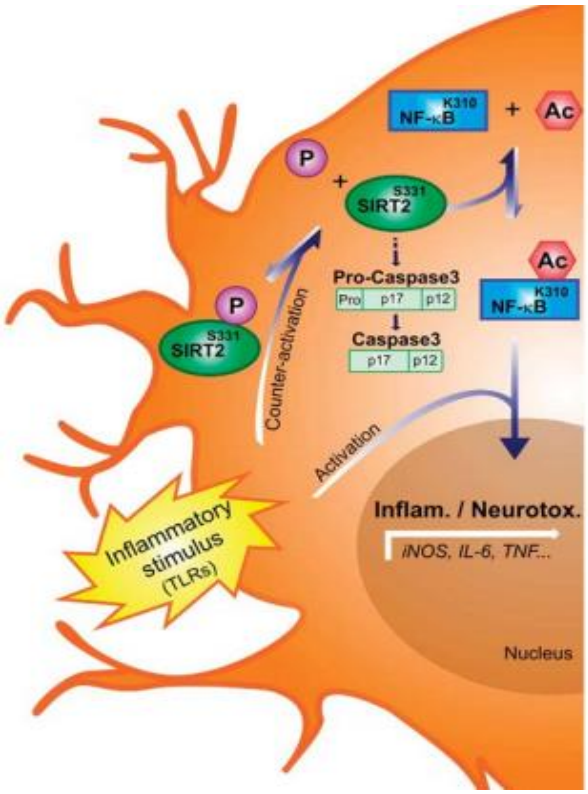

Figure 10: SIRT2 orchestrates the pro-inflammatory response of microglia. Upon inflammatory stimulus, SIRT2 is dephosphorylated, which turns on an increase on its deacetylases activity. Therefore, SIRT2 directly deacetylates the p65 subunit of NF-κB, leading to the reduction the pro-inflammatory gene expression that depends of NF-κB (Pais et al., 2013).

4.4 Intrinsic pathways of axonal regeneration

Mammal's neurons have the intrinsic capability to replace and repair the not useful axons by regeneration, keeping an optimal nervous system throughout lifetime. Nerve disconnection will trigger the degeneration of the distal nerve stump through a mechanism know as Wallerian degeneration (Waller, 1850). This reaction is characterized by a progressive degeneration of the axon and by the change of the molecular programs of the affected neurons. This change is known as axonal reaction and chromatolysis (explained previously). Once the neuron gets over the insult, it must reextend its axon until target organ. Several factors will determine an efficient functional recovery after nerve injury: a rapid shift towards a pro-regenerative phenotype, the activation of neurite elongation pathways, the distance upon target approach and an effective synapse rebuilding. Different pathways are postulated to increase nerve regeneration (Tedeschi, 2012). Hereinafter, we will discuss one of the most common molecular pathways that are activated in neurons to increase the velocity of axonal re-growth.

Nowadays, the most studied pathway that directs axonal growth is the PI3K/AKT molecular network. Neurotrophic factors bind to the Tyrosine kinase receptors, which activate PI3K and consequently AKT (Caporali et al., 2008). The activation of this pathway culminates with mTOR and its role in transduction. PI3K is very sensitive to the phosphatase and tensin homologue (PTEN), which can blocks PI3K and reduce the axis power (Berry et al., 2016). Several approaches like PTEN deletion (Park et al., 2008) or its pharmacological inhibition (Ohtake et al., 2014) raised axonal re-growth after nervous system injury. Nevertheless, the suppression of PTEN activity has no clinical translation due to its tumor-suppressor role (Tolkacheva and Chan, 2000).

If the PTEN step is overpassed, AKT will become active and will phosphorylate mTOR. In spite that several phosphorylation residues have been identified on the three isoforms of AKT, the Ser 473 one is highly correlated with axonal growth and mTOR activation in different publications, suggesting an intrinsic relationship between AKT/mTOR axis and axonal elongation (Ransome and Turnley, 2008; Rahman and Haugh, 2017). mTOR is also able to phosphorylate AKT at the same residue. This indicates a highly regulated molecular circuitries for axonal regeneration (Blenis, 2004). Although there are no studies performed in adult MNs, mTOR kinase activity has been linked with axonal growth in sensory neurons (Leibinger et al., 2012; Duan et al., 2015). mTOR kinase activity, through the activation of the 70-kDa ribosomal protein S6 kinase (p70s6k), leads to an increase of cell growth and protein synthesis (Blenis, 2004; Magnuson et al., 2012).

Concurrently, the activity of AKT inhibits FOXOs by direct phosphorialtion (Brunet et al., 1999). At this point, some discrepancies arise. The homologue of FOXOs in *C. Elegans* organism is the *daf-16* TF. Its activity extends lifespan, avoids nerve degeneration and enhances nerve growth in worms (Kenyon et al., 1993; Calixto et al., 2012; Byrne et al., 2014). Thus, its activity increases axonal growh and the *daf-18* (PTEN in mammals) blocks this effect. Curiously, the receptor *daf-2* (the homologue of IGF1 receptor), which improves nerve growth on mammal models through the PI3K/AKT axis activation, inhibits *daf*-16 and also blocks its pro-regenerative effect (Byrne et al., 2014). Nowadays, regarding the regrowth of mammal axons, no studies describe the exact role of FOXOs on it, but the

publications suggest that the phosphorylation of FOXO1 and 3 by AKT avoids its entrance to nucleus (Brunet et al., 1999; Caporali et al., 2008). This reduces FOXOs transcriptional activity. Moreover, the activation of PI3K/AKT by neurotrophic factors holds the FOXO1 at the cytoplasm repressing its gene expression (Gan et al., 2005). Therefore, the role of FOXOs on regeneration of mammalian axons remains unknown.

5. Therapy for peripheral nerve lesions

The complete motor functional recovery after nerve injury require four main steps: i) sustain survival of axotomized motoneurons; ii) promote axonal regrowth across the glial scar formed at the ventral-root intermediate zone; iii) enhance axonal elongation through the degenerated distal nerve stump until the target muscle; iv) establish functional connections to denervated muscle and prevent muscle atrophy. After PNL, the injured neurons counteract the insult by triggering endogenous neuroprotective mechanisms to switch from neurotransmission state to a pro-regenerative one (Casas et al., 2015). Once the neurons survive against the injury, they need to extend their axon through the distal stump. To favor a more pro-regenerative environment, the distal stump of the nerve will suffer Wallerian degeneration to set the stage for axonal regrowth. The last step for a correct recovery is a properly growth of the regenerated axon towards the target organ and the rebuild of a functional synapse with it. Besides this, the final outcome will depend on other factors such as the patient's age, the type of lesion, the distance between the injury and the target organs, and the delay and the type of surgical repair (Navarro et al., 2007).

5.1 Actual therapies to promote MN survival

Several therapeutically approximations to sustain MNs viability after RA have been described (**Table 2**). Although survival of MNs is achieved, it translation to the human healthcare has never been performed. For example, the Pre084 compound is a good neuroprotectant, but its systemic treatment induced the apparition of neuropathic pain, averting its clinical application (Roh et al., 2011; Pyun et al., 2014). Other compounds are also able to maintain MN survival, but its

ability to enhance nerve regeneration has never been analyzed. Only Riluzole, Lithium and an inhibitor of the proteoglycan receptor (ISP) have been tested in a model of RA combined with immediate reimplantation of roots, showing MN preservation and a slightly effect on nerve regeneration. Nevertheless, their effects on functional recovery can be mediated by the increase on MN survival and not by a specific effect on axonal regeneration.

Table 2. Published therapies to sustain MN survival in different RA models.

Drug	Model	Ref
Riluzole	Spinal Root Avulsion + Reimplantation	(Nogradi and Vrbova, 2001) (Pintér et al., 2010)
Glatiramer acetate	Spinal Root Avulsion	(Scorisa et al., 2009)
GM-1 Ganglioside	Spinal Root Avulsion	(Oliveira and Langone, 2000)
Pre084	Spinal Root Avulsion	(Penas et al., 2011b)
Cerebrolysin	Spinal Root Avulsion	(Haninec et al., 2003)
Valproic acid	Spinal Root Avulsion	(Wu et al., 2013)
Minocycline	Spinal Root Avulsion	(Chin et al., 2017)
Phorbol-12-myristate-13-acetate	Spinal Root Avulsion	(Zhao et al., 2012)
N-Acetyl-cysteine	Spinal Root Avulsion	(Zhang et al., 2005)
Lithium	Spinal Root Avulsion + Reimplantation	(Fang et al., 2016)
Erythropoietin	Spinal Root Avulsion	(Noguchi et al., 2015)
ISP (Intracellular Sigma Peptide)	Spinal Root Avulsion + Reimplantation	(Li et al., 2015)
Paclitaxel	Spinal Root Avulsion	(Sim et al., 2015)
Vitamin E	Facial nerve avulsion	(Hoshida et al., 2009)
BDNF+GDNF	Facial nerve avulsion	(Blits et al., 2004)
Pregabalin	Facial nerve avulsion	(Moriya et al., 2017)
T-588 (derivative of acetylcholine)	Facial nerve avulsion	(Ikeda et al., 2003)
Nitroarginine (NOS inhibitor)	Facial nerve avulsion	(Wu et al., 2003)
Ro5-48654	Facial nerve avulsion	(Mills et al., 2008)
Riluzole + GDNF	Spinal Root Avulsion + Reimplantation	(Bergerot et al., 2004)

5.2 Actual strategies to promote regeneration

Nowadays and in the best scenario, only 10 % of the axons will regenerate until target organs after a nerve transection (Janjic and Gorantla, 2017). The “gold standard” clinical treatment, when direct suture between stumps cannot be achieved, is the nerve grafting, which can be from the same patient (autograft) or from a donor (allograft) (Glaus et al., 2011). Nowadays, to avoid the use of allografts, conductive tubes based in chitosan (Meyer et al., 2016) or in cell therapy are used, but the functional recovery is slightly increased (Georgiou et al., 2015). Therefore,

once the PNL is repaired, a co-adjuvant therapy is needed to enhance nerve regeneration, reduce muscle atrophy and suppress the functional impairments. Neurotherapeutic approaches to increase nerve regeneration such as FK506, Geldanamycin, N-acetylcysteine, acetyl-L-carnitine, IGF1 and Chondroitinase ABC are described (Navarro et al., 2001; Welin et al., 2009; Sun et al., 2012; Farahpour and Ghayour, 2014; Kostereva et al., 2016). On the other side, treatment with neurotrophic factors like BDNF and NGF, or stem cell therapy are also described in literature to enhance nerve regeneration (Janjic and Gorantla, 2017). Although they promoted an increase on the regenerative rate of the nerve after PNL, their clinical translation is not performed. Fk-506 has immunosuppressant effects, impairing its administration to humans for PNL. On the other side, neurotrophic factors can induced tumorigenesis, promoting the formation of neuroma and blocking a correct nerve regeneration due to the "candy-store effect" (Tannemaat et al., 2008). So, a co-adjuvant therapy to enhance nerve regeneration is needed to reduce the functional impairments after a PNL.

6 New strategies for drug discovery

To develop new therapies, different approximations can be performed. Them go from new drug discovery to the unravelling of new indications for the pre-existing drugs. Hereinafter, we will focus in one that is based on Systems biology and drug repurposing.

6.1 Systems biology and artificial neural networks

During last decades, the high amount of information related with proteins state and their interactions, and the genome-sequencing; have delivered a massive knowledge about genes and genes products present in most of the organisms, including humans, and how them modify cell behavior. If we take this information alone, we only observe the cell physiology through a very small window, and we lose those key points by which the biological systems combine many discrete functions for a correct functionality. From this idea was born the network analysis, which is based in the mathematical analyze of a circuit composed by different interconnected components. Thus, network analysis, instead of molecular biology, is useful to

elucidate the intricate connections that form the biological systems and how they are disturbed in disease conditions (Barabási, 2007). Several subtypes of molecular networks can be performed based on: RNA, gene-regulatory, protein-protein interactions (PPI) and metabolic information (Barabási et al., 2011b). From this holistic point of view was born the Systems Biology approach, which main goal is the integration of the biological information obtained from experimental and computational studies (Kitano, 2002). Systems biology has delivered a huge information about human diseases, from those monogenic to the oligogenic (Zanzoni et al., 2009) and for complex diseases such as diabetes or chronic lung obstruction (Jain et al., 2013; Najafi et al., 2014)

System biology has opened a new gate of opportunities to find new therapeutic targets and new drug treatments. During last years, the "single-drug, single-target" paradigm has reached its limits. Currently, instead of modulating a single protein that can have a dual role in determined pathology (i.e. p53 on cancer disease), we need to shift the whole cell network taking into consideration the cell intrinsic pathways and its environmental context (Barabási and Oltvai, 2004; Jaeger and Aloy, 2012). In the same way, the deletion of an specific protein or gene can affect the whole cell behavior being even more harmful (Jeong et al., 2001). Thus, we need to treat the network instead of a single target. This strategy also gives information about new mechanistic actions, toxicity and sided effects of new and old drugs (Berger and Iyengar, 2009). For example, systems biology has been useful to find a new drug combination to treat an incurable pancreatic adenocarcinoma (Azmi et al., 2010).

Artificial neural networks (ANNs) are computational models that share similarities with the interconnections of neurons in the brain. Basically, each neuron receives inputs from several axons and if the income information reaches an specific threshold, neuron is depolarized and fires (Presnell and Cohen, 1993). ANN acts as a black box, it learns from complex dynamics states and it is able to theoretically predict the characteristics of an output after a properly-detailed input (Arce-Medina and Paz-Paredes, 2009). The combination of ANNs with System biology can be a useful approach to characterize complex pathologies and to discover new therapeutic treatments with reduced side effects.

6.1 Drug repurposing

The discovery of new drugs, its production and its translation to human healthcare takes several years and sources (Li and Jones, 2012). Therefore, take advantage of the pre-existing drugs for human therapy has raised interest during last years. Intriguingly, although it is thought that a specific drug has a single target, once it reaches the organism it will interact with at least two different proteins (its described target and the enzyme that metabolizes its degradation). Indeed, it is described that a single drug interacts with a mean of 6 different targets (Mestres et al., 2009). The concept of drug repurposing arises from the idea of take benefit from the side effects of traditional drugs, from which the safety, pharmacokinetics and pharmacodynamics are well established in humans. Therefore, the drug repurposing reduces drastically the timelines between the animal experimental studies and the toxicity and efficacy assays in human (Ashburn and Thor, 2004).

Several strategies for drug repurposing are reported in literature. They range from a rational discovery of its repurposing capability (i.e. the drug is able to modify a target or pathway relevant in other disease) to an unexpected side effects found in clinical trials (Li and Jones, 2012). The first evidence of drug repurposing was carried out with the Thalidomide, a drug that caused several skeletal defects in new-borns. Although drug was banned in the market, few years later it was rediscovered as treatment for *erythema nodosum leprosum* due to its blockage of TNFα action (Ashburn and Thor, 2004). Since then, drug repositioning has shown evidences in several medical areas. The survival of patients with glioblastoma cancer is increased after the treatment with a repurposed GSK3β inhibitor (Furuta et al., 2017). In the same way, two antidiabetic drugs exert neuroprotection in mice with AD and in patients with PD (Aviles-Olmos et al., 2013; Hettich et al., 2014).

6.2 Systems Biology and artificial intelligence for drug discovery

Several informatics-based approaches use the network-centric thinking to discover new drug effects for human diseases (Shahreza et al., 2017). This thesis starts from one of these approaches, the therapeutic performance mapping system, hereinafter TPMS. TPMS is a bioinformatic patented tool used by ANAXOMICS

BIOTECH S.L. company (www.anaxomics.com) (Valls et al., 2013). TPMS is based on the building of a network for a desired condition (either normal or pathological), using network and systems biology approaches (Pujol et al., 2010). Thereafter, thousands of drug combinations used in human healthcare are thrown into the undesired condition and the disturbances that they provoke to the network are analyzed. This tool is also enriched using ANNs. For more details see: www.anaxomics.com/our-technology/tpms.

This approximation yielded several drug combinations with a putative potential to shift one physiological condition to other more desired. TPMS unravel a new therapeutic effect of nutraceuticals to ameliorate liver diseases (Perera et al., 2014) and discovered new drug combinations to treat ALS (Herrando-Grabulosa et al., 2016). Although these positive results, the TPMS analysis needs to be taken with caution. The starting data must be very accurate. In fact, TPMS predicted as a neuroprotective compound a proton pump inhibitor for AD, but at the end it exerted detrimental effects and accelerated the progression of the disease (Badiola et al., 2013). In this case, the study was performed with uncompleted networks, and it resulted in an incorrect study of drug repurposing. This thesis was initiated with accurate data concerning two different states that MNs suffer after two different PNL. The RA, that provokes death of MNs, and the DA which does not affect the MNs survival and allows their regeneration. This data was analyzed through a systems biology approach and the TPMS raised different drug combinations with a putative score to induce neuroprotection in RA model.

HYPHOTESIS & OBJECTIVES

Hypothesis & Objectives

Combination of Network and System biology approaches can be an effective strategy to found neuroprotectants for complex pathologies, in our case for PNL and specifically for death of MNs after RA. Therefore, our main objective is to test whether a drug-based therapy obtained through Systems biology-based approach can be effective for different PNLs.

With this aim, the thesis has been divided in two different blocks with a total of 4 different chapters that are composed by different specific objectives:

NEUROPROTECTION

Chapter 1: Neuroprotective Drug for Nerve Trauma Revealed Using Artificial Intelligence

1.1 To validate the efficiency of a systems biology-based bioinformatic tool to elucidate new neuroprotective therapies for PNL

1.2 To assess if oral NH can be a plausible treatment for RA and therefore for PNL

1.3 To evaluate if NH enhances functional recovery after PNL

1.4 To check if Mechanism of action predicted by TPMS was ascertained for the NH

1.5 To elucidate the role of SIRT1 in survival of MNs after RA

Chapter 2: Neuroprotection of Disconnected Motoneurons requires Sirtuin 1 activation but Sirtuin 2 depletion or inhibition with AK-7 is detrimental.

2.1 To discern SIRT1 and SIRT2 activities after hypoglossal nerve injury within MNs

2.2 To clarify SIRT1 and SIRT2 role's in *in vitro* models of endoplasmic reticulum stress

2.3 To asses if SIRT1 activation and SIRT2 inhibition will exert MN neuroprotection after hypoglossal axotomy

Chapter 3: NeuroHeal Confers Neonatal Neuroprotection Inducing SIRT1-Dependent Autophagy

3.2 To characterize which are the molecular mechanisms that promote death of MNs after neonatal PNL

3.3 To assess the anti-apoptotic effect of NH

3.4 To elucidate if NH is able to sustain MN viability during neonatal stages after PNL

3.5 To check if NH induces autophagy and through which mechanisms it is induced

Preclinical model of MN death and regeneration

Chapter 4: Boosted regeneration and reduced denervated muscle atrophy by NeuroHeal in a pre-clinical model of lumbar root avulsion with delayed reimplantaiton

4.1 To corroborate the therapeutic potential of NH in a pre-clinical model of RA combined with delayed root reimplantation

4.2 To elucidate the possible role of NH on muscle atrophy after long nerve denervation

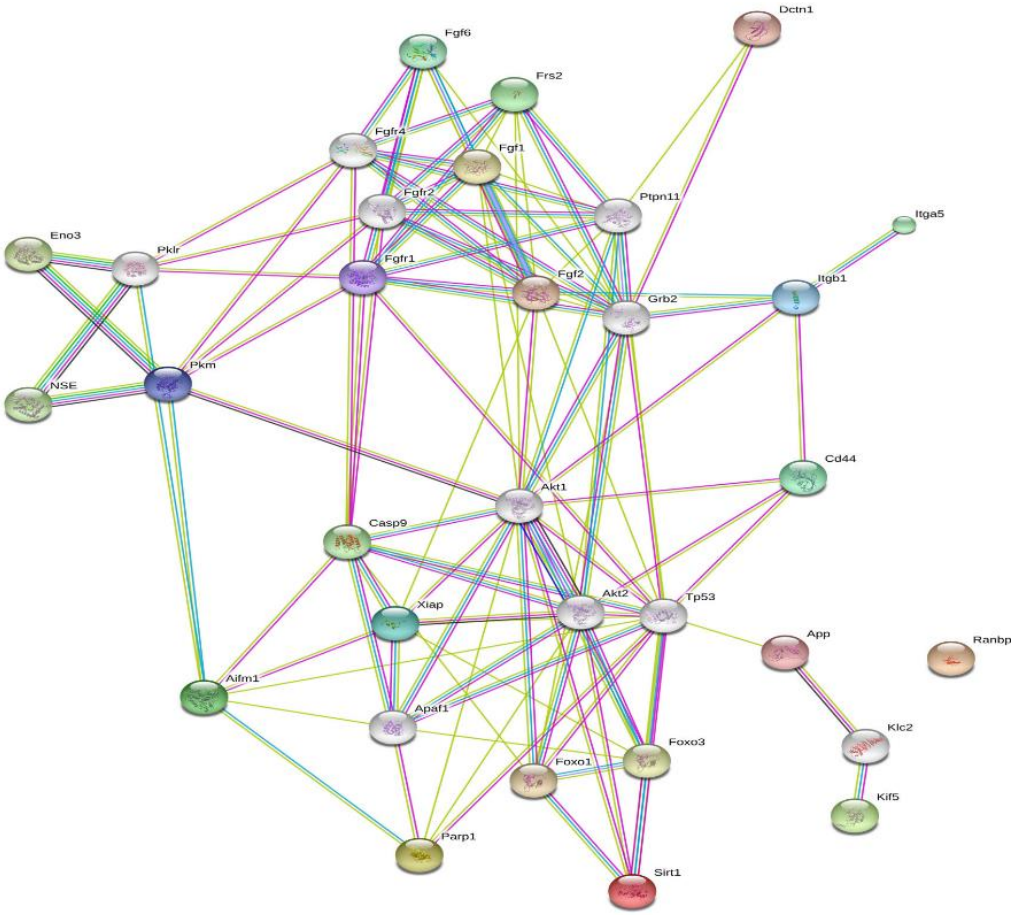
Dctn1
Fgf6
Frs2
Fgfr4
Fgf1
Fgfr2
Ptpn11
Itga5
Eno3
Pklr
Fgfr1
Fgf2
Itgb1
Grb2
Pkm
NSE
Cd44
Akt1
Casp9
Akt2
Tp53
Xiap
App
Ranbp
Aifm1
Apaf1
Klc2
Foxo3
Foxo1
Kif5
Parp1
Sirt1

CHAPTER 1

Neuroprotective Drug for Nerve Trauma Revealed Using Artificial Intelligence

David Romeo-Guitart[1], Joaquim Forés[2], Mireia Herrando-Grabulosa[1], Raquel Valls[3], Tatiana Leiva-Rodríguez[1], Elena Galea[4], Francisco González-Pérez[1], Xavier Navarro[1], Valerie Petegnief[5], Assumpció Bosch[6], Mireia Coma[3], José Manuel Mas[3], Caty Casas[1*]

Affiliations

[1] *Institut de Neurociències* (INc) and Department of Cell Biology, Physiology and Immunology, *Universitat Autònoma de Barcelona* (UAB), & *Centro de Investigación Biomédica en Red sobre Enfermedades Neurodegenerativas* (CIBERNED), Bellaterra, Barcelona, Spain

[2] Hand and Peripheral Nerve Unit, Hospital Clínic i Provincial, *Universitat de Barcelona*, Barcelona, Spain

[3]Anaxomics Biotech, S.L, Barcelona, Spain

[4] *Institut de Neurociències* (INc), Biochemistry and Molecular Biology, UAB and *ICREA*, Passeig Lluís Companys 23, 08010, Barcelona, Spain

[5] Department of Brain Ischemia and Neurodegeneration, Institute for Biomedical Research of Barcelona (IIBB), Spanish Research Council (CSIC), *Institut d'Investigacions Biomèdiques August Pi Sunyer* (IDIBAPS), Barcelona, Spain

[6] INc and Department of Biochemistry and Molecular Biology, UAB and CIBERNED, Spain

*To whom correspondence should be addressed: Caty Casas Louzao, *Unitat de Fisiologia Mèdica*, *Facultat de Medicina*, *Universitat Autònoma de Barcelona*, E-08193 Bellaterra, Barcelona, Spain. Tel: +34-935811324, Fax: +34-935812986, E-mail: Caty.Casas@uab.cat

Running title: Network-based drug discovery for CNS trauma

ABSTRACT

Here we used a systems biology approach and artificial intelligence to identify a neuroprotective agent for the treatment of peripheral nerve root avulsion. Based on accumulated knowledge of the neurodegenerative and neuroprotective processes that occur in motoneurons after root avulsion, we built up protein networks and converted them into mathematical models. Unbiased proteomic data from our preclinical models were used for machine learning algorithms and for restrictions to be imposed on mathematical solutions. Solutions allowed us to identified combinations of repurposed drugs as potential neuroprotective agents and validated them in our preclinical models. The best one, NeuroHeal, neuroprotected motoneurons, exert anti-inflammatory properties and promoted functional locomotor recovery. NeuroHeal endorsed the activation of Sirtuin 1, which was essential for its neuroprotective effect. These results support the value of network-centric approaches for drug discovery and demonstrate the efficacy of NeuroHeal as adjuvant treatment with surgical repair for nervous-system trauma.

Keywords: neurodegeneration; motoneurons; axon regeneration; systems biology; sirtuin 1.

INTRODUCTION

Common diseases of the central nervous system (CNS), including psychiatric disorders and neurodegeneration, are caused by multiple molecular abnormalities as opposed to individual defects. Likewise, recovery from CNS trauma requires multiple strategies encompassing neuroprotection and repair and regeneration of CNS cells. It follows that effective therapies must target multiple pathways rather than single proteins. Systems biology is an indispensable analytical tool in drug discovery for complex diseases. First, it allows for a necessary shift from a gene-centric to a network-centric view that takes protein targets back to their physiological context, such that a systemic perspective of the environment is gained without losing molecular details. Second, it facilitates the generation of multi-component therapies by repurposing existing drugs with well-established safety, bioavailability, and pharmacology profiles.

Here we report the discovery of a neuroprotective and pro-regenerative drug combination with the therapeutic performance mapping system (TPMS), a platform for drug discovery based on systems biology and artificial intelligence (www.Anaxomics.com). TPMS facilitates the screening of drugs for their capacity to shift the profile of topological molecular maps from pathological to beneficial (Herrando-Grabulosa et al., 2016). We used TPMS to identify known drugs likely to be beneficial in treatment of peripheral nerve lesions caused by trauma, tumors, or autoimmune reactions. The economic cost of treating injured patients is considerable due to both direct and indirect expenses, as the injuries tend to cause functional inability in previously productive people (Dias and Garcia-Elias, 2006). Nerve root avulsion (RA) leads to the most severe degree of nerve injury because nerves are completely separated from the spinal cord and sensory ganglia, thus causing loss of motor, sensory, and autonomic functions in the affected extremities (Berman et al., 1998). RA often leads to deafferentation pain that may develop into central sensitization and severe neuropathic pain that is refractory to pharmacotherapy (Cohen and Mao, 2014b). Detached nerves may be reimplanted but successful repair is time-dependent due to the existence of massive retrograde degeneration of motoneurons (MNs) (Penas et al., 2009a). Thus, effective

therapeutic agents should target multiple mechanisms in order to maintain MN viability, promote regenerative capabilities, and minimize glial reactivity.

In order to discover such a multifunctional therapy, we built molecular maps using TPMS and quantitative and unbiased proteomic data obtained from a pre-clinical rat model of RA that leads to retrograde degeneration of MNs and from a rat model of distal axotomy (DA) and suture that leads to MN survival and nerve regeneration (Casas et al., 2015). We screened these maps for neuroprotective combinations of FDA-approved drugs, and we validated the selected combinations in the RA model. We found that the combination of acamprosate (ACA) plus ribavirin (RIB), which we called NeuroHeal, promotes neuroprotection, nerve regeneration, and functional recovery and, unlike existing drugs, is not pro-nociceptive. The mechanism of action of NeuroHeal involves sirtuin 1 (SIRT1), an actively pursued therapeutic target. NeuroHeal thus warrants further evaluation for early treatment after peripheral nerve and RA injuries.

MATERIALS AND METHODS

TPMS technology

TPMS is a top-down systems biology approach with applications in drug repositioning (Mas et al., 2010; Herrando-Grabulosa et al., 2016; Iborra-egea et al., 2017). It is based on artificial intelligence and pattern recognition models that integrate all available biological, pharmacological, and medical knowledge to create mathematical models that simulate *in silico* the behaviour of human physiology. The process encompasses five steps: i) A manually curated collection of molecular effectors (seeds) that characterize degeneration after RA and neuroprotection after DA, respectively, were created; ii) condition-specific molecular maps were prepared from these seeds that incorporate all the available functional relationships; iii) each static map was converted into mathematical models (topological maps) capable of reproducing existing knowledge and predicting new data; iv) our own proteomic data from RA and DA models were used to feed machine learning and generate a set of restrictions that make up the truth table, and v) mathematical models were solved

to obtain multicomponent drug neuroprotective candidates for RA and a minimal description of its synergic MoA.

Generation of molecular maps. We manual curated a list of proteins (seed proteins) relevant for the processes of neurodegeneration and neuroprotection (Casas et al., 2015). Manual curation was performed through an extensive and careful review of full-length articles in the PubMed database that included the strings defined in Figure 1B. The search was expanded using the "related articles" function and article reference list. The map generation and extension process was conducted through the incorporation of all known relationships of the seed proteins in the map based on the following sources: KEGG (Kanehisa et al., 2006), REACTOME (Croft et al., 2014), BIOGRID (Salwinski et al., 2009), INTACT (Brooksbank et al., 2003) (Salwinski et al., 2009), HDPR (Keshava Prasad et al., 2009), MATRIXDB (Chautard et al., 2011), MIPS (Mewes et al., 2011), DIP (Xenarios et al., 2000), and MINT (Licata et al., 2012). The final map included 12,000 proteins and 180,000 links connecting the proteins.

Generation and solving mathematical models. Models were generated through the use of ANN and pattern recognition (Sampling methods) techniques based on optimization of genetic algorithms (Goldberg, n.d.; Kirkpatrick et al., 1983). The specific algorithm used for ANN was a multilayer perceptron (MLP) neural network classifier (Rosenblatt, 1961; Cybenko, 1989) with a backpropagation training method that typically consists of an input layer of nodes, an output layer, and one or more middle hidden layers of nodes in between (Arce-Medina and Paz-Paredes, 2009). The input layer is the raw data introduced. The learning methodology used consisted of an architecture of stratified ensembles of neural networks as a model, trained with a gradient descent algorithm to approximate values of a given truth table. MLP gradient descent training depends on randomization initialization. In order to generate each of the ensembles, 1000 MLPs were trained with the training subset. The best 100 were used as the ensemble. The model identified the relationships between drug targets and clinical elements of the network with a 98% of accuracy after applying cross-fold validation process. The truth table is a set of restrictions corresponding to the available biological knowledge about the constructed networks, together with the knowledge derived from DrugBank, GEO

(Lopes et al., 2010) and our own dictionary called Biological Effectors Database (BED) (http://www.anaxomics.com/our- technology/tpms/#tpms). The BED database contains the molecular description and details of 212 clinical terms cited in DrugBank (Wishart et al., 2008) summing more than 3500 proteins in 200 pathological conditions covering 98.5% of all clinical terms included (Valls et al., 2013). We added to BED our own proteomic data from RA and DA models (Casas et al 2015). The models should be able to reproduce every single rule contained in the truth table so that the error of a model is calculated as the sum of all the rules with which the model did not comply. To validate our models, we used a previously reported neuroprotective drug (PRE084) as a positive control in our RA model (Penas et al., 2011b).

Sampling methods were used to generate mathematical models with stratified ensembles that comply with the truth table. Each drug combination was considered an input signal that stimulates and changes the model. The integration of the input signals consisted of the sum of all input values that arrive at the node. This signal was submitted to a sigmoid function to produce a normalized output in the range [-1,1], this output-signal being the input-signal for the next node. The topology was initialised by random values for all the links in each of the 100 initial models. Each model is evaluated against the human functional description. In the present work the best model was that closest to the regenerative model. The worst models were discarded, and new models with different initialization values for the links were created. This iterative process was optimized by a stochastic optimization strategy exploring between 10^6 and 10^9 models as described previously (Mitchell, 1998). The accuracy of the best 100 models improved with each new cycle of iteration. This process continued until the models did not improve with more cycles of iteration.

Models result in both “global” predicted mechanisms that account for the majority of the population, and “cluster” mechanisms of action, which are more accurate for population subgroups. The MoA was validated in a two-step process. First, we checked that each link was accurate (i.e., was already described in the literature). Second, we ensured that the MoA made sense overall, featuring pathways coherent within the living system. A normalized synergism score (SE) was

obtained from the protein involved in the synergism between two drugs of the combination. SE, based on the ponderation of the number of solutions for a particular node affected by both drugs, and the synergistic effect (rather than additive) of both drugs over the node, were determined with the maximum score according to this calculation being 0.5.

Subjects and surgical procedures

Sprague–Dawley female rats aged 12 weeks were kept under standard conditions of light and temperature and given food and water *ad libitum.* We performed surgical procedures under anaesthesia with a cocktail of ketamine/xylazine (0.1 mL/100 g weight) intraperitoneally (i.p.) as reported previously (Penas et al., 2009). To perform extravertebral avulsion of the L4-L5 roots (the RA model) we made a midline skin incision and applied a moderate traction on the selected roots away from the intervertebral foramina, exposing the mixed spinal nerves that contained the motor and sensory roots and dorsal root ganglia. To carry out the sciatic nerve crush injury, we exposed the right sciatic nerve and crushed it in three different orientations using fine forceps (Dumont no. 5) for 30 seconds. The wound was sutured by planes and disinfected with povidone iodine, and the animals were allowed to recover in a warm environment. For intrathecal delivery of vehicle or drugs to the avulsed animals we used iPrecio programmable pumps (Data Science International, Italy), placed subcutaneously on the lumbar left side of the animal. The catheter connected to the pump was inserted into the magna cistern in the brain stem and fixed with surgical adhesive (Huhn, 1991). The pumps were programmed to release 30 µL from 18 to 20 hours after injury to reach the desired concentration in the CSF after a 1:5 dilution. Then, a continuous flow of 1 µL/h was released during 20 days from the day following RA until sacrifice to maintain the desired concentration in the CSF. All procedures involving animals were approved by the ethics committee (*Comissió d'Ètica i experimentació animal i Humana*) of the *Universitat Autònoma de Barcelona* and *Comité de Seguretat i Salut de la Generalitat de Catalunya*, and followed the European Council Directive 2010/63/EU

Electrophysiological and functional examination

All experiments were conducted in a blinded fashion. For electrophysiological examination, rats were anaesthetized. The sciatic nerve was stimulated by transcutaneuous electrodes placed at the sciatic notch and the compound muscle potential (CMAP) was recorded by placing electrodes on the gastrocnemius and the plantar interosseus muscles. The evoked action potentials were displayed on a storage oscilloscope (Synergy Medelec, Viasys HealthCare) at settings appropriate to measuring the amplitude from baseline to peak and latency to onset. For the functional analysis of locomotion, we painted the plantar surface of rat hindpaws with acrylic paint and allowed the rat to walk along a corridor with white paper. Footprints from operated and intact paws were analysed by measuring the print length (PL), the distance between 1st and 5th (TS) or 2nd and 4th (IT) toes with a precision device. The three parameters were combined to obtain the Sciatic Functional Index (SFI) (de Medinaceli, 1988), which quantifies the changes in walking pattern (0 for uninjured; -100 for maximally impaired gait).

Drugs

Pre084 (Tocris, Ellisville, MO, USA), mefloquine (Mef), alitetrinoin (Ali), S-adenosylmethionine (SAM), ephedrine (EPHE), acamprosate calcium (ACA), ribavirin (RIB; Norman), and Ex-527 (Sigma-Aldrich, Saint Louis, MO, USA) were diluted in artificial cerebrospinal fluid (aCSF: 124 mM NaCl, 3 mM KCl, 26 mM $NaHCO_3$, 2 mM $CaCl_2 \cdot 2H_2O$, 1 mM $MgSO_4 \cdot 7H_2O$, 1.25 mM KH_2PO_4, and 10 mM D-glucose) used as a vehicle alone or with 0.01% DMSO in the case of comparative studies with Ex-527. The concentrations prepared in the pumps were 5X the desired final concentration in animal CSF: 0.015 mM for MEF, 0.15 mM for ALI, 5 mM for ACA, 20 µM for RIB, 36.5 µM for EPHE, 187 µM for SAM, 50 µM for Pre084, and 7 mM for Ex-527. We added spermidine (Sigma-Aldrich) to the drinking water; it was freshly added at 30 mM concentration every 2-3 days for 21 days as described elsewhere (Eisenberg et al., 2009). For oral administration, ACA (Merck, Darmstadt, Germany) and RIB (Normon, Madrid, Spain) were dissolved in water at a final concentration of 2.2 mM and 1 mM, respectively for dose 2 (0.25X group).

Construction, purification, and infection with recombinant adeno-associated vectors

The *SIRT1* cDNA was cloned into *Nhe*I and *Xho*I sites between the ITRs of AAV2, under the regulation of *CMV* promoter and the woodchuck hepatitis virus responsive element (WPRE) (Loeb et al., 1999). AAV2/rh10 vector was generated as previously described (Zolotukhin et al., 1999) by triple transfection of HEK 293-AAV cells (Stratagene, San Diego, CA, USA) with branched polyethylenimine (PEI; Sigma-Aldrich) with the plasmid containing the ITRs of AAV2, the AAV helper plasmid containing Rep2 and Cap for rh10 (kindly provided by JM Wilson, University of Pennsylvania, Philadelphia, PA, USA) and the pXX6 plasmid containing helper adenoviral genes (Piedra et al., 2015). Recombinant vectors were clarified after benzonase treatment (50 U/mL, Novagen) and polyethylene glycol (PEG 8000, Sigma-Aldrich) precipitation. Vectors were purified by iodixanol gradient by the Vector Production Unit at UAB (http://sct.uab.cat/upv), following standard operating procedures. Viral genomes per ml (vg/ml) were quantified by picogreen (Invitrogen, Carlsbad, CA, USA).

Intrathecal administration of $4x10^{-10}$ viral genomes was performed at the lumbar region of isoflurane-anaesthetized animals using a 33-gauge needle and a Hamilton syringe. After lateral spine exposure by paravertebral muscle dissection, 10 µl of viral vectors were slowly injected into the CSF between vertebrae L3 and L4. Appropriate access to the intrathecal space was confirmed by animal tail flick. The needle was held in place at the injection site for one additional minute, after which muscle and skin were sutured.

In vitro model

We used the NSC-34 motoneuron-like cell line cultured in Dulbecco's modified Eagle's medium high-glucose (DMEM, Biochrom, Berlin) supplemented with 10% fetal bovine serum and 1X penicillin/streptomycin solution (Sigma-Aldrich), on collagen-coated plates (Thermo-Fisher, Waltham, Massachusetts, USA) in a humidified incubator at 37 °C under 5% CO_2. We plated the cells at a density of $2.5x10^5$/cm2. After 5 days of cell culture without changing the medium, NSC-34 cells

presented a differentiated-like phenotype characterized by the presence of long neurite extensions. Then we added tunicamycin (0, 0.1, 1, or 10 μg/ml; Sigma-Aldrich) or vehicle (0.02% DMSO) to the medium to induce endoplasmic reticulum (ER) stress together with either vehicle or drug combinations to assess their neuroprotective effect in vitro. Twenty-four hours after treatments, we analyzed cell viability by incubating the cells with 5 mg/ml MTT solution for 4 hours at 37 ˚C and, after medium removal, the MTT salts were dissolved with DMSO for 5 minutes. Absorbance at 570 nm was measured with a Biotek Elx800 microplate reader. The synergistic effect of C1 was observed by evaluation of Zmix, where Zmix=((z-z0)*100)/(100-z0), z is the value used for normalization and the z0 is the reference (the total dose of both compounds equals 0) as previously described (Tallarida, 2000a; Salwinski et al., 2009).

Immunohistochemistry and image analysis

After deep anaesthesia with pentobarbital, we transcardially perfused the animals with a saline solution containing 10 U/ml heparin, followed by 4% paraformaldehyde in a 0.1 M phosphate buffer, pH 7.2 for tissue fixation at 21 dpi (n=4 for each condition), and removed the L4 and L5 segments (5-mm total length) of the spinal cord, which were post-fixed in the same fixative for an extra 4 hours and cryopreserved in 30% sucrose overnight. Serial transverse sections (20-μm thick) were obtained on gelatinized slides using a cryotome (Leica, Heidelberg, Germany) and preserved them at -20 ˚C until use. We treated the slides with blocking solution (Tris-buffered saline (TBS) with 0.3% Triton-X-100 and 10% bovine serum) for 1 hour and incubated thereafter with primary antibodies: rabbit anti-glial fibrillary acidic protein (GFAP; 1:1000, Dako), rabbit anti-ionized calcium binding adaptor molecule 1 (Iba1; 1:1000, Dako), rabbit anti-growth associated protein-43 (GAP43; 1:50, Millipore, Billerica, MA, USA), rabbit anti-subunit β1 integrin (ITGb1; 1:100, Millipore), rabbit anti-kinesin 5c (Kif5c; 1:1000, Abcam, Cambridge, UK), rabbit anti-dynactin 1 (DCTN1; 1:200, Antibodies-online, Acton, MA, USA), rabbit-anti NAD-dependent deacetylase sirtuin-1 (SIRT1; 1:100, Millipore), rabbit anti-acetyl-Histone H3 (Lys9) (Acetyl H3-K9; 1:50, Millipore), and rabbit anti-acetyl-p53 (Lys373) (Acetyl p53-K373; 1:500, Millipore). After several washes with TBS with 0.1% Tween-20, the sections were incubated for 2 hour with

Cy-3-conjugated donkey anti-rabbit antibodies (Jackson Immunoresearch, West Grove, PA, USA). We counterstained the sections with DAPI (Sigma-Aldrich), or NeuroTrace Fluorescent Nissl Stain (Molecular Probes, Leiden, Netherlands). Sections to be compared were processed together on the same slide and on the same day. Images of the spinal cord samples from different treatments and controls were taken under the same exposure time, sensibility, and resolution for each marker analysed with the aid of a digital camera (Olympus DP50) attached to the microscope (Olympus BX51). We analysed signal intensity with the ImageJ software (National Institutes of Health; available at http://rsb.info.nih.gov/ij/). For GFAP and Iba1, microphotographs were taken at 40X, and then we transformed them to grey scale and analysed immunoreactivity by measuring the integrated density of a region of interest (ROI) after defining a threshold for background correction (Penas et al., 2009). The ROIs were selected on the grey matter at the ventral horn and had an area of 0.12 mm^2 for GFAP and Iba1 and the same ROI size but in the white matter for GAP43 and DCTN-1. Measurements were performed from 8 spinal cord sections (separated 220 μm between pairs) of each animal.

Confocal microphotographs of nuclei of MNs were taken in identical conditions of exposure (Zeiss LSM 700; Zeiss, Jena, Germany). For SIRT1 and deacetylase activity substrate (p53K373 and H3k9) analysis, single-cell densitometry was performed by pre-defining the threshold for each section for background correction and measuring the total area of the encircled MN nucleus. Then the ratio of integrated density/area was used as an index to classify at least 15-20 MNs per section.

Motor neuron counting

Spinal cord sections were selected with a random start and then sampled systematically (every 12^{th} section) to generate serial subsamples from each lumbar spinal cord of animals at 21 dpi. Eight series of 10 sections (separated by 100 μm) of each processed L4-L5 spinal cord were stained with fluorescent NeuroTrace (Life Technologies, Carlsbad, CA, USA) following the manufacturer's protocol. Sequential microphotographs were taken covering the lateral ventral horn at 10X. Large MNs were identified by their localization in the lateral ventral horn of lumbar spinal cord

sections and only MNs with diameters of 30-70 μm with prominent nucleoli and polyglonal shapes located at the layer IX of the ventral horn were counted. The mean number of MNs per section was calculated. For comparisons, the estimated number of MNs present in the ventral horn of the avulsed side was expressed as a percentage of the contralateral side.

Neuromuscular junction reinnervation analysis

We cut the plantar interossei muscles into serial transverse sections (40 μm thick) using a cryotome and preserved them at -20 ˚C until use. The slides were incubated with chicken anti-Neuro Filament 200 (NF-200; 1:1000, Millipore) as described above. After several washes Cy3-conjugated secondary antibody was added. Finally, we incubated slices with α-bungarotoxin labelling solution (Life Technologies) following the manufacturer's protocol to reveal motor endplate machinery. Sequential microphotographs were taken covering all the plantar muscle at 20X. Only motor end plates with NF-200 co-labelling were counted as reinnervated.

Statistical analysis

All values are presented as means ± standard errors of the means (SEM). For statistical analysis, we analyzed data with GraphPad Prism 5 software (San Diego, CA, USA) using unpaired t-tests or one-way analysis of variances (ANOVA) followed by Bonferroni's multiple comparison tests. We considered differences significant at $p<0.05$.

RESULTS

Identification of putative neuroprotective drug combinations

To identify potential neuroprotective drug combinations, we applied machine-learning tools as depicted in **Figure 1A**. To generate our systems biology-based networks, the starting material was a manually curated list composed of proteins clustered in motives likely to be involved in either "neuroprotection" or

"neurodegeneration" (Casas et al., 2015) and obtained from a perusal of the literature in PubMed. The initial list was expanded to generate network maps that included 3,296 proteins for regeneration and 3,836 proteins for degeneration with an overlap of 2,232 proteins. Snapshot of the maps are shown in **Figure 1B**. The maps were converted into mathematical models incorporating all biological knowledge available including drug targets and clinical trials results (Badiola et al., 2013; Gómez-serrano et al., 2016; Herrando-Grabulosa et al., 2016; Iborra-egea et al., 2017). Drug repositioning solutions were acquired by perturbing the models with stimulus (drugs) and approximating the best solution to the neuroprotection model. We incorporated our experimental proteomic data from the RA and DA models previously published (Casas et al., 2015) and categorized as degeneration and neuroprotection conditions, respectively, for machine training to generate physiological responses facing any perturbation. These data resulted in a set of restrictions that all mathematical solutions should accomplish. In addition the drugs screened were required to: i) have an outstanding safety profile, ii) not cause neuropathic pain, iii) have no known effects on CNS/PNS regeneration, and iv) be able to cross the brain-blood barrier. A total of 5,440 drugs that generated approximately 15 million binary combinations were screened. From the scored resulting binary combinations (**Fig. 1C**) we selected the best for further experimental validation: ACA plus RIB (Combination C1); ACA plus ephedrine (EPHE) (C2), and S-adenosylmethionine (SAM) plus EPHE (C3).

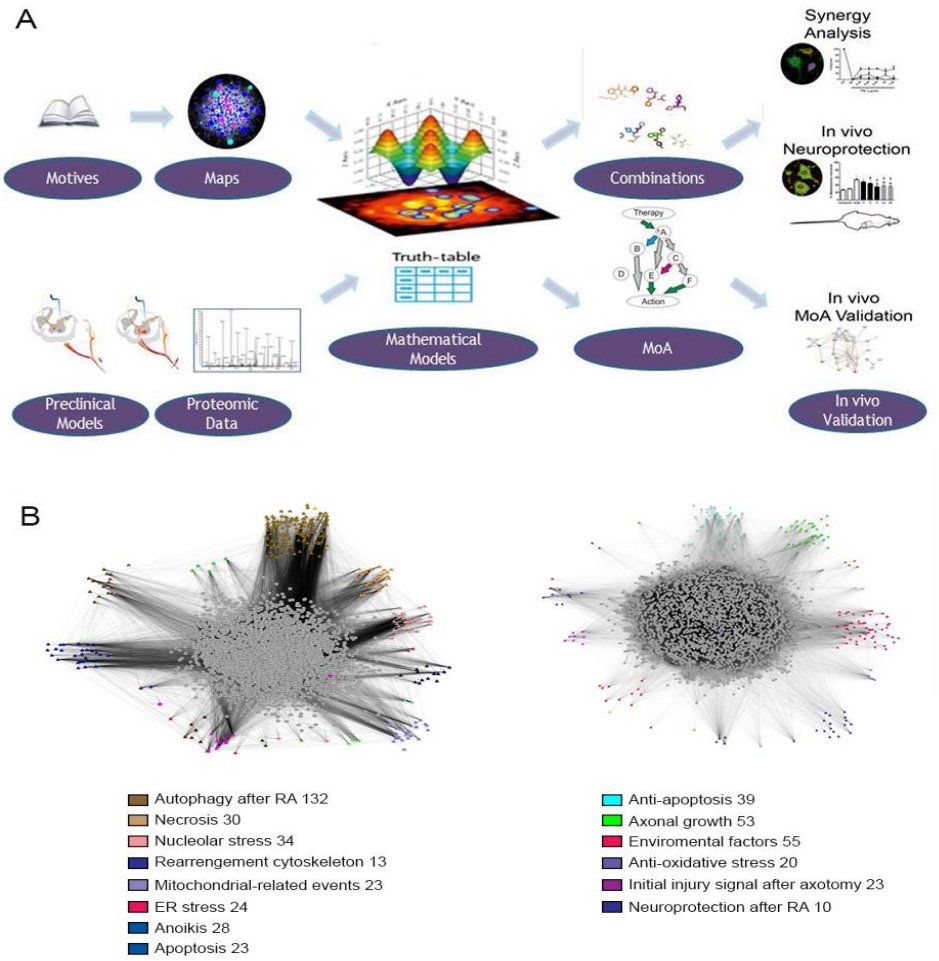

C

Potential neuroprotective drug combinations					
Drug A		Drug B		Prediction values	
ID	Name	ID	Name	Regeneration	Neuropathic pain
DB00118	S-Adenosylmethionine	DB01364	Ephedrine	75.7	2.1
DB00150	L-Tryptophan	DB00811	Ribavirin		9.6
DB00699	Nicergoline	DB01587	Ketazolam	29.2	3
DB00150	L-Tryptophan	DB01587	Ketazolam	28.6	9.6
DB00118	S-Adenosylmethionine	DB00659	Acamprosate	76.1	2.1
DB00659	Acamprosate	DB00811	Ribavirin	75.6	2.1
DB00530	Erlotinib	DB00659	Acamprosate	36.1	2.1
DB00659	Acamprosate	DB01364	Ephedrine	31	9.8
DB00659	Acamprosate	DB00699	Nicergoline	30.7	16.2

Figure 1. **Experimental design. (A)** The starting material was a manually curated list of key proteins clustered in motives that allowed construction of condition-specific networks for neurodegeneration after RA and for neuroprotection after DA. Using TPMS, network static maps were converted into topological maps associated with mathematical equations. The available data from unbiased proteomic analysis generated from RA and DA models (Casas et al., 2015) was used to build a set of restrictions collated into a truth table with which all models generated had to comply. Drug screening *in silico* was used to perturb the neurodegeneration-associated mathematical model and drug combinations that approximated the model to the neuroprotective state were identified. The algorithms used also allowed specification of key proteins involved in the mode of action (MoA) of each drug combination. Finally, we validated new combinations for its neuroprotective effect and putative MoA *in vivo* and *in vitro*. **(B)** Snapshots of the full protein networks associated with

the neurodegenerative condition after RA (left, 3,836 nodes, average links per node 13.4) and with the neuroprotective condition after DA (right, 3,296 nodes, average links per node 13.9) visualized through the Cytoscape software platform (Lopes et al., 2010). Seed proteins for different motives are labelled by colour as indicated. Some seeds belong to more than one motive. **(C)** List of potential neuroprotective drug combinations identified using the *in silico* screen.

In vitro and in vivo validation of drug combinations

To validate the neuroprotective effect of the drug combinations and the synergy between their components we used an *in vitro* model of endoplasmic reticulum (ER) stress, since this is a hallmark of the RA neurodegenerative process (Penas et al., 2011a). We treated differentiated NSC-34 MN-like cells with tunicamycin (TN, an ER stressor), vehicle, individual drugs, or one of the drug combinations (C1-C3) and assessed viability with the MTT assay. Drug combinations, but not single drugs with the exception of SAM, protected the cells against ER stress (**Fig. 2A**).

We next performed RA in animals that received treatment with vehicle, single drugs, or drug combinations using subcutaneous implanted programmable pumps for continuous intrathecal infusion during 20 days post-injury. We used Pre084, a selective agonist of receptor σ1 (Penas et al., 2011b), as a positive control of neuroprotection; Pre084 has no clinical value as it is pro-nociceptive (Roh et al., 2011; Pyun et al., 2014). Among all combinations, only C1 yielded a similar rate of MN survival as Pre084. Treatment with single C1 components ACA or RIB alone did not promote neuroprotection (**Fig. 2B**). Next, in order to determine the specificity of neuroprotection, we treated RA animals with a non-relevant combination composed of meflokine (MEF) and alitretionion (ALI), which we previously discovered using a similar systems biology approach for amyotrophic lateral sclerosis (Herrando-Grabulosa et al., 2016). The drug combination reached its target after a continuously pumped infusion because there was upregulation of choline acetyl transferase (ChAT) expression within the MNs of treated RA animals (**Fig. 2C**) as previously demonstrated (Herrando-Grabulosa et al., 2016). However, the combination was not neuroprotective (**Fig. 2D**), suggesting that the results obtained with TPMS were highly pathology-specific.

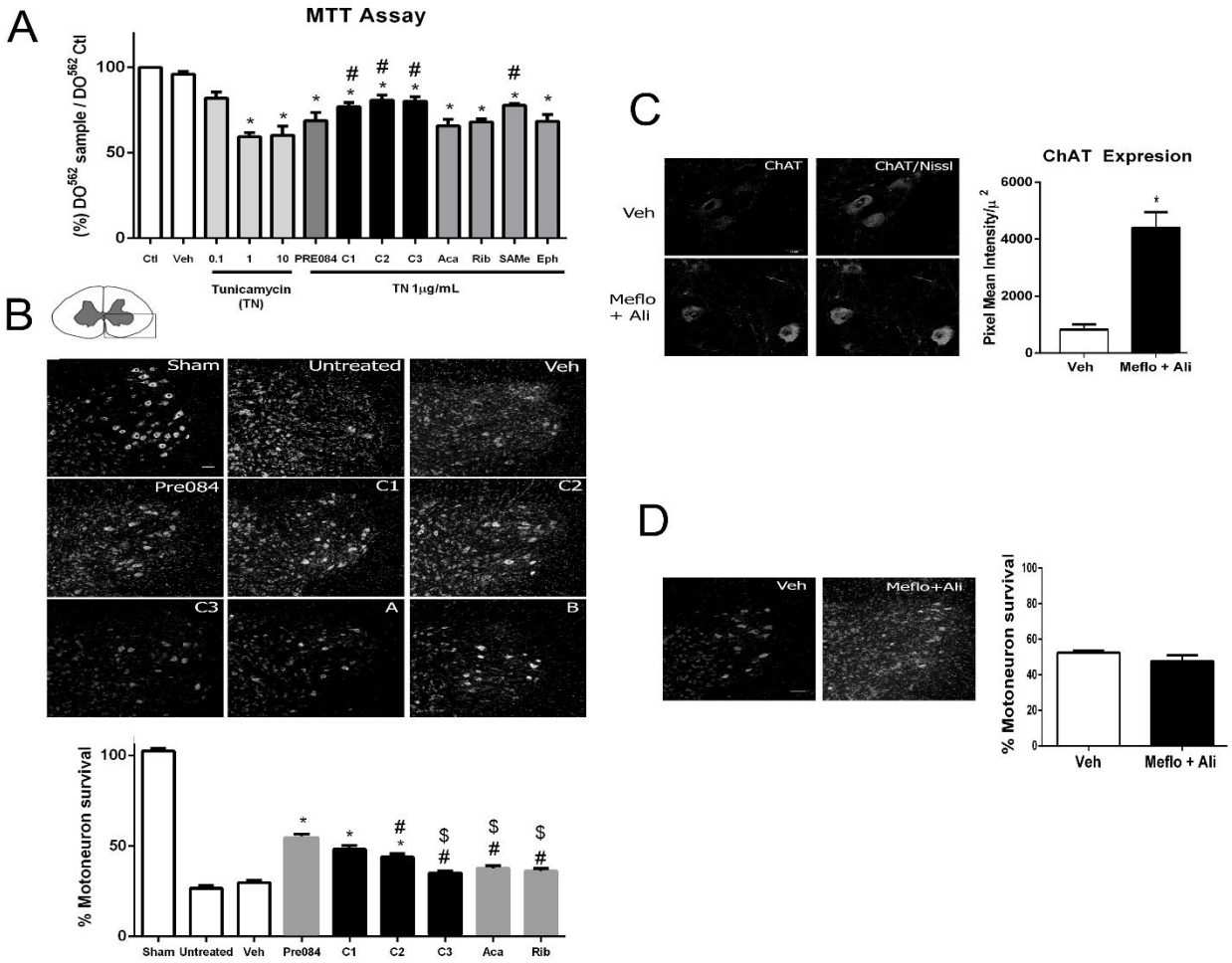

Figure 2. Neuroprotection by drug combinations identified *in silico.* (A) Bar graph showing the percentage of cell survival ± SEM after treatment with different doses of TN, which causes ER stress, to establish the optimal concentration to be used *in vitro* (fixed at 1 µg/ml TN). Neurotoxicity was evaluated with an MTT assay on differentiated NSC-34 MN-like cells in the absence of treatment (control, ctrl) or vehicle (veh) or presence of a single drug (Pre084, ACA, Rib, SAM, or EPHE or drug combinations (C1-C3) analysed 24 h after adding treatments (n=3-8, *p<0.05 vs. vehicle, #p<0.05 vs. 1 µg/ml TN). **(B)** ***Top,*** representative microphotographs of spinal cord ventral horns at L4-L5 from sham-operated control or the ipsilateral side of RA animals stained with fluorescent Nissl. Animals were intrathecally treated using programmable infusion pumps with either vehicle (artificial cerebrospinal fluid), PRE084 (positive control), single drugs, or combination of drugs: C1= ACA (drug A) + RIB (drug B); C2= EPHE + ACA; and C3= SAM + EPHE. Scale bar = 100 µm. ***Bottom,*** bar graph of the average relative number of surviving motoneurons ± SEM on the ipsilateral side with respect to the contralateral side after 21 days post injury (dpi; n=3 for Sham, PRE084, C3; n=6 for injured; n=4 for other groups, ANOVA, post hoc Bonferroni * p<0.05 vs. vehicle, # p<0.05 vs. PRE084, $ p<0.05 vs. C1). **(C)** Microphotographs of ChAT immunohistochemistry in the ventral horn MNs from RA animals treated with vehicle (veh) or with a non-related drug combination of Mef and Ali at 14 dpi. Ali reduces expression of ChAT. Histogram of immunoreactivity intensity per area within MNs (Nissl-positive). **(D)** Representative microphotographs of MNs of the ipsilateral

ventral horn stained by Nissl. Histogram showing the average number of MNs ± SEM on the ipsilateral with respect to the contralateral side of spinal cord from animals treated with either vehicle or the combination of Mef and Ali at 14 dpi.

C1 and C3 treatments, in contrast to C2, reduced both microgliosis and astrogliosis after RA, as determined by immunohistochemical analysis of GFAP-positive astrocytes and Iba1-positive microglia (**Fig. 3A, B**). Of drugs given individually only RIB slightly reduced astrogliosis (**Fig. 3B**). To examine the existence of a pro-regenerative profile within MNs, we analyzed the expression of GAP43, a protein associated with proliferation, in the motor axonal branches on the lateral-ventral side of the ipsilateral *versus* contralateral spinal cord sections. Most of the combinations analyzed and ACA alone, but not after Pre084 or RIB, increased GAP43 levels (**Fig. 3B**). We scored all drug combinations with regards to neuroprotection, reduction of inflammation, regeneration, and ER stress protection *in vitro* (**Fig. 3C**). C1 was the best in all readouts, and we named it NeuroHeal.

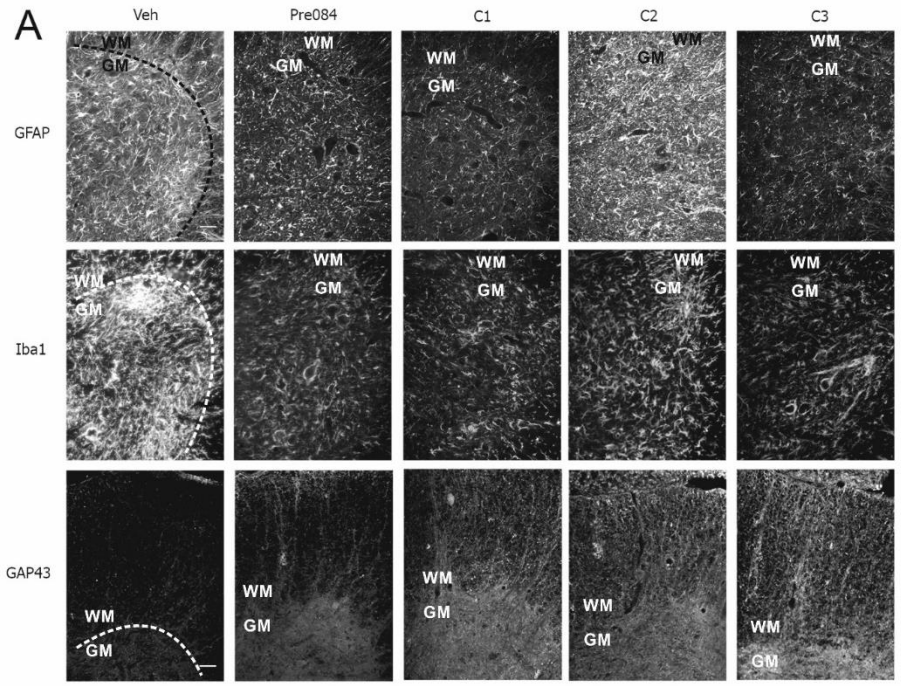

C

Therapeutic value & Score						
Drug	Neuroprotection in vivo	Astrogliosis reduction	Microgliosis reduction	Pro-regenerative profile	ER-stress neuroprotection in vitro	Final Score
C1	1	1	1	1	1	5
C2	1	0	0	1	1	3
C3	0	1	0	0	1	2
Pre084	1	1	0	1	0	3
ACA	0	0	0	1	0	1
RIB	0	1	0	0	0	1

Figure 3. All drug combinations reduce microgliosis and astrogliosis and promote neuronal regeneration. (A) Representative fluorescence microphotographs at low magnification of the ipsilateral ventral horns of the spinal cord from RA injured animals treated with vehicle (Veh), Pre084, or drug combinations (C). Top and middle panels, staining for astrocytes (GFAP) and (middle panel) microglia (Iba1), respectively, in grey matter (GM)—delimited with dashed lines. Bottom panels, GAP43-positive neurites at the white matter (WM) of the ipsilateral ventral horns. Scale bar = 100 μm. **(B)** Histograms of average immunoreactivity intensities in GM for GFAP and Iba1 and in WM for GAP43 (* $p<0.05$ vs. Veh, # $p<0.05$ vs. C1). **(C)** Table summarizing dichotomy scores for MN survival, gliosis, and pro-regenerative effects *in vivo* and neuroprotective effects *in vitro* (1 is beneficial effect and 0 indicated no effect).

Determination of drug synergy in NeuroHeal

In order to determine the optimal dose combination we assayed ACA and RIB in different concentrations, changing by approximately 10-fold the amount of one drug with respect to the other. The fixed, 1X concentrations were 0.22 mM for ACA and 4 μM for RIB. We measured protection against cellular death caused by ER stress using the MTT assay. Neuroprotection was observed in a range of 0.1X to 1X for individual drugs, but not with higher doses (10X) (**Fig. 4A, left**). We next narrowed the range of concentrations from 0 to 2X. ACA or RIB treatment alone had no significant neuroprotective effect. In contrast, C1 afforded neuroprotection from 0.1X until less than 1X (**Fig. 4A**). Statistical analysis performed as previously described (Tallarida, 2000b) revealed a supra-additive effect when the drugs were combined to form NeuroHeal. Thus, for *in vivo* testing, we chose two doses with the best outcomes: 0.22 mM ACA plus 0.4 μM RIB and 0.06 mM ACA plus 1 μM RIB.

We administered these doses orally in RA injured animals because both drugs cross the blood-brain barrier in animals. The oral doses required to achieve effective of 0.22 mM ACA plus 0.4 μM RIB (dose 1) and 0.06 mM ACA plus 1 μM RIB (dose 2) in the CNS were estimated on the basis of previous pharmacokinetic studies of ACA and RIB in rats (Daoust et al., 1992; Mason et al., 2002; Tsubota et al., 2003; Zornoza et al., 2003). Both dose 1 and dose 2 caused a significant increase in MN survival as compared with vehicle-treated rats, although dose 2 was slightly more effective than dose 1 (**Fig. 4B**). We chose dose2 for further works and found that it reduced gliosis and promoted overexpression of GAP43 (**Fig. 4C**).

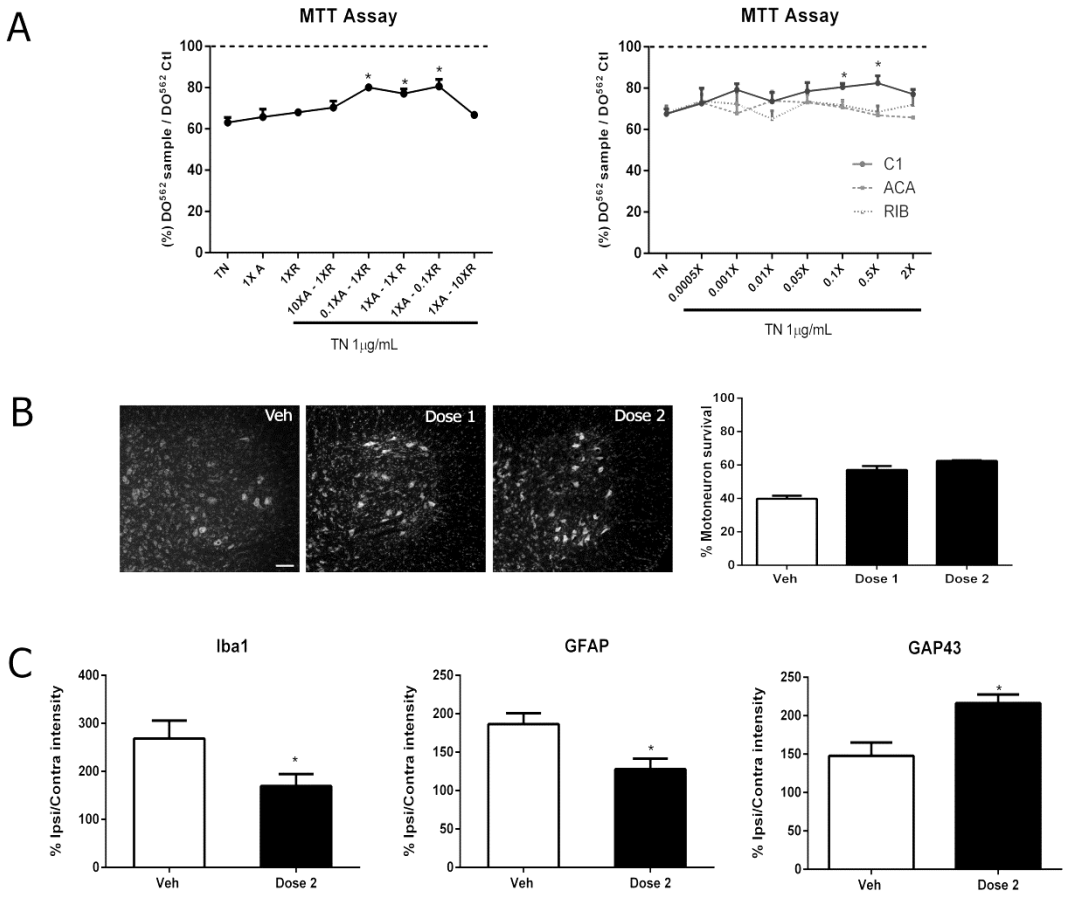

Figure 4. NeuroHeal has a supra-additive neuroprotective effect and is effective upon oral administration. (A) ***Left,*** Histogram of NSC-34 cell survival upon ER stress measured by MTT assay at different dose ratios of ACA (A; 1X = 0.22 mM) to RIB (B; 1X B = 4 μM). ***Right,*** Effect of range of doses within 0-2X with NeuroHeal or with single drugs at 1X ($p<0.05$ with respect to TN alone). **(B)** Representative microphotographs of MNs stained by Nissl at the ipsilateral ventral horns of RA animals treated orally with either vehicle or dose 1 (0.22 mM ACA + 0.4 μM RIB) or dose 2 (0.06 mM ACA + 1 μM RIB), and bar graph of the percentage of surviving MN cells at the ipsilateral side with respect to the contralateral side. **(C)** Histograms of average immunoreactivity intensity for GFAP, Iba1, and GAP43 in a fixed region of interest in the ipsilateral ventral horn in grey matter for GFAP and Iba1 staining or white matter for GAP43 (n=4; *$p<0.05$ vs. vehicle).

NeuroHeal promotes functional recovery

The regenerative potential of NeuroHeal was confirmed in a model of crush injury of the sciatic nerve. The compound muscle action potentials (CMAP) evoked in response to sciatic nerve stimulation were recorded in gastronecmius and plantar muscles to assess functional recovery of denervated muscles. NeuroHeal led to a significant increase in CMAP amplitude in both muscles during the follow-up (**Fig.**

5A). After 28 days, there was reinnervation of the plantar muscle in all of the treated rats but in only 40% of the untreated (**Fig. 5B**), suggesting that NeuroHeal accelerated nerve regeneration. Furthermore, NeuroHeal improved the recovery of motor function, evaluated with the sciatic functional index (**Fig. 5C**), and increased the number of reinnervated neuromuscular junctions, assessed with co-localization of NF-200 with α-bungarotoxin (**Fig. 5D**). The numbers of MNs in rats after nerve crush were not significantly different in vehicle and NeuroHeal treated animals (**Fig. 5E**).

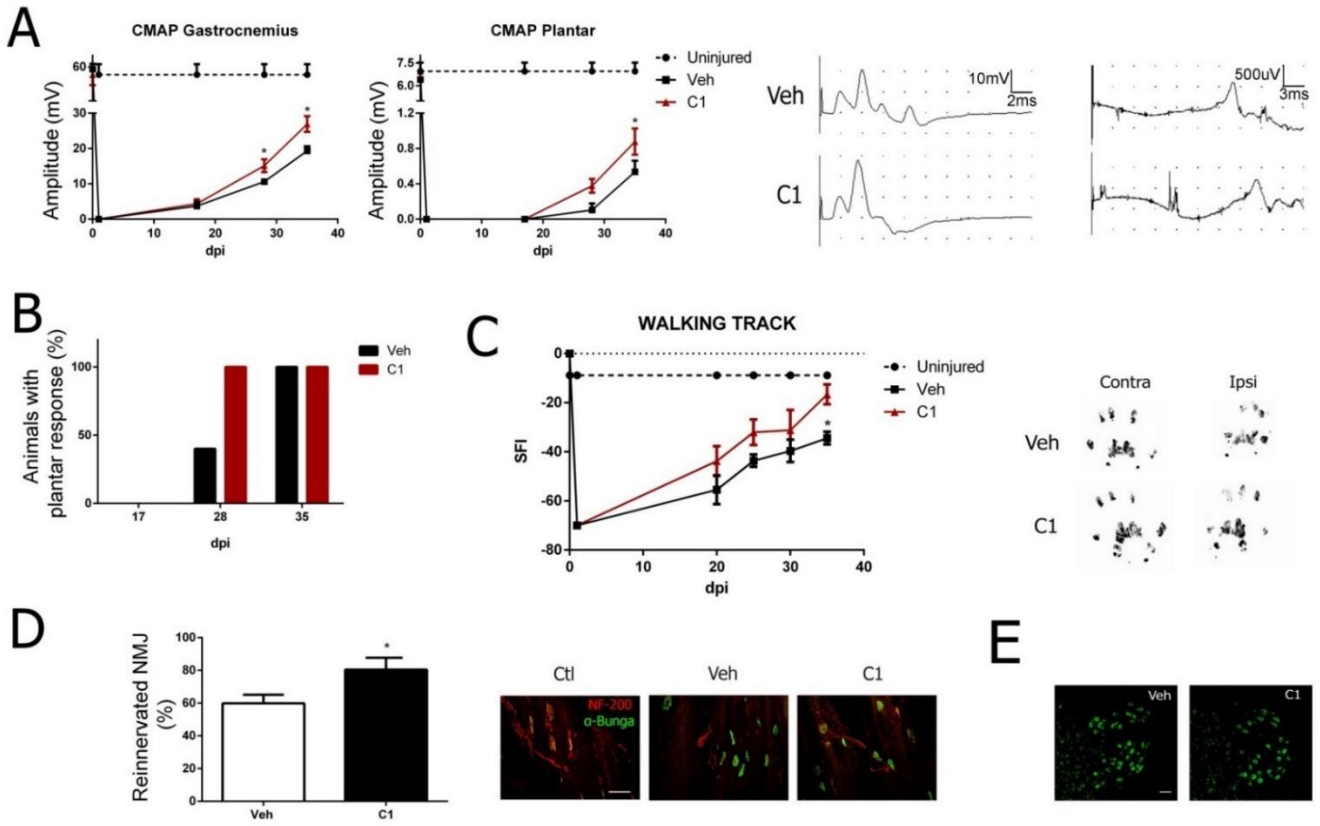

Figure 5. NeuroHeal accelerates nerve regeneration and improves muscle reinnervation and functional recovery after nerve crush injury. (A) ***Left panels,*** mean amplitudes of CMAP from ipsilateral gastrocnemius and plantar muscles after sciatic nerve crush of animals treated with vehicle (Veh) or NeuroHeal (C1; n=5, ANOVA, post hoc Bonferroni*p<0.05 vs. Veh). ***Right panels***, representative recordings. **(B)** Histograms of the percentages of treated animals that presented electrophysiological evidence of reinnervation at the plantar muscle at different time-points. **(C)** ***Left,*** plot of the sciatic functional index (SFI) obtained with walking track analysis of sciatic nerve in RA animals treated with either vehicle (Veh) or NeuroHeal (C1). ***Right***, Representative footprints from ipsi- and contralateral paws at 35 days post injury (dpi). **(D)** ***Left,*** bar graph showing the percentage of reinnervated motor endplates at plantar muscle. ***Right***, representative pictures of reinnervated neuromuscular junctions showing nerve fibers immunostained by NF200 (red) and end-plates labeled with bungarotoxin (green). **(E)** Microphotographs of spinal MNs stained with Nissl green at the ventral horn showing no signs of cell death due to nerve crush at 3 weeks post-injury.

The mechanism of action of NeuroHeal

TPMS analysis allowed the identification of putative proteins that mediate the synergistic mechanism of action (MoA) for NeuroHeal. The manually curated collection of molecular effectors (seeds) used in the model are listed in **Fig. 6A**. We used STRING platform STRING and literature perusal to establish functional relationships among these proteins and the known targets of each drug composing NeuroHeal (**Fig. 6B, S1**). The known actions of ACA (DB00659) include the antagonism of the N-methyl-d-aspartate (NMDA) receptor and the metabotropic glutamate receptor 5 and the positive modulation of GABA receptor (A) (GABAR(A)). Hyperpolarization caused by Cl^- entry due to GABAR(A)) stimulation is normally proceeded by a depolarization caused by L-type voltage-gated calcium channel activation (Gutiérrez et al., 2014). The consequent entry of Ca^{2+} may trigger different pathways, importantly PI3K activation (Feng et al., 2013). PI3K activation may lead to the pro-survival AKT and FOXO pathway activation (Zhan et al., 2012) and also to an increase in cytoskeletal dynamics (Zhao et al., 2007). In particular, it may favor vesicle trafficking such as the gephyrin-mediated transport of GABA receptors to the surface membrane helped by dynactin, Kif5, and Hap1 (Twelvetrees et al., 2010; Papadopoulos et al., 2016) and nucleocytoplasmic shuttling mediated by Ran-binding proteins (RANBP) (Yoon et al., 2008). PI3K activation may also promote the activation of Src-integrin complex which in turn confers anti-anoikis properties (Kang et al., 2011a; Dai et al., 2016). In particular, the Src-integrin complex together with ranbp9 may favour endocytosis, which is anti-amyloidogenic (Woo et al., 2012). Other ranbp proteins may be also activated, such as ranbp9, which is linked to active endocytosis and prevents the generation of amyloid peptide.

RIB (DB00811) inhibits inosine-5'-monophosphate dehydrogenase 1, an enzyme that catalyzes the conversion of inosine 5'-phosphate to xanthosine 5'-phosphate and acts as immunodulator (Koh et al., 2014). Since this reaction consumes NAD^+, its inhibition may lead to NAD^+ accumulation. Hence, SIRT1, a nicotinamide adenine dinucleotide (NAD^+)-dependent histone deacetylase and sensor of the NAD^+/NADH balance (Liu et al., 2009) may activate NAD^+/NADH metabolism in a process involving PDK1 and PKM (Vachharajani et al., 2016). This

leads to deacetylation of p53, which inhibits apoptosis (Wątroba and Szukiewicz, 2016) and deacetylation and reinforced activation of AKT and FOXO (Sedding, 2008; Pallàs et al., 2009), which regulates microtubule dynamics resulting in neuroprotection in a process that involves PLK1 and Dynactin (Kim et al., 2015). Indeed, PLK1 has been shown to reduce cell death mediated by amyloid peptide (Song et al., 2011).

In order to validate this putative MoA, we evaluated the effect of NeuroHeal on expression of some of these proteins such as the subunit b1 of integrin (ITGb1), kinesin family member Kif5c (Casas et al., 2015), SIRT1, and the dynactin subunit DCTN1 in MNs at the ipsilateral site after 21 days post injury (dpi) in the RA model. We found that NeuroHeal increased the cytosolic expression of ITGb1, Kif5c, DCTN1, and SIRT1 in the ipsilateral horn with respect to the contralateral (**Fig. 6C**). Of note, the normalized levels of cytosolic SIRT1 in NeuroHeal treated rats was mostly due to the reduction in injury-induced nuclear expression of the protein. DCTN1 analysis showed that the expression of the target protein was modulated exclusively on the ipsilateral side, suggesting that the MoA of NeuroHeal may be specific to the damage context.

A

Candidate key proteins to MoA in NH synergism		
Uniprot ID	Name	Effect
P08592	A4	Amyloid beta A4 protein
P28023	DCTN1	Dynactin subunit 1
Q9R0I6	XIAP	E3 ubiquitin-protein ligase XIAP
Q9JM53	AIFM1	Apoptosis-inducing factor 1
P11980	KPYM	Pyruvate kinase PKM
F1LTP2	SIRT1	Protein Sirt1
D4A2G9	RANBP1	RAN-binding protein 1
Q04589	FGFR1	Fibroblast growth factor receptor 1 (FGFR-1)
P26051	CD44	CD44 antigen
P27008	PARP1	Poly [ADP-ribose] polymerase 1

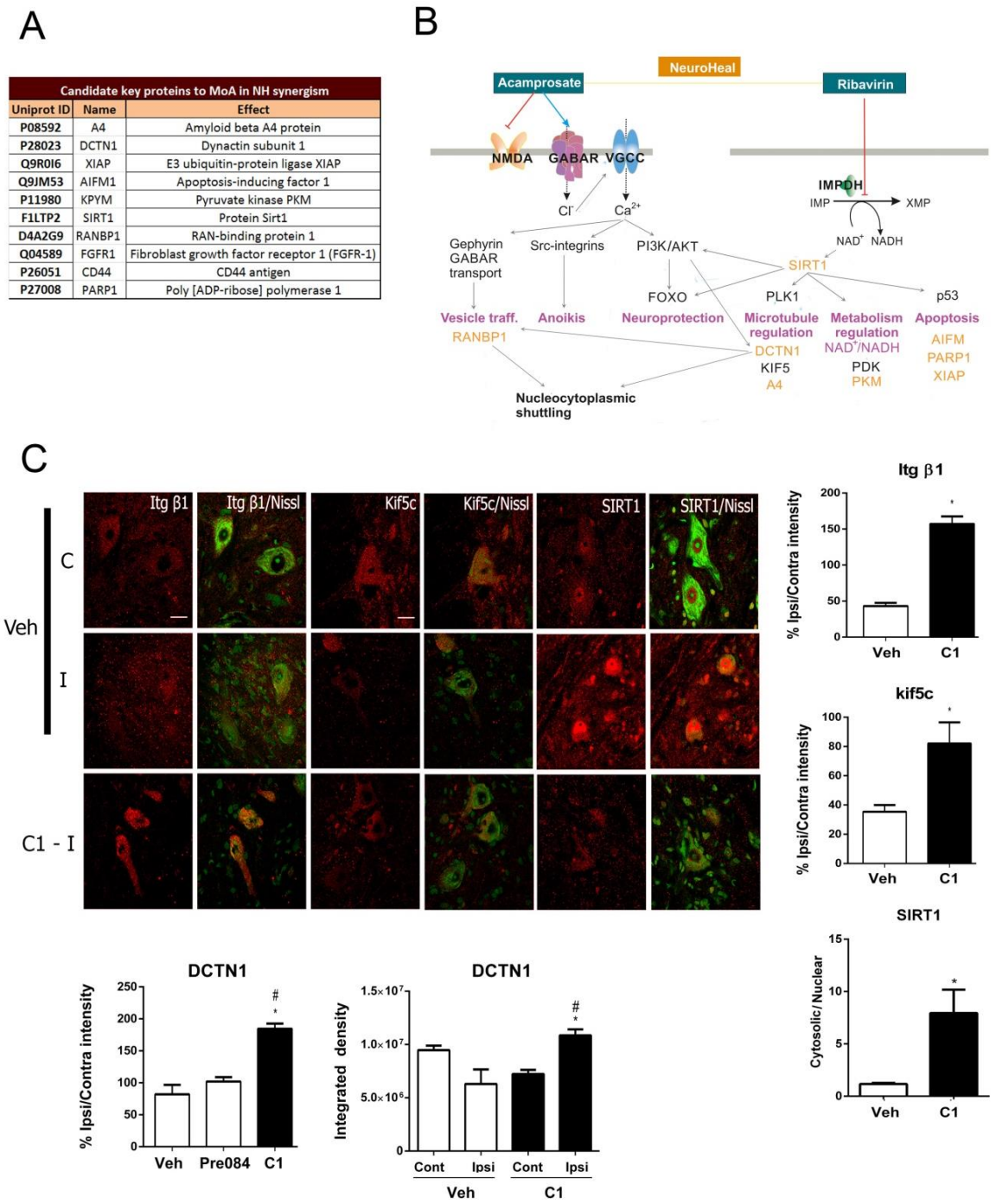

Figure 6. Molecular targets of NeuroHeal. (A) List of seed proteins predicted to be key synergic targets in the action of NeuroHeal. **(B)** Representation of putative NeuroHeal MoA from initial ACA and RIB targets to downstream possible effects to yield the synergic effects (pink) through its targets (orange). Representation is based on analysis using STRING and IntAct platforms and manual scrutiny of relevant literature. **(C)** ***Left,*** microphotographs of ipsilateral (I) and contralateral (C) ventral horns immunostained to reveal Itgb1, Kif5c, and SIRT1 in MNs (red) counterstained with green fluorescent Nissl (merged pictures) in animals treated with vehicle (Veh) or NeuroHeal (C1). Scale bar = 50 μm. ***Right and Bottom***, bar graphs of the average ratios of immunofluorescence intensity (IF) between ipsi- and contralateral sides within an equivalent pre-determined region of interest (ROI) localized in the lateral grey matter for all conditions except for DCTN1, which was measured in the

white matter (n=4 animals, 5 MN/section, 3 sections, *p<0.05). The bottom right histogram of DCTN1 analysis shows the quantification of total integrated intensity on each side to document that NeuroHeal only changes expression on the injured site (n=4 animals, 5 MN/section, 3 sections, *p<0.05).

Due to the importance of SIRT1 in many pathological conditions and in life span (Hubbard and Sinclair, 2014), we investigated further whether SIRT1 was activated by NeuroHeal. First, we sought to determine whether viral overexpression of SIRT1 mimics resulted in neuroprotection after RA since, due to NAD^+ depletion promoted by SIRT1, SIRT1 does not always promote neuroprotection (Liu et al., 2009). We cloned the *SIRT1* gene into a recombinant adeno-associated viral vector 10 (AAVrh10), which we previously had reported as being highly specific to MNs when intrathecally delivered to the spinal cord (Homs et al., 2014). SIRT1 overexpression was localized in MNs, mainly in the cytoplasm **(Fig. 7A**). Within avulsed MNs, infection with AAVrh10-GFP did not change the nuclear ring-like pattern of SIRT1 expression induced by RA, but infection with AAVrh10-SIRT1 led to accumulation of SIRT1 predominantly in the cytoplasm of MNs, similar to NeuroHeal's effect (**Fig. 7A**).

Second, we measured the deacetylase activity of SIRT1 by assessing the contents of histone-H3 acetylated at Lys9 (H3-K9) and of p53 acetylated at Lys373 (p53-K373) residues (Vaquero et al., 2004),(Vaziri et al., 2001),. In RA animals treated with AAVrh10-SIRT1we observed: i) a decrease in both H3-K9 and p53-K373 acetylated forms, suggesting that SIRT1 overexpression caused an activity increase (**Fig. 7B**) and ii) a significant increase in MN survival (up to 52.90% ± 1.79) (**Fig. 7C**). Together these results suggest that overexpression and subsequent enhanced activation of SIRT1 is neuroprotective in severe peripheral nerve lesions.

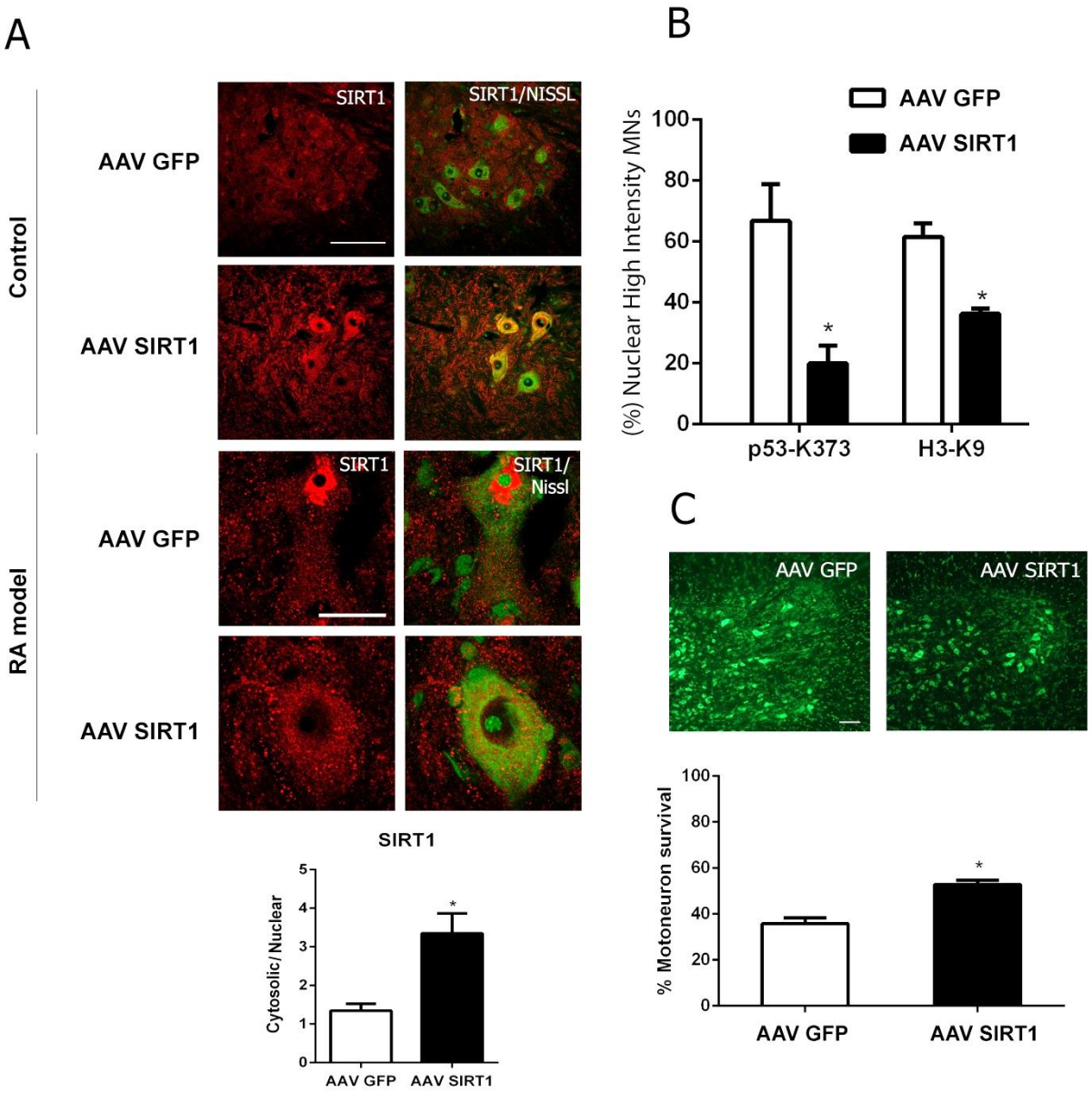

Figure 7. SIRT1 overexpression promotes MN survival after RA. **(A)** ***Top***, representative microphotographs of SIRT1 immunolabelling (red) in infected MNs in control animals (*upper*) and RA injured animals (*lower*) treated with either AAVrh10-GFP or AAVrh10-SIRT1 and counterstained with green fluorescent Nissl. Scale bar = 100 µm (top); 25 µm (bottom). ***Bottom*,** histogram of cytosolic versus nuclear SIRT1 localization in the RA-injured MNs 21dpi after damage. **(B)** Histogram of the percentage of avulsed MNs with high nuclear immunofluorescence intensity for each acetylated form of either H3 (H3-K9) or p53 (p53-K373) at the ipsilateral side of RA animals infected with either vector (n=4, *p<0.05 vs. AAV-GFP). **(C)** Representative microphotographs of Nissl-labelled MNs (green) at the ipsilateral ventral horns of RA animals treated with either AAVrh10-GFP or AAVrh10-SIRT1and histogram of MN survival ± SEM expressed as % of MN on the contralateral side (contra) (n=4, *p<0.05 vs. AAVrh10-GFP).

Third, we evaluated the effect of NeuroHeal in combination with either a specific inhibitor of SIRT1, Ex-527, which promotes the persistence of acetylated forms, or spermidine, an inhibitor of acetylases that causes the persistence of deacetylated forms (Eisenberg et al., 2009). Rats were treated with NeuroHeal and either Ex-527 or spermidine using the continuous intrathecal pump perfusion system for 20 days post RA injury. As readouts, we used nuclear SIRT1, H3-K9, and p53-K373 in injured MNs at the ipsilateral ventral horn. Maximal expression of all markers was observed in untreated and vehicle-treated mice. Spermidine did not alter SIRT1 distribution but, as expected, reduced H3-K9 and p53-K373 levels (**Fig.8A**). NeuroHeal reduced levels of SIRT1 and acetylated forms of H3 and p53 and this effect was reversed by Ex-527 but not spermidine (**Fig. 8A**). Accordingly, spermidine, either alone or in combination with NeuroHeal, increased the survival rate of MN whereas Ex-527 abolished the neuroprotective effect exerted by the drug (**Fig. 8B**).

Finally, we compared the regenerative and anti-inflammatory capacities of NeuroHeal with those of virally transduced SIRT1 and spermidine. Although all treatments were neuroprotective, only NeuroHeal promoted GAP43 expression and reduced microgliosis and astrogliosis (**Fig. 8C, D**). These results demonstrate that deacetylation is important for the NeuroHeal-mediated neuroprotection after RA and that, synergistically acting through multiple targets, NeuroHeal performs better than single-target drugs.

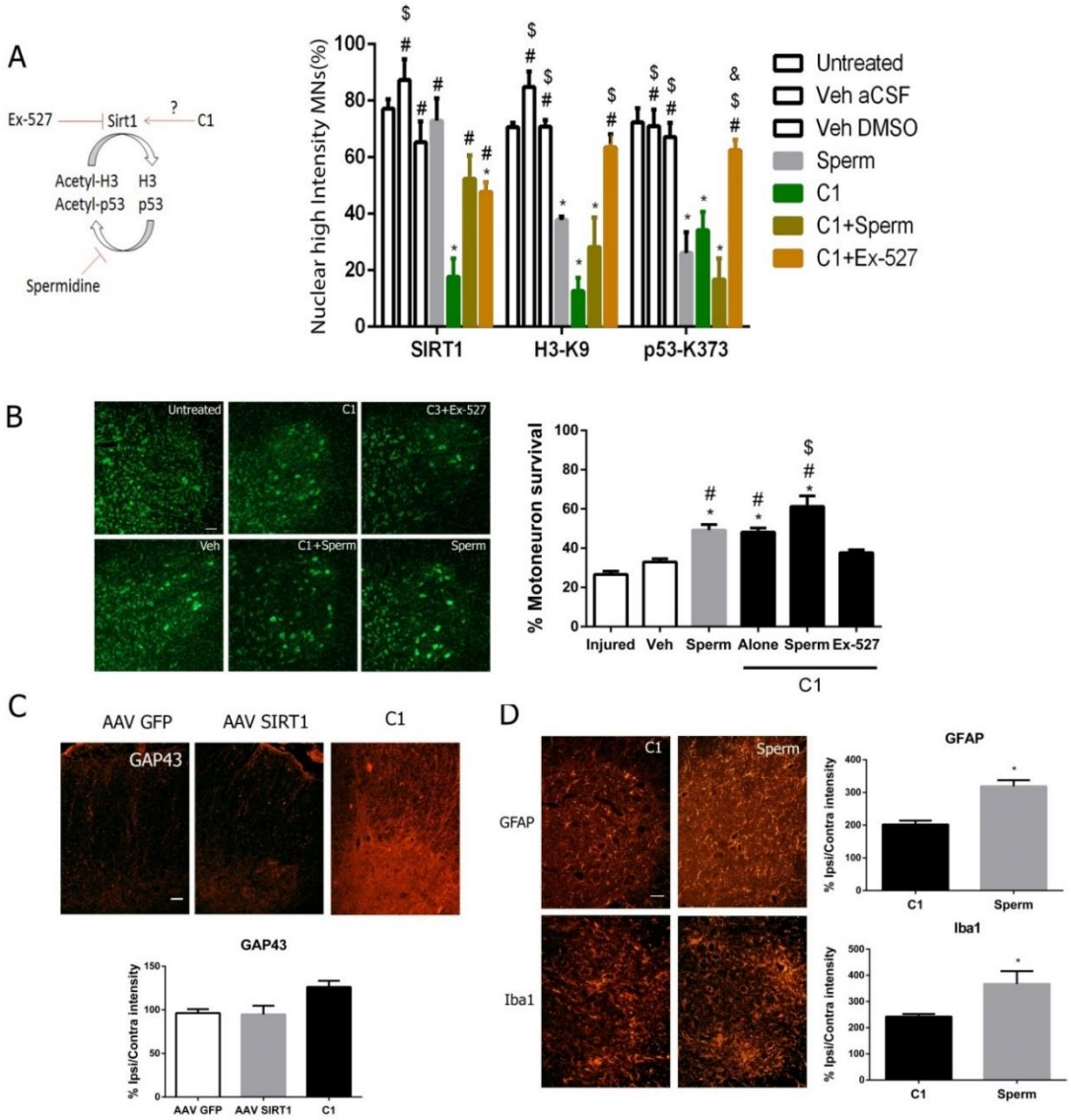

Figure 8. SIRT1 mediates the neuroprotective effect of NeuroHeal. (A) Diagram of the mechanisms of action of spermidine and Ex-527 and histogram of the percentage of avulsed MNs with high nuclear immunofluorescence intensity for each marker on the ipsilateral side of RA animals treated with different drugs (n= 6 for untreated; n=3 for Veh DMSO; n=4 other groups, ANOVA, post hoc Bonferroni*p<0.05 vs, #p<0.05 vs. C1, $p<0.05 vs. C1+Sperm, & p<0.05 vs. Sperm). **(B)** Representative microphotographs of MNs on the ipsilateral sides and associated histogram of the average percentage of MN survival ± SEM in animals intrathecally treated with spermidine (Sperm) or Ex-527 with or without NeuroHeal (C1) (n=4, ANOVA, post hoc Bonferroni *p<0.05 vs. untreated, # p<0.05 vs. veh, $ p<0.05 vs. C1+Ex-527, *p<0.05). Scale bar = 100 µm. **(C)** Microphotographs of GAP43 immunostaining at the ventral horns of the ipsilateral sides from animals treated with either AAVrh10-GFP, AAVrh10-SIRT1 or C1. Scale bar = 100 µm. Bar graph of the average immunoreactivity in a fixed region of interest of the white matter (n=3-4, *p<0.05 vs. AAVrh10-GFP). **(D)** Representative microphotographs of astrocyte (GFAP) or microglia (Iba1) staining at the ventral horns of the ipsilateral sides of RA animals treated with either NeuroHeal (C1) or spermidine (Sperm). Scale bar=100 µm. Associated histograms of the average immunoreactivity in a fixed region of interest of the grey matter (*p<0.05 vs. C1).

DISCUSSION

Network medicine has become increasingly important for identifying novel disease mechanisms and predicting drug effects. This network-based approach enables elucidation of the underlying molecular mechanisms, mainly in terms of disease modules, disease phenotypes, and disease-disease associations (Barabási et al., 2011a; Chen and Butte, 2013; Zhou et al., 2014). A number of studies have investigated the disease modules associated with specific disease phenotypes such as asthma, diabetes, and cancer, for which a single disease module would mainly be detected (Wang et al., 2013; Sharma et al., 2015). That there should be a shift in the paradigm of drug discovery from a focus on single targets to the systems has been argued (He et al., 2016a), particularly in neuropathology (Margineanu, 2016).

We reasoned that proteomic profiles from suitable preclinical models of MN neurodegeneration would provide unbiased data for use as input to machine learning and mathematical modeling to search for novel drug combinations. We took advantage of the existence of advanced molecular knowledge of the dissimilar reactions in MNs after either proximal or distal axotomy with opposite readouts (degeneration vs. survival, respectively). The rationale was that mimicking the endogenous mechanism that MNs engage in after distal axotomy should be neuroprotective. Computational tools available allowed us to screen for known drugs that *in silico* perturb the RA model to convert it into a DA model. We validated that some of the synergic drug combinations discovered *in silico* were neuroprotective in cell culture models and *in vivo*. The combination we call NeuroHeal had anti-inflammatory properties and induced pre-regenerative profiles in MNs. Furthermore, we identified the molecular downstream pathway that is modulated by NeuroHeal: SIRT1 is an important node in the network. Moreover, we validated that activation of SIRT1 mediated the neuroprotective action of NeuroHeal in a rat model of RA. To our knowledge this is the first work to demonstrate discovery of repurposed drug combinations using a network-centric approach with learning machine computational tools that moves forward from theory to practice and validates both the efficacy and mechanism of action using preclinical *in vivo* models. Previous partial studies have paved the way (Sirota et al., 2011; Zhao et al., 2011; Lecca and Re, 2017).

Combined actions of ACA and RIB in NeuroHeal resulted in neuroprotection probably by exerting anti-apoptosis and anti-anoikis actions that we previously had shown to be key elements to activate the endogenous mechanisms of neuroprotection in axotomized MNs (Casas et al., 2015). In the same report and in others (Penas et al., 2009a), the importance of cytoskeletal rearrangements for neuroprotection was also revealed; these rearrangements also appear to be facilitated by the NeuroHeal MoA. It would be interesting to validate the role of these and the others described processes in NeuroHeal MoA, similarly to what we have done for SIRT1.

NeuroHeal activated SIRT1 in damaged MNs after axonal disconnection. This is an interesting discovery because SIRT1 activators have long been sought due to the beneficial effects likely for several diseases (Blander and Guarente, 2004; Bordone and Guarente, 2005; Milne et al., 2007). Although SIRT1 is important for neurodegeneration (Haigis and Guarente, 2006), it does not always lead to neuroprotection because it exhausts NAD^+ resources (Liu et al., 2009). The main advantage of NeuroHeal as compared to other recently discovered small-molecule sirtuin-activating compounds (e.g., STAC) (Hubbard and Sinclair, 2014) is that its components have been proven to be safe for humans and cross the blood-brain barrier. Of note, NeuroHeal has effects beyond SIRT1 activation since it also promotes the expression of the pro-regenerative marker GAP43, while overexpression of SIRT1 does not. Finally, although we found that spermidine also affords neuroprotection of MNs after RA, its use in the clinic has been avoided as it is nociceptive (Gewehr et al., 2011). Our work indicates that the role of epigenetic switches in neuroprotection deserves further investigation.

Unexpectedly, we found that NeuroHeal promoted nerve regeneration and functional recovery after nerve crush. This finding suggested that the proteomic data used from DA models may contain intrinsically pro-regenerative factors. It would be worth testing this hypothesis in more severe models to study CNS axon regeneration.

The properties of NeuroHeal make it a first-in-class therapeutic agent for nerve root disconnection or entrapments. The translation of NeuroHeal to the clinic will be facilitated because it is composed of already FDA-approved drugs.

Knowledge about formulation is also advanced because we assessed the effect of different stoichiometry combinations of single drugs to achieve neuroprotective synergism.

We conclude that our network-centric discovery approach encompassing proteomic data relevant to disease and artificial intelligence is a powerful and promising methodology for the design of effective treatments based on drug repurposing. Repurposing speeds up the clinical translation of treatments for complex pathological conditions. Patent protection of NeuroHeal is currently in progress and funding is being raised in order to test the drug in a clinical trial.

ACKNOWLEDGEMENTS

We thank Marta Morell for taking excellent care of the animals and Ariadna Arasanz for helping with culture maintenance. We thank Tomas Santalucía for guidance with SIRT1 plasmid and Alex Vaquero for providing H3-K9 antibody. **Funding:** This work was mainly supported by a grant from Fundació La Marató-TV3 (#110432, CC, AB & VP) that funded the work and contracts of TLR and MHG and partially by the Ministerio de Economía y Competitividad of Spain (#SAF 2014-59701, CC, DRG, & TLR). We are also grateful for support from CIBERNED and funding from the European Union Seventh Framework Programme for research, technological development, and demonstration (# 306240, XN, FRP &CC).

AUTHOR CONTRIBUTIONS

DRG performed the experiments, analyzed the results, and wrote part of the manuscript. JF performed all the surgeries. MHG and TLR set up the in vitro models and provided technical help. FGP and XN conceived and performed the electrophysiological analysis. JMM conceived, MC coordinated, and AP and RV carried out the in silico experiments and analysis. VP and AB generated the AAVrh10 viral vector and made a critical reading of the manuscript. EG did a critical edit of the manuscript. CC conceived, designed, supervised, and analyzed all the experiments and wrote the manuscript.

ADDITIONAL INFORMATION

Competing Financial Interest: MC and RV are employees and JMM is founder and CEO of Anaxomics Biotech. JMM contributed to the design of TPMS. The other authors DR, JF, MHG, TLR, EG, FRP, XN, VP, AB, and CC declare no competing interests. NeuroHeal is currently under patent review.

SUPPLEMENTARY DATA

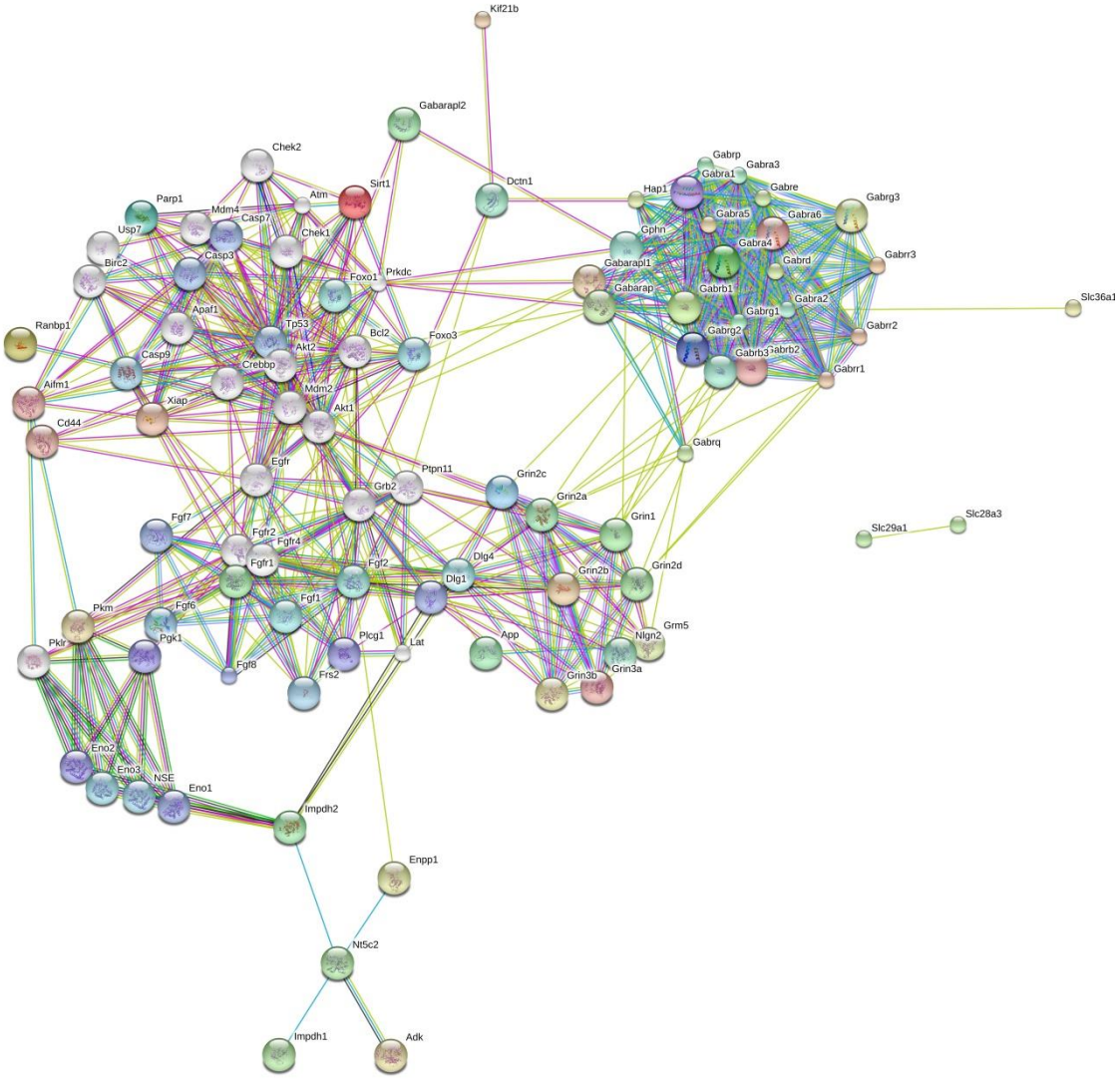

Supplemental Figure 1. Extended protein-protein interaction network resulting from STRING analysis with default parameters. Initial seeds used were NH synergic MoA-related proteins and known targets from ACA and RIB.

REFERENCES

Arce-Medina E, Paz-Paredes JI (2009) Artificial neural network modeling techniques applied to the hydrodesulfurization process. Math Comput Model 49:207–214

Badiola N, Alcalde V, Pujol A, Münter L-M, Multhaup G, Lleó A, Coma M, Soler-López M, Aloy P (2013) The proton-pump inhibitor lansoprazole enhances amyloid beta production. PLoS One 8:e58837

Barabási A-L, Gulbahce N, Loscalzo J (2011) Network medicine: a network-based approach to human disease. Nat Rev Genet 12:56–68.

Berman JS, Birch R, Anand P (1998) Pain following human brachial plexus injury with spinal cord root avulsion and the effect of surgery. Pain 75:199–207 Blander G, Guarente L (2004) The Sir2 family of protein deacetylases. Annu Rev Biochem 73:417–435.

Bordone L, Guarente L (2005) Calorie restriction, SIRT1 and metabolism: understanding longevity. Nat Rev Mol Cell Biol 6:298–305.

Brooksbank C, Camon E, Harris MA, Magrane M, Martin MJ, Mulder N, O'Donovan C, Parkinson H, Tuli MA, Apweiler R, Birney E, Brazma A, Henrick K, Lopez R, Stoesser G, Stoehr P, Cameron G (2003) The European Bioinformatics Institute's data resources. Nucleic Acids Res 31:43–50.

Casas C, Isus L, Herrando-Grabulosa M, Mancuso FM, Borrás E, Sabidó E, Forés J, Aloy P (2015) Network-based proteomic approaches reveal the neurodegenerative, neuroprotective and pain-related mechanisms involved after retrograde axonal damage. Sci Rep 5:9185

Chautard E, Fatoux-Ardore M, Ballut L, Thierry-Mieg N, Ricard-Blum S (2011) MatrixDB, the extracellular matrix interaction database. Nucleic Acids Res 39:D235-40.

Chen B, Butte AJ (2013) Network Medicine in Disease Analysis and Therapeutics. Clin Pharmacol Ther 94:627–629.

Cohen SP, Mao J (2014) Neuropathic pain: mechanisms and their clinical implications. BMJ 348:f7656

Croft D et al. (2014) The Reactome pathway knowledgebase. Nucleic Acids Res 42:D472-7.

Cybenko G (1989) Approximation by superpositions of a sigmoidal function. Math

Control Signals, Syst 2:303–314.

Dai H, Lv Y, Yan G, Meng G, Zhang X, Guo Q (2016) RanBP9 / TSSC3 complex cooperates to suppress anoikis resistance and metastasis via inhibiting Src-mediated Akt signaling in osteosarcoma. Nat Publ Gr 7:e2572-12.

Daoust M, Legrand E, Gewiss M, Heidbreder C, DeWitte P, Tran G, Durbin P (1992) Acamprosate modulates synaptosomal GABA transmission in chronically alcoholised rats. Pharmacol Biochem Behav 41:669–674.

de Medinaceli L (1988) Functional consequences of experimental nerve lesions: Effects of reinnervation blend. Exp Neurol 100:166–178.

Dias JJ, Garcia-Elias M (2006) Hand injury costs. Injury 37:1071–1077.

Eisenberg T et al. (2009) Induction of autophagy by spermidine promotes longevity. Nat Cell Biol 11:1305–1314

Feng Y, Wang B, Du F, Li H, Wang S, Hu C, Zhu C (2013) The Involvement of PI3K-Mediated and L-VGCC-Gated Transient Ca 2 + Influx in 17β-Estradiol-Mediated Protection of Retinal Cells from H 2 O 2 -Induced Apoptosis with Ca 2 + Overload. 8:1–12.

Gewehr C, da Silva MA, dos Santos GT, Rossato MF, de Oliveira SM, Drewes CC, Pazini AM, Guerra GP, Rubin MA, Ferreira J (2011) Contribution of peripheral vanilloid receptor to the nociception induced by injection of spermine in mice. Pharmacol Biochem Behav 99:775–781.

Goldberg DE (n.d.) Genetic Algorithms in Search, Optimization, and Machine Learning, 1st ed. Addison-Wesley.

Gómez-serrano M, Camafeita E, García-santos E, López JA, Rubio MA, Sánchez-pernaute A, Torres A, Vázquez J (2016) Proteome-wide alterations on adipose tissue from obese patients as age- , diabetes- and gender-specific hallmarks. Sci Rep 6:25756.

Gutiérrez ML, Ferreri MC, Gravielle MC (2014) GABA-induced uncoupling of GABA/benzodiazepine site interactions is mediated by increased GABAA receptor internalization and associated with a change in subunit composition. Neuroscience 257:119–129.

Haigis MC, Guarente LP (2006) Mammalian sirtuins--emerging roles in physiology, aging, and calorie restriction. Genes Dev 20:2913–2921.

He B, Lu C, Zheng G, He X, Wang M, Chen G, Zhang G, Lu A (2016) Combination

therapeutics in complex diseases. J Cell Mol Med 20:2231–2240.

Herrando-Grabulosa M, Mulet R, Pujol A, Mas JM, Navarro X, Aloy P, Coma M, Casas C (2016) Novel Neuroprotective Multicomponent Therapy for Amyotrophic Lateral Sclerosis Designed by Networked Systems. PLoS One 11:e0147626.

Homs J, Pagès G, Ariza L, Casas C, Chillón M, Navarro X, Bosch A (2014) Intrathecal administration of IGF-I by AAVrh10 improves sensory and motor deficits in a mouse model of diabetic neuropathy. Mol Ther — Methods Clin Dev 1:7.

Hubbard BP, Sinclair DA (2014) Small molecule SIRT1 activators for the treatment of aging and age-related diseases. Trends Pharmacol Sci 35:146–154.

Huhn SL (1991) Technical note. 29:943–946.

Iborra-egea O, Gálvez-montón C, Roura S, Perea-gil I, Prat-vidal C, Soler-botija C (2017) Mechanisms of action of sacubitril / valsartan on cardiac remodeling : a systems biology approach. npj Syst Biol Appl:1–8.

Kanehisa M, Goto S, Hattori M, Aoki-Kinoshita KF, Itoh M, Kawashima S, Katayama T, Araki M, Hirakawa M (2006) From genomics to chemical genomics: new developments in KEGG. Nucleic Acids Res 34:D354–D357.

Kang DE, Roh SE, Woo JA, Liu T (2011) The Interface between Cytoskeletal Aberrations and Mitochondrial Dysfunction in Alzheimer ' s Disease and Related Disorders. 20:67–80.

Keshava Prasad TS et al. (2009) Human Protein Reference Database--2009 update. Nucleic Acids Res 37:D767–D772.

Kim J, Gil N, Zhang XH, Chun K, Fang G, Kim J, Cho H, Jang C, Cha H (2015) Sirt1 Regulates Microtubule Dynamics Through Negative Regulation of Plk1 in Mitosis. 1897:1888–1897.

Kirkpatrick S, Gelatt CD, Vecchi MP (1983) Optimization by simulated annealing. Science 220:671–680.

Koh C, Abdalla A, Gara N, Sarkar S, Thomas E (2014) Effect of Ribavirin on Viral Kinetics and Liver Gene Expression in Chronic Hepatitis C. Gut 63:1–26.

Lecca P, Re A (2017) Network-Oriented Approaches to Anticancer Drug Response. Methods Mol Biol 1513:101–117.

Licata L, Briganti L, Peluso D, Perfetto L, Iannuccelli M, Galeota E, Sacco F, Palma A, Nardozza AP, Santonico E, Castagnoli L, Cesareni G (2012) MINT, the molecular interaction database: 2012 update. Nucleic Acids Res 40:D857-61.

Liu D, Gharavi R, Pitta M, Gleichmann M, Mattson MP (2009) Nicotinamide prevents NAD+ depletion and protects neurons against excitotoxicity and cerebral ischemia: NAD+ consumption by SIRT1 may endanger energetically compromised neurons. Neuromolecular Med 11:28–42.

Loeb JE, Cordier WS, Harris ME, Weitzman MD, Hope TJ (1999) Enhanced expression of transgenes from adeno-associated virus vectors with the woodchuck hepatitis virus posttranscriptional regulatory element: implications for gene therapy. Hum Gene Ther 10:2295–2305

Lopes CT, Franz M, Kazi F, Donaldson SL, Morris Q, Bader GD (2010) Cytoscape Web: an interactive web-based network browser. Bioinformatics 26:2347–2348.

Margineanu DG (2016) Neuropharmacology beyond reductionism – A likely prospect. Biosystems 141:1–9.

Mas J, Pujol A, Farrés J, Aloy P (2010) Methods and systems for identifying molecules or processes of biological interest by using knowledge discovery in biological data.

Mason BJ, Goodman AM, Dixon RM, Hameed MHA, Hulot T, Wesnes K, Hunter JA, Boyeson MG (2002) A pharmacokinetic and pharmacodynamic drug interaction study of acamprosate and naltrexone. Neuropsychopharmacology 27:596–606.

Mewes HW, Ruepp A, Theis F, Rattei T, Walter M, Frishman D, Suhre K, Spannagl M, Mayer KFX, Stümpflen V, Antonov A (2011) MIPS: curated databases and comprehensive secondary data resources in 2010. Nucleic Acids Res 39:D220-4.

Milne JC et al. (2007) Small molecule activators of SIRT1 as therapeutics for the treatment of type 2 diabetes. Nature 450:712–716.

Mitchell M (1998) An Introduction to Genetic Algorithms (Complex Adaptive Systems).

Pallàs M, Casadesús G, Smith MA, Coto-montes A, Pelegri C, Vilaplana J, Camins A (2009) Resveratrol and Neurodegenerative Diseases : Activation of SIRT1 as the Potential Pathway towards Neuroprotection. :70–81.

Papadopoulos T, Rhee HJ, Subramanian D, Paraskevopoulou F, Mueller R, Schultz C, Brose N, Rhee J, Betz H (2016) Endosomal Phosphatidylinositol-3-Phosphate Promotes Gephyrin Clustering and GABAergic Neurotransmission at Inhibitory

Postsynapses. J Biol Chem 292:1160–1177.

Penas C, Casas C, Robert I, Fores J, Navarro X (2009) Cytoskeletal and activity-related changes in spinal motoneurons after root avulsion. J Neurotrauma 26:763–779.

Penas C, Font-Nieves M, Forés J, Petegnief V, Planas a, Navarro X, Casas C (2011a) Autophagy, and BiP level decrease are early key events in retrograde degeneration of motoneurons. Cell Death Differ 18:1617–1627

Penas C, Pascual-Font A, Mancuso R, Forés J, Casas C, Navarro X (2011b) Sigma receptor agonist 2-(4-morpholinethyl)1 phenylcyclohexanecarboxylate (Pre084) increases GDNF and BiP expression and promotes neuroprotection after root avulsion injury. J Neurotrauma 28:831–840

Piedra J, Ontiveros M, Miravet S, Penalva C, Monfar M, Chillon M (2015) Development of a rapid, robust, and universal picogreen-based method to titer adeno-associated vectors. Hum Gene Ther Methods 26:35–42.

Pyun K, Son JS, Kwon YB (2014) Chronic activation of sigma-1 receptor evokes nociceptive activation of trigeminal nucleus caudalis in rats. Pharmacol Biochem Behav 124C:278–283.

Roh D-H, Choi S-R, Yoon S-Y, Kang S-Y, Moon J-Y, Kwon S-G, Han H-J, Beitz AJ, Lee J-H (2011) Spinal nNOS activation mediates sigma-1 receptor-induced mechanical and thermal hypersensitivity in mice: involvement of PKC-dependent NR1 phosphorylation. Br J Pharmacol.

Rosenblatt F (1961) PRINCIPLES OF NEURODYNAMICS. PERCEPTRONS AND THE THEORY OF BRAIN MECHANISMS. Spartan Books.

Salwinski L, Licata L, Winter A, Thorneycroft D, Khadake J, Ceol A, Aryamontri AC, Oughtred R, Livstone M, Boucher L, Botstein D, Dolinski K, Berardini T, Huala E, Tyers M, Eisenberg D, Cesareni G, Hermjakob H (2009) Recurated protein interaction datasets. Nat Methods 6:860–861.

Sedding DG (2008) FoxO transcription factors in oxidative stress response and ageing – a new fork on the way to longevity ? 389:279–283.

Sharma A et al. (2015) A disease module in the interactome explains disease heterogeneity, drug response and captures novel pathways and genes in asthma. Hum Mol Genet 24:3005–3020.

Sirota M, Dudley JT, Kim J, Chiang AP, Morgan AA, Sweet-Cordero A, Sage J, Butte AJ

(2011) Discovery and Preclinical Validation of Drug Indications Using Compendia of Public Gene Expression Data. Sci Transl Med 3:96ra77-96ra77.

Song B, Davis K, Liu XS, Lee H, Smith M, Liu X (2011) Inhibition of Polo - like kinase 1 reduces beta - amyloid - induced neuronal cell death in Alzheimer ' s disease. 3:846–851.

Tallarida RJ (2000a) Drug Synergism and Dose-Effect Data Analysis.

Tallarida RJ (2000b) Drug synergism and dose-effect dasta analysis. Chapman and Hall/CRC.

Tsubota A, Hirose Y, Izumi N, Kumada H (2003) Pharmacokinetics of ribavirin in combined interferon-alpha 2b and ribavirin therapy for chronic hepatitis C virus infection. Br J Clin Pharmacol 55:360–367.

Twelvetrees AE, Yuen EY, Arancibia-carcamo IL, Andrew F, Rostaing P, Lumb MJ, Humbert S, Triller A, Saudou F, Yan Z, Kittler JT (2010) Deslivery of GABA Rs to synapses is mediated by HAP1-KIF5 and A disrupted by mutant huntingtin. Neuron 65:53–65.

Vachharajani VT, Liu T, Wang X, Hoth JJ, Yoza BK, Mccall CE (2016) Sirtuins Link Inflammation and Metabolism. 2016.

Valls R, Pujol A, Artigas L (2013) Anaxomics' methodologies: understanding the complexity of biological processes. white Pap.

Vaquero A, Scher M, Lee D, Erdjument-Bromage H, Tempst P, Reinberg D (2004) Human SirT1 interacts with histone H1 and promotes formation of facultative heterochromatin. Mol Cell 16:93–105.

Vaziri H, Dessain SK, Eaton EN, Imai SI, Frye R a., Pandita TK, Guarente L, Weinberg R a. (2001) hSIR2SIRT1 functions as an NAD-dependent p53 deacetylase. Cell 107:149–159.

Wang C-P, Li J-L, Zhang L-Z, Zhang X-C, Yu S, Liang X-M, Ding F, Wang Z-W (2013) Isoquercetin protects cortical neurons from oxygen-glucose deprivation-reperfusion induced injury via suppression of TLR4-NF-κB signal pathway. Neurochem Int 63:741–749.

Wątroba M, Szukiewicz D (2016) The role of sirtuins in aging and age-related diseases. Adv Med Sci 61:52–62.

Wishart DS, Knox C, Guo AC, Cheng D, Shrivastava S, Tzur D, Gautam B, Hassanali M (2008) DrugBank: a knowledgebase for drugs, drug actions and drug targets.

Nucleic Acids Res 36:D901-6.

Woo JA, Jung AR, Lakshmana MK, Bedrossian A, Lim Y, Bu JH, Park SA, Koo EH, Kang DE (2012) Pivotal role of the RanBP9-cofilin pathway in A b -induced apoptosis and neurodegeneration. :1413–1423.

Xenarios I, Rice DW, Salwinski L, Baron MK, Marcotte EM, Eisenberg D (2000) DIP: the database of interacting proteins. Nucleic Acids Res 28:289–291.

Yoon SO, Shin S, Liu Y, Ballif BA, Woo MS, Gygi SP, Blenis J (2008) Ran-Binding Protein 3 Phosphorylation Links the Ras and PI3-Kinase Pathways to Nucleocytoplasmic Transport. Mol Cell 29:362–375.

Zhan L, Li D, Liang D, Wu B, Zhu P, Wang Y, Sun W, Xu E (2012) Activation of Akt/FoxO and inactivation of MEK/ERK pathways contribute to induction of neuroprotection against transient global cerebral ischemia by delayed hypoxic postconditioning in adult rats. Neuropharmacology 63:873–882.

Zhao X-M, Iskar M, Zeller G, Kuhn M, van Noort V, Bork P (2011) Prediction of drug combinations by integrating molecular and pharmacological data. PLoS Comput Biol 7:e1002323.

Zhao Y, Gaidarov I, Keen JH (2007) Phosphoinositide 3-Kinase C2 ? Links Clathrin to. 282:1249–1256.

Zhou X, Menche J, Barabási A-L, Sharma A (2014) Human symptoms–disease network. Nat Commun 5:4212.

Zolotukhin S, Byrne BJ, Mason E, Zolotukhin I, Potter M, Chesnut K, Summerford C, Samulski RJ, Muzyczka N (1999) Recombinant adeno-associated virus purification using novel methods improves infectious titer and yield. Gene Ther 6:973–985.

Zornoza T, Cano MJ, Polache A, Granero L (2003) Pharmacology of acamprosate: an overview. CNS Drug Rev 9:359–374.

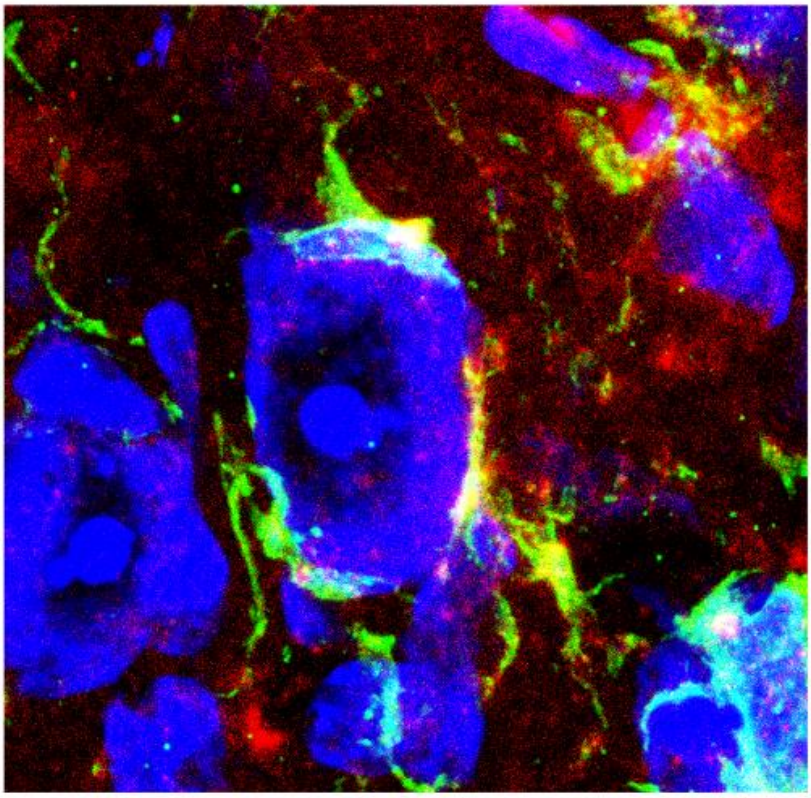

CHAPTER 2

Neuroprotection of Disconnected Motoneurons requires Sirtuin 1 activation but Sirtuin 2 depletion or inhibition with AK-7 is detrimental

David Romeo-Guitart[1], Tatiana Leiva-Rodríguez[1], Núria Sima[2], Alex Vaquero[2], Helena Domínguez-Martín,[3,4], Diego Ruano[3,4], Caty Casas[1]

Affiliations

[1] *Institut de Neurociències* (INc) and Department of Cell Biology, Physiology and Immunology, *Universitat Autònoma de Barcelona* (UAB), & *Centro de Investigación Biomédica en Red sobre Enfermedades Neurodegenerativas* (CIBERNED), Bellaterra, Barcelona, Spain,

[2] Chromatin Biology Laboratory, Cancer Epigenetics and Biology Program, *Institut d'Investigació Biomèdica de Bellvitge,* Barcelona, Spain.

[3] *Departamento de Bioquímica y Biología Molecular, Facultad de Farmacia, Universidad de Sevilla*, 41012, Sevilla, Spain.

[4] *Instituto de Biomedicina de Sevilla (IBiS)-Hospital Universitario Virgen del Rocío/Consejo Superior de Investigaciones Científicas/Universidad de Sevilla*, 41013, Sevilla, Spain.

To whom correspondence should be addressed: Caty Casas Louzao, *Unitat de Fisiologia Mèdica*, *Facultat de Medicina*, *Universitat Autònoma de Barcelona*, E-08193 Bellaterra, Barcelona, Spain. Tel: +34-935811324, Fax: +34-935812986, E-mail: Caty.Casas@uab.cat

Running title: Motor Neuroprotection by SIRT1 and SIRT2

ABSTRACT

Over the last years, the enzyme family described as sirtuin (SIRT) has been related with neurological dysfunctions and traumatic injuries. SIRT1 activity exerts neuroprotection in neurodegenerative diseases, and recently we have demonstrated its relevant role in the retrograde degenerative process accounted to motoneurons (MNs) after proximal nerve injury. Among the other sirtuins, the SIRT2 has been described as the opposite player of SIRT1. Nowadays, the role of SIRT2 in neurodegeneration and neuron response after nerve injury response remains controversial and unknown. Since SIRT2 role in cytoskeleton integrity and autophagy is well known, we aimed to elucidate its contribution to retrograde MN degeneration provoked by nerve axotomy. We used a mice model of hypoglossal nerve axotomy, which transection induces a reduction of 50% MN population within 21 days post injury, and we have assessed SIRT1 and SIRT2 relevance in the subsequent neurodegenerative process. We tested the hypothesis that activation of SIRT1 increases survival of MNs, and that SIRT2 activity would prevent the reactive gliosis that is considered one of the most important hallmark of neurodegenerative diseases. We also tested the neuroprotective effect of both enzymes on in vitro models of endoplasmic reticulum (ER) stress. Regarding SIRT2, we discerned that its activity is detrimental for MNs under ER stress, otherwise, it acts as a gatekeeper of the inflammatory response. The obtained data support the neuroprotective roles of SIRT1 and SIRT2 to sustain MN viability upon insult, and suggests that the modulation of its activity can be an effective therapeutic target for neurodegenerative diseases.

Keywords: NeuroHeal; Motoneuron; Neuroprotection; Endoplasmic Reticulum stress; Unfolding Protein Response; Neuroinflammation; Sirtuin; Hypoglossal nerve injury.

INTRODUCTION

Axonopathy is a common early characteristic of neurodegenerative processes in the central nervous system (CNS) (Conforti et al., 2014). Axon degeneration often leads to retrograde neuronal cell death or atrophy and progressive permanent loss of vital neuronal functions. Deciphering the signaling involved is a key step toward developing the effective neuroprotectants that are greatly needed in the clinics. Transgenic models of neurodegenerative diseases are broadly used but represent one piece of the puzzle. Non-transgenic models of neurodegeneration shed also valuable information of the "natural occurring process" after neuronal soma-axon disconnection. By exploiting the anatomical and technical advantages of several axotomized models, it has been revealed the presence of multiple parallel running signaling programs in neuronal soma characterizing the retrograde neurodegenerative process which is non-apoptotic (Penas et al., 2011; Casas et al., 2015).

We have recently demonstrated that this knowledge is useful to shed effective neuroprotectants such as the newly discovery therapy NeuroHeal (NH) (Romeo-Guitart et al., 2017a; Romeo-Guitart, 2017b). NH was discovered using unbiased proteomic data from two models that represented pure regenerative and pure neurodegenerative conditions after nerve or RA injuries, respectively. The data served to build bona fide state-specific molecular maps and mathematical models of this human biological system that allowed us to screen databases of drugs to identify putatively neuroprotective combinations. NeuroHeal is a combination of acamprosate and ribavirin, two FDA-approved drugs without non-described adverse effects and with a well described pharmacokinetics and pharmacodynamics. Activation of sirtuin 1 (SIRT1) was shown to be necessary for the neuroprotective action of NeuroHeal after nerve root avulsion(Romeo-Guitart et al., 2017a). Sirtuins constitute a highly conserved family of deacetylases play an important role in the regulation of cellular homeostasis (Kupis et al., 2016). Seven homologs of yeast Sir2 (SIRT1–7) which share a conserved catalytic domain have been identified in mammals (Frye, 2000). Among them SIRT1 and SIRT2 have been targets in the design of neuroprotectans for degenerative conditions but also for traumatic injuries (Mellini et al., 2015). SIRT1 regulates a number of pathways

associated with normal metabolism and functioning of individual organs in mammals (Houtkooper et al., 2012) with several targets such as Histone 3, p53 and NF-kB among others (Chang and Guarente, 2014) . SIRT2 is the most abundant sirtuin in the brain and colocalizes with microtubules and deacetylates the main component of microtubules, α-tubulin, at lysine 40 (North et al., 2003). In this way, regulates microtubule dynamics (Chen et al., 2015b).

Both SIRT1 activation and SIRT2 inhibition have been identified as good strategies for neurodegenerative diseases. In the present work, we aimed to validate whether these strategies could be extended to disconnected neurons using a model of axotomy of the hypoglossal nuclei which contain highly vulnerable motoneurons (Lavezzi et al., 2010) (Hayashi, 2010)(Kanning et al., 2010) that differ in their properties from the spinal motoneurons (Tadros et al., 2016).

MATERIALS & METHODS

Animals

All procedures involving animals were approved by the Ethics Committee of Universitat Autònoma de Barcelona, and followed the European Community Council Directive 2010/63/EU

Knock-out Sirt2 mice (KO Sirt2):

The SIRT2-/- C57-BL6 mice used in these experiments were kindly given by Dr Alejandro Vaquero. This mice were generated in Tong´s lab using the original ES cells (Serrano et al., 2013).

Transgenic mice overexpressing Sirt1 (Tg Sirt1):

Mice with an extra copy of murine SIRT1 gene was kindly given by Dr Jesús Ruberte. This transgenic line was generated following a previously described protocol (Herranz et al., 2010).

Surgical procedures

Wild type C57BL/6 (Charles River) and KO SIRT2 mice aged two months-old, and transgenic mice of SIRT1 weighted 24.92 ± 1.66 g (average ± SEM), were maintained under standard conditions of temperature and light and fed with food and water *ad libitum*. We performed surgical procedures under anaesthesia with ketamine (90 mg/kg, i.m.) and xylazine (10 mg/kg, i.m.). We carried out the neurotmesis of the hypoglossal nerve, hereinafter hypoglossal axotomu (HA) as described elsewhere (Yamada and Jinno, 2013). Briefly, the right digastric muscle was opened using blunt end dissection with a pair of scissors and the right hypoglossal nerve was exposed. We transected the nerve with a pair of scissors at the proximal side of the hypoglossal nerve bifurcation, and removed 3 mm from the distal stump. Finally, we separated the nerve stumps to avoid spontaneous axon regrowth. Besides this, we sutured the muscle, closed the wound by planes and disinfected it with povidone iodine. The animals were allowed to recover in a warm environment.

For neonatal sciatic crush injury, pregnant rats were maintained under standard conditions of light, temperature and fed *ab libitum* until breeding. For surgical intervention, we deeply anesthetise pups at 4 days of age reducing its body temperature with ice, dissected the right sciatic nerve and we crushed it twice with a fine forceps during 10s. Besides, we closed the bound with suture, allowed the animals to recover in a warm environment and returned to the dam.

Drug treatments

The NeuroHeal treatment(NH) is composed by Acamprosate (Merck, Darmstadt, Germany) and Ribavirin (Normon, Madrid, Spain) (Romeo-Guitart et al., 2017a) In the *in vivo* experiments, NH compounds were added at tip water at final concentration of 2.2mM for Aca and 1mM for Rib. Water was changed every 3 days and fresh drugs were dissolved For the *in vitro* studies, we diluted both drugs (Sigma-Aldrich, Saint Louis, MO) in distilled water and added to NSC34 cell line or organotypic cultures at 55 µM Acamprosate and 1 µM Ribavirin. AK7 (Sigma-Aldrich, Saint Louis, MO) was dissolved in DMSO to obtain the stock solution and

used *in vitro* at 25 μM final concentration. *In vivo*, the stock was diluted in saline and administered 20 mg/kg i.p daily until end-stage.

In vitro models

NSC-34 line

We cultured the NSC-34 motoneuron-like cell line in Dulbecco's modified Eagle's medium high-glucose (DMEM, Biochrom, Berlin) supplemented with 10% fetal bovine serum and 1X penicillin/streptomycin solution (Sigma-Aldrich) on collagen-coated plates (Thermo-Fisher, Waltham, Massachusetts, USA) in a humidified incubator at 37 °C under 5% CO2. We transfected a million cells with 2 μg GFP or SIRT1 plasmid using the Amaxa Nucleofector II TM (Lonza,Norwalk) and the Nucleofactor V kit following manufacturer's recommendations. After 4 days of cell culture without changing the medium, we freshly prepared the drugs in DMEM at 10 X concentration. For endoplasmic reticulum (ER) stress induction, we added 1 μg/mL Tunicamycin (TN, Sigma-Aldrich) at final concentration. Treatments with NH or AK7 were performed together with TN-containing media. Twenty-four hours after treatments, we analysed cell viability by incubating the cells with 4 mg/ml MTT solution for 1 hours at 37 ˚C. After medium removal, the MTT salts were dissolved with DMSO and the absorbance was measured at 570 nm with a Biotek Elx800 microplate reader. The % of cell survival was obtained comparing each group with the absorbance value derived from the control group of each plate.

Spinal cord organotypic cultures

We prepared spinal cord organotypic cultures (SOCs) from lumbar sections of 8-days old Sprague Dawley pups as previously described (Herrando-Grabulosa et al., 2016). Briefly, we collected the spinal cords from the pups and placed them into cold high glucose-containing (6.4 mg/ml) Gey's Balanced Salt Solution (GBSS) (Sigma-Aldrich, Steinheim, Germany). After removing the meninges and roots, we cut them into 350 μm transverse sections with a McIlwain Tissue Chopper. Each 4 lumbar sections were transferred onto 30-mm-diameter 0.4 μm Millicell-CM nets (Millipore, Billerica, USA) in 6-well plates (Thermo Fisher Scientific, Waltham, MA, USA) containing 1 mL of medium, based in 50% (v/v) minimal essential medium

(MEM), 2 mM glutamine, 25 (v/v) Hank's Balanced Solution (HBSS, Sigma-Aldrich) supplemented with 25.6 mg/mL glucose and 25 mM Hepes; pH = 7.2 and maintained at 37ºC in a 5% CO_2 air humidified environment. Medium was unchanged during the first week of culture and then changed twice per week. After 15 of in vitro (DIV) culture, we added TN at 1µg/mL of final concentration alone or in combination with NH or AK7. After 6 hours or two days post-treatment we fixed the SOCs with 4% paraformaldehyde in a 0.1 M phosphate buffer at pH 7.2 during 1 hour at RT. We washed the SOCs with 0,3% Triton in TBS solution, blocked them with 10% of normal donkey serum with TBS and incubated during 2 days with mouse anti-Neurofilament H Non-Phosphorylated (SMI32; 1:1000; Biolegend) at 4ºC. Then, we washed the SOCs with 0,1% Tween-20 of TBS solution and incubated with Alexa 488-conjugated donkey anti-mouse antibodies (1:200; Jackson Immunoresearch, West Grove, PA, USA) during 2h at RT. After several washes, we counterstained with DAPI and mounted with Fluoromount-G mounting medium (SouthernBiotech). We took pictures with the aid of a digital camera (Olympus DP76) attached to the microscope (Olympus BX51) and assesse motorneuron survival counting all SMI32 posotive neurons at the ventral horn for each spinal cord hemisection. Six different SOCs were used for each experimental condition.

Immunohistochemistry and Image analysis

After deep anaesthesia with pentobarbital, we transcardially perfused the animals with a saline solution containing 10 U/ml heparin, followed by 4% paraformaldehyde in a 0.1 M phosphate buffer, pH 7.2 for tissue fixation at 3, 7, or 21 dpi (n=4 for each condition), and removed the brainstem, which was post-fixed in the same fixative overnigth at 4ºC hours and cryopreserved in 30% sucrose until processed. We isolated the brainstem zone containing the hypoglossal nuclei using a brain mould and we cut it into serial transversal sections (10-µm thick) with the aid of a cryotome (Leica, Heidelberg, Germany) on gelatinized slides and preserved them at -20 ˚C until use. For neonatal rats, we perfused them as explained previously at 10dpi, extracted the L4-L6 spinal cord segment and cut it into transversal serial sections of 20-µm thick. We treated the slides of brainstem, spinal cords or SOCs with blocking solution (Tris-buffered saline (TBS) with 0.3% Triton-X-100 and 10% bovine serum) for 1 hour and incubated it r with the following primary antibodies:

rabbit anti-ionized calcium binding adaptor molecule 1 (Iba1; 1:1000, Wako), rabbit-anti NAD-dependent deacetylase sirtuin-1 (SIRT1; 1:100, Millipore), rabbit anti-acetyl-Histone H3 (Lys9) (Acetyl H3-K9; 1:50, Millipore), rabbit anti-acetyl-p53 (Lys373) (Acetyl p53-K373; 1:500, Millipore), rabbit-anti NAD-dependent deacetylase sirtuin-2 (SIRT2; 1:200, Sigma-Aldrich), mouse-anti α-tubulin (α-Tub; 1:500; Sigma Aldrich), mouse-anti acetylated α-tubulin (Acetyl α-Tub; 1:500; Hybridoma Bank), mouse-anti anti-Neurofilament H Non-Phosphorylated (SMI32; 1:1000; Biolegend, San Diego, CA, USA), rabbit-anti Nuclear Factor κB p65 subunit (NF-κB; 1:1000, Cell Signaling, Danver, MA, USA), rat-anti CD86 (CD86; 1:200; BD Biosciences, San Jose, CA, USA), rabbit anti-cleaved caspase 3 (Casp3 act.; 1:200;Cell Signaling) and rabbit apoptosis inducing factor 1 (AIF1; 1:200; Antibodies-online). After several washes with 0.1% Tween-20 TBS solution, the sections were incubated for 2 hour with Cy-3/Cy-2/Alexa 488/Alexa 594-conjugated donkey anti-rabbit or anti-mouse antibodies (1:200; Jackson Immunoresearch, West Grove, PA, USA) and washed with 0,3% TritonX-100 in TBS We counterstained the sections with DAPI (Sigma-Aldrich) or NeuroTrace Fluorescent Nissl Stain (Molecular Probes, Leiden, Netherlands), and mounted with Fluoromount-G mounting medium (SouthernBiotech). Sections to be compared were processed together on the same slide and on the same day. Images from sections ofdifferent treatments and controls were taken under the same exposure time, sensibility, and resolution for each analysed marker.). Confocal images were obtained using two separate photomultiplier channels with a 1.4 numerical aperture oil-immnersion objective of 20 or 40 X. Images were separately projected and merged using a pseudocolor display. We analysed fluorescence signal intensity using the ImageJ software (National Institutes of Health; available at http://rsb.info.nih.gov/ij/). The analysis of the images to be compared was performed the same day. We delimited an area as region of interest (ROI) with the aid of Nissl labelling for MN cytoplasm or DAPI for MN nuclei. Therefore, the integrated density inside the ROI was obtained for at least 15 MNs/animal per each marker from three 100-µm distant different sections.

Western blot

We deeply anesthetized mice with pentobarbital from control, injured and treated groups at 3 dpi (N=4) to obtain whole brain tissue for western blot analysis. We snap-frozen the brains into liquid nitrogen to store for further dissection. We removed the the hypoglossal nuclei with the aid of a brain mould and homogenizated with lysis buffer (Hepes 20 mM, Sucrose 250 mM, EDTA 1 mM, EGTA 1 mM and a cocktail of protease (Sigma) and phosphatase inhibitors (Roche) with potter homogenizer on ice. We centrifuged the lysate during 20 min at 800 xg at 4ºC and collected the supernatant as cytosolic fraction. Then, we mixed the pellet with nuclear buffer (Hepes 20mM, Tritxon-X-100 0,1%, EGTA 0,2 Mm, EDTA 0,2 mM, KCl 1M and a cocktail of protease (Sigma) and phosphatase inhibitors (Roche)) and we mae vortex at 1400 rpm during 20 min at 4ºC. We centrifuged the lysate at 10000xg during 10 min at 4ºc and harvested the supernatant as nuclear fraction. Finally, we quantified the cytosolic and nuclear fraction by BCA assay (assay (Pierce Chemical Co.; Rockford, IL, USA).

For western blotting, we mixed equally samples from four animals and we loaded 10µg of cytosolic or nuclear fractions from hypoglossal nuclei. Then, we mixed it with loading buffer and loaded onto a 10% SDS-polyacrylamide gels to perform electrophoretic separation of the proteins followed by its transference to a PVDF membrane in a BioRad cubette system in 25 mM Tris, 192 mM glycine, 20% (v/v) methanol, pH 8.4. After blocking the membrane with 0,1% Tween-20 TBS with 5% of milk, it was incubated overnight at 4ºc with the primary antibody: rabbit anti-inositol-requiring protein-1 alpha (IRE1a; 1:1000, Cell Signalling) and rabbit anti-X-box binding protein 1 (Xbp1; 1:1000, Cell Signaling. The following day, we washed and incubated the membranes during 1 h with an appropriate secondary antibody conjugated with horseradish peroxidase (1:5000, Vector) at RT. Proteins were developed using a chemoluminiscent method (ECL Clarity kit, Bio-Rad Laboratories, Berkeley, CA, USA) and the images were captured and analysed with Image Lab Software (Bio-Rad Laboratories).

RNA extraction, reverse transcription and Real-time PCR

For PCR analysis, total RNA was extracted using the Tripure Isolation Reagent (Roche, Mannheim, Germany) according to the instructions of the manufacturer. The recovery of RNA was similar in young and aged rats. Reverse transcription was performed using random hexamers primers exactly as previously described. PCR was performed in an ABI Prism 7000 sequence detector (Applied Biosystems, Madrid, Spain) using cDNA diluted in sterile water as template. The Tnf-α, IL-1β and the housekeeper genes were amplified using specific Taqman probes supplied by Applied Biosystems, Madrid, Spain. Threshold cycle (Ct) values were calculated using the software supplied by Applied Biosystems, Madrid, Spain.

Fluoro-Jade C staining

Brainstem Sections were randomly selected and stained with Fluoresecent Fluorojade C (Chemicon) following the manufacturer's protocol. Summarizing, the slices were immersed in a solution of 80% EtOH with 1% of NaOH during 5 min. Then, we rinsed them for 2 min in 70% EtOH, washed 2 min in distilled water and we incubated them during 10 min with 0,06% permanganate solution. After wash with water, we transferred the slices to a solution of 0,0001 % of Fluoro-Jade C dissolved in 0,1% acetic acid dissolution during 10 min. Then, the slices are washed with water, counterstained with DAPI and mounted with DPX (Sigma). We took confocal images the same day of the staining to avoid fluorescence loss.

Motor neuron counting

Sixteen brainstem sections (separated by 50 μm each one) including the hypoglossal nuclei were randomly selected and stained with Fluoresecent Neurotracer (Life technologies) following the manufacturer's protocol. We took sequential microphotographs from the injured and contralateral hypoglossal MN pull at 20 with the aid of a digital camera (Olympus DP76) attached to the microscope (Olympus BX51). We count thoseMNs with diameters bigger than 17 μm (area of 320 μm2)(Haenggeli and Kato, 2002b; Ferrucci et al., 2010), prominent nucleous, poligonal shape and located in the hypoglossal nucleus and calculated the

the percentage of MN survival after compare the injured site with the contralateral non-injured side and obtain the mean of each animal.

Statistical analysis

All data is presented as mean ± standard error of the mean (SEM). We performed the statistical analysis with GraphPad Prism 5 software (San Diego, CA, USA) using unpaired t-test (one or two tails) or one-way analysis of variances (ANOVA) followed by Bonferroni's multiple test depending on the scientific paradigm. Significant differences were considered at $p<0.05$.

RESULTS

In order to evaluate the implication of SIRT1 and 2 in neuroprotection of motoneurons after proximal nerve injury we chose the hypoglossal axotomy model (Kiryu-Seo et al., 2005) (**Fig. 1a**). We characterized the pace of MN cell death at the hypoglossal nucleus at different time points post injury. We observed that the process slowly proceeded achieving 48.72 %± 2.20 after 21 days post injury (dpi) (**Fig. 1a**). This neurodegenerative process was not related to apoptotic hallmarks such as activation of caspase 3 or AIF nuclearization (**Fig. 1b**) at 7pi. We also check that injured MNs are degenerating by Fluoro-Jade C staining (**Fig. 1b**). Considering this similarity to our previous reported model of nerve root avulsion, we explore whether there was activation of some hallmarks of endoplasmic reticulum (ER) stress like activation of the IRE1a pathway. Once active, IRE1, autophosphorylates itself, dimerizes and acquires ribonuclease activity, which is translated into the splicing of the mRNA of the X-box binding protein 1 (Xbp-1) (Sidrauski and Walter, 1997). In this sense, we observed an increase in the amount of phosphorylated IRE1α (pIREα) protein and a higher ratio of XBP1s/XBP1u in injured animals respect to control **(Fig. 1c**). These results suggested that the neurodegenerative pathway of cranial MN death was non apoptotic and presented some hallmarks of ER stress.

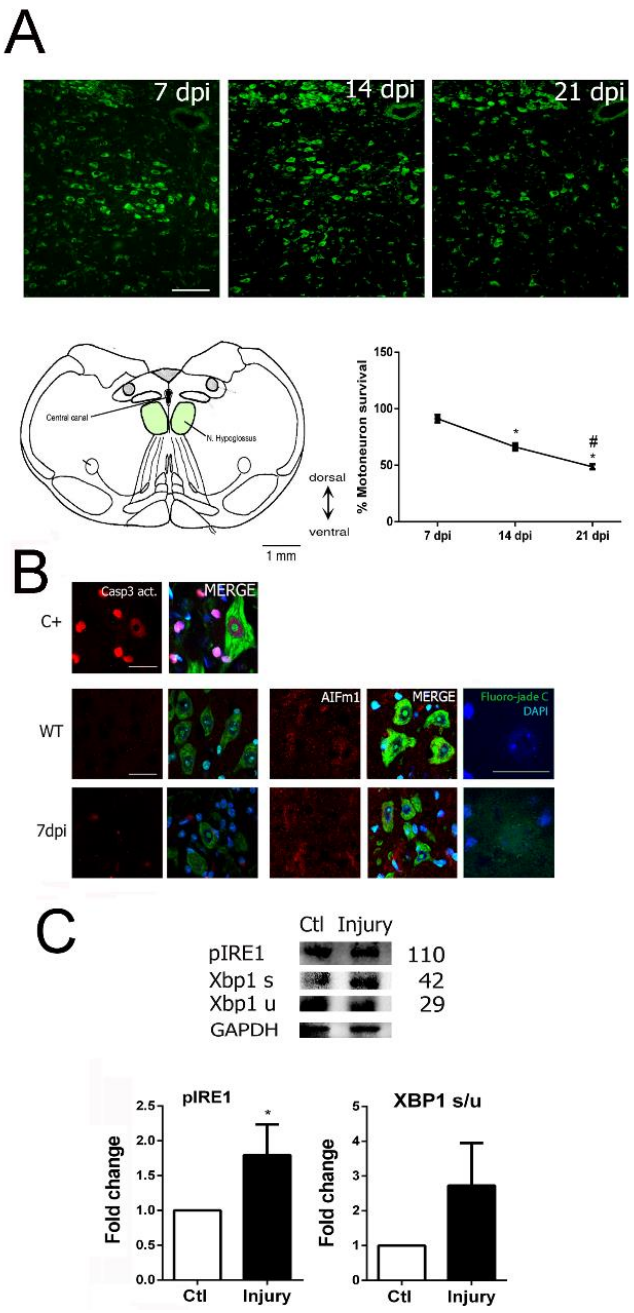

Figure 1. The MNs death that occurs after hypoglossal nerve injury is not apoptotic and presents UPR hallmarks (A) Nissl microphotographs from hypoglossal nucleus of HA injured animals at ipsilateral side at 7, 14 and 21 dpi. Drawing highlighting the hypoglossal nuclei in the brainstem of the mice. Graphic showing the fall of the MN survival at different dpi at the ipsilateral side with respect to the contralateral after HA (n=4 for 14dpi and n=5 for other groups, ANOVA, post hoc Bonferroni #p<0.05 vs 7dpi and *p<0.05 vs 14dpi). (**B**) ***Left***, Representative confocal images of MNs from hypoglossal nuclei immunolabelled against Cleaved caspase 3 (Casp3. Act) or AIF1 in red, Fluoronissl in green and DAPI from wild type or 7dpi animals. Note that we added a positive control from spinal cord samples of neonatal rats submitted to sciatic crush injury (C+) for the Casp3. Act. labelling. Scale bars= 25µm. ***Right,*** Confocal microphotographs of Fluoro-jade C stained hypoglossal nuclei counterstained with DAPI from CTL and Injured animals at 7dpi (**C**) Western blots and histogram showing the analysis of pIRE1α and Xbp1 protein levels in control (Ctl) and injured animals at 3dpi.

Some authors reported that activation of SIRT11 or inhibition of SIRT22 promotes neuroprotection in some neurodegenerative mouse models (Herskovits and Guarente, 2013). Thus, we nalysed the effect of axotomy of the hypoglossal nerve on the expression and activity of SIRT1 and SIRT2. We observed that SIRT1 was overexpressed at the nuclei of axotomized MNs at 7 dpi (**Fig. 2a**). We measured the deacetylase activity of SIRT1 by assessing the contents of histone-H3 acetylated at Lys9 (H3-K9) and of p53 acetylated at Lys373 (p53-K373) residues (Vaziri et al., 2001; Vaquero et al., 2004). We observed that both were significantly accumulated in the nucleus of damaged MNs at the same time post injury compared to in control animals (**Fig. 2a**). SIRT2 was down-represented in axotomized MNs at 7 dpi respect to controls (**Fig. 2b**) and displayed an immunolocalization with a characteristic pointed localization probably corresponding to the ER-Golgi intermediate compartment (ERGIC) as reported. Despite the total abundance of alpha tubulin diminished after injury, relative levels of the acetylated form of alpha tubulin were higher than the same ratio in controls (**Fig. 2b**). These results suggested that the activity of both sirtuins was reduced early after injury. Whether these were detrimental or part of the endogenous neuroprotective mechanism was unknown.

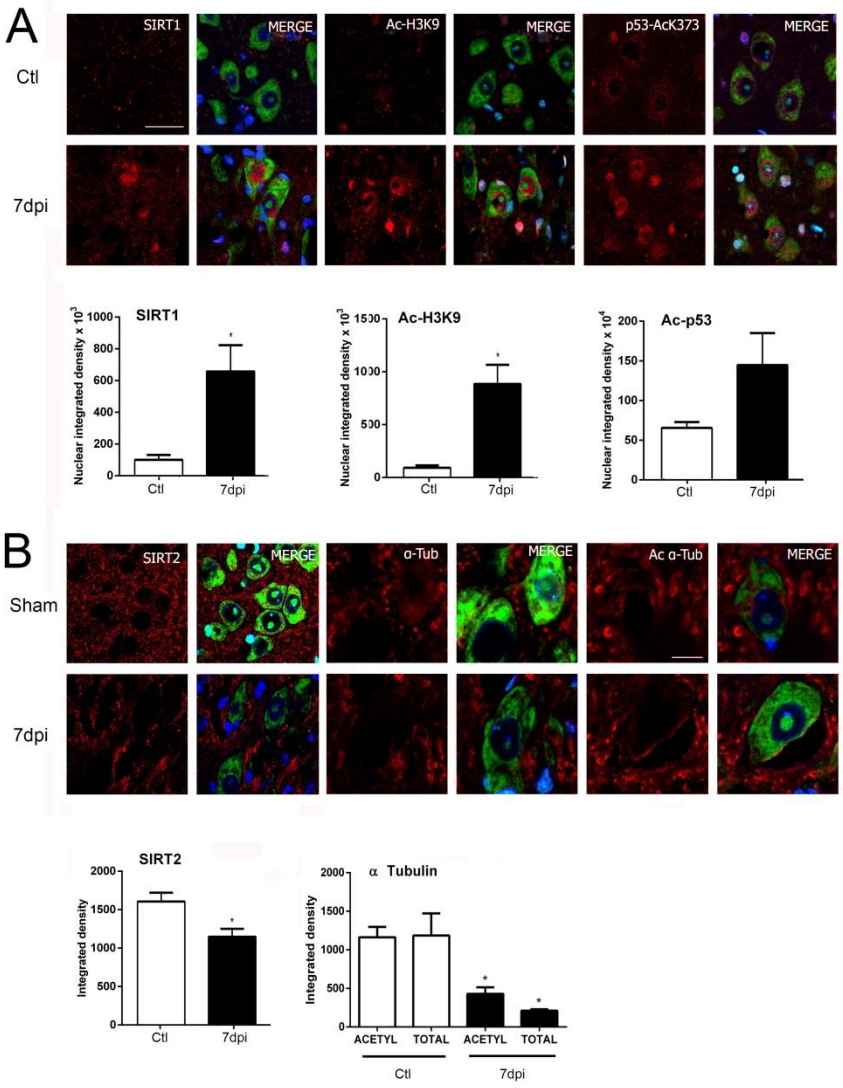

Figure 2. Deacetylase activity of Sirt1 and Sirt2 is reduced after nerve injury. (A) ***Top***, Confocal images of MNs immunolabelled against SIRT1, Histone H3 acetylated at Lys-9 (Ac-H3k9), and p53 acetylated at Lys-373 (p53 Ack373) in red and counterstained with green fluorescent Nissl and DAPI from hypoglossal nuclei of wild type (WT) and injured animals (HA) at 7dpi. ***Bottom***, Histograms of the mean of the immunofluorescence for each marker inside the nuclei of MNs (n=4 animals, t-test, *p<0.05 vs WT). (**B**) ***Top***, Representative confocal microphotographs of SIRT2, α-tubulin (α-Tub) and acetylated α-tubulin (Ac α-Tub) immunolabelling in red, counterstained with green Fluoronissl and DAPI from hypoglossal nuclei of wild type or injured animals at 7dpi. ***Bottom***, Quantification of the integrated density for each marker into the cytosol of MNs for both groups (n=4 animals, t-test, *p<0.05 vs WT). Scale bar= 25µm for all images except 10µm for α-tub and acetyl α-tub.

We used a model of ER stress *in vitro* using Tunicamycin (TUN) as stressor agent on NSC-34 MN-like cells to test whether an SIRT1 activation and SIRT2 inhibition were neuroprotective. TUN exerted 59.58 %±1.82M cell death by MTT assay 24h post insult (**Fig. 3a**). Cells overexpressing SIRT1 promoted survival of ER

stressed cells (20%) compared to GFP overexpressing insulted cells (**Fig. 3a**). Treatment of ER stressed cells with NH, activator of SIRT1 under ER-stress conditions (**Fig. S1**)(Romeo-Guitart et al., 2017a)(Romeo-Guitart et al., 2017a)(Romeo-Guitart et al., 2017a)(Romeo-Guitart et al., 2017a)(Romeo-Guitart et al., 2017a), was neuroprotective for these cells (**Fig. 3a**). To analyse SIRT2 implication, we used AK-7, SIRT2 inhibitor reported to exert neuroprotection in some models of neurodegenerative diseases. Treatment of the stressed cells with AK-7 was also neuroprotective.

Then, we verified that administration of these drugs in vivo exerted their effects in the brain. NH treatment in vivo let to a decrease of Ac-H3-K9 levels within the nucleus of MNs compared to vehicle treatment (**Fig. 3b**). Similarly, AK-7 treatment promoted a raise in acetyl-a-tubulin in the hypoglossal nuclei at 21 dpi respect to vehicle as expected for a SIRT2 inhibitor (**Fig. 3c**). Overall, these results suggested that these strategies may neuroprotect in our model.

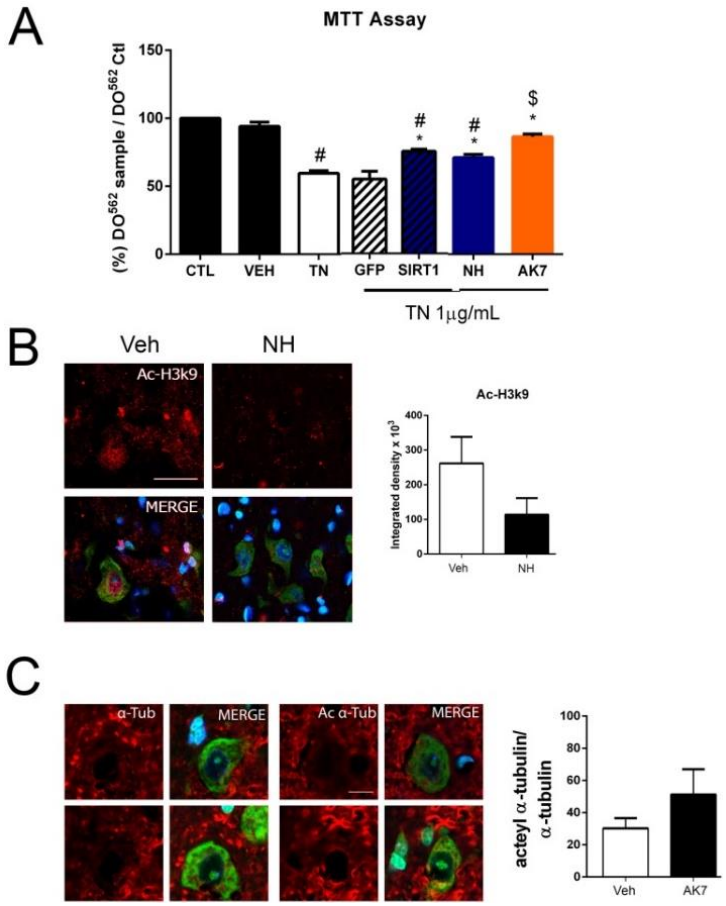

Figure 3. SIRT1 and SIRT2 role in endoplasmic reticulum (ER) stress-induced cell death in vitro and its activity modulation by NH and AK7 in mice brain (A) Bar graph showing the percentage of cell survival ± SEM after the treatment with tunicamycin (TN) at

1µg/mL alone or in combination with the NeuroHeal or AK7 drugs. Also observe the cell survival after adding to transfected cell with SIRT1 or GFP the same concentration of TN. (n=4-10, ANOVA, post hoc Bonferroni #p<0.05 vs Veh, *p<0.05 vs TN, $p<0.05 vs TN-GFP). (**B**) ***Left***, Confocal images of acetylated H3k9 from injured animals after NH treatment, counterstained with Fluoronissl green and DAPI at 21 dpi. ***Right***, Histogram showing the integrated density of nuclear acetyl-H3k9 immunolabelling from injured MNs in the vehicle or NH-treated groups at 21 dpi (n=4, t-test, *p<0.05 vs Veh). Scale bar= 25µm. (**C**) ***Left***, Immunohistochemical images of acetylated and total α-tubulin (red), countersainted with Fluoronissl green and DAPI from animals treated with Veh or AK7 at 21 dpi. ***Right***, Histogram showing the ratio of the acetylalted form versus total of α-tubulin within the MNs in both groups (n=4, t-test, *p<0.05 vs Veh). Scale bar= 10µm.

Hence, in light of the *in vitro* results suggesting that activating SIRT1 or inhibiting SIRT2 might be neuroprotective in our model, we used both pharmacological and genetic approach to test these hypotheses. Injured animals treated with NH presented increased percentage of MN survival than those vehicle-treated **(Fig. 4a)**. Similarly, a higher number of MN survival was observed when injured a transgenic animal overexpressing SIRT1 (tg-SIRT1) (Herranz et al., 2010) compared to its injured WT littermates (**Fig. 4a).** We compared the quantification of survival MNs from axotomized animals treated with daily administration of AK-7 to those in the injured knockout mice of SIRT2 (KO-SIRT2) (Serrano et al., 2013) at 21 dpi (**Fig. 4b**). Unexpectedly, we observed a reduction in the number of survived MNs in both cases compared to vehicle-treated or wild-type littermates, respectively.

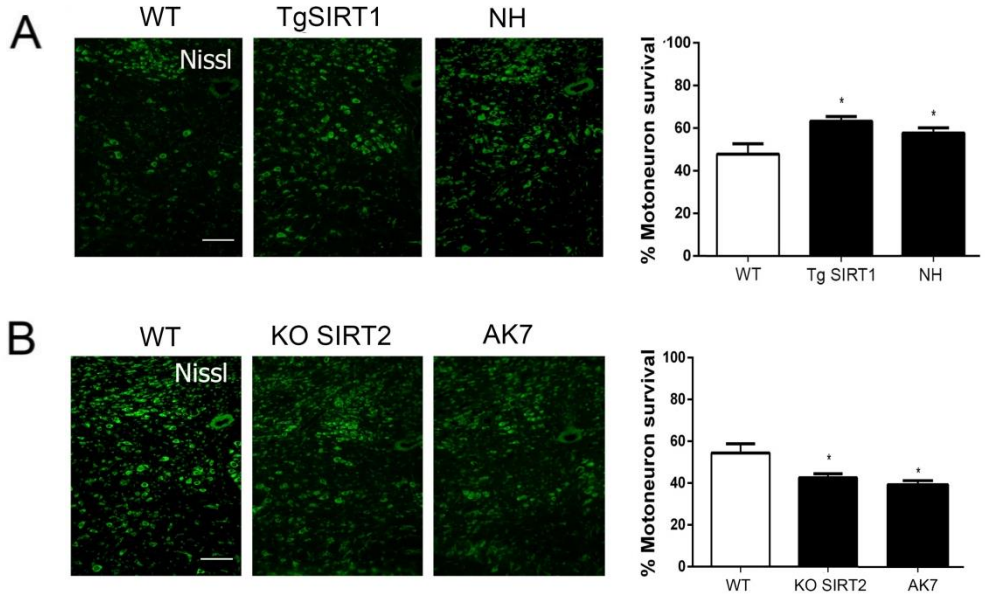

Figure 4. SIRT1 and SIRT2 activities are essential for survival of MNs after HA nerve injury. (A) Representative microphotographs of Nissl stained ipsilateral hypoglossal nuclei from WT, SIRT1-overexpressing (Tg SIRT1) or NH-treated mice at 21dpi. The histogram represents the mean percentage ± SEM of surviving MNs in the ipsilateral side respect to the contralateral side (n=4-5, ANOVA, post hoc Bonferroni, *p<0.05 vs WT). (**B**) Hypoglossal nuclei stained with Nissl from WT, knock out (KO) for SIRT2 and AK7-treated (20 mg/kg i.p, daily) mice at 21 dpi. Plots of the percentage ± SEM of the counted MNs at the ipsilateral side respect the contralateral for different experimental groups at 21 dpi (n=4, ANOVA, post hoc Bonferroni, *p<0.05 v Scale bar= 100μm.

Overall these results suggested that inhibition of SIRT2 is detrimental *in vivo*, although not *in vitro*, while fostering SIRT1 activity is beneficial for MN survival after axotomy of the hypoglossal nerve.

Due to differences between *in vitro* and *in vivo* results regarding neuroprotection provided by AK7 treatment, we used an intermediate model, the spinal cord organotypic model (SOCs) (Herrando-Grabulosa et al., 2016) to know whether the presence of glial cells in the culture might be the cause of this discrepancy. We observed that TUN treatment produced a decline in SMI-32 positive MN pool compared to control or vehicle treatment (**Fig. 5a**). We observed that TN treatment drastically reduced the activity of SIRT1 as nerve injury *in vivo*, but in this case, this stress enhanced the activity of SIRT2 (**Fig. S1 and 2**). In this model of MNs death, we observed that NH-treated SOCs better preserved the survival of MNs while AK7 treatment yielded similar readouts than TUN alone (**Fig. 5a).** Hence, regarding AK7, the results obtained in SOCs were unlike to those obtained in the NSC-34 model but similar to the *in vivo* model.

Considering that one of the main differences in both *in vitro* models is the presence of glia cells, we wondered whether AK7 influenced in this particular cell type and thus reverting MN destiny. One of the possibilities to be explored was that AK7 treatment could influence in microglia and render it more reactive (Pais et al., 2013). Considering that NF-κb is a transcription factor implicated in the production of pro-inflammatory cytokines (Pais et al., 2013), we investigated its protein levels at the nuclei of microglia in SOCs. We did not observe a significative increase of NF-κb in TUN-treated SOCs compared to those vehicle-treated or control (**fig. 5b**). In contrast, while there was a considerable decrease of nuclear NF-κb in microglia of NH-treated stressed SOCs, AK7 treatment increase significantly its presence (**Fig.**

5b). Accordingly, we observed a trend to increase in the levels of *IL-1β* and *TNF-a* gene expression in AK7-treated SOCs respect to TUN or control samples (**Fig. 5c**).

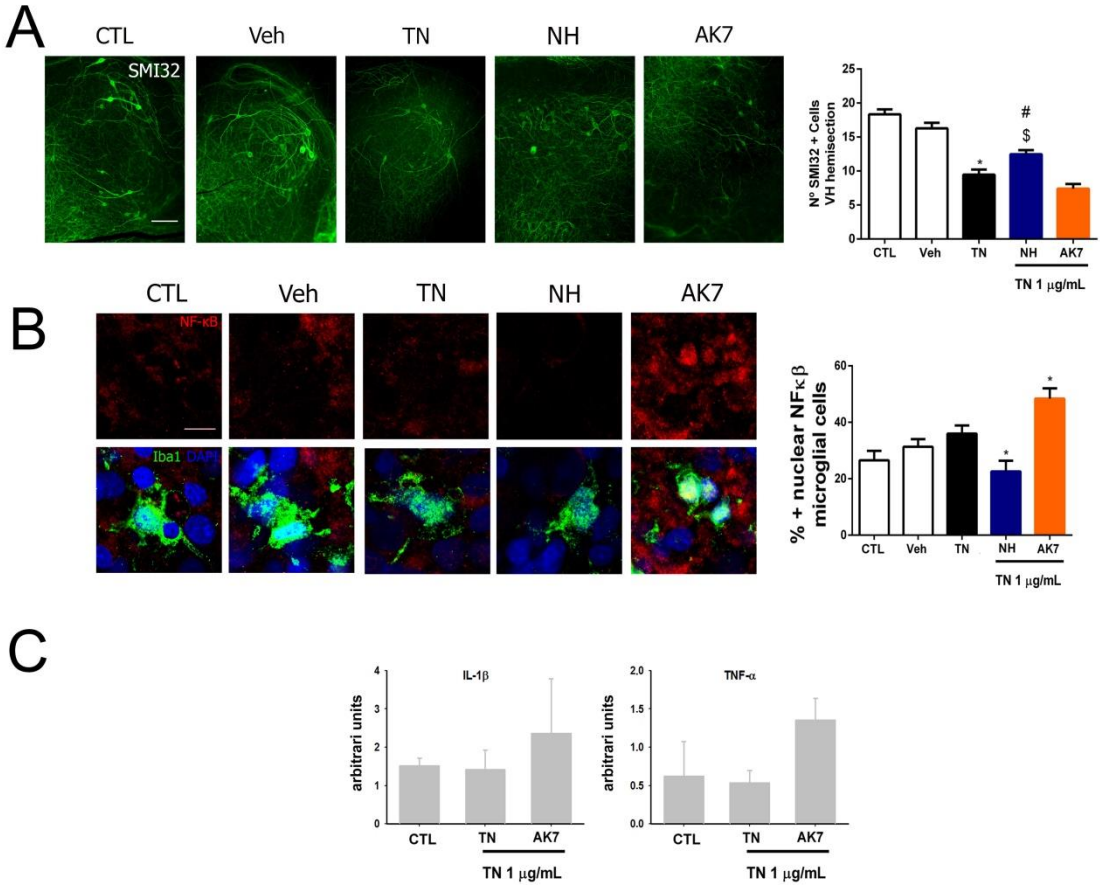

Figure 5. SIRT1 and SIRT2 activities maintains neuron survival in an in vitro model of ER stress in SOCs. (A) ***Left,*** SMI-32 representative microphotographs from the ventral horn of the SOCs after two days of treatment with TN with or without the NH or AK7 co-treatment. ***Right***, Bar graphs showing the number ± SEM of SMI-32 positive cells in the ventral horn of each hemi-section of the spinal cord slice (n=5-10 complete spinal cord slices, ANOVA, post hoc Bonferroni *p<0.05 vs Veh, #p<0.05 vs TN, $p<0.05 vs AK7). Scale bar = 100µm (**B**) ***Left***, Confocal microphotographs of the immunolabelling of p65 subunit of NF-κB in red, Iba1 in green and DAPI in blue from different experimental conditions 6h after of TN adding. ***Right***, Histogram showing the percentage of microglial cells with positive nuclear labelling of NF-κB for each experimental group. (n=4, ANOVA post hoc Dunnett *p<0.05 vs TN). Scale bar= 10µm. (**C**) Histogram of mean values obtained by quantitative real-time PCR for IL-1β and TNFα mRNA in the control (CTL), TN or TN plus AK7 SOCs at 6 h post-treatment.

To confirm that it might be what it happened *in vivo*, we analyzed AK7-treated injured animals, and we observed an increased in CD86, marker of M1 phenotype (Wachholz et al., 2016) was also increased in microglial cells treated with AK7 at 3 dpi (**Fig. 6a**). Accordingly, we observed a major quantity of NF-κb in the nucleus of microglia of AK7 treated injured animals than control (**Fig. 6b**). In

addition, we observed an increased in the expression of *IL-1β* and *TNFα* genes promoted by AK7 treatment at the same time (**Fig. 6c**).

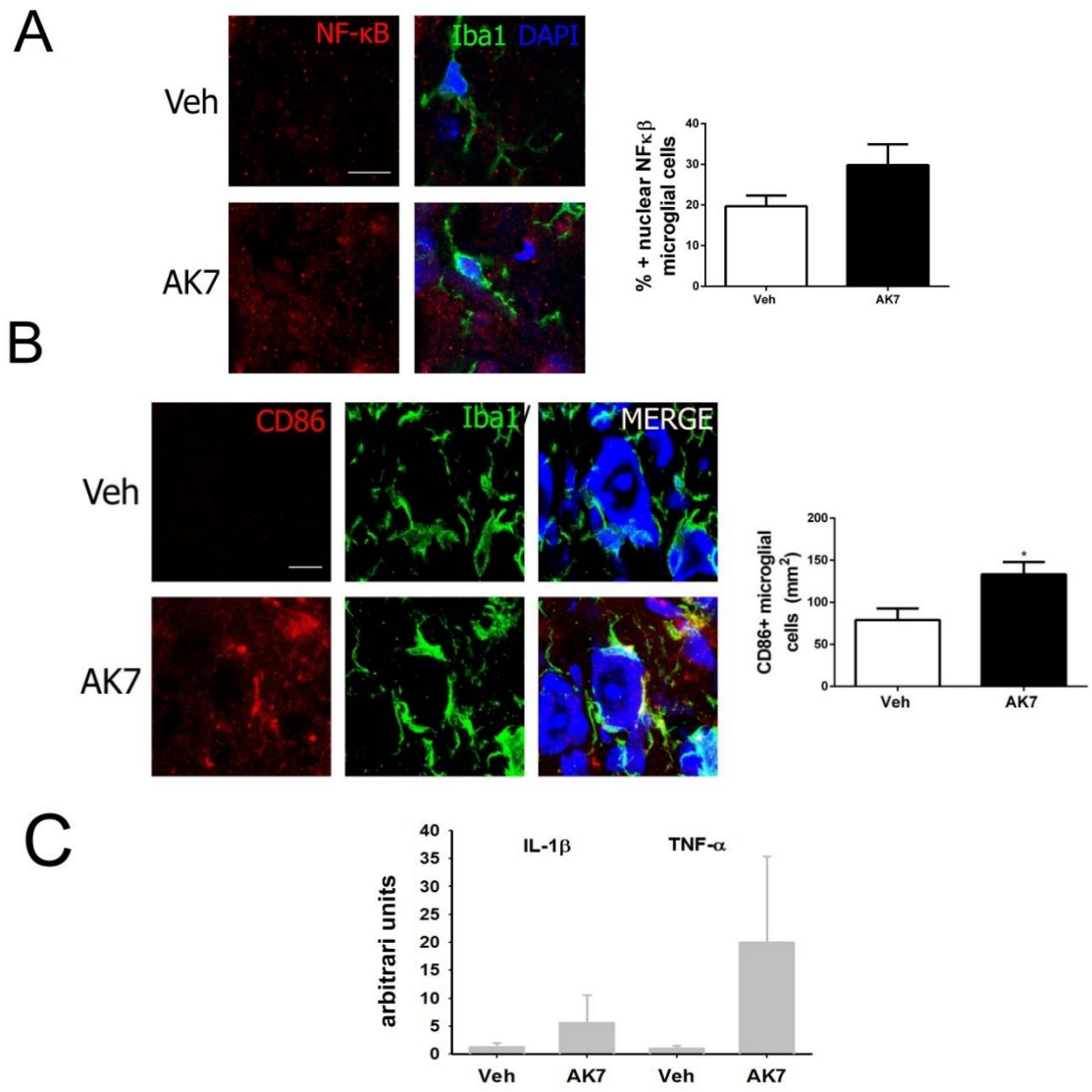

Figure 6. Sirt2 inhibition exacerbates microglial reaction and compromise MN survival after nerve neurotmesis. (A, B) ***Left***, Immunohistochemical analysis of NF-κB and CD86 in red, versus Iba1 in green and counterstained with DAPI and blue FluoroNissl from vehicle or AK7 treated animals at 3dpi. **(A, B)** ***Right***, Histograms showing the mean ± SEM of the % of microglial cells with positive nuclear NF-κB labelling or the number of microglial cells per mm2 with CD86 labelling for both groups (n=3 for veh and 4 for AK7, t-test, *p<0.05 vs Veh). Scale bar= 10μm. (**C**) Histogram of mean values obtained by quantitative real-time PCR for IL-1β and TNFα mRNA in the hypoglossal nuclei from Veh or AK7-treated animals at 3dpi.

Thus, overall the results suggested that although SIRT2 inhibition might be beneficial for the neuronal survival itself, important issues regarding accompanying glial cells should be also considered, since the overproduction of pro-inflammatory interleukins might override all the beneficial aspect to the neurons.

DISCUSSION

Impediment in communication among nerve cells and their tissue target is a common issue in neurodegeneration. In neurodegenerative diseases, in addition to their particular protein hallmarks, all of them face the neuronal death related to soma isolation due to neurite retraction. Deciphering the programs activated by neurons to cope with this damage may add valuable information to obtain robust pipelines for neuroprotective therapy.

The purpose of the present study was to assess the implication of SIRT1 and 2 for neuroprotection of disconnected central neurons using the hypoglossal nerve axotomy model. Axotomized cranial motoneurons suffered a non-apoptotic neurodegenerative process characterized by the activation of IRE1a branch of the unfolded protein response (UPR). We demonstrated that pharmacological activation with NeuroHeal or overexpression of SIRT1 is beneficial, whereas pharmacological or genetical inhibition of SIRT2 is detrimental for axotomized neuron survival. Nevertheless, SIRT2 inhibition with AK-7 could exert neuroprotection in a motoneuron-like cell line but not to MNs in organotypic culture with the presence of glia, submitted to ER stress. AK-7 treatment in the organotypic and in the *in vivo* model promoted an overproduction of pro-inflammatory cytokines and "M1" or pro-cytotoxic microglia population that can explain its deleterious effect.

We have demonstrated that activation of SIRT1 with NeuroHeal is important for neuroprotection of disconnected cranial motoneurons in mice as it was for root avulsed spinal motoneurons in rats (Romeo-Guitart et al., 2017a). We have recently reported that its treatment produced long-lasting neuroprotection and also accelerated nerve regeneration and reduced muscle atrophy in a pre-clinical model of root avulsion with delay repair (Romeo-Guitart et al., 2017b). *In vitro*, NeuroHeal was able to rescue neurons *in vitro* from ER stress insults although the mechanisms involved are still to be elucidated. We previously showed that SIRT1 activation was necessary for NeuroHeal neuroprotection although this drug composition is essentially multitarget (REF). SIRT1 has been repeatedly reported to be important for neuroprotection in several models of neurodegenerative diseases (e.g

Alzheimer's disease, Huntington's disease) (Kim et al., 2007; Jeong et al., 2012; Jęśko et al., 2017) and crucial in cerebral ischemia and preconditioning (Khoury et al., 2017). Thus, we confirm that activation of SIRT1, but in particular through the treatment with NeuroHeal, is a promising therapeutic option for disconnected neurons.

Surprising results were obtained regarding SIRT2 inhibition with AK-7. We expected AK-7 and deletion of SIRT2 to be neuroprotective since SIRT2 inhibition has been reported for some age-related disorders such as PD (Outeiro et al., 2007; Luthi-Carter et al., 2010; Taylor et al., 2011)(Chen et al., 2015b); (Di Fruscia et al., 2015) and Huntington disease models (Pallos et al., 2008); (Chopra et al., 2012). On the contrary, our results indicated that AK-7 treatment resulted deleterious for disconnected MN survival. Although in cell lines the treatment was beneficious, recreation the complex microenvironment of the nervous system and adding the time necessary to favour the apparition of chronic circumstances such as inflammation are crucial to ascertain with proper neuroprotectants towards the clinics. In our organotypic and in vivo models, AK-7 treatment render microglia cells more prone to generate pro-inflammatory cytokines which might override any putative protection that the treatment might do to the neurons specifically. After axotomy, primary injury induces the apparition of inflammatory reaction with cytokines and chemokines released and spread to peri-lesional areas. Microglial activation, a key process in the propagation of inflammation to neighbouring tissue, may lead to impaired neuronal survival in the peri-lesional regions as a result of the generation of cytokines and reactive oxygen species. Our data indicated that AK-7 treatment results in enhanced microglial activation at the injury site, indicating that SIRT2 inhibition might aggravate the acute inflammatory response. Accordingly, SIRT2 is reported to interact with p65, an NF-κB subunit in the cytoplasm, and to deacetylate it at Lys310 in vitro and in vivo (Rothgiesser et al., 2010)). After TNFa stimulation, p65 is hyperacetylated in SIRT2-deficient cells, which results in increased expression of a subset of p65 target genes (Rothgiesser et al., 2010). This is in agreement with recent reports that have indicated that SIRT2 targets Lys310 of p65 to influence pro-inflammatory gene transcription in microglia (Lin et al., 2013); (Pais et al., 2013). Together, these data indicate that post-translational

deacetylation of p65 by SIRT2 might be one of the mechanisms that contribute toward its anti-inflammatory properties

Our results are in agreement with others reporting no-beneficial effect of AK-7 where the control of microglial reaction is crucial for neuronal survival such as in amyotrophic lateral sclerosis (Chen et al., 2015b) or traumatic brain injury (Yuan et al., 2016). Another study, using SIRT2 knock-out mice, revealed an increase in microglial activation and pro-inflammatory cytokines upon intra- cortical injection of LPS (Pais et al., 2013). SIRT2 deletion also promotes inflammatory responses in a dextran sulfate sodium (DSS)-induced model of colitis (Lo Sasso et al., 2014). When recombined SIRT2 protein is transduced into murine macrophages, it inhibits LPS-induced expression of cytokines as well as activation of NF-κB and MAPKs ((Kim et al., 2013), further demonstrating a role for SIRT2 activation in the suppression of the inflammatory response. However, other contradictory results imply that SIRT2 might play a detrimental role under inflammatory conditions. In one study, SIRT2 inhibition by genetic and pharmacological mediators and reactive oxygen species by macrophages via a mechanism involving degradation of IκBα and nuclear translocation of p65 (Lee et al., 2014; Chen et al., 2015a). The systems of study are different what might explain the controversy, nevertheless this call for caution when extrapolate for therapy design.

A very interesting recent study demonstrate that release of cytokines such as *IL-1β* and *TNF-a* y by classically-activated neuroinflammatory microglia induce a subtype of astrocytes termed A1 reactive astrocytes which are neurotoxic for axotomized neurons and are present in human neurodegenerative diseases (Liddelow et al., 2017).

ACKNOWLEDGEMENTS

We are sincerely grateful to Dr Jesús Ruberte and Noaya Araujo from Universitat Autònoma de Barcelona for kindly proportionate Sirt1 transgenic mice. This work was mainly supported by the Ministerio de Economía y Competitividad of Spain (#SAF 2014-59701). We are also grateful for support from CIBERNED.

AUTHOR CONTRIBUTIONS

DRG conceived, designed and performed the experiments, analyzed the results and wrote part of the paper. HR did the PCR experiments and analyzed together with DR. In addition, DR helped in discussion together with CC who conceived, designed, supervised and analyzed all the experiments and wrote the paper.

COMPETING INTEREST

The authors declare no competing interests. NeuroHeal is currently under PCT extension.

SUPPLEMENTARY FIGURES

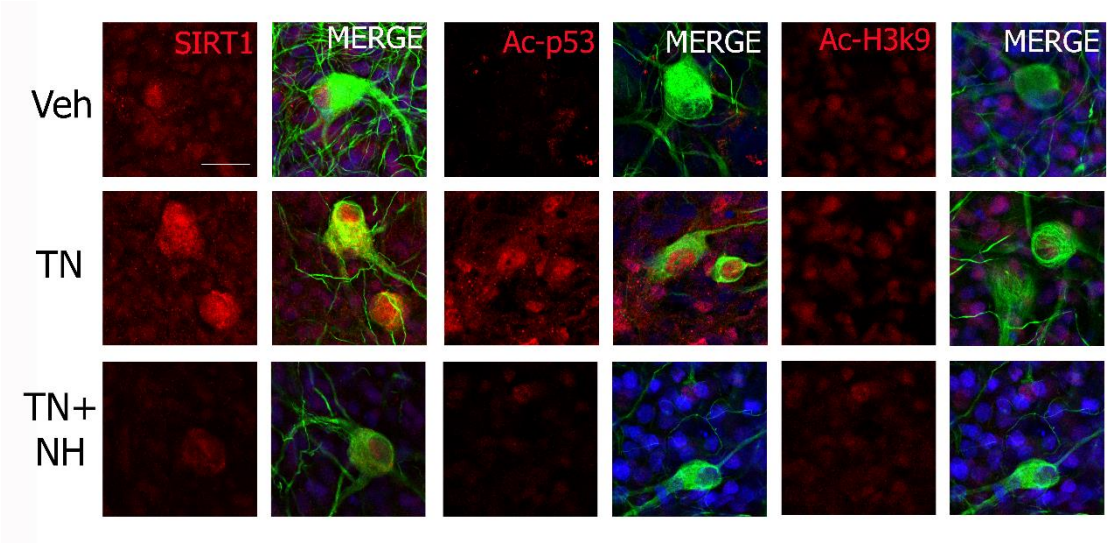

Figure S1. TN reduces SIRT1 activity and NH reverts this blockage. **(A)** Confocal microphotographs of immunolabelled SOCs against SIRT1, Ac-p53 and Ac-H3k9 in red, SMI3-32 in green and DAPI in blue for each group after 2 days with different treatments. Scale bar= 25µm

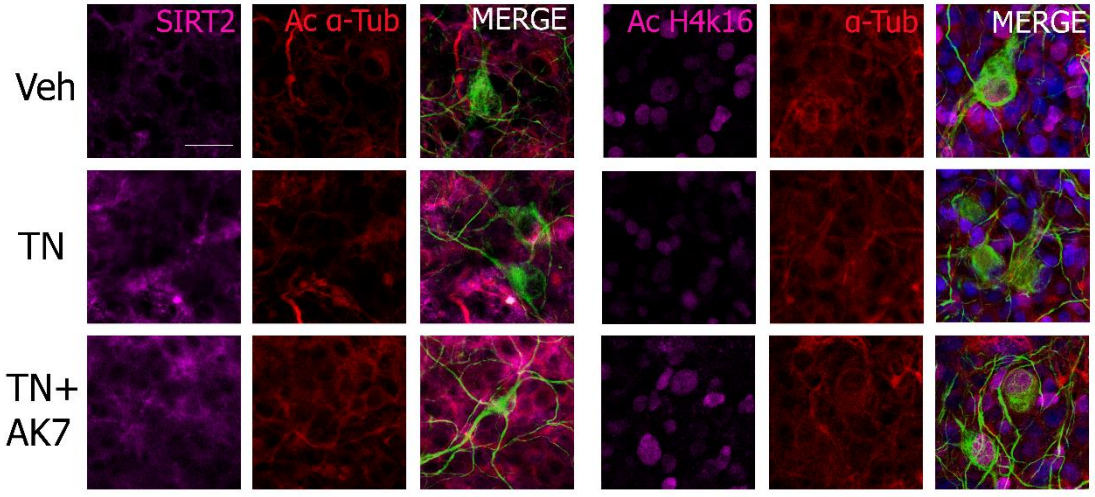

Figure S2. ER stress increases SIRT2 activity and AK7 blocks it (A) Confocal microphotographs of immunolabelled SOCs against SIRT2 or Ac-H4K16 in magenta, Ac or total α-tubulin in red, SMI3-32 in green and DAPI in blue for different groups 6 hours after Veh, TN or TN+AK7 treatment. Scale bar= 25µm

REFERENCES

Casas C, Isus L, Herrando-Grabulosa M, Mancuso FM, Borrás E, Sabidó E, Forés J, Aloy P (2015) Network-based proteomic approaches reveal the neurodegenerative, neuroprotective and pain-related mechanisms involved after retrograde axonal damage. Sci Rep 5:9185

Chang H-C, Guarente L (2014) SIRT1 and other sirtuins in metabolism. Trends Endocrinol Metab 25:138–145.

Chen H, Wu D, Ding X, Ying W (2015a) SIRT2 is required for lipopolysaccharide-induced activation of BV2 microglia. 2:88–93.

Chen X, Wales P, Quinti L, Zuo F, Moniot S, Herisson F, Rauf NA, Wang H, Silverman RB, Ayata C, Maxwell MM, Steegborn C, Schwarzschild MA, Outeiro TF, Kazantsev AG (2015b) The sirtuin-2 inhibitor AK7 is neuroprotective in models of parkinson's disease but not amyotrophic lateral sclerosis and cerebral ischemia. PLoS One 10:1–15.

Chopra V, Quinti L, Kim J, Vollor L, Narayanan KL, Edgerly C, Cipicchio PM, Lauver MA, Choi SH, Silverman RB, Ferrante RJ, Hersch S, Kazantsev AG (2012) The Sirtuin 2 Inhibitor AK-7 Is Neuroprotective in Huntington's Disease Mouse Models. Cell Rep 2:1492–1497

Conforti L, Gilley J, Coleman MP (2014) Wallerian degeneration: an emerging axon death pathway linking injury and disease. Nat Rev Neurosci 15:394–409

Di Fruscia P, Zacharioudakis E, Liu C, Moniot S, Laohasinnarong S, Khongkow M, Harrison IF, Koltsida K, Reynolds CR, Schmidtkunz K, Jung M, Chapman KL, Steegborn C, Dexter DT, Sternberg MJE, Lam EW-F, Fuchter MJ (2015) The Discovery of a Highly Selective 5,6,7,8-Tetrahydrobenzo[4,5]thieno[2,3- *d*]pyrimidin-4(3 *H*)-one SIRT2 Inhibitor that is Neuroprotective in an in vitro Parkinson's Disease Model. ChemMedChem 10:69–82.

Ferrucci M, Spalloni A, Bartalucci A, Cantafora E, Fulceri F, Nutini M, Longone P, Paparelli A, Fornai F (2010) A systematic study of brainstem motor nuclei in a mouse model of ALS, the effects of lithium. Neurobiol Dis 37:370–383.

Frye RA (2000) Phylogenetic classification of prokaryotic and eukaryotic Sir2-like proteins. Biochem Biophys Res Commun 273:793–798.

Haenggeli C, Kato AC (2002) Differential vulnerability of cranial motoneurons in

mouse models with motor neuron degeneration. Neurosci Lett 335:39–43.

Hayashi M (2010) Is developmental neuropathology of the motor neurons the key to resolving the mystery in motor neuron diseases? Brain Dev 32:265–267.

Herrando-Grabulosa M, Mulet R, Pujol A, Mas JM, Navarro X, Aloy P, Coma M, Casas C (2016) Novel Neuroprotective Multicomponent Therapy for Amyotrophic Lateral Sclerosis Designed by Networked Systems. PLoS One 11:e0147626.

Herranz D, Muñoz-Martin M, Cañamero M, Mulero F, Martinez-Pastor B, Fernandez-Capetillo O, Serrano M (2010) Sirt1 improves healthy ageing and protects from metabolic syndrome-associated cancer. Nat Commun 1:3.

Herskovits AZ, Guarente L (2013) Sirtuin deacetylases in neurodegenerative diseases of aging. Cell Res 23:746–758

Houtkooper RH, Pirinen E, Auwerx J (2012) Sirtuins as regulators of metabolism and healthspan. Nat Rev Mol Cell Biol 13:225–238

Jeong H, Cohen DE, Cui L, Supinski a, Savas JN, Mazzulli JR, Yates 3rd JR, Bordone L, Guarente L, Krainc D (2012) Sirt1 mediates neuroprotection from mutant huntingtin by activation of the TORC1 and CREB transcriptional pathway. Nat Med 18:159–165

Jęśko H, Wencel P, Strosznajder RP, Strosznajder JB (2017) Sirtuins and Their Roles in Brain Aging and Neurodegenerative Disorders. Neurochem Res 42:876–890.

Kanning KC, Kaplan A, Henderson CE (2010) Motor neuron diversity in development and disease. Annu Rev Neurosci 33:409–440.

Khoury N, Koronowski KB, Young JI, Perez-Pinzon MA (2017) The NAD $^{+}$ -Dependent Family of Sirtuins in Cerebral Ischemia and Preconditioning. Antioxid Redox Signal 0:ars.2017.7258.

Kim D, Nguyen MD, Dobbin MM, Fischer A, Sananbenesi F, Rodgers JT, Delalle I, Baur JA, Sui G, Armour SM, Puigserver P, Sinclair DA, Tsai L-H (2007) SIRT1 deacetylase protects against neurodegeneration in models for Alzheimer's disease and amyotrophic lateral sclerosis. EMBO J 26:3169–3179

Kim MJ, Kim DW, Park JH, Kim SJ, Lee CH, Yong JI, Ryu EJ, Cho S Bin, Yeo HJ, Hyeon J, Cho S-W, Kim D-S, Son O, Park J, Han KH, Cho YS, Eum WS, Choi SY (2013) PEP-1-SIRT2 inhibits inflammatory response and oxidative stress-induced cell death via expression of antioxidant enzymes in murine macrophages. Free Radic Biol Med 63:432–445

Kiryu-Seo S, Hirayama T, Kato R, Kiyama H (2005) Noxa is a critical mediator of p53-dependent motor neuron death after nerve injury in adult mouse. J Neurosci 25:1442–1447.

Kupis W, Pałyga J, Tomal E, Niewiadomska E (2016) The role of sirtuins in cellular homeostasis. J Physiol Biochem 72:371–380.

Lavezzi AM, Corna M, Mingrone R, Matturri L (2010) Study of the human hypoglossal nucleus : Normal development and morpho-functional alterations in sudden unexplained late fetal and infant death. Brain Dev 32:275–284.

Lee AS, Jung YJ, Kim D, Nguyen-Thanh T, Kang KP, Lee S, Park SK, Kim W (2014) SIRT2 ameliorates lipopolysaccharide-induced inflammation in macrophages. Biochem Biophys Res Commun 450:1363–1369.

Liddelow SA et al. (2017) Neurotoxic reactive astrocytes are induced by activated microglia. Nature 541:481–487.

Lin J, Sun B, Jiang C, Hong H, Zheng Y (2013) Sirt2 suppresses inflammatory responses in collagen-induced arthritis. Biochem Biophys Res Commun 441:897–903

Lo Sasso G, Menzies KJ, Mottis A, Piersigilli A, Perino A, Yamamoto H, Schoonjans K, Auwerx J (2014) SIRT2 Deficiency Modulates Macrophage Polarization and Susceptibility to Experimental Colitis Heimesaat MM, ed. PLoS One 9:e103573.

Luthi-Carter R, Taylor DM, Pallos J, Lambert E, Amore A, Parker A, Moffitt H, Smith DL, Runne H, Gokce O, Kuhn A, Xiang Z, Maxwell MM, Reeves SA, Bates GP, Neri C, Thompson LM, Marsh JL, Kazantsev AG (2010) SIRT2 inhibition achieves neuroprotection by decreasing sterol biosynthesis. Proc Natl Acad Sci U S A 107:7927–7932.

Mellini P, Valente S, Mai A (2015) Sirtuin modulators: an updated patent review (2012 - 2014). Expert Opin Ther Pat 25:5–15.

North BJ, Marshall BL, Borra MT, Denu JM, Verdin E, Francisco S (2003) The Human Sir2 Ortholog, SIRT2, Is an NAD+-Dependent Tubulin Deacetylase Brian. Mol Cell 11:437–444.

Outeiro TF, Kontopoulos E, Altmann SM, Kufareva I, Strathearn KE, Amore AM, Volk CB, Maxwell MM, Rochet J-C, McLean PJ, Young AB, Abagyan R, Feany MB, Hyman BT, Kazantsev AG (2007) Sirtuin 2 inhibitors rescue alpha-synuclein-mediated toxicity in models of Parkinson's disease. Science 317:516–519.

Pais TF, Marques O, Miller-fleming L, Antas P, Oliveira RM De, Kasapoglu B, Outeiro TF (2013) The NAD-dependent deacetylase sirtuin 2 is a suppressor of microglial activation and brain. :2603–2616.

Pallos J, Bodai L, Lukacsovich T, Purcell JM, Steffan JS, Thompson LM, Marsh JL (2008) Inhibition of specific HDACs and sirtuins suppresses pathogenesis in a Drosophila model of Huntington's disease. Hum Mol Genet 17:3767–3775.

Penas C, Font-Nieves M, Forés J, Petegnief V, Planas A, Navarro X, Casas C (2011) Autophagy, and BiP level decrease are early key events in retrograde degeneration of motoneurons. Cell Death Differ 18:1617–1627.

Romeo-Guitart D, Forés J, Herrando-Grabulosa M, Valls R, Leiva-Rodríguez T, Galea E, González-Pérez F, Navarro X, Petegnief V, Bosch A, Coma M, Mas J, Casas C (2017a) Neuroprotective Drug for Nerve Trauma Revealed Using Artificial Intelligence. Sci Rep Submitted.

Romeo-Guitart D, Forés J, Navarro X, Casas C (2017b) Boosted Regeneration and Reduced Denervated Muscle Atrophy by NeuroHeal in a Pre-clinical Model of Lumbar Root Avulsion with Delayed Reimplantation. Sci Rep 7:12028

Rothgiesser KM, Erener S, Waibel S, Lüscher B, Hottiger MO (2010) SIRT2 regulates NF-κB dependent gene expression through deacetylation of p65 Lys310. J Cell Sci 123:4251–4258

Serrano L, Martínez-Redondo P, Marazuela-Duque A, Vazquez BN, Dooley SJ, Voigt P, Beck DB, Kane-Goldsmith N, Tong Q, Rabanal RM, Fondevila D, Muñoz P, Krüger M, Tischfield JA, Vaquero A (2013) The tumor suppressor SirT2 regulates cell cycle progression and genome stability by modulating the mitotic deposition of H4K20 methylation. Genes Dev 27:639–653.

Sidrauski C, Walter P (1997) The transmembrane kinase Ire1p is a site-specific endonuclease that initiates mRNA splicing in the unfolded protein response. Cell 90:1031–1039.

Tadros MA, Fuglevand AJ, Brichta AM, Callister RJ (2016) Intrinsic excitability differs between murine hypoglossal and spinal motoneurons. J Neurophysiol:jn.01114.2015.

Taylor DM, Balabadra U, Xiang Z, Woodman B, Meade S, Amore A, Maxwell MM, Reeves S, Bates GP, Luthi-Carter R, Lowden PAS, Kazantsev AG (2011) A brain-permeable small molecule reduces neuronal cholesterol by inhibiting activity

of sirtuin 2 deacetylase. ACS Chem Biol 6:540–546.

Vaquero A, Scher M, Lee D, Erdjument-Bromage H, Tempst P, Reinberg D (2004) Human SirT1 interacts with histone H1 and promotes formation of facultative heterochromatin. Mol Cell 16:93–105.

Vaziri H, Dessain SK, Eaton EN, Imai SI, Frye R a., Pandita TK, Guarente L, Weinberg R a. (2001) hSIR2SIRT1 functions as an NAD-dependent p53 deacetylase. Cell 107:149–159.

Wachholz S, Esslinger M, Plumper J, Manitz M-P, Juckel G, Friebe A (2016) Microglia activation is associated with IFN-alpha induced depressive-like behavior. Brain Behav Immun 55:105–113.

Yamada J, Jinno S (2013) Novel objective classification of reactive microglia following hypoglossal axotomy using hierarchical cluster analysis. J Comp Neurol 521:1184–1201.

Yuan F, Xu ZM, Lu LY, Nie H, Ding J, Ying WH, Tian HL (2016) SIRT2 inhibition exacerbates neuroinflammation and blood-brain barrier disruption in experimental traumatic brain injury by enhancing NF-κB p65 acetylation and activation. J Neurochem 136:581–593.

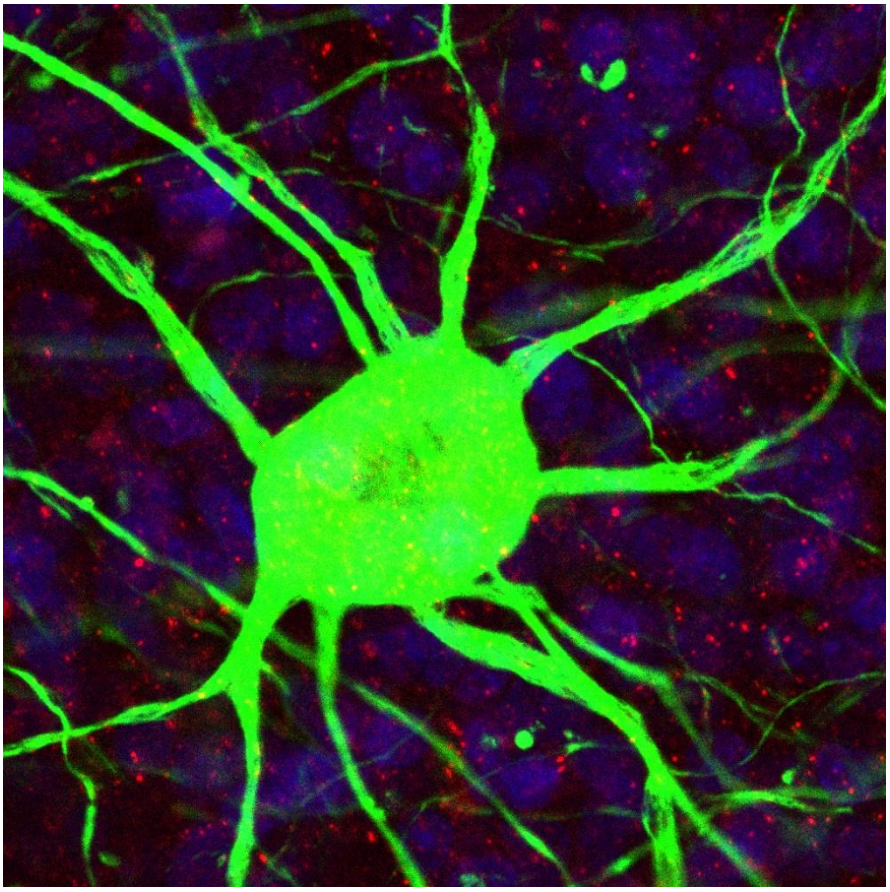

CHAPTER 3

NeuroHeal Confers Neonatal Neuroprotection Inducing SIRT1-Dependent Autophagy

David Romeo-Guitart[1], Xavier Navarro[1], Caty Casas[1*]

Affiliations

[1] *Institut de Neurociències* (INc) and Department of Cell Biology, Physiology and Immunology, *Universitat Autònoma de Barcelona* (UAB), & *Centro de Investigación Biomédica en Red sobre Enfermedades Neurodegenerativas* (CIBERNED), Bellaterra, Barcelona, Spain

*To whom correspondence should be addressed: Caty Casas Louzao, *Unitat de Fisiologia Mèdica*, *Facultat de Medicina*, *Universitat Autònoma de Barcelona*, E-08193 Bellaterra, Barcelona, Spain. Tel: +34-935811324, Fax: +34-935812986, E-mail: Caty.Casas@uab.cat

Running title: Neonatal Therapy for spinal root injuries

ABSTRACT

Sustain viability of motoneurons (MN) after the target deprivation during early postnatal stages can enhance functional recovery of patients whom suffered a nerve injury. Nowadays, new-born child who suffered a nerve injury only receive reparative surgery as therapy, being this insufficient to obtain an optimal motor recovery. MNs perish after the target deprivation due to an axonal disconnection, being this reduction the main cause of the future functional impairment. Currently, no neuroprotective therapies at clinical level are described to sustain MN viability until muscle reinnervation. We have recently discovered a drug combination called as NeuroHeal (NH), which is able to avert MN demise after nerve injury in adult stages. On the other side, it is also able to raise SIRT1 activity in different models characterized by massive MN death. We found that SIRT1 deacetylase activity is reduced within neonatal MNs after nerve injury. Target deprivation also induces the presence of apoptotic activation hallmarks such as caspase 3 and PARP cleavage were at the nuclei of injured MNs. The treatment with NH averted MN apoptotic death after sciatic nerve injury, modulated the post-transductional state of FOXO3a and increased the autophagic flux. NH had also long-lasting effects and did not affected the normal development of the peripheral nervous system. Thus, NeuroHeal is a promising treatment for the nerve injuries that occur during early stages of development.

Keywords: obstetric injuries, target deprivation, nerve crush, motoneurons, apoptosis, cell death, NeuroHeal, neuroprotection, Sirtuin 1, autophagy.

INTRODUCTION

Previous attempts to discover neuroprotective agents by identifying single therapeutic targets from pathological signalling cascades have failed to translate to efficacious therapies for neurodegenerative processes. We hypothesized that studying the molecular determinants of endogenous neuroprotection using systems biology approach in a well-established paradigm of self-neuroprotection against neuronal disconnection which is the distal peripheral nerve axotomy model (Casas et al., 2015), would reveal new neuroprotective agents (Romeo-Guitart et al., 2017a). Using artificial neural intelligence we discovered NeuroHeal, a combination of two repurposed drugs, acamprosate and ribavirin (Romeo-Guitart et al., 2017a). NeuroHeal was demonstrated to be neuroprotective for adult MNs after proximal axotomy (Romeo-Guitart et al., 2017b) and root avulsions (Romeo-Guitart et al., 2017c) which suffer a non-apoptotic neurodegenerative process. However, it is known that axotomized neonatal MNs dye by an apoptotic process (Oliveira *et al.*, 1997; Sun and Oppenheim, 2003). So, we did not know whether NeuroHeal could be neuroprotective for that.

Nervous system is extremely susceptible to external insults during the early days of development. Those injuries that disrupt the neuron-target organ connection, such as facial palsy or brachial plexus avulsion during obstetric interventions, will change the whole life of the new-born. Brachial injuries affects 2-3 of 1000 births (Pondaag et al., 2004). Although nerve regeneration is greater in new-borns than in adults and reparative surgery can be performed (Kennedy, 1903), functional deficits are not fully reversed and between 20 and 30% of those patients will not have an optimal spontaneous recovery (Pondaag et al., 2004; Malessy and Pondaag, 2009) or central developmental disabilities (Buitenhuis et al., 2012). The main cause that prevent the functional recovery is the fast and massive motoneurons (MNs) death that occurs after target deprivation (Lowrie et al., 1994). Therefore, sustain MN viability until axonal regrowth and the consequent organ reinnervation are achieved is essential to warranty a correct functional recovery.

The NAD-dependent deacetylase sirtuin-1, hereinafter SIRT1, has emerged as a neuroprotective player in several neurodegenerative models and in adult death

of MNs after root avulsion (Langley and Sauve, 2013; Romeo-Guitart et al., 2017a). SIRT1 is able to induce autophagy by the modulation of autophagy related genes (ATG) and the mammalian Target of Rapamycin (mTOR) (Lee et al., 2008; Ghosh et al., 2010). Parallelly to SIRT1 and acting co-ordinately, the phosphatidylinositol-4,5-bisphosphate 3-kinase (PI3K)/AKT axis also modulates autophagy depending on the cell paradigm (Jung et al., 2010; Wang et al., 2012b; Kaur and Sharma, 2017). Regarding our apoptotic death of MN, some studies suggest that autophagy can bypasses apoptotic outcome in other cell types and therefore avoid cellular death (Kondo et al., 2005; Maiuri et al., 2007)

The Forkhead box 0 proteins (FOXO) are a well-known transcription factors (TF) that drive cell metabolism, stress response and lifespan (van der Horst and Burgering, 2007). Among them, FOXO3a drives autophagic flux in different cell types such as hematopoietic (Israeli, 2013), cardiomyocytes (Sengupta et al., 2009) and muscle (Mammucari et al., 2007) conferring cell protection or modulating cell size. FOXO3a is downregulated after nerve or spinal cord injury (Wang et al., 2009a; Zhang et al., 2013), and exerts neuroprotection *in vitro* and in *C. elegans* models of MN death (Mojsilovic-Petrovic et al., 2009). The FOXO3a activity as TF is orchestrated by the direct AKT-phosphorylation and Sirt1-deacetylation, being both of them direct inhibitors of its activity. Nevertheless, it was recently SIRT1 promotes FOXO3a-depedent gene expression to exert neuroprotection in Huntington disease model (Jiang et al., 2012). So SIRT1 seems to drive the FOXO3a activity enhancing or repressing a set of transcriptional networks.

NeuroHeal, promotes SIRT1 Gain-of-Function and activates the AKT pathway. Therefore, we hypothesize that NH can induces autophagy after neonatal nerve injury and bypass the apoptotic death by dual modulation of FOXO3a. To achieve this aim, we used *in vivo* and *in vitro* models of neonatal MN death after nerve injury, we modulated SIRT1 and the PI3K/AKT axis and analysed FOXO3a state to test the hypothesis.

MATERIAL AND METHODS

Subjects and surgical procedures

All the procedures used in this work that involved animals were approved by the of Universitat Autònoma de Barcelona and Generalitat de Catalunya, and follow the European Community Council Directive 2010/63/EU. Pregnant rats were maintained under standard conditions of light, CO_2 and fed *ab libitum*. Once born, the litter was individualized for each rat and maintained with the same conditions. For surgical intervention, we deeply anesthetise pups at 4 days of age reducing its body temperature with ice. Besides this, we dissected the right sciatic nerve, we crushed it twice with a fine forceps during 10s and we closed the bound with suture. Animals were placed on a warm environment and once recovered, they were returned with its dam. For bilateral sciatic nerve injury, we crushed both nerve and sutured the bounds immediately.

Drug treatments

We purchased Acamprasate Calcium (Aca), Ribavirin (Rib), Ex-527, Nicotinamide (NAM), 3-Methyladenine (3MA) and LY-294,002 hydrochloride (Sigma-Aldrich, Saint Louis, MO), diluted H_2O or DMSO and added at 55µM, 1µM, 10µm, 5mM, 10µm and 10µm respectively to the *in vitro* SCOCs. The *in vivo* oral treatment NeuroHeal is composed by two diferent drugs: Aca (Merck, Darmstadt, Germany) and Rib (Normon, Madrid, Spain). We ground pills from both compounds into fine powder and added in tap water of the dams at final concentration of 2.2 mM and 1mM for Aca and Rib respectively. Nicotinamide was purchased from Sigma-Aldrich and dissolved into fresh water at final concentration of 5 mM. We added the NH or the NH+NAM drugs at the drinking water the previous day of the injury to ensure the pup treatment the same day of the injury. We added drugs to fresh water every 3 days. Vehicle water was also changed every 3 days.

Electrophysiological test

At 28 and 42 dpi, we deeply anesthetize animals with with ketamine/xylazine (100:10 mg/kg weight, i.p) and evaluated motor nerve conduction and reinnervation using an electromyography equipment (Synergy Medelec, Viasys

HealthCare). Body temperature was kept constant (34-36ºC) with the aid of a thermostated flat coil. We inserted two needle electrodes percutaneously at the sciatic notch and applied single rectangular pulses of 20μs with increasing voltage until generate the maximal evoked response. The compound muscle action potentials (CMAP) at gastrocnemius and plantar muscles were registered with microneedle electrodes, amplified, displayed and analyzed with the appropriate settings. We measured the onset of peak (latency, ms) and the distance between from baseline until top of the peak (Amplitude, mV). Once evaluated, the animals were allowed to recover in a warm environment.

Spinal organotypic cultures (SOCs)

We removed the spinal cord from 7-days old Sprague Dawley rats and placed it in 30% glucose cold Gey's balance salt solution (Sigma-Aldrich). Besides this, we cleaned it from meninges, cut it into 350μM–thickness slices and placed onto Millicell-CM of 30-mm-diameter (0,4μm, Millipore, Billerica, USA) within 6-weel plates (Thermo Fisher Scientific, Waltham, MA, usa) containing 1mL of culture medium. Culturing media is based in 50% (v/v) minimal essential medium (MEM), 2mM glutamine, 25 (v/v) Hank's Balanced Solution (HBSS, Simga-Aldrich) supplemented with 25.6 mg/mL glucose and 25 mM Hepes at pH=7,2. Cultures were maintained in a 5% CO2 air humidified environment at 37ºC. The following day after seed the SCOCs, we changed the media and added the different drug treatments: H_2O+DMSO as vehicle, NH, NH+Ex-527, NH+NAM, NH+3-MA and NH+LY294. Medium was changed twice per week. After 2 weeks of treatment, we removed the media, post-fixed the spinal cords with cold 4% PFA solution in a 0.1 M phosphate buffer at pH 7.2 for 1 hour, washed them with TBS several times and incubated during 48h with primary antibodies combined with mouse-anti anti-Neurofilament H Non-Phosphorylated (SMI32; 1:1000; Biolegend) at 4ºC. Confocal microphotographs of a predefined Z-stack were taken covering ventral horn of each SOCs and MN presence was assessed counting SMI32+ neurons for each SOC hemisection.

Tissue processing for histology

We euthanized at 10dpi or 42dpi the animals with dolethal injection (60 mg/kg i.p), and perfused them with transcarrdially infusion of a saline solution of heparine (10 U/mL) followed by 0.1M PBS buffer solution of 4% paraformaldehyde. We collected the L4-L5 spinal cord segments and the contra- and ipsilateral gastrocnemius muscles. The spinal cord were post-fixed 2 h with the same solution and introduced into a 30% sucrose solution for cryopreservation at 4ºC. Muscles weighted and transferred to the same sucrose solution. Muscle atrophy was assessed by the ratio between ipsi and contra muscle weight. We froze the spinal cords with Tissue-tek (Sakura Finetek) and cut them into serial slices of 20-µm (20 slices of 10 slides each) with the aid of cryotome (Leica, Heidelberg, Germany) and kept them at 20ºC until used.

Immunohistochemistry

For immunolabelling, we washed the spinal cord slides with Tris-buffered saline (TBS), treated them with TBS-Glycine 0,1mM and with blocking solution TBS with 0,3% Triton-X-100 and 10% donkey serum for 1h at RT. Then, we incubated overnight at ºC with the following primary antibodies: rabbit anti-ionized calcium binding adaptor molecule 1 (Iba1; 1:1000, Wako), rabbit anti-glial fibrillary acidic protein (GFAP; 1:1000, Dako), rabbit-anti NAD-dependent deacetylase sirtuin-1 (SIRT1; 1:100, Millipore), rabbit anti-acetyl-Histone H3 (Lys9) (Acetyl H3-K9; 1:50, Millipore), rabbit anti-acetyl-p53 (Lys373) (Acetyl p53-K373; 1:500, Millipore), rabbit rabbit-anti cleaved caspase 3 (Casp3 act.; 1:200;Cell Signaling), rabbit anti-lysosomal-associated membrane protein 1 (LAMP1; 1:200, Antibodies-online), mouse anti-autophagy protein 5 (ATG5; 1:200, Nanotool), mouse anti-nucleoporin 62 (p62; 1:100; BD Trasduction Laboratories), rabbit anti-phospho FOXO3a (Ser-253) (pFOXO3a; 1:500, Abcam), rabbit anti-FOXO3a (FOXO3a; Novus Biologicals, 1:200), rabbit anti-phospho Protein Kinase B/AKT (Ser-473) (pAKT; 1:500, Santa cruz), rabbit anti-C terminal of Poly [ADP-ribose] polymerase 1/2 (PARP1/2; 1:200; Santa Cruz) and goat anti-choline Acetyl-transferase (ChAT; Millipore, 1:50). After several washes with TBS with Tween-20 at 0,1%, we added specific donkey-Cy3 or Alexa488 against primary antibody (1:200; Jackson Immunoresearch) during 1h

and 30' at RT. We removed the exceeding secondary antibody washing with TBS-0,3Triton-X-100 and counterstained the slices with fluorescent green or blue NeuroTracer Nissl Stain (Molecular Probes, Leiden, Netherlands) and DAPI (Sigma, St Louis, MO, USA). The slices were washed with TBS and TB, and were mounted with Fluoromount-G mounting medium (SouthernBiotech).

We examined under confocal microscope with a Confocal Laser Scanning Microscope (Zeiss LSM 700; Zeiss, Jena, Germany) the spinal cord from different animals and experimental groups. Confocal images were systematically adquiered using three separate photomultiplier channels with a 1.4 numerial aperture objective of 20x under the same conditions of sensibility, resolution and exposure time for each analysed marker. Images were separately projected and merged using a pseudocolor display. Signal intensity was analysed with the aid of the ImageJ software (National Institutes of Health; available at http://rsb.info.nih.gov/ij/). The Nissl or DAPI labelling were used as ROI (Region of interest) to enclose the MN cytosolic or nuclei respectively area, and the integrated density within the ROI was obtained for at least 15 MNs extracted from three different sections (separated 100 μm between each one) per animal for each marker.

For gliotic response, we acquired images from at least five spinal cord sections (separated by 200-μm between pairs) immunolabelled against Iba1 and GFAP at 20X with the aid of a digital camera (Olympus DP76) attached to a microscope (Olympus BX51). The integrated density of marked ROI covering the whole ventral horn was calculated.

Immunohistochemistry of the sections to be compared between them were processed together on the same slide and on the same day. The analysis of the images to be compared was also performed the same day.

Western blotting and immunoprecipitation

To detect proteins by immunoblotting we collected 4 different SOCS for each "n" at 3 div or pup spinal cords (L4-L6 segments) at 3 dpi, added lysis buffer (50 Mm Tris, 2mM EDTA, 10 mM Nicotinamide, 0.5% Triton-X-100 and a cocktail of protease (Sigma) and phosphatase inhibitors (Roche); pH=6.8) homogenised with a Pellet pestle (Sigma-Aldrich) on ice, and sonicated with a Ultrasonic homogenizer (Model

3000, Biologics Inc). We centrifuged at during 10 min at 13000g at 4ºC, harvested the supernatant and was quantified it by BCA assay (Pierce Chemical Co.; Rockford, IL, USA). An equal amount of protein (10µg/well) were resolved in SDS-Page and transferred to a nitrocellulose membrane in a BioRad cubette system in 25 mM Tris, 192 mM glycine, 20% (v/v) methanol, pH 8.4. We blocked the membrane with 5% milk solution in 0.1% Tween-TBS for 1 hour at RT and incubated overnight with different primary antibodies: rabbit anti-C terminal of Poly [ADP-ribose] polymerase 1/2 (PARP1/2; 1:500; Santa Cruz), rabbit anti-phospho ulk1 (Ser 555) (pUlk1; 1:1000; Millipore), mouse anti-autophagy protein 5 (Atg5; 1:1000; Nanotools), rabbit anti-microtubule-associated proteins 1A/1B light chain 3B (LC3; 1:1000; Abcam), rabbit anti-phospho FOXO3a (Ser-253) (pFOXO3a; 1:1000, Abcam), rabbit anti-FOXO3a (FOXO3a; Novus Biologicals, 1:500), rabbit anti-phospho Protein Kinase B/AKT (pAKT; 1:1000; Cell Signalling), rabbit anti-AKT (AKT, 1:1000; Cell Signalling) and anti-β-actin (Actin; 1:3000; Sigma Aldrich). After wash the membrane, it was incubated for 1 h with an appropriate secondary antibody conjugated with horseradish peroxidase (1:5000, Vector). The membrane was visualized using a chemoluminiscent method (ECL Clarity kit, Bio-Rad Laboratories, Berkeley, CA, USA) and the images were captured and quantified with Image Lab Software (Bio-Rad Laboratories).

For Immunoprecipitation, we followed the manufacturer's protocol (Life Technologies). Briefly, we linked the anti-Acetylated lysine antibodies (Ac-Lys; 1:200; Sigma) to the magnetics particles on a rotatory wheel during 10 min at RT, washed them and incubated with 20µg of protein extract during 10 mins at RT on a rotatory wheel. After elution, proteins were denaturalized, resolved in SDS-Page gel of 10%, transferred to a nitrocellulose membrane, incubated with primary and secondary antibody as previously described.

Transmission Electronic microscopy

After perfusing the animals as explained previously, we submerged the L4-L6 spinal cord segment in a fixative solution of 2.5% (v/v) glutaraldehyde (EM grade, Merck, Darmstadt, Germany and 2% (w/v) PFA in PB 0.1M, pH 7.4 and placed them on a rocking platform for 2h. Besides this, we fixed in 1% (w/v) PFA and subsequently post-fixed with 1% (w/v) osmium tetroxide (TAAB Lab., UK)

containing 0.08% (w/v) potassium hexocyanoferrate (Sigma-Aldrich) in PB for 2 additional hours at 4ºC, and after 4 washed with deionized water, we dehidatrated them with sequential washes of acetone (Ref Alex). We embedded samples in EPON resin and polymerized it at 60ºC for 48h to obtain semithin sections (1µm) with a Leica ultracut UCT microtome (Leica Microsystems GmbH, Wetzlar, Germany). Besides this, we stained the sections with 1% (w/v) aqueous toluidine blue solution and examined with a light microscope to identify the ventral horn area. We cut with diamond knife ultrathin sections (70 nm), placed on coated grids and contrasted with conventional uranyl acetate and Reynolds lead citrate solutions. Finally, we observed the sections with a transmission electron microscope (EM) (Jeol1400 Ltd, Tokyo, Japan) equipped with a Gatan Ultrascan ES1000CCD Camera. We analyzed 3-4 MNs/animal.

Motor neuron counting

We stained with FluoroNissl (Life Technologies) green 20 slides (separated by 100 µm) covering all the L4-L5 medullar segment of every animals during 20 min following the manufacturer's protocol. We systemically took sequential microphotographs from the lateral funiculus of contra- and ipsilateral sides of each animal with the aid of a digital camera (Olympus DP76) attached to a microscope (Olympus BX51) at 20X. Only those MNs localized in the more lateral neuron pool of the grey matter with a prominent nuclear and higher soma of 900 μm^2 were counted as MN. The percentage of MN survival was calculated as the number of surviving MNs at the ipsilateral side respect to the contralateral for each animal.

Statistical analysis

Data is presented as mean ± standard error of the mean (SEM). We performed the statistical analysis with the aid of the GraphPad Prism 5 software. We performed Unpaired t-test, to compare two groups, or One-way analysis of variance (ANOVA), to compare three or more groups followed by Bonferroni's multiple comparison test. Significant differences were taken under a $p<0.05$ value.

RESULTS

NeuroHeal neuroprotects neonatal axotomized MNs in vivo and in vitro

To explore the neuroprotective potential of NH treatment of injured neonatal motoneurons we used a model of neonatal axotomy of the sciatic nerve by the postnatal day 4 of age (P4) (**Figure 1A**). Injury rapidly provoke the mortality of more than 38% of L4-L5 ipsilateral MNs regarding contralateral side (Figure 1B). Nourished mother was orally administered with NH at a particular concentration within the optimal therapeutic range (Romeo-Guitart et al., 2017a) expecting to arrive to sucking pups. We observed that NH treatment increased the percentage of MN survival compared to vehicle treatment (**Fig. 1B**). Since we previously reported that NH activated SIRT1 and this was relevant for survival to avulsed adult MNs (Romeo-Guitart et al., 2017a), we tested whether it was similar for neonatal MNs. We orally administered nicotinamide (NAM), a non-specific inhibitor of sirtuins' activity, concomitant to NH to suckled mothers. We observed that NAM treatment blocked the neuroprotective effect promoted by NH (**Fig. 1B**). We corroborate the effects of treatment on SIRT1 activity by analysing the acetylated levels of two of its substrates such as Histone H3 acetylated at Lys9 (Ac-H3k9) and p53 acetylated at Lys373 (Ac-p53) as direct readout (Imai et al., 2000; Luo et al., 2001a, 2001b). Axotomy produced an aberrant SIRT1 nuclear accumulation, but an overacetylation of both substrates indicating that SIRT1 activity was drastically reduced by injury (**Fig. 1C**). The treatment with NH normalized SIRT1 levels and the acetylation state of p53 and H3. This normalization effect produced by NH was blocked with the co-treatment with NAM suggesting that SIRT1 mediated the effect (**Fig. 1C**).

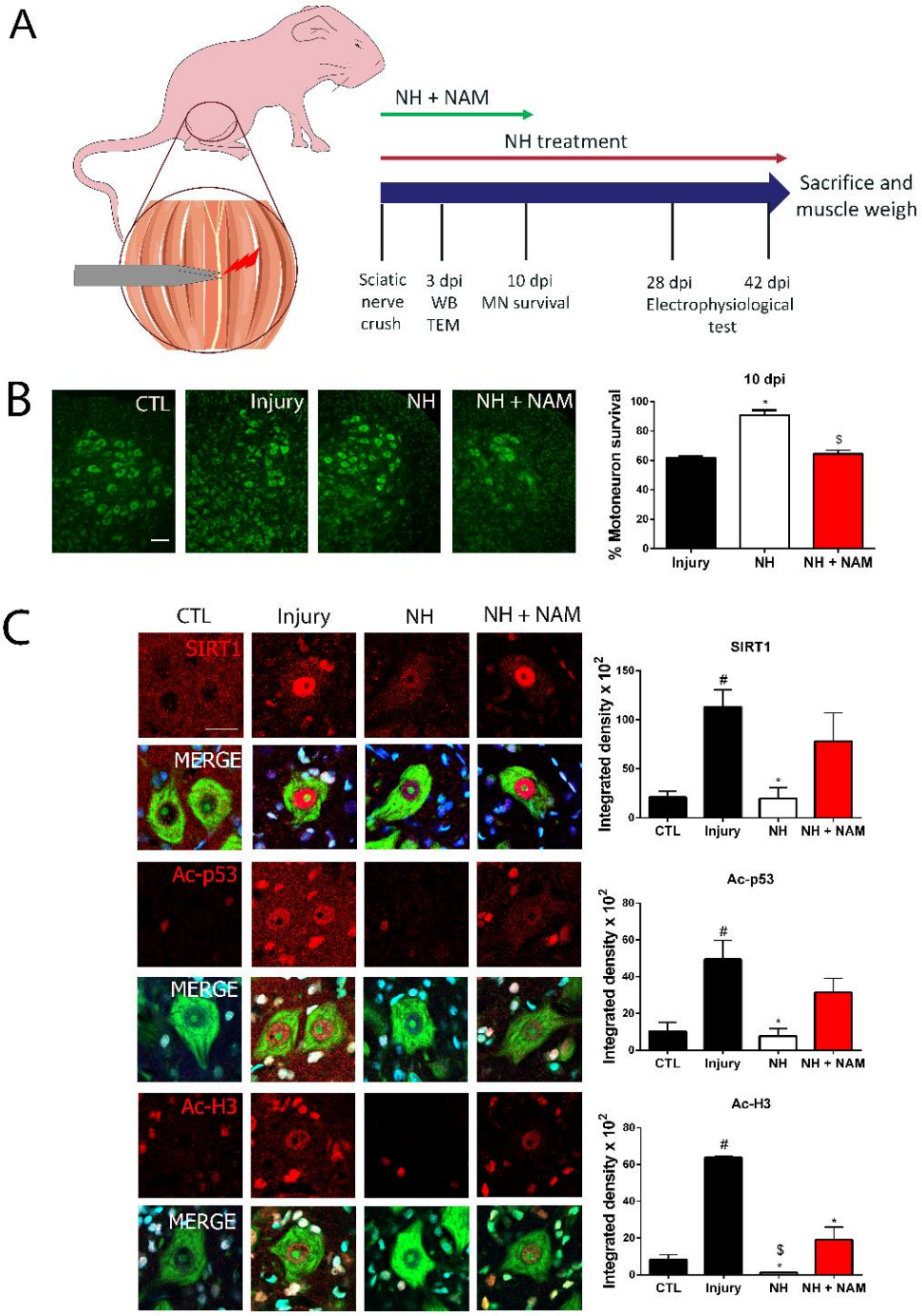

Figure 1: NH treatment reduces MN demise by SIRT1 Gain-of-Function. (A) Schematic and workflow of the experimental designof the procedure. At 4 days post birth, sciatic nerve from newborn-rats was crushed, and the animals were untreated or treated with NH or NH+NAM. At 3 days post injury (dpi), we extrated the L4-L5 spinal segments for Western blot (WB) and transmiscion electronic microscopy (TEM), for different groups. At 10 dpi, we extracted spinal cords to analyse motoneuron survival. Some untreated or NH-treated animals were electrophisiologycally tested at 28 or 42 dpi. **(B)** ***Left,*** Nissl microphotographs from spinal cords from control (CTL) or sciatic nerve crushed animals at 10 dpi. ***Right,*** Graphic showing the MN survival at the ipsilateral side with respect to the contralateral for injury, and injured treated with NeuroHeal (NH) or NH plus Nicotinamide (NAM) (n=4 group, ANOVA, post hoc Bonferroni *p<0.05 vs Injury). (**C**) ***Left,*** Confocal images of MNs

immunolabelled against SIRT1, Histone H3 acetylated at Lys-9 (Ac-H3k9), and p53 acetylated at Lys-373 (p53 Ack373) in red and counterstained with green fluorescent Nissl and DAPI from MNs of CTL and injured animals from different groups at 10dpi. ***Bottom***, Histograms of the mean of the immunofluorescence for each marker inside the nuclei of MNs (n=4 animals, ANOVA, post hoc Bonferroni, *p<0.05 vs NH, #p<0.05 vs CTL and $<0.05 vs NH+NAM). Scale bars= 100µm (B) and 25µm (C).

Injured-induced Apoptosis is not inhibited by NeuroHeal but it diminishes PARP1/2 cleavage

Since axotomy to neonatal MNs mainly engages the apoptotic pathway (Oliveira et al., 1997; Sun and Oppenheim, 2003), we investigated whether NH acted as an anti-apoptotic agent. We analysed the presence of cleaved casp3 as the last executer of the apoptotic pathway. As expected, cleaved casp3 was present in the nuclei of damaged MNs what was unchanged by NH treatment (Figure **2A**). PARP-1 is one of several known cellular substrates of caspases. Cleavage of Poly (ADP-ribose) polymerase (PARP-1/2) by caspases to yield an 85-kD PARP-1 fragment is considered to be a hallmark of apoptosis(Chaitanya et al., 2010b) .

By immunoblotting of L4-L5 spinal cord segments from neonatal injured pups at 3 dpi, we observed an increase of the 89-kD fragment after injury (**Fig. 2B**). However, NH treatment reduced the apparition of whole PARP1/2 (115 kDa band) and also the relative abundance of the active cleaved form of 89 kDa (**Fig. 2B**). In agreement, immunohistochemical analysis of PARP1/2 localization revealed that this enzyme was overrepresented within the nuclei and dispersed in the cytosol of injured MNs as expected (**Fig. 2C**). However, NH treatment drastically reduced its overall presence. Curiously, NAM co-treatment abolished the effect observed produced by NH (**Fig. 2C**). These results suggested that NH might prevent late apoptotic events downstream of caspase 3.

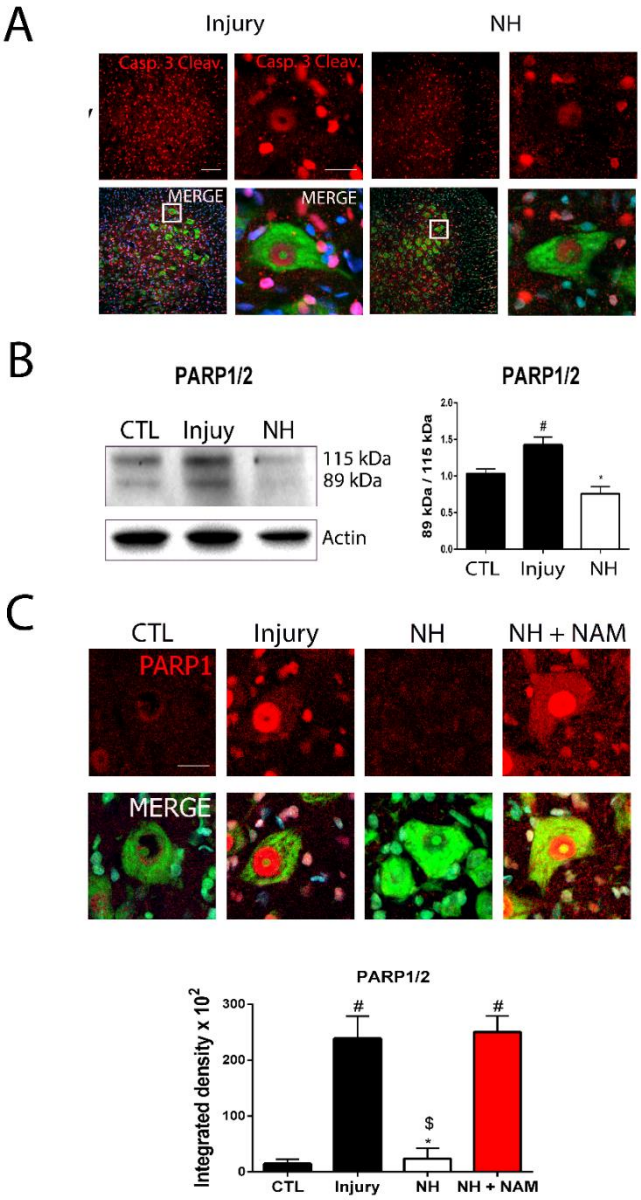

Figure 2: Apoptosis is engaged and inhibited at PARP1 level. (A) Representative confocal images of MNs from spinal cords immunolabelled against Cleaved caspase 3 (Casp3. Act) in red, Fluoronissl in green and DAPI from injury with or without NH treatment at 10dpi. Scale bar= 100µm high magnification and 20µm low magnification. (**B**) Western blots and histogram showing the analysis of PARP1 protein levels in control (CTL), injury and injury with NH treatment animals at 3dpi. (n=4 animals, ANOVA, post hoc Bonferroni, *p<0.05 vs NH, #p<0.05 vs CTL). (**C**) ***Top***, Confocal microphotographs of the immunolabelling of PARP1 in red, Fluoronissl in green and DAPI in blue of MNs from different experimental conditions at 10dpi. ***Bottom***, Quantification of the integrated density of PARP1 into the nuclei of MNs for different experimental groups (n=4 animals, ANOVA, post hoc Bonferroni, *p<0.05 vs Injury, #p<0.05 vs CTL and $p<0.05 vs NH+NAM) Scale bar= 20µm.

We further investigated the effects of axotomy and the neuroprotective potential of NH using an *in vitro* model of neonatal axotomy based on organotypic

culture of postnatal spinal cord (SOC) (Guzmán-Lenis et al., 2009b). Chopped spinal cord slices devoid of its roots provoked a natural death of 25% of MNs along 15 DIV (**Fig. 3A**). Similarly, to the *in vivo* results, we observed that NH promoted neuroprotection of axotomized MNs in the SOCs (**Fig. 3A**). We analysed caspase 3 and PARP1 cleavage. Similarly, axotomy provoked accumulation of cleaved caspase 3 within the MN nuclei in both vehicle and NH-treated SOCs (**Fig. 3B**). Axotomy induced an increase of the PARP1 89 KDa fragment which was attenuated by NH treatment (**Fig. 3C**). These results suggested that the *in vitro* model of axotomy further reproduced the *in vivo* model.

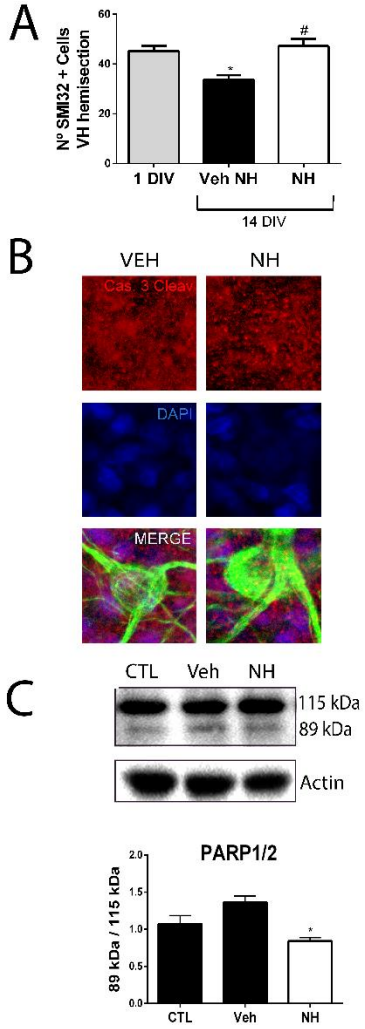

Figure 3: NH neuroprotects axotomized MNs *in vitro.* (A) Bar graphs showing the number ± SEM of SMI-32 positive cells in the ventral horn of each hemi-section of the spinal cord slice (n=8-12 complete spinal cord slices, ANOVA, post hoc Bonferroni *p<0.05 vs 1DIV, #p<0.05 vs Veh) (**B**) Confocal micropothographs of Cleaved caspase 3 (Casp3. Cleav) in red, SMI32 in green and DAPI from CTL, Veh or NH-Treated SOCs at 15DIV. Scale bar= 20µm **(C)** Western blots and histogram showing the analysis of PARP1 protein levels from CTL, Veh or NH treated SOCs at 2 days post treatment (n=4, ANOVA, post hoc Bonferroni, *p<0.05 vs Veh).

SIRT1 and PI3K downstream FOXO3a modifications are targeted by NeuroHeal

We analysed FOXO3a transcription factor whose phosphorylation by PI3K (Brunet et al., 1999) or deacetylation by SIRT1 (Brunet et al., 2004; Motta et al., 2004) may drive survival or death (van der Horst and Burgering, 2007). We found that FOXO3a is abundantly expressed in neonatal spinal MNs both *in vivo* and in the cultured SOCs at 15 DIV (**Fig. 4A**). FOXO3a can be phosphorylated by AKT at Ser 253 (Brunet et al., 1999). We found that injury provoked an increase of pAKT which is not altered by treatment with NH alone or in combination with NAM (**Fig. 4B**). This increase correlated with an increase of pFOXO3a which was sustained by NH but abrogated when added NAM (**Fig, 4C**). Subcellular localization of pFOXO3a was determined by immunohistochemical analysis. We found that pFOXO3a was mainly cytosolic after injury but NH treatment forced its localization to be nuclear which was abolished by co-treatment with NAM (**Fig. 4D**). Since acetylation also influence in activity and localization of FOXO3a (van der Horst and Burgering, 2007), we investigated the amount of this isoform by immunoblotting. The amount of acetylated form of pFOXO3a was significantly higher after injury respect to control, and NH treatment reduced its levels (**Fig. 4E**). Similarly, *in vitro*, we verified that pFOXO3a levels and its entrance to nucleus were increased by NH (**Fig. 4F**). Co-treatment of NH with an specific SIRT1 inhibitor, EX-527, abolished these increment (**Fig. 4G**) and trendy with NAM co-incubation. Axotomy also increased Ac-pFOXO3a and NH reduced its presence (**Fig. 4H**).

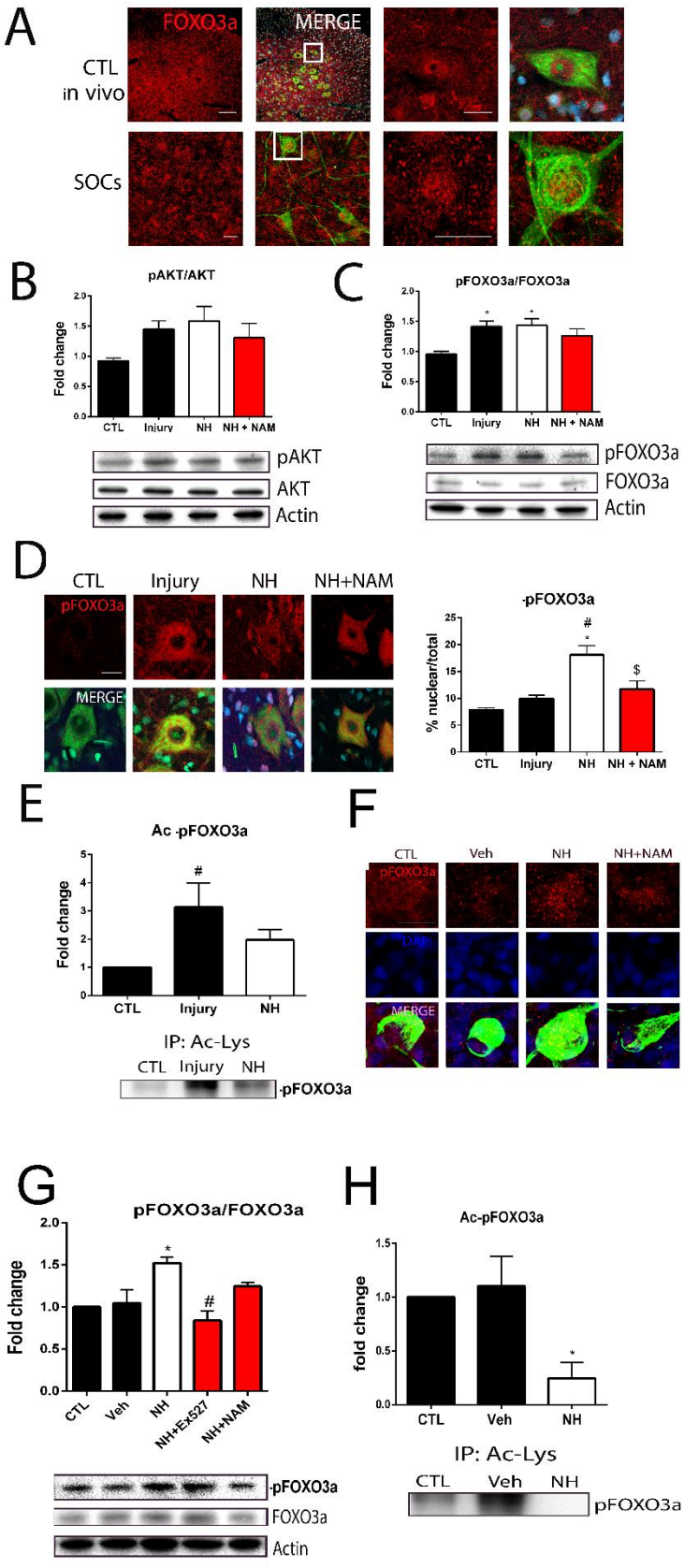

Figure 4: NH modulates FOXO3a. (A) Confocal microphotographs showing the expression of FOXO3a in red, colabeled with Nissl or SMI32 in green and DAPI, from CTL spinal cord from 15 days old animals or untreated SOCs at 15 DIV. Scale bar=100µ for high

magnification of the *in vivo* and 20µm for other (**B**, **C)** Western blots and histogram showing the analysis of pFOXO3a (Ser 253), FOXO3a, pAKT and AKT protein levels in different experimental groups at 3dpi. (n=4 animals, ANOVA, post hoc Bonferroni, *p<0.05 vs NH, #p<0.05 vs CTL). (**D**) ***Left,*** Confocal microphotographs labelled against pFOXO3a in red, and Fluronissl and DAPI as colabeling from different analysed conditions Scale bar= 20µm ***Right,*** Histogram showing the % of nuclear fluorescence of pFOXO3 respect the total labelling within MNs for different experimental conditions (n=4 animals, ANOVA, post hoc Bonferroni, *p<0.05 vs CTL, #p<0.05 vs Injury and $p<0.05 vs NH+NAM). (**E)** Western blots and histogram showing the analysis of immunoprecipitated Ac-pFOXO3a (Ser 253), levels in different *in vivo* experimental groups at 3dpi. (n=4 animals, ANOVA, post hoc Bonferroni, #p<0.05 CTL). (**F**) Confocal microphotographs labelled against pFOXO3a in red, and SMI32 in green and DAPI as colabeling from SOCs in diferent groups at 15DIV Scale bar= 20µm. (**G**) Western blots and histogram showing the analysis of pFOXO3a (Ser 253) and FOXO3a from different SOC-treated groups at 3DIV (n=4, ANOVA, post hoc Bonferroni, *p<0.05 vs Veh, #p<0.05 vs NH). (**H)** Western blots and histogram showing the analysis of immunoprecipitated Ac-pFOXO3a (Ser 253) protein levels in different experimental groups at 3dpi. (n=4 animals, ANOVA, post hoc Bonferroni, *p<0.05 vs NH, #p<0.05 vs CTL).

SIRT1 activation is necessary for autophagy induction by NeuroHeal

In order to further analyse the way NH promote neuroprotection to neonatal axotomized MNs, and considering that several studies reported the existence of crosstalk between apoptosis and autophagy which are used by some cancer cells to bypass pro-apoptotic chemotherapy (Kondo et al., 2005), we analysed the autophagic flux after NH treatment. We evaluated the presence of autophagy markers such as LC3II formation, Ulk1 phosphorylation at Ser 555 and the presence of conjugated ATG5/ATG12 (Klionsky et al., 2016) by western blot at 3dpi. We found that all these markers were increased in injured tissue by NH treatment, and that these effects were abolished with the NAM co-treatment (**Fig. 5A**). Accordingly, NH treatment reduced the presence of p62 and increases LAMP1 and ATG5 within the cytosol of MNs at 10 dpi (**Fig. 5B**). Moreover, TEM images confirmed the presence of autophagosomes and autolysosomes only after NH treatment at 3dpi (**Fig. 5C**).

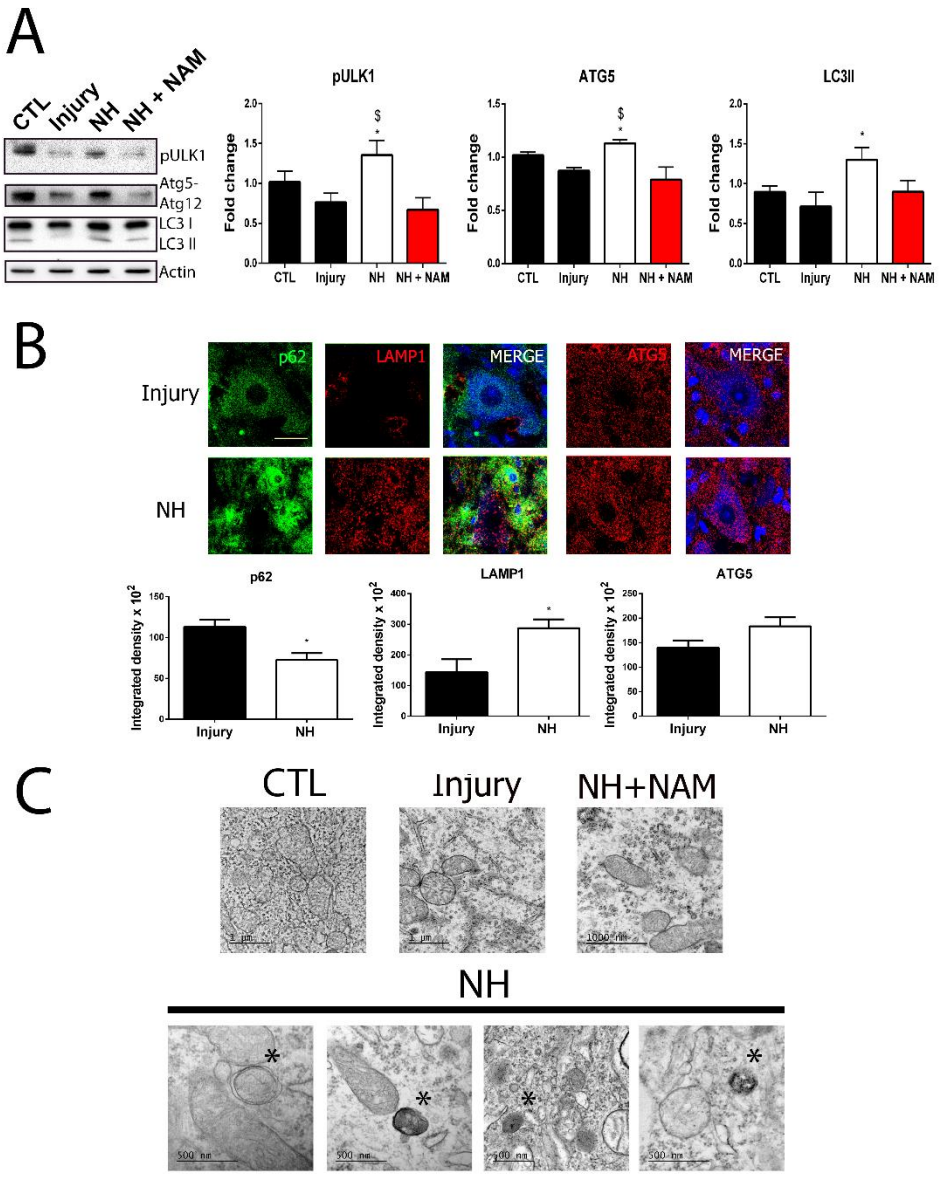

Figure 5: NH treatment induces autophagy and this depends on SIRT1 activity. (A) Western blots and histogram showing the analysis of pUlk1 (Ser555), ATG5-ATG12 and LC3II protein levels in different experimental groups at 3dpi. (n=4 animals, ANOVA, post hoc Bonferroni, *p<0.05 vs NH, #p<0.05 vs CTL). **(B)** ***Top,*** Confocal microphotographs labelled against p62 in green, LAMP1 and ATG5 in red, and counterstained with Fluoronissl blue and DAPI, from injury and NH treated animals. ***Bottom,*** Histograms of the mean of the immunofluorescence for each marker within the MNs (n=4 animals, t-test, *p<0.05 vs Injury). Scale bar= 25 µm. (**C**) Transmission electronic images from CTL, injury, NH and NH+NAM animals at 3dpi. Note that only autophagosomes or autolysosomes, marked with an asterisk, are detected in NH-treated MNs.

Further investigation revealed that NH treatment promoted autophagy to injured slices observed by an increase in LC3II, pUlk1 and ATG5 presence (**Fig. 6A**). These increments were abolished when NH treatment was combined with

autophagy inhibitors such as 3MA or LY294, a well described inhibitors of Phosphatidylinositol 3-kinases (PI-3K). In addition, specific inhibition of SIRT1 with EX-527 or with NAM, also blocked autophagy induction promoted by NH (**Fig. 6A**). Both SIRT1 inhibitors were verified to increase the acetylated forms of p53 and H3, as expected (**Fig. S1**). Accordingly, NH-promoted neuroprotection was abolished either when co-treatment with SIRT1 inhibitors or autophagy inhibitors (**Fig. 6B**).

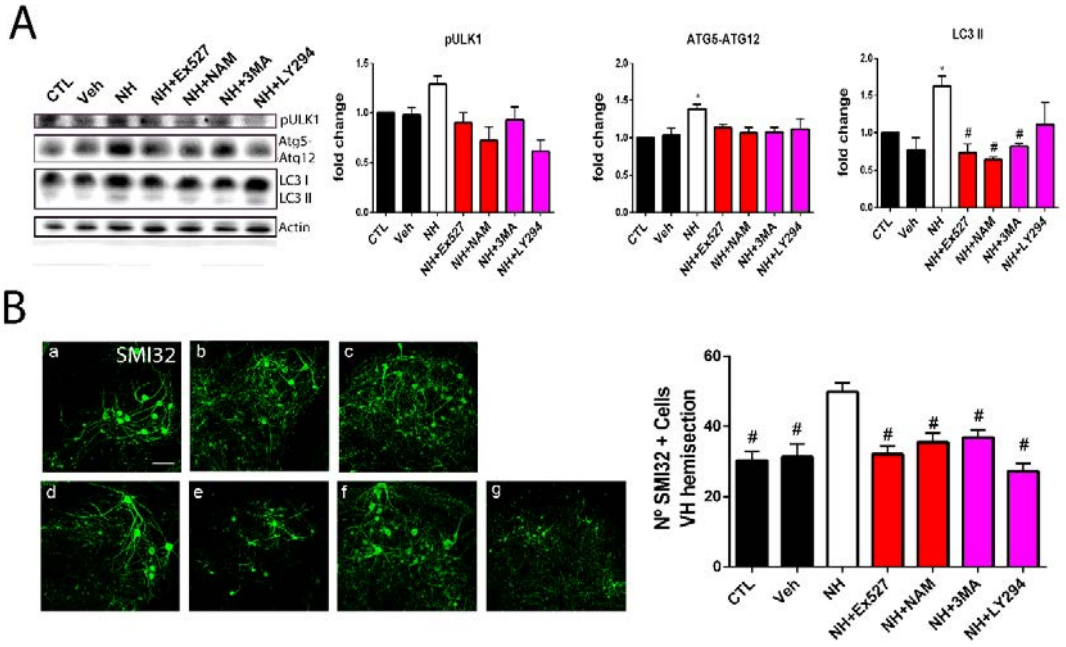

Figure 6: NH neuroprotects axotomized MNs by AKT/SIRT1 axes. (A) Western blots and histogram showing the analysis of pUlk1 (Ser555), ATG5-ATG12 and LC3II protein levels from SOCs after 2 days of treatment with NH alone or in combination with SIRT1 or PI3K inhibitors (n=4, ANOVA, post hoc Bonferroni, *p<0.05 vs Veh, #p<0.05 vs NH). (**B)** ***Left,*** SMI-32 representative microphotographs from the ventral horn of the SOCs after two weeks of treatment with NH alone or in combination with SIRT1 or PI3K inhibitors. Scale bar=100µm ***Right***, Bar graphs showing the number ± SEM of SMI-32 positive cells in the ventral horn of each hemi-section of the spinal cord slice (n=8-12 complete spinal cord slices, ANOVA, post hoc Bonferroni #p<0.05 vs NH) Scale bar = 100µm.

These results suggested that the model reproduces well what seems to account *in vivo* and NH may promote neuroprotection through autophagy induction where SIRT1 and PI3K activation seem to be necessary.

Sustainability of endogenous neonatal nerve regenerative capability by NeuroHeal

After nerve crush, pups are able to regenerate the nerve (Kashihara et al., 1987). We previously reported that NH was capable to accelerate nerve regeneration after crush injury (Romeo-Guitart et al., 2017a) or avulsion and reimplantation of nerve roots (Romeo-Guitart et al., 2017b) in the adult. Thus, we analyzed any effect by NH on motor nerve regeneration in the axotomized pups. We observed that the compound muscle action potential (CMAP) amplitude and latency were not modified by NH treatment in contralateral and injured side at 28 and 42 dpi (**Fig. 7A**). In the same way, muscle atrophy and its recovery after nerve injury was not altered between both groups (**Fig. 7B**), indicating that after the injury the NH did not averted a correct muscle development. Regarding neuroprotection, the treatment with NH gave a raise in MN survival (**Fig. 7C**) and reduced astroglial and microglial reactivity at 42 dpi (**Fig. 7D**). At this time post injury, cleaved caspase 3 disappeared from the nuclei in both groups, indicating that the MN faced up the insult and survived. To check if the behaviour of remaining MNs is normal, we analysed the Choline Acetyltransferase (ChAT) by IHC as marker of mature neuron, and we observed that MNs from both groups had similar levels of this enzyme (**Fig. 7D**).

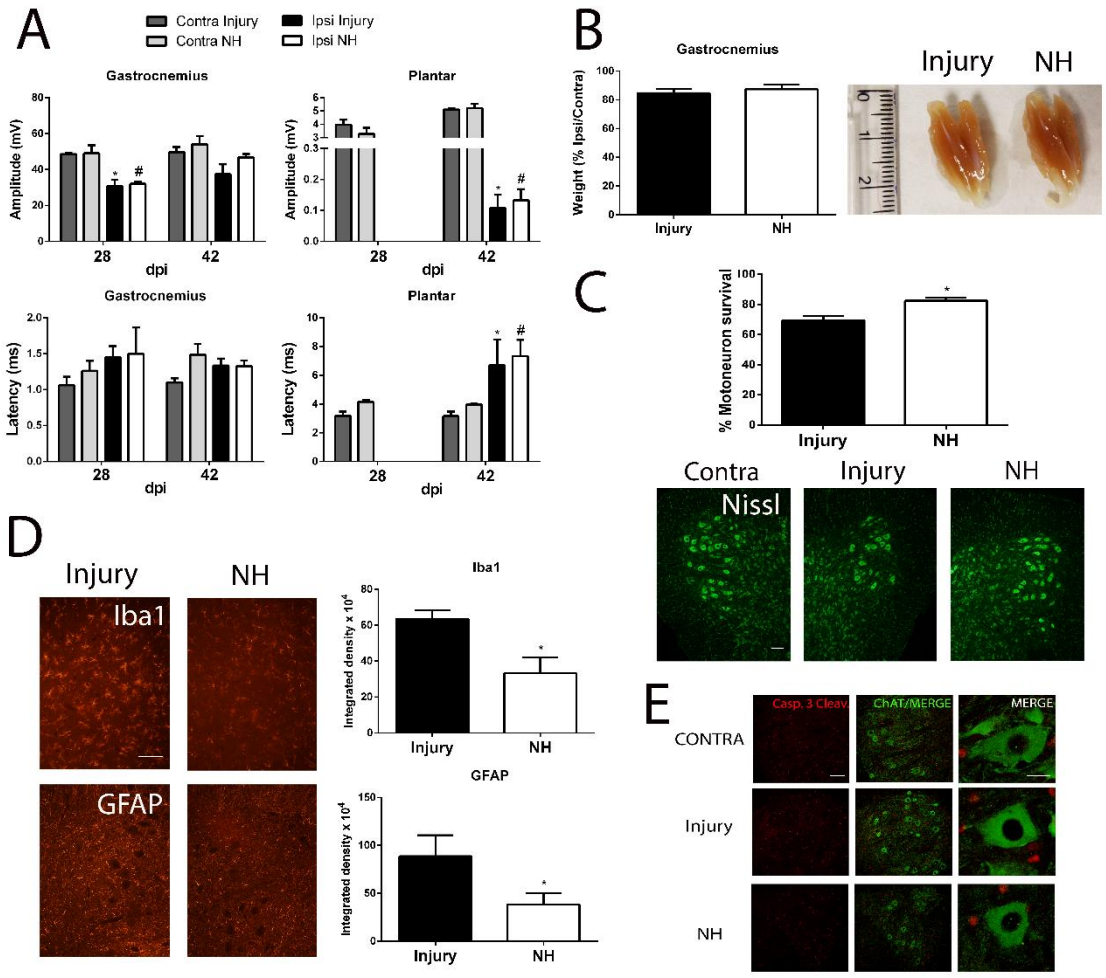

Figure 7. NH effects are maintained until adulthood and did not affected peripheral nervous system development. Mean amplitudes (± SEM) and time latency values of CMAP recordings obtained during follow-up post injury from Gastrocnemius and Plantar muscles (n=4, ANOVA, post hoc Bonferroni, * p<0.05 vs Contra injury, #p<0.05 vs Contra NH). (**B)** Representative photographs of GA muscle from injured side from untreated and NH-treated rats with the histograms of weight ratio between ipsilateral and contralateral muscles at end stage (n=4; t-test, * p<0.05 Injury) (**C**) Representative microphotographs of ventral horns of sciatic-crushed spinal cords stained with fluorescent Nissl at 42 dpi from injured untreated or NH-treated and the bar graphs showing the average percentage of surviving MNs ± SEM (n=4; t-test, * p<0.05 Injury). Scale bar = 100 (**D)** ***Left,*** Representative microphotographs of ventral horns from injured animals with labeled microglia (Iba1) and astrocytes (GFAP). ***Right***, Histograms of the averaged immunoreactivity in the fixed region of interest at the ventral horn from different groups (n=4; t-test, * p<0.05 Injury). Scale bar = 100 µm. (**E**) Confocal microphotographs of MNs labeled against Cleaved Caspase 3 in red or ChAT in green at low (left) and high magnification (right) at end stage.

.

DISCUSSION

In this study, we investigated the involvement of SIRT1 and PI3K activation in neuroprotection of neonatal axotomized MNs *in vivo* and *in vitro*. Neonatal axotomy produced apoptosis to MNs with casp3 and downstream substrate PARP1 cleavage. We showed that the SIRT1 activator NeuroHeal exerted neuroprotection by promoting a notably reduction of the apoptotic hallmark fragment of PARP1(Chaitanya et al., 2010a) despite persistent cleaved caspase 3. Investigating the mechanisms by which NeuroHeal exerted neuroprotection we revealed that it triggered SIRT1 and PI3K-dependent autophagy which was essential for MN survival. Detailed downstream analysis pointed to pFOXO3a deacetylation by SIRT1 as a relevant implicated factor although further analysis would determine the degree of its implication in NH-induced autophagy. NeuroHeal exerted no-avert effects on normal nerve regenerative process which is important for its therapeutic potential for the treatment of traumatic injury after birth.

Neuroprotective strategies are still clinical demanded by society. NeuroHeal was envisaged as an agent to boost endogenous mechanisms of self-neuroprotection(Romeo-Guitart et al., 2017a, 2017b). It was discovered through a systems biology approach to analyse comparative proteomic data between a model of MN degeneration (proximal injury) and another of MN survival and regeneration (distal injury) after axotomy obtained by simply changing the distance of injury in the adult rat (Romeo-Guitart et al., 2017a). In the present work, we observed that axotomy to neonatal nerves produced MN apoptosis in agreement with previously reported studies (Deckwerth et al., 1996b; Chan et al., 2001; Sun and Oppenheim, 2003). We observed that it was characterized by the presence of caspase 3 and PARP1 cleavage but also with an increase of p-AKT and accordingly, a huge accumulation of cytoplasmic phosphorylated FOXO3a (Tzivion et al., 2011; Brunet et al., 1999). However, importantly, phosphorylation by AKT and other kinases such as, IKK, and ERK, also constitutes a signal for poly-ubiquitination and proteasomal degradation of FOXO transcription factors (Matsuzaki et al., 2003; Huang and Tindall, 2011) which is the opposite we observed after axotomy suggesting that proteasomal degradation of FOXO3a might be compromised. Since AKT activation by PI3K phosphorylation is commonly accepted as a pro-survival signal, we

considered this activation as an unsuccessful attempt of MNs to cope with the injury. The same for the AKT-dependent FOXO3a cytoplasmic export preventing the transcription factor induce the expression of several pro-apoptotic genes such as BiM (Hagenbuchner et al., 2012) or BH3-only protein Puma (Ekoff et al., 2007).

SIRT1 however is inactivated within MNs after injury as observed by accumulation of acetylated targets such as p53 (Luo et al., 2001a) and H3 (Imai et al., 2000). SIRT1 activity induces p53 deacetylation to avoid apoptotic cell death (Luo et al., 2001a) and neurodegeneration (Hasegawa and Yoshikawa, 2008). After axotomy, SIRT1 might be inactivated probably due to its dependence of NAD+ levels. Axotomy disrupt membrane integrity allowing massive calcium entry into the neuron which may produce energy depletion and run out NAD+ stock which as requirement for SIRT1 activation (Petegnief and Planas, 2013). SIRT1 is also affecting FOXO3a destiny by deacetylation. Sirt1 deacetylates FoxOs and regulates FoxO-dependent gene transcription either positively or negatively (Brunet et al., 2004)(Motta et al., 2004). Indeed, it was observed that the same sites are either acetylated or ubiquitinated for proteasomal targeting (Huang and Tindall, 2011). Hence, sirt1 inactivation after axotomy would render foxo3a acetylated that is a more stable form which explain the huge cytosolic accumulation observed.

In this scenario, NH treatment sustained pAKT levels but promoted activation of SIRT1 as well. As a consequence, levels of phosphorylated foxo3a drastically decrease in the cytosol in agreement with its deacetylation state more prone to be degraded. Curiously, although, reduced levels, there was an increased proportion of pFoxo3a in the nucleus. In the literature, the dogma is that once phosphorylated it is out of nuclei and hence inactive. But it is non-reported what can be doing a version of foxo3a which is phosphorylated and deacetylated in the nucleus. If it is active as a transcription factor, it would be interesting to analyse the levels of transcription for several of their target genes, particularly those pro-autophagic genes such as ULK2, Beclin 1, VPS34, Bnip3 and Bnip3L, Atg 12, Atg4B, LC3, and GABAR- APL1 (Kroemer et al., 2010) that have been reported upregulated by foxo3a in several models (Hariharan et al., 2010; Ni et al., 2013; Warr et al., 2013; Sun et al., 2017). Consistently, the transcription of ATG genes will push the apparition of autophagy and would help explaining the apparition of SIRT-

dependent autophagy promoted by NH. In addition to this putative increase of ATG gene expression which might not be sufficient to fully engage autophagy, it is probably that other activated SIRT1-dependent actions might also be involved. SIRT1 can deacetylate Atg5, Atg7 and LC3 (Lee et al., 2008). Besides, a cytoplasm-restricted mutant of Sirt1 could stimulate autophagy (Morselli et al., 2010).

Although largely nuclear in many cell types, Sirt1 could also be cytoplasmic or mitochondrial localized (Aquilano et al., 2013). We observed that SIRT1 was strongly accumulated within the nuclei of the neonatal MNs after injury leading to inactivation. Curiously, NAM blocked the SIRT1 level and activity restoration promoted by NH. These results suggested that SIRT1 might be deacetylated by a NAD+ dependent deacetylase, maybe itself, and this may lead to degradation. It has been reported recently that SIRT1 deacetylate SIRT3 in the mitochondria and this is affect its activity and stability (Kwon et al., 2017). Although, the acetylation status of SIRT1 is not documented it is possible that it happens similarly. This would explain, why NH treatment downregulated SIRT1 levels but increased its activity.

Indeed, autophagy promoted by NH is sensible to the use of SIRT1 as well as to PI3K inhibitors. Both PI3K inhibitors used blocked the formation of Ptdns (3)P which is widely reported to be necessary for the formation of autophagosome (Klionsky et al., 2016). The particular case of LY294002, which inhibits class I PI3K, inhibits also AKT phosphorylation. The implication of AKT in autophagy is dual since it activates mTOR, which is supposed to inhibit autophagy (Jung et al., 2010; Kaur and Sharma, 2017), and phosphorylated Beclin-1 which clearly inhibit autophagy (Wang et al., 2012b). But, on the opposite, AKT is translocated and needed for the formation of the autolysosome (Matsuda-Lennikov et al., 2014). Thus, the interplay between Sirt1 and AKT that directly interact and act on several common targets, may fine tune the degree of autophagy to promote survival otherwise too excessive autophagy is detrimental for the neuron.

ACKNOWLEDGEMENTS

We thank Ariadna Arbat for helping with the neonatal axotomy model. This work was mainly supported by the Ministerio de Economía y Competitividad of Spain (#SAF 2014-59701). We are also grateful for support from CIBERNED and TERCEL. The RT97, antibody was obtained from the Developmental Studies Hybridoma Bank developed under the auspices of the NICHD and maintained by the University of Iowa, Department of Biology.

AUTHOR CONTRIBUTIONS

DRG performed the experiments, analyzed the results, and wrote part of the paper. XN conceived experiment with this model and helped with electrophysiological analyses and contributed to writing of the paper. CC conceived most of the experimental design, supervised, and analyzed all the results and wrote the paper.

COMPETING INTEREST

The authors declare no competing interests. NeuroHeal is currently under patent review.

SUPPLEMENTARY MATERIAL

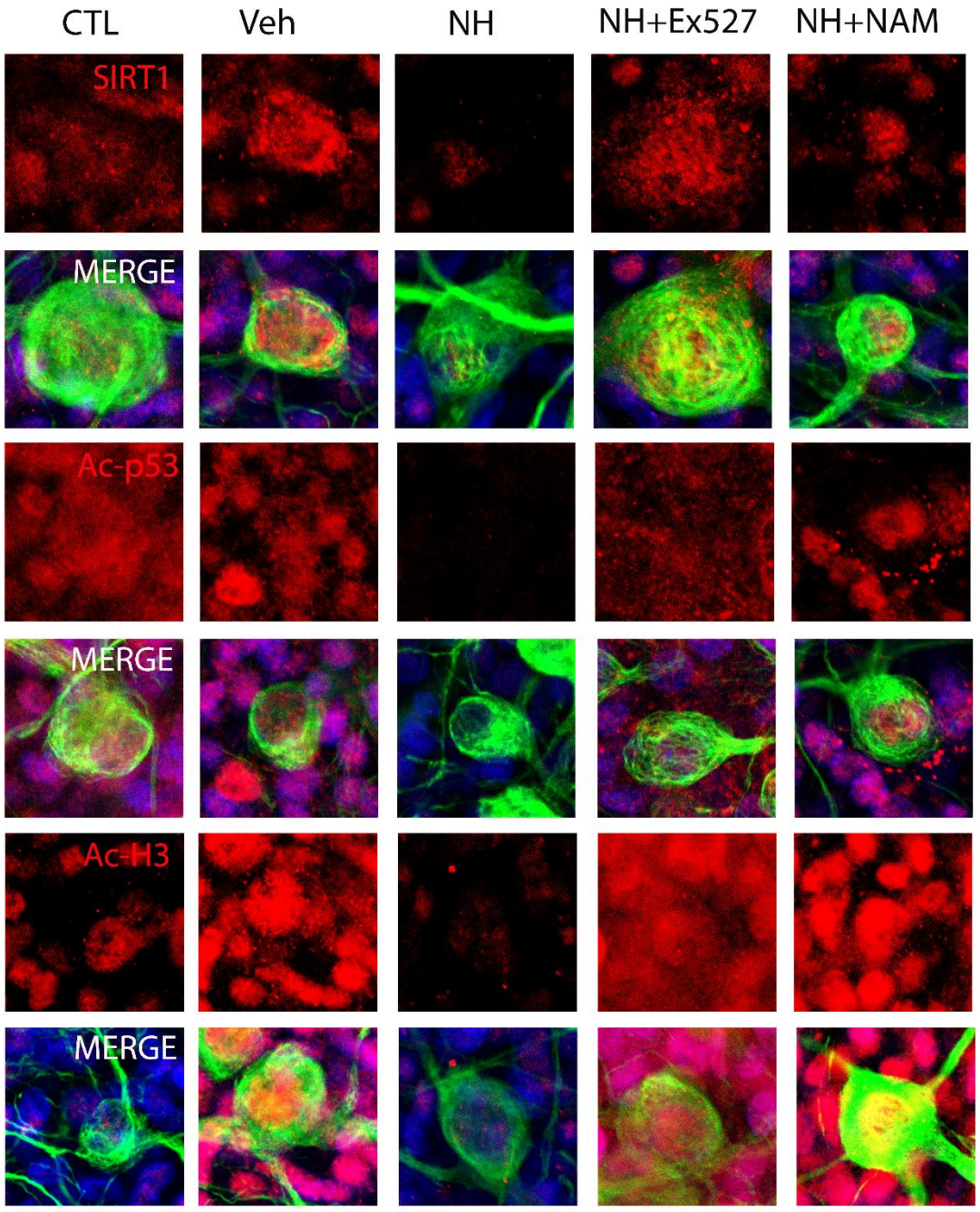

Figure S1. NH increases SIRT1 activity in SOCs. Confocal microphotographs of immunolabelled SOCs against SIRT1, Ac-p53 and Ac-H3k9 in red, SMI3-32 in green and DAPI in blue for each group 15 div after the treatment with NH or NH+SIRT1 inhibitors. Scale bar= 25μm.

REFERENCES

Aquilano K, Baldelli S, Pagliei B, Ciriolo M (2013) Extranuclear localization of SIRT1 and PGC-1α: an insight into possible roles in diseases associated with mitochondrial dysfunction. Curr Mol Med 13:140–54.

Brunet A, Bonni A, Zigmond MJ, Lin MZ, Juo P, Hu LS, Anderson MJ, Arden KC, Blenis J, Greenberg ME (1999) Akt Promotes Cell Survival by Phosphorylating and Inhibiting a Forkhead Transcription Factor. Cell 96:857–868.

Brunet A, Sweeney LB, Sturgill JF, Chua KF, Greer PL, Lin Y, Tran H, Ross SE, Mostoslavsky R, Cohen HY, Hu LS, Cheng H-L, Jedrychowski MP, Gygi SP, Sinclair DA, Alt FW, Greenberg ME (2004) Stress-dependent regulation of FOXO transcription factors by the SIRT1 deacetylase. Science 303:2011–2015

Buitenhuis S, van Wijlen-Hempel RS, Pondaag W, Malessy MJA (2012) Obstetric brachial plexus lesions and central developmental disability. Early Hum Dev 88:731–734.

Casas C, Isus L, Herrando-Grabulosa M, Mancuso FM, Borrás E, Sabidó E, Forés J, Aloy P (2015) Network-based proteomic approaches reveal the neurodegenerative, neuroprotective and pain-related mechanisms involved after retrograde axonal damage. Sci Rep 5:9185

Chaitanya G, Alexander JS, Babu P (2010a) PARP-1 cleavage fragments: signatures of cell-death proteases in neurodegeneration. Cell Commun Signal 8:31.

Chaitanya G V, Steven AJ, Babu PP (2010b) PARP-1 cleavage fragments: signatures of cell-death proteases in neurodegeneration. Cell Commun Signal 8:31

Chan YM, Wu W, Yip HK, So KF, Oppenheim RW (2001) Caspase inhibitors promote the survival of avulsed spinal motoneurons in neonatal rats. Neuroreport 12:541–545.

Deckwerth TL, Elliott JL, Knudson CM, Johnson EM, Snider WD, Korsmeyer SJ (1996) BAX is required for neuronal death after trophic factor deprivation and during development. Neuron 17:401–411.

Ekoff M, Kaufmann T, Engström M, Motoyama N, Villunger A, Jönsson J-I, Strasser A, Nilsson G (2007) The BH3-only protein Puma plays an essential role in cytokine deprivation–induced apoptosis of mast cells. Blood 110:3209–3217.

Ghosh HS, McBurney M, Robbins PD (2010) SIRT1 negatively regulates the

mammalian target of rapamycin. PLoS One 5:1–8.

Guzmán-Lenis MS, Navarro X, Casas C (2009) Drug screening of neuroprotective agents on an organotypic-based model of spinal cord excitotoxic damage. Restor Neurol Neurosci 27:335–349.

Hagenbuchner J, Kuznetsov a., Hermann M, Hausott B, Obexer P, Ausserlechner MJ (2012) FOXO3-induced reactive oxygen species are regulated by BCL2L11 (Bim) and SESN3. J Cell Sci 125:1191–1203.

Hariharan N, Maejima Y, Nakae J, Paik J, Depinho RA, Sadoshima J (2010) Deacetylation of FoxO by Sirt1 plays an essential role in mediating starvation-induced autophagy in cardiac myocytes. Circ Res 107:1470–1482.

Hasegawa K, Yoshikawa K (2008) Necdin regulates p53 acetylation via Sirtuin1 to modulate DNA damage response in cortical neurons.

Huang H, Tindall DJ (2011) Regulation of FoxO protein stability via ubiquitination and proteasome degradation. 1813:1961–1964.

Imai S, Armstrong CM, Kaeberlein M, Guarente L (2000) Transcriptional silencing and longevity protein Sir2 is an NAD-dependent histone deacetylase. Nature 403:795–800.

Israeli E (2013) FOXO3A directs a protective autophagy program in hematopoietic stem cells. Isr Med Assoc J 15:225.

Jiang M et al. (2012) Neuroprotective role of Sirt1 in mammalian models of Huntington's disease through activation of multiple Sirt1 targets. Nat Med 18:153–158

Jung CH, Ro SH, Cao J, Otto NM, Kim DH (2010) MTOR regulation of autophagy. FEBS Lett 584:1287–1295.

Kashihara Y, Kuno M, Miyata Y (1987) Cell death of axotomized motoneurones in neonatal rats, and its prevention by peripheral reinnervation. J Physiol 386:135–148.

Kaur A, Sharma S (2017) Mammalian target of rapamycin (mTOR) as a potential therapeutic target in various diseases. Inflammopharmacology 25:293–312.

Kennedy R (1903) SUTURE of the BRACHIAL PLEXUS in BIRTH PARALYSIS of the UPPER EXTREMITY. Br Med J 1:298–301

Klionsky DJ et al. (2016) Guidelines for the use and interpretation of assays for monitoring autophagy (3rd edition). Autophagy 12:1–222.

Kondo Y, Kanzawa T, Sawaya R, Kondo S (2005) The role of autophagy in cancer development and response to therapy. Nat Rev Cancer 5:726–734.

Kroemer G, Mariño G, Levine B (2010) Autophagy and the Integrated Stress Response. Mol Cell 40:280–293.

Kwon S, Seok S, Yau P, Li X, Kemper B, Kemper JK (2017) Obesity and aging diminish SIRT1-mediated deacetylation of SIRT3, leading to hyperacetylation and decreased activity and stability of SIRT3. J Biol Chem:jbc.M117.778720.

Langley B, Sauve A (2013) Sirtuin Deacetylases as Therapeutic Targets in the Nervous System. Neurotherapeutics 10:605–620.

Lee IH, Cao L, Mostoslavsky R, Lombard DB, Liu J, Bruns NE, Tsokos M, Alt FW, Finkel T (2008) A role for the NAD-dependent deacetylase Sirt1 in the regulation of autophagy. Proc Natl Acad Sci U S A 105:3374–3379.

Lowrie MB, Lavalette D, Davies CE (1994) Time Course of Motoneurone Death after Neonatal Sciatic Nerve Crush in the Rat. Dev Neurosci 16:279–284

Luo J, Nikolaev AY, Imai S, Chen D, Su F, Shiloh A, Guarente L, Gu W (2001a) Negative control of p53 by Sir2alpha promotes cell survival under stress. Cell 107:137–148.

Luo J, Nikolaev AY, Imai S, Chen D, Su F, Shiloh A, Guarente L, Gu W (2001b) Negative control of p53 by Sir2alpha promotes cell survival under stress. Cell 107:137–148

Maiuri MC, Zalckvar E, Kimchi A, Kroemer G (2007) Self-eating and self-killing: crosstalk between autophagy and apoptosis. Nat Rev Mol Cell Biol 8:741–752

Malessy MJA, Pondaag W (2009) Obstetric Brachial Plexus Injuries. Neurosurg Clin N Am 20:1–14

Mammucari C, Milan G, Romanello V, Masiero E, Rudolf R, Del Piccolo P, Burden SJ, Di Lisi R, Sandri C, Zhao J, Goldberg AL, Schiaffino S, Sandri M (2007) FoxO3 Controls Autophagy in Skeletal Muscle In Vivo. Cell Metab 6:458–471.

Matsuda-Lennikov M, Suizu F, Hirata N, Hashimoto M, Kimura K, Nagamine T, Fujioka Y, Ohba Y, Iwanaga T, Noguchi M (2014) Lysosomal interaction of Akt with Phafin2: A critical step in the induction of autophagy. PLoS One 9.

Matsuzaki H, Daitoku H, Hatta M, Tanaka K, Fukamizu A (2003) Insulin-induced phosphorylation of FKHR (Foxo1) targets to proteasomal degradation. Proc Natl Acad Sci U S A 100:11285–11290.

Mojsilovic-Petrovic J, Nedelsky N, Boccitto M, Mano I, Georgiades SN, Zhou W, Liu Y, Neve RL, Taylor JP, Driscoll M, Clardy J, Merry D, Kalb RG (2009) FOXO3a Is Broadly Neuroprotective In Vitro and In Vivo against Insults Implicated in Motor Neuron Diseases. J Neurosci 29:8236–8247

Morselli E, Maiuri MC, Markaki M, Megalou E, Pasparaki A, Palikaras K, Criollo A, Galluzzi L, Malik SA, Vitale I, Michaud M, Madeo F, Tavernarakis N, Kroemer G (2010) Caloric restriction and resveratrol promote longevity through the Sirtuin-1-dependent induction of autophagy. Cell Death Dis 1:e10.

Motta MC, Divecha N, Lemieux M, Kamel C, Chen D, Gu W, Bultsma Y, McBurney M, Guarente L (2004) Mammalian SIRT1 Represses Forkhead Transcription Factors. Cell 116:551–563.

Ni HM, Du K, You M, Ding WX (2013) Critical role of FoxO3a in alcohol-induced autophagy and hepatotoxicity. Am J Pathol 183:1815–1825.

Oliveira AL, Risling M, Deckner M, Lindholm T, Langone F, Cullheim S (1997) Neonatal sciatic nerve transection induces TUNEL labeling of neurons in the rat spinal cord and DRG. Neuroreport 8:2837–2840.

Petegnief V, Planas AM (2013) SIRT1 Regulation Modulates Stroke Outcome. Transl Stroke Res 4:663–671.

Pondaag W, A Malessy MJ, Gert van Dijk J, W M Thomeer RT (2004) Natural history of obstetric brachial plexus palsy: a systematic review. Dev Med Child Neurol 2004, 46:138–144

Romeo-Guitart D, Forés J, Herrando-Grabulosa M, Valls R, Leiva-Rodríguez T, Galea E, González-Pérez F, Navarro X, Petegnief V, Bosch A, Coma M, Mas J, Casas C (2017a) Neuroprotective Drug for Nerve Trauma Revealed Using Artificial Intelligence. Sci Rep, *Submitted.*

Romeo-Guitart D, Forés J, Navarro X, Casas C (2017b) Boosted Regeneration and Reduced Denervated Muscle Atrophy by NeuroHeal in a Pre-clinical Model of Lumbar Root Avulsion with Delayed Reimplantation. Sci Rep 7:12028

Romeo-Guitart D, Leiva-Rodríguez T, Sima N, Vaquero A, Domínguez-Martí H, Ruano D, Casas C (2017c) Neuroprotection of Disconnected Motoneurons requires Sirtuin 1 activation but Sirtuin 2 depletion or inhibition with AK-7 is detrimental. *In prep.*

Sengupta A, Molkentin JD, Yutzey KE (2009) FoxO transcription factors promote

autophagy in cardiomyocytes. J Biol Chem 284:28319–28331.

Sun L, Zhao M, Liu M, Su P, Zhang J, Li Y, Yang X, Wu Z (2017) Suppression of FoxO3a attenuates neurobehavioral deficits after traumatic brain injury through inhibiting neuronal autophagy. Behav Brain Res

Sun W, Oppenheim RW (2003) Response of motoneurons to neonatal sciatic nerve axotomy in Bax-knockout mice. Mol Cell Neurosci 24:875–886

Tzivion G, Dobson M, Ramakrishnan G (2011) FoxO transcription factors; Regulation by AKT and 14-3-3 proteins. Biochim Biophys Acta - Mol Cell Res 1813:1938–1945.

van der Horst A, Burgering BMT (2007) Stressing the role of FoxO proteins in lifespan and disease. Nat Rev Mol Cell Biol 8:440–450

Wang RC, Wei Y, An Z, Zou Z, Xiao G, Bhagat G, White M, Reichelt J, Levine B (2012) Akt-Mediated Regulation of Autophagy and Tumorigenesis Through Beclin 1 Phosphorylation. Science (80-) 338:956–959.

Wang Y, Liu Y, Chen Y, Shi S, Qin J, Xiao F, Zhou D, Lu M, Lu Q, Shen A (2009) Peripheral nerve injury induces down-regulation of Foxo3a and p27kip1 in rat dorsal root ganglia. Neurochem Res 34:891–898

Warr MR, Binnewies M, Flach J, Reynaud D, Garg T, Malhotra R, Debnath J, Passegué E (2013) FoxO3a Directs a Protective Autophagy Program in Hematopoietic Stem Cells. 494:323–327.

Zhang S, Huan W, Wei H, Shi J, Fan J, Zhao J, Shen A, Teng H (2013) FOXO3a/p27kip1 expression and essential role after acute spinal cord injury in adult rat. J Cell Biochem 114:354–365.

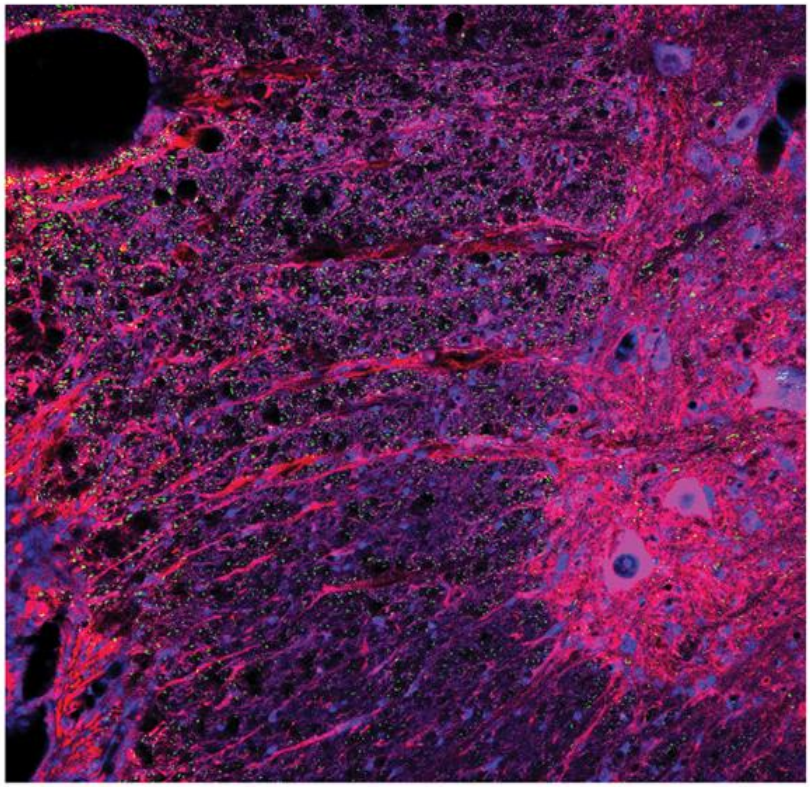

CHAPTER 4

www.nature.com/scientificreports

OPEN

Received: 25 April 2017
Accepted: 9 August 2017
Published online: 20 September 2017

Boosted Regeneration and Reduced Denervated Muscle Atrophy by NeuroHeal in a Pre-clinical Model of Lumbar Root Avulsion with Delayed Reimplantation

David Romeo-Guitart[1], Joaquim Forés[2], Xavier Navarro[1] & Caty Casas[1]

The "gold standard" treatment of patients with spinal root injuries consists of delayed surgical reconnection of nerves. The sooner, the better, but problems such as injury-induced motor neuronal death and muscle atrophy due to long-term denervation mean that normal movement is not restored. Herein we describe a preclinical model of root avulsion with delayed reimplantation of lumbar roots that was used to establish a new adjuvant pharmacological treatment. Chronic treatment (up to 6 months) with NeuroHeal, a new combination drug therapy identified using a systems biology approach, exerted long-lasting neuroprotection, reduced gliosis and matrix proteoglycan content, accelerated nerve regeneration by activating the AKT pathway, promoted the formation of functional neuromuscular junctions, and reduced denervation-induced muscular atrophy. Thus, NeuroHeal is a promising treatment for spinal nerve root injuries and axonal regeneration after trauma.

Traumatic injuries to the spinal roots and brachial or lumbar nerve plexus usually result in permanent loss of motor and sensory functions in the affected members. Advanced microsurgical interventions by neurotization and nerve transfer[1] or, in some cases, by direct nerve reimplantation of injured roots has been shown to allow some functional recovery in cases with brachial plexus avulsion[2–4]. Although the outcome is dependent on age of the patient and delay of intervention, generally protective sensation is recovered, but there is considerable muscle atrophy and poor motor functional recovery[5].

Proximal nerve injuries result in three main problems. First, the rupture of the ventral roots results in a progressive retrograde neurodegeneration of axotomized motoneurons (MN)[6–8] that compromises motor functional recovery. Second, the long distances that injured motor axons have to regrow to reach the muscles of denervated limb makes the chances for reinnervation very limited[9,10]. Third, there is muscle atrophy due to long-term denervation[2]. Therefore, any envisaged therapeutic strategy must consider these aspects as a whole.

In animal models of root avulsion (root avulsion, RA), immediate reimplantation of the avulsed roots increases MN survival and allows some reinnervation of limb muscles although with limited functional recovery that is worse in lumbar than in cervical root injuries, likely due to the differences in length[11–14]. To prevent MN atrophy and enhance axonal outgrowth and fiber density along roots, several experimental studies have induced expression of neurotrophic factors by gene therapy with some positive effects; however, in areas with continuously elevated levels of neurotrophic factor the axons remain trapped and do not grow to distal targets[15,16]. Grafting of mesenchymal stem cells into the injured spinal cord segments have shown some benefit[17,18]. Drugs, such as riluzole[13], lithium[19], and intracellular sigma peptide (ISP, a mimetic of the proteoglycan receptor PTPσ)[20], have been tested only after immediate reimplantation of the avulsed roots and so have limited translational potential.

In order to bring efficient therapeutic strategies to the clinic, we developed a preclinical model based on RA plus delayed surgical reimplantation of lumbar roots to test a new promising drug combination called

[1]Institut de Neurociències (INc) and Department of Cell Biology, Physiology and Immunology, Universitat Autònoma de Barcelona (UAB), Bellaterra, Barcelona, Spain. [2]Hand and Peripheral Nerve Unit, Hospital Clínic i Provincial, Universitat de Barcelona, Barcelona, Spain. Correspondence and requests for materials should be addressed to C.C. (email: Caty.Casas@uab.cat)

NeuroHeal[7]. NeuroHeal was discovered using unbiased proteomic data from two models that represented pure regenerative and pure neurodegenerative conditions after nerve or RA injuries, respectively. The data served to build bona fide state-specific molecular maps and mathematical models of this human biological system that allowed us to screen databases of drugs to identify putatively neuroprotective combinations. NeuroHeal is a combination of FDA-approved drugs. Results presented here evaluating NeuroHeal in a preclinical model demonstrate the promise of this coadjuvant agent for the clinical treatment of root and plexus injuries.

Results

NeuroHeal promotes motoneuron survival and reduction of glial scars in a preclinical model of RA with delayed repair of lumbar roots. We performed RA by traction of the L3 to L6 ventral spinal roots followed by reimplantation (RE) at 14 days post-injury (dpi). To facilitate root handling, we maintained the transected roots in a small silicone tube during the 14-day period prior to reimplantation (Fig. 1A). After reimplantation, we evaluated the animals using electrophysiological tests over 6 months. NeuroHeal-treated animals were given the combination therapy in drinking water from the day of injury. Although we observed, rats were drinking the half during the first 2 days, they continue to drink regularly during the 6 months that the treatment last. At the end of the follow-up period, we injected True Blue retrotracer to label regenerated MNs (Fig. 1B). At 14 days after RA none of the animals had compound muscle action potential (CMAP) responses in the tested muscles, indicating complete loss of motor function and confirming the effectiveness of the surgical approach (Fig. 1C).

Neuronal survival was assessed as the ipsilateral to contralateral ratio of MNs located in the lamina IX of the ventral horn (Fig. 2A). In the sham RE group, animals were subjected to RA and then to mock surgery at 14 dpi. As expected, sham animals presented with a significant drop in the number of avulsed MNs in the ipsilateral side at 21 days post-RA relative to the contralateral side (Fig. 2A). The animals subjected to RA and to RE (group RE) had increased MN survival compared to unrepaired rats but the difference was not significant (RE 49.44% $\pm$ 2.48; sham RE 36.2% $\pm$ 2.73). In contrast, RA avulsed animals subjected to either NeuroHeal treatment (NH group) or to reimplantation in addition to NeuroHeal treatment (RE + NH group) showed an increased proportion of surviving MNs of 61.71% and 64.62% respectively compared to sham RE group at 1 week after RE (Fig. 2A, short term: 3 weeks after RA or one week after RE in already RA injured animals). At 6 months, the animals treated with NeuroHeal had higher number of surviving MNs than those in the RE group, indicating a beneficial long-lasting effect of the treatment (Fig. 2A, long term).

Immunoreactivity against Iba 1 and GFAP was used to analyze the degree of microglial and astroglial reactivity after lesion, respectively. At 21 days post RA, there was similar glial reactivity in both the sham RE and RE groups (Fig. 2B,C). In contrast, Iba1 immunoreactivity was significantly reduced in all the animals treated with NeuroHeal at both early and late time points (Fig. 2B); however, there was no significant reduction of astroglial reactivity at any time (Fig. 2C; short term: 170.58% $\pm$ 33.65 in sham RE, 98.39 $\pm$ 47.96% in NH, and 100.97 $\pm$ 47.78% in NH + RE groups; and long term: 106.52 $\pm$ 13.27% in RE and 91.75 $\pm$ 11.52% in NH + RE). We did observed a significant reduction in chondroitin sulfate proteoglycan (CSPG) content, a matrix component of the glial scar reaction, in all the treated groups with respect to the untreated sham group at the time of its formation by 7 days after RE (Fig. 2D). These results suggested that NeuroHeal treatment exerted long lasting neuroprotection when begun after delayed surgical repair of avulsed lumbar roots.

NeuroHeal treatment enhances regeneration of motoneurons. At 6 months after RE, by retrograde labeling by injection of True Blue into the tibialis anterior and gastrocnemius, we observed 2 fold more regenerated MNs in NeuroHeal-treated reimplanted animals compared to those reimplanted but untreated (Fig. 3A). We then evaluated the presence of pro-regenerative molecular marker GAP43 and activation of putative NeuroHeal target such as AKT[7]. NeuroHeal treatment increased GAP43 and phosphorylated AKT levels, suggesting activation of pro-regenerative programs (Fig. 3B,C). Expression of phosphorylated p70S6k (Thr 389), a downstream AKT/mTOR target, was markedly increased within MNs in the NeuroHeal-treated RE animals compared with untreated animals (Fig. 3D).

Long-term NeuroHeal treatment accelerates nerve regeneration and recovery. In addition to confirming neuroprotection exerted by NeuroHeal, we investigated whether NeuroHeal treatment improved motor recovery in our model by using electrophysiological tests monthly. CMAPs were observed in the NeuroHeal-treated group between 2 and 3 months after RE. In contrast, no responses were observed in the untreated group until 4 months after RE (Fig. 4A), indicating that NeuroHeal treatment accelerated axonal growth by at least 4 weeks ($p = 0.0276$ in TA; $p = 0.0053$ from GA). By 4 months, all the NeuroHeal-treated rats presented electrophysiological evidence of reinnervation in both muscles, whereas in 11% of untreated animals there was no evidence of reinnervation at 6 months. Moreover, the NeuroHeal-treated group had significantly higher CMAP amplitudes compared to the untreated group at 5, and 6 months ($p < 0.05$, Fig. 4B). No significant differences in the CMAP latencies were observed (Fig. 4C).

Analysis of spinal cords at L4-L6 showed abundant acetyl cholinesterase-positive ($ChAT^+$) motor fibers along the ventral horn in NeuroHeal-treated animals at 6 months after RE (Fig. 5A). Accordingly, in the sciatic nerve there were significantly higher numbers of $ChAT^+$ motor axons from surviving MNs (up to 11.30% of the total L4-L6 pool) and a trend to a higher number of regenerative $GAP43^+$ fibers entering the reimplanted root in NH-treated animals compared to those in the RE group (Fig. 5B).

Reduced muscle atrophy and increased functional endplates observed in NH-treated rats. We also evaluated recovery from muscle atrophy due to denervation. Muscle weight is a sensitive measure of muscle

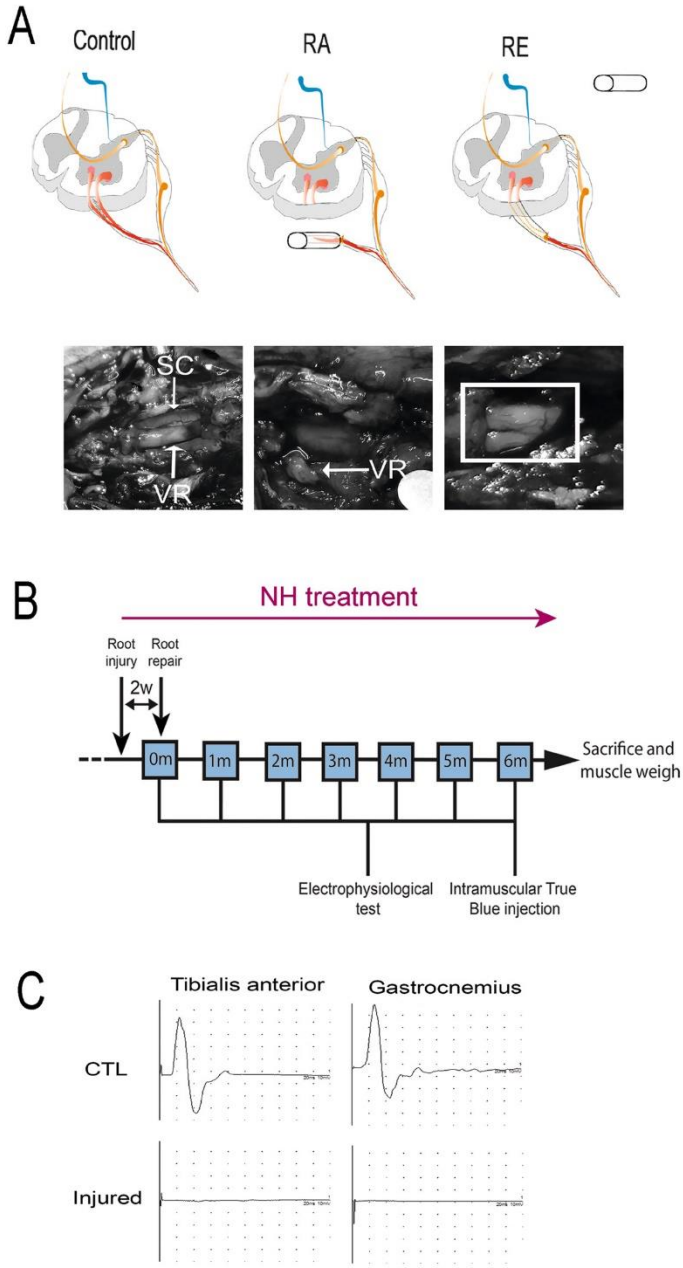

Figure 1. *In vivo* preclinical model of RA injury with delayed reimplantation of lumbar roots and experimental design. **(A)** Schematic of the procedure. Spinal cord with the nerve roots from control, root-avulsed (RA), and reimplanted (RE) animals. The L3-L6 spinal roots were detached and inserted into a silicone tube after RA injury. At 14 dpi, the tube was removed, and the injured spinal roots were re-inserted onto the spinal cord at the same lumbar level. Photographs showing the spinal cord (SC) and ventral roots (VR) inside the tube (left), root appearance after removing the tube (middle) and once roots were apposed underneath the spinal cord (right), during reimplantation surgery at 14 dpi. **(B)** Workflow of the experimental design. NH treatment was administered from the day of injury dissolved in the drinking water refreshed every three days for 6 months. Fourteen days post avulsion, a group of animals were reimplanted. A week later, some animals were sacrificed to evaluate MN survival (short-term period: 3 weeks post-RA injury or 1 week post-RE). The rest of animals were evaluated once per month with electrophysiological tests. One week before the end of the 6-month follow up period, we intramuscularly injected True Blue retrotracer at the tibialis anterior (TA) and the gastrocnemius (GA). **(C)** Electrophysiological CMAP recordings of control animals (CTL) and animals after RA and before RE (Injured).

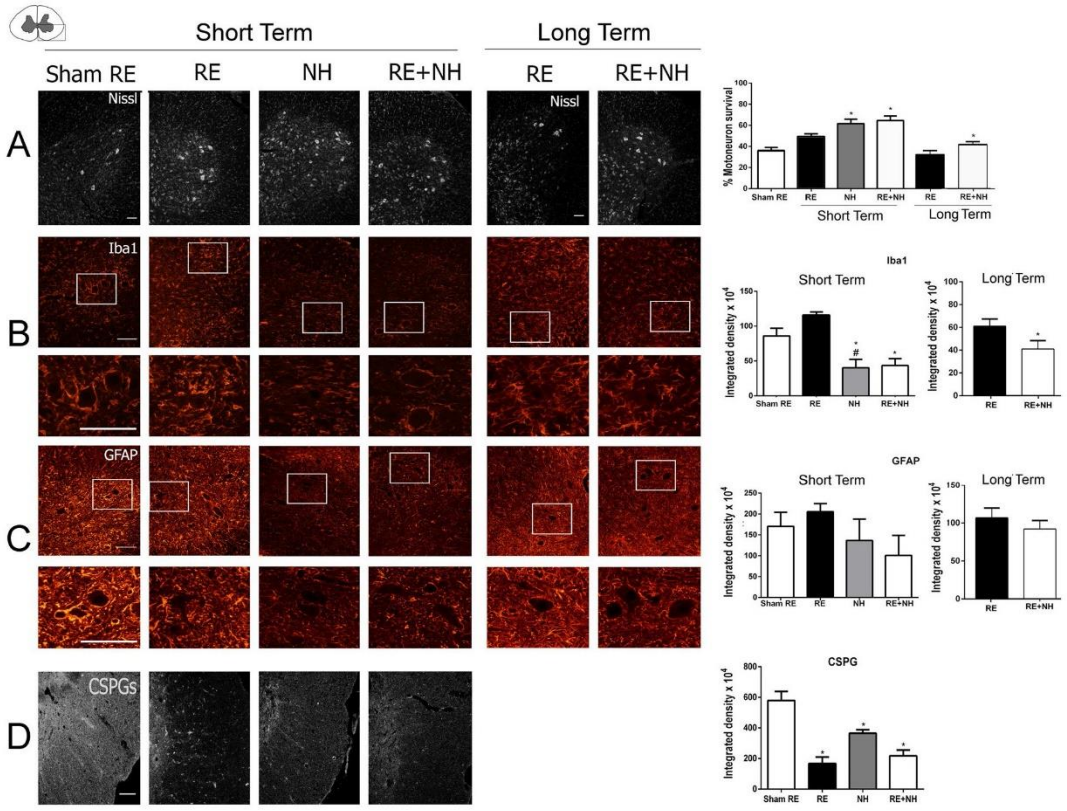

Figure 2. NH treatment has short- and long-term neuroprotective effects in the preclinical model. (**A**) ***Left***, Representative microphotographs of ventral horns of root-avulsed spinal cords stained with fluorescent Nissl, which specifically labels MNs, at 21 dpi post RA and 1 week post RE (short term) or at 6 month post RE (long term) from RA injured untreated animals (sham RE) or NeuroHeal-treated animals (NH and RE + NH). ***Right***, Bar graphs showing the average percentage of surviving MNs ± SEM on the injured side with respect to the contralateral side. **(B–D)** ***Left***, Representative microphotographs of ventral horns from injured animals with labeled microglia (Iba1), astrocytes (GFAP), at low (top) and high magnification (below), or chondroitin sulfate proteoglycans (CSPGs), respectively. ***Right***, Histograms of the averaged immunoreactivity in the fixed region of interest at the ventral horn from different groups (n = 4 for each group, ANOVA, post hoc Bonferroni, *$p < 0.05$ RE + NH vs. Sham RE or RE). Scale bar = 100 µm.

atrophy. We harvested and weighted the gastrocnemius and tibialis anterior muscles of both ipsi- and contralateral sides from the NH-treated and untreated animals. We found an average 83% reduction in the weight of both TA and GA ipsilateral muscles compared to contralateral muscles in the RE group consistent with persistent long-term denervation-induced atrophy. In contrast, NH treatment reduced muscle atrophy compared to untreated rats with muscle reduction of about 72% with respect to the contralateral side ($p < 0.05$, Fig. 6A). Long-term denervated muscle fibers have cells with shrunken cytoplasms, show signs of fibrosis, and cluster into groups[21,22]. In addition, the more widespread the denervation, the greater the percentage of small muscle fibers[23]. To evaluate muscle fibers, we analyzed muscle sections histologically. The RE group of animals had fibers with small cross-sectional areas and numerous fibroblast nuclei within the endomysium suggesting fibrosis (Fig. 6B). In contrast, NH treatment fibers presented clear myocyte nuclei and no apparent fibrosis. In addition, in the RE group, fibers were contracted by 82% relative to contralateral regions of RE rats, but animals treated with NH had fibers contracted only 58% relative to controls ($p < 0.001$, Fig. 6c). In muscle sections from the RE group we observed clustering of small fibers; most were smaller than 400 μm^2. NH treatment resulted in a more distributed mean cross-sectional area with the most abundant fibers those between 400 and 800 μm^2 (Fig. 6C). These observations are consistent with the extension of reinnervated motor endplates in the muscles.

We then analyzed the folds of neuromuscular junctions (NMJs) of GA muscle using NF-200 to stain axon terminals and FITC-conjugated α-bungarotoxin to stain acetyl-choline receptors (AchRs). There was a significantly higher percentage of reinnervated motor endplates in the NH-treated group than in the RE group (Fig. 6D). Recently it has been proposed that failure of motor recovery after long-term denervation might be due to failure in pre-synaptic function at NMJs despite physical contact[24,25]. Thus, we performed immunolabeling for syntaxin

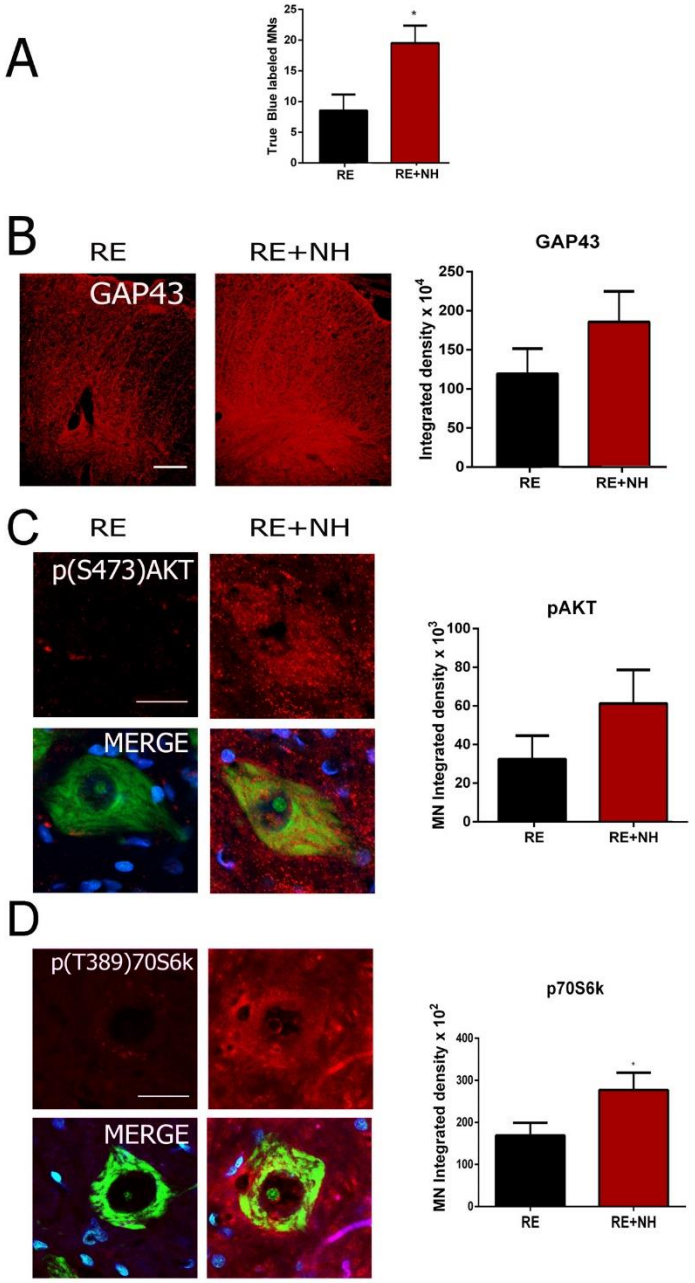

Figure 3. Molecular markers of regeneration are modulated by NH treatment. **(A)** Histogram showing the average number (±SEM) of MNs labeled after intramuscular injection of True Blue into the TA and GA on the injured side. The number of positive MNs were counted in the L4-L5 segments of the spinal cords from animals at 6 months post RE for animals in RE group (not treated) or NH-treated groups (RE + NH). **(B)** ***Left***, Representative microphotographs of GAP43 immunolabeling of neuronal processes at the white matter ventral horns from injured animals. ***Right***, Bar graph of the mean immunolabeling intensity for GAP43 in a region inside the white matter from injured spinal cords. **(C,D)** ***Left***, Confocal images of MNs immunolabeled for (**C**) phosphorylated AKT at S-473 and D) p70S6K at T-389 and counterstained with Fluoro Nissl Green and DAPI (blue) in injured spinal cord at 6 months post RE. ***Right***, Histograms of the mean of the immunofluorescence intensity for each marker inside the cytoplasm of injured MNs ($n = 4$ animals, t-test, $^*p < 0.05$ RE + NH vs. RE). Scale bar = 100 μm in **B**; 25 μm in **C** and **D**.

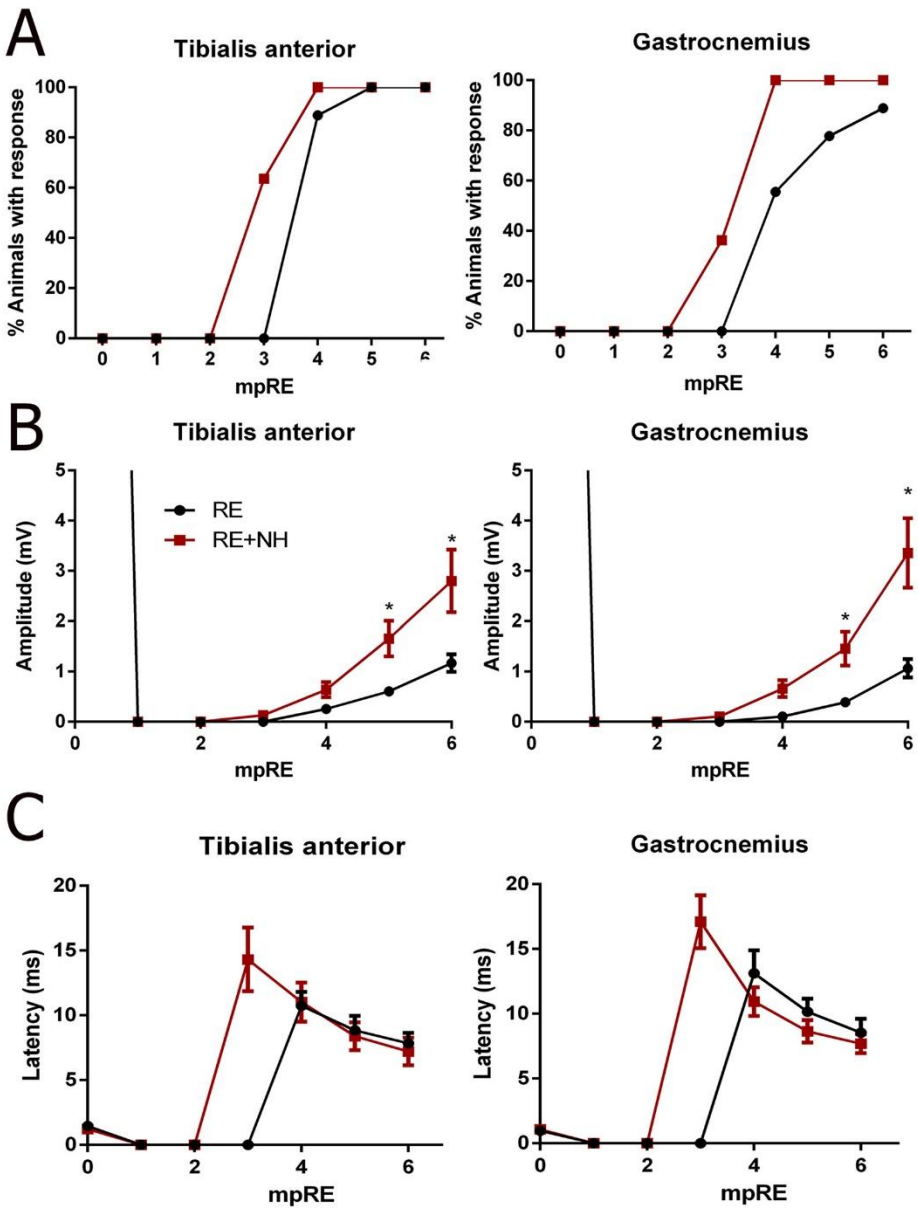

Figure 4. Nerve regeneration and CMAP amplitudes are enhanced by NH treatment. **(A)** Graphs summarizing the percentages of animals in RE group (not treated) or NH-treated groups (RE + NH) with electrophysiological signals of muscle reinnervation in TA and GA muscles at indicated times after RE. **(B)** Mean amplitudes (±SEM) and **(C)** time latency values of CMAP recordings obtained during follow-up post RE from TA and GA muscles (n = 9–11, ANOVA, post hoc Bonferroni, *$p < 0.05$ RE + NH vs. RE).

1 (SYT1), a protein key to functional release of neurotransmitters at presynaptic terminals. We observed that this marker was present only in control and NH-treated animals and not in the RE group rats (Fig. 6E). These observations suggested that NH-treatment may promote muscle recovery and formation of functional motor endplates.

Discussion

The findings of this work indicate that NeuroHeal treatment after root avulsion and delayed reimplantation of the lumbar roots remarkably promoted regeneration resulting in (1) long-lasting protection of motoneurons from retrograde neurodegeneration; (2) activation of a pro-regenerative profile via pAKT-mTOR signaling; (3)

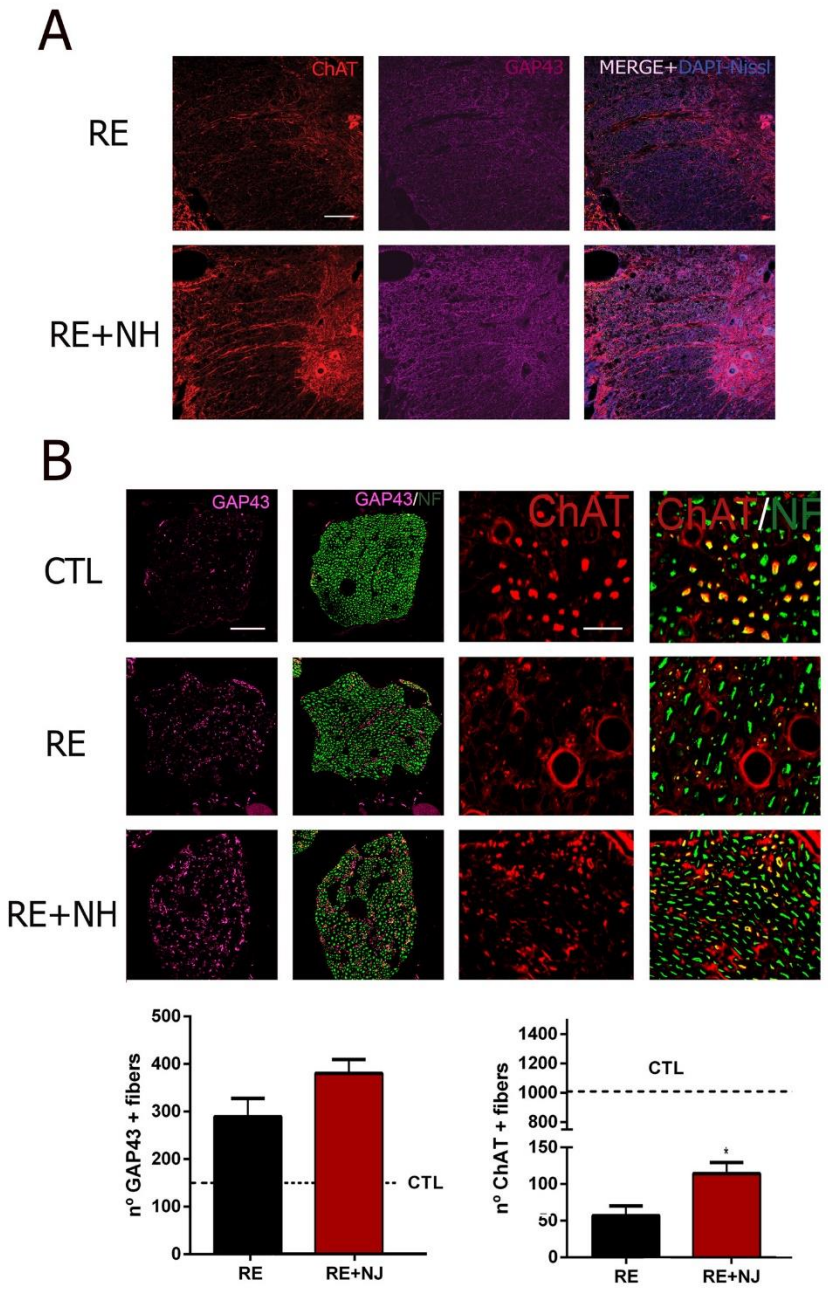

Figure 5. Regeneration of motor axons increased by NH treatment. **(A)** White matter of the spinal cord immunostained against ChAT (red), GAP43 (purple), and counterstained with DAPI (blue, for nuclei) and Fluoro Nissl Blue (for MNs) RE and NH-treated (RE + NH) animals at 6 months post RE. **(B)** ***Top***, Microphotographs showing co-localization of GAP43 (purple) or ChAT (red) with neurofilament NF200 (NF, green) at mid-level of sciatic nerves obtained from controlateral (CTL), RE, and RE + NH groups at 6 months post RE. ***Bottom***, Bar graphs showing the average (±SEM) of the number of immunohistochemically detected $GAP43^{+}$ (left) and $ChAT^{+}$ (right) fibers at midlevel of sciatic nerve. Dotted lines indicate control value means for GAP43 and ChAT, respectively (n = 3 for CTL group and n = 4 for RE and RE + NH; t-test, $*p < 0.05$ RE + NH vs. RE). Scale bar = 100 µm for **A** and for GAP43/NF in **B**, and 25 µm for ChAT/NF in **B**.

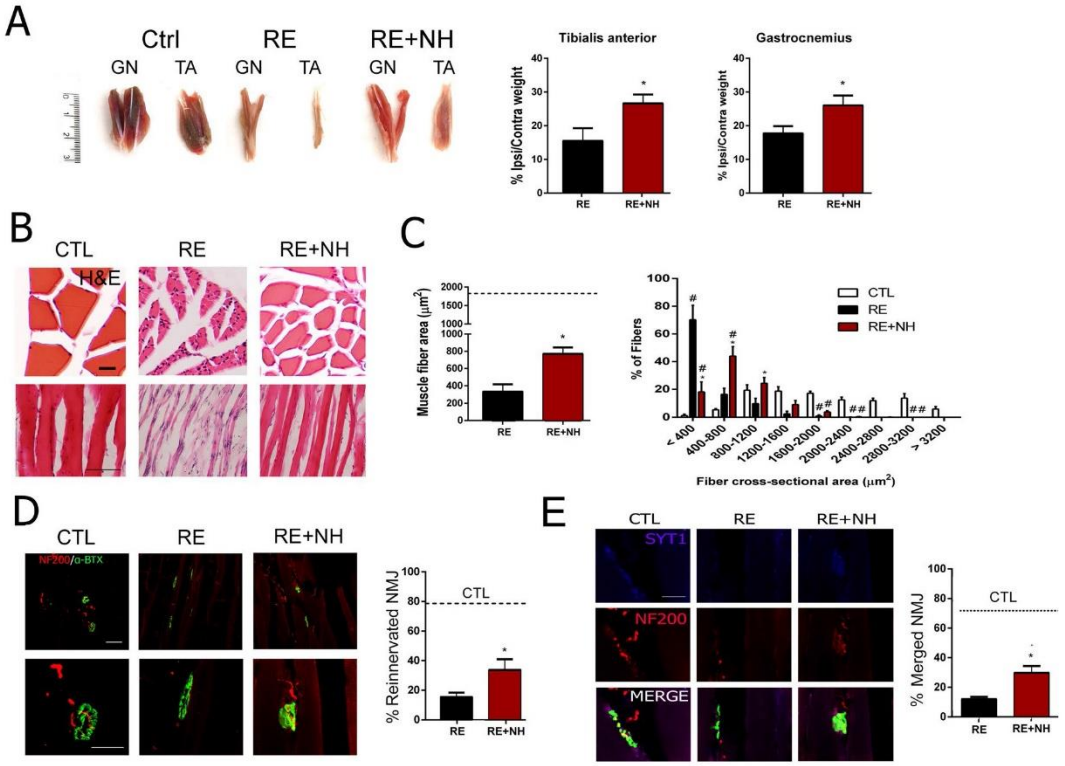

Figure 6. Muscle atrophy is reduced and numbers of functional endplates are increased by NH treatment. **(A)** ***Left***, Representative photographs of GA and TA muscles from contralateral regions of RE rats (CTL) and ipsilateral from untreated (RE) and NH-treated (NH + RE) rats at 6 months post RE. ***Right***, Histograms of weight ratio between ipsilateral and contralateral TA and GA muscles at 6 months post RE ($n = 7–8$; t-test, $^*p < 0.05$ RE + NH vs. RE). **(B)** Representative microphotographs of cross (upper panel) and longitudinal (lower panel) TA and GA muscle sections with H&E staining from CTL, RE, and RE + NH groups at 6 months post RE. **(C)** ***Left***, Means (±SEM) of the fiber cross-sectional areas (μm^2) from GA muscles of indicated groups at 6 months post RE. Dotted line indicates the mean obtained from the CTL muscles ($n = 4$ per group; t-test, $^*p < 0.05$ RE + NH vs. RE). ***Right***, Histogram of the cross-sectional area distribution of fibers in GA. Each interval of the distribution contains ranges of 400 μm^2 between the extremes ($n = 4$ per group), ANOVA, post hoc Bonferroni $^*p < 0.05$ RE + NH vs. RE). **(D)** ***Left***, Representative confocal images of GA transversal sections stained for NF200 (NF, red) and FITC-conjugated α-bungarotoxin (α-btx, green) from contralateral side of RE rats (CTL), ipsilateral side of RE rats, and NH-treated animals (RE + NH) at 6 months post RE. ***Right***, Quantification of the percentage of reinnervated NMJs (red and green overlapping signal) analyzed with ImageJ software in RE and RE + NH groups compared to CTL (dotted line; $n = 3–4$; t-test, $^*p < 0.05$ RE + NH vs. RE). **(E)** Representative microphotographs of SYT1 immunolabeling (magenta) and NF co-localization (red) in α-btx (green) neuromuscular junctions (NMJs). Scale bars = 20 μm in B (bottom panel) and E; 25 μm in D (bottom panel); 50 μm in D (upper panel); and 100 μm in B (upper panel).

evidenced motor axonal regrowth with reduced gliosis formation at the transitional zone; (4) accelerated motor axonal regeneration; (5) enhanced functional reconnection of endplates, and (6) reduced long-term muscle atrophy.

The effective recovery of motor function after spinal root injuries depends on neuroprotection and axonal regeneration toward the muscle targets. In human patients, reimplanting the avulsed spinal roots into the spinal cord partially restores motor function but only if the repair procedure is performed less than 1 month after injury[2]. After brachial plexus or proximal nerve injuries the proximal muscles in the limb may recover good function, whereas distal muscles, such as intrinsic muscles of the hand, rarely regain any useful activity, although this has been described in some patients[26].

Any therapeutic strategy must be tested in a relevant experimental model and must show significant effects on neuroprotection and nerve regeneration after long-term denervation. Here we first characterized a rat model of root avulsion with delayed reimplantation of lumbar roots. We evaluated the effects of NeuroHeal given orally in this model. One of the most remarkable effects exerted by NeuroHeal was the acceleration of axonal regeneration. Very few strategies have demonstrated this property with exceptions of the treatment with FK506[27] and

the use of brief electrical stimulation (ES)[28,29]. Although FK506 accelerated axonal regeneration by still unknown mechanisms, its secondary effects as immunosuppressant preclude clinical use. FK506 and geldanamycin, which also accelerates axonal regeneration, do not reduce muscle atrophy as NH does[30]. ES to the nerve is being used clinically[31]. Results obtained by ES and by NH treatment are comparable since both advanced axonal regeneration at least 4 weeks. However, nerve ES has not been shown to reduce muscle atrophy. NH may act specifically to preserve muscle integrity during the time of denervation. Recently, failure of motor recovery after long-term denervation has been demonstrated to be due to failure in pre-synaptic function of endplates despite physical contact[24,25]. Evidence indicates that there is an apparent mismatch in the correlation of nerve recovery and function recovery as demonstrated in a study of over 300 patients followed for 3–18 years after sciatic nerve injury[32]. Thus, the reduction in muscle atrophy that we observed here in rats treated with NH should be further investigated.

NH is a multitarget compound that was specifically designed for treatment of root avulsion injuries. Multitargeting gives the opportunity to act through several pathways in parallel to support a neuroprotective and pro-regenerative phenotype. In the present study we confirmed that one of these targets is the AKT pathway as suggested previously based on studies *in silico*[7]. The essential role of PI3K/AKT signaling in stimulating axon regenerative processes in the adult central and peripheral nervous systems is well documented[33–36]. Activation of PI3K/AKT signaling appears to result from ablation of its cell intrinsic antagonist, the phospholipid phosphatase PTEN[37]. The clinical use of PTEN inhibitors is not straightforward due to its anti-oncogenic properties[38]. NH offers a promising alternative since it is based on the repurposing of two already FDA-approved drugs. In addition, this multitarget aspect also may favor its concurrent action on several other critical tissues in addition to the nervous system.

Our results suggest that NH triggers specific pathways to prevent muscle degeneration. In particular, the AKT/mTOR/p70S6K pathway is known to increase protein synthesis that is necessary to maintain muscle mass[39,40], although the role of mTOR in muscle atrophy is still controversial[41]. Another possibility is that NH activates of SIRT1[7], a nicotinamide adenosine dinucleotide-dependent histone deacetylase that plays an essential role in regulating multiple biological processes[42]. Previous studies showed that SIRT1 overexpression induced through impeding FoxOs and NF-κB expression is capable of thwarting the loss of muscle mass, as well as inducing hypertrophy of normal muscle[43]. Indeed, SIRT1 transgenic muscle exhibits a decreased expression of the atrophy gene program[44]. Thus it would be very interesting to know whether NH prevents muscle atrophy by ameliorating related pathologies. In conclusion, we believe the treatment with NH offers interesting possibilities for treatment after nervous system trauma or upon other forms of neurological damage as in lesioned optic nerves or corticospinal tract in which central nervous system axons must regenerate to enable normal function.

Materials and Methods

Animals and surgical procedures. Sprague-Dawley female rats aged 12 weeks (weight at time of surgery: 250–300 g, Animal Service, *Universitat Autònoma de Barcelona*) were kept under standard conditions of light and temperature and fed with food and water ad libitum. We performed surgical procedures under anesthesia with ketamine/xylazine (100:10 mg/kg weight, i.p). For RA-injury, a midline skin incision was made, the paravertebral muscles were smoothly retracted avoiding muscle damage. Then a laminectomy of around 1 cm was made at T12-L1 level using the last rib as reference and the pia matter was opened to expose the spinal ventral roots. The L3-L6 ventral roots were detached from their entrance into the spinal cord using moderate traction with a hook, disrupting nerve integrity, as previously reported[8]. We placed the ventral roots in a silicone tube (2 mm i.d., 3 mm lenght) that was placed into the laminectomized space close to the spinal cord, avoiding damage and preventing spontaneous axon regeneration into the avulsed root. Fasciae were sutured and the skin closed with planes. Two weeks after RA injury, we anesthethized the animals, confirm denervation by electrophysiological test and proceed with the reimplantation (RE) surgery. We localized the silicone tube after blunt dissected paraventral muscles. The avulsed ventral roots were dissected back into scar-free, healthy-appearing nerve tissue, and tensionlessly were equidistantly apposed 1 mm-approximately underneath the corresponding spinal cord segment adjacent to the avulsion zone. Paravertebral muscles were opposed and pressing onto the spinal cord to avoid root misleading. In pilot studies, we had assured this procedure was enough to maintain physical connection without damaging the spinal cord in contrast of being sutured by analyzing the existence of ChAT- labeled axons in the replanted roots 14 days after reparative RE. After RE surgery, the wound was sutured by planes and disinfected with povidone iodine, and the animals were allowed to recover in a warm environment. RE-sham animals were submitted to RA-injury and re-opened two weeks after injury to remove the silicone tube. When sacrifice the animals, we visually checked that re-implanted nerve roots still remain in contact with the injured spinal cord. All procedures involving animals were approved by the Ethics Committee of *Universitat Autònoma de Barcelona*, and followed the European Community Council Directive 2010/63/EU. Groups for short-term analysis (21 dpi) were: Group Sham-RE, vehicle-treated RA-injured animals that have been just re-opened two weeks after injury; Group NH, NH-treated RA-injured animals that have been just re-opened two weeks after injury; Group RE, vehicle-treated RA-injured animals with root reimplant two weeks after injury; Group RE + NH, NH-treated RA-injured animals with root reimplant two weeks after injury. For the long-term analysis, groups were composed with RA-injured animals reimplanted at two weeks post injury treated with either vehicle (group RE) or NH (group RE + NH) for 6 months.

Electrophysiological tests. For electrophysiological evaluation, rats were anaesthetized with ketamine/xylazine (100:10 mg/kg weight, i.p) every month after 1-month post RE surgery. The sciatic nerve was stimulated by transcutaneuous electrodes placed at the sciatic notch by single pulses (20 μs), and the CMAP was recorded by placing electrodes on the gastrocnemius and tibialis anterior. Stimulus intensity was applied gradually until reach the supramaximal stimulus, which correspond to the maximum CMAP amplitude. The evoked action potentials were displayed on a storage oscilloscope (Synergy Medelec, Viasys HealthCare) at settings appropriate to measure

the amplitude from baseline to peak and the latency to the onset after every stimulus. (n = 9–11). After testing, animals were allowed to recover in a warm environment.

Retrograde axonal tracing. To identify regenerated avulsed MNs that had reinnervated the gastrocnemius medialis and tibilais anterior muscles, we applied True Blue (Setareh Biotech) retrotracer to the muscle one week before euthanizing the animals as described elsewhere[45]. Briefly, under anesthesia with ketamine/xylazine as mentioned, we made a small cut to the skin to expose the muscle and retrotracer (6 µL) was distributed throughout the body of the muscle with a glass pipette using a Picospritzer. Pipette was maintained 10 s after injection to avoid reflux and then the animals were allowed to recover in a warm environment.

Drug treatment. The Neuroheal mixture is composed of Acamprosate (Merck, Darmstadt, Germany) and Ribavirin (Normon, Madrid, Spain). Pills of both compounds were ground into fine powder and dissolved in drinking water at final concentration of 2.2 mM and 1 mM, respectively. Rats in the NH treatment group were given water containing drugs from the day of RA injury. Fresh drug solutions were made every 3 days.

Tissue processing for histology. Rats were sacrified at 21 days post RA to evaluate MN survival or at 6 months after RE for analysis of nerve regeneration with dolethal (60 mg/kg, i.p.). We then transcardially perfused the animals with a saline solution containing heparin (10 U/mL), followed by 4% paraformaldehyde in 0.1 M phosphate buffer, pH 7.2, for tissue fixation. We removed L4-L5 spinal cord segments (5 mm total length), sciatic nerve from lumbar plexus to sciatic notch of the avulsed side, and tibialis anterior and gastrocnemius muscles. Spinal cord and sciatic nerve were post-fixed in the same fixative solution for 2 hours or 30 min, respectively, and cryopreserved in 30% sucrose. For muscle analysis, we weighed the ipsilateral and contralateral muscles and placed them into cryopreservation solution to avoid autofluorescence. The ratio of ipsilateral to contralateral muscle weight was calculated to assess the extent of muscle atrophy. For spinal cord analysis, we cut the samples into serial transverse sections of 20-µm thickness, obtaining 30 series with 10 sections. For sciatic nerve analysis we obtained 10 series of eight 15-µm sections. Samples were sectioned using a cryotome (Leica) and preserved at −20 °C until use. We cut gastrocnemius muscle at midlevel into 10-µm serial transverse or longitudinal sections obtaining five series with 10 sections/each. Spinal nerve ventral roots were harvested at 14 days post RE and cut at 15 µm transversal sections obtaining 3 slices with of 10 slides.

Immunohistochemistry and image analysis. We treated slides with Tris-buffered saline (TBS), TBS with 0.3% Triton-X-100 and 10% bovine serum for 1 h and incubated overnight at 4 °C with different primary antibodies: goat anti-choline acetyltransferase (ChAT; 1:50; Millipore), chicken anti-Neuro Filament 200 (NF-200; 1:1000, Millipore), mouse anti-Neuro Filament (RT97, 1:200, Hybridoma Bank), rabbit anti-glial fibrillary acidic protein (GFAP; 1:1000, Dako), rabbit anti-ionized calcium binding adaptor molecule 1 (Iba1; 1:1000, Wako), rabbit anti-growth associated protein-43 (GAP43; 1:50, Millipore), mouse anti-chondroitin sulfate proteoglycan (CSPG; 1:100, Hybridoma Bank), mouse anti-Syntaxin 1 (SYT1; 1:100, Hybridoma Bank), rabbit anti-phospho ribosomal protein S6 kinase (Thr 389) (p-pRPS6KB 1; 1:100, Antibodies Online), and rabbit anti-phospho protein kinase B (Ser473) (pAKT; 1:500, SantaCruz Biotechnology). After several washes with TBS with 0.1% Tween-20, the sections were incubated 1.5 h at room temperature with the appropriate Cy-3, Cy-2, or Alexa 647 conjugated secondary antibodies (Jackson Immunoresearch, West Grove, PA, USA). After TBS with 0.3% Triton-X-100 and TBS, Ce counterstained the sections with DAPI (Sigma, St Louis, MO, USA) and NeuroTrace Fluorescent Nissl Stain (Molecular Probes, Leiden, Netherlands) and mounted the slices with Fluoromount-G mounting medium (SouthernBiotech). Immunolabeling of different groups to be compared, and image captured were performed the same day.

We acquired images under the same exposure, sensitivity, and resolution from spinal cord samples of the different treatments or controls for each marker (n = 4/group). Images were captured with the aid of a digital camera (Olympus DP76) attached to the microscope (Olympus BX51) and analyzed with ImageJ software (National Institutes of Health; available at http://rsb.info.nih.gov/ij/). We transformed the microphotographs to a gray scale and analyzed immunoreactivity by calculating the integrated density of a region of interest (ROI) after defining a threshold for background correction.

Glial reactivity was measured on eight spinal cord sections (separated by 200 µm between pairs) immunolabeled against GFAP and Iba1 per animal. Images were taken at 20× and the integrated density of a ROI of 0.11 mm^2 selected on the gray matter of the ventral horn was calculated. CSPG and GAP43 immunoreactivity was assessed after image capturing at 20× within the white matter located in front of the ventral horn. For both markers, a ROI of 0.11 mm^2 was used.

To count the number of $ChAT^+$ or $GAP43^+$ fibers in the nerve sections, images at 10X were taken of one series of eight sections at midlevel of sciatic nerve. For both markers, fibers were counted as positive when co-localization between Neurofilament and ChAT or GAP43 was found.

Confocal microscope examinations were made with a Confocal Laser Scanning Microscope (Zeiss LSM 700) for p-RPS6KB1 and pAKT. Images were collected with a 1.4 numerical aperture oil-immersion 20 or 40X objective. Confocal images were obtained using two separate photomultiplier channels, either concurrently or in separate runs, and were separately projected and merged using a pseudocolor display showing green for Nissl, red for Cy-3, and blue for DAPI. MN area was taken using Nissl green as the ROI, and the integrated density was obtained for at least 15 MN per animal.

Motor neuron counting. Six slices covering all the L4-L5 segment (separated by 100-µm; n = 4 per group) of eight sections of every animal were incubated 20 min with fluorescence Nissl labeling solution (Life

Technologies) following the manufacturer's protocol. We took sequential microphotographs covering ventral horn (L4 and L5 segments) at 10X with a digital camera (Olympus DP76) attached to a microscope (Olympus BX51). Only MNs localized in the lateral ventral horn with prominent nuclei and soma diameter larger than 30 μm were counted. MN survival was calculated as the percentage of the number of surviving MNs on the ipsilateral side with respect to the contralateral non-injured side of each animal. For retrogradely labeled MNs, the same sections used for MN survival were observed under fluorescence, and the number of labeled neurons counted in every fifth section following the fractionator principle[46].

Neuromuscular junction analysis. Gastrocnemius muscle longitudinal slices were washed with TBS, blocked with NDS during 1 h and incubated overnight at 4 °C with chicken anti-Neuro Filament 200 (NF-200; 1:1000, Millipore) as described above. After after several washes, Cy3-conjugated secondary antibody was added. Finally, we washed and incubated slices with FITC-conjugated α-bungarotoxin labeling solution (Life Technologies) to reveal the motor end plates during 20 minutes. Systematic analyses were performed through three different sections of each animal. Bungarotoxin positive endplates (100) were classified as positive and negative for NF-200. Only motor endplates with NF-200 co-labeling were counted as reinnervated per animal (n = 4 animals per group).

Muscle fiber area analysis. Transversal and longitudinal gastrocnemius muscle sections were stained with H&E. Briefly, nuclei were stained with Harris hematoxylin for 6 minutes followed by differentiation with acid solution of 0.01% HCl in ethanol. Cytoplasm was stained with eosin for 1 minute. Sections were dehydrated by graded ethanol (50%, 70%, 96%, and 100%, and glycerol; twice, 5 minutes each solution) and mounted with DPX. We randomly took images under light microscopy at 20× or 40×, and the areas of at least 100 muscle fibers from three different images were calculated. The mean and area distribution for each animal was analyzed (n = 4 per group).

Statistical analysis. All values are presented as means ± standard error of the mean (SEM). Statistical analyses were performed using GraphPad Prism 5 software by unpaired t-tests or two or one-way analysis of variance (ANOVA) followed by Bonferroni's multiple comparison tests. CMAP apparition was analyzed using the Mantel-Cox test, being each CMAP an event. A p value of 0.05 was taken to indicate significant difference.

Data Availability. The datasets generated during and/or analysed during the current study are available from the corresponding author on reasonable request.

References

1. Rochkind, S., Filmar, G., Kluger, Y. & Alon, M. Microsurgical management of penetrating peripheral nerve injuries: pre, intra- and postoperative analysis and results. *Acta Neurochir. Suppl.* **100**, 21–4 (2007).
2. Carlstedt, T. New Treatments for Spinal Nerve Root Avulsion Injury. *Front. Neurol.* **7**, 23–26 (2016).
3. Chalfoun, C. T., Wirth, G. A. & Evans, G. R. D. Tissue engineered nerve constructs: where do we stand? *J. Cell. Mol. Med.* **10**, 309–17 (2006).
4. Rochkind, S., Shapira, Y. & Nevo, Z. The potential clinical utility of novel methods for peripheral nerve regeneration: where are we now? *Future Neurol.* **9**, 105–107 (2014).
5. Chuang, D. C. *et al.* Traction avulsion amputation of the major upper limb: a proposed new classification, guidelines for acute management, and strategies for secondary reconstruction. *Plast. Reconstr. Surg.* **108**, 1624–38 (2001).
6. Koliatsos, V. E., Price, W. L., Pardo, C. A. & Price, D. L. Ventral root avulsion: an experimental model of death of adult motor neurons. *J Comp Neurol* **342**, 35–44 (1994).
7. Casas, C. *et al.* Network-based proteomic approaches reveal the neurodegenerative, neuroprotective and pain-related mechanisms involved after retrograde axonal damage. *Sci. Rep.* **5**, 9185 (2015).
8. Penas, C., Casas, C., Robert, L, Forés, J. & Navarro, X. Cytoskeletal and activity-related changes in spinal motoneurons after root avulsion. *J. Neurotrauma* **26**, 763–79 (2009).
9. Eggers, R., Tannemaat, M. R., De Winter, F., Malessy, M. J. A. & Verhaagen, J. Clinical and neurobiological advances in promoting regeneration of the ventral root avulsion lesion. *Eur. J. Neurosci.* **43**, 318–335 (2016).
10. Seddon, H. J., Medawar, P. B. & Smith, H. Rate of regeneration of peripheral nerves in man. *J. Physiol.* **102**, 191–215 (1943).
11. Hoang, T. X. & Havton, L. A. A single re-implanted ventral root exerts neurotropic effects over multiple spinal cord segments in the adult rat. *Exp. brain Res.* **169**, 208–17 (2006).
12. Gu, H.-Y. *et al.* Survival, regeneration and functional recovery of motoneurons after delayed reimplantation of avulsed spinal root in adult rat. *Exp. Neurol.* **192**, 89–99 (2005).
13. Pintér, S., Gloviczki, B., Szabó, A., Márton, G. & Nógrádi, A. Increased survival and reinnervation of cervical motoneurons by riluzole after avulsion of the C7 ventral root. *J. Neurotrauma* **27**, 2273–2282 (2010).
14. Eggers, R., Tannemaat, M. R., Ehlert, E. M. & Verhaagen, J. A spatio-temporal analysis of motoneuron survival, axonal regeneration and neurotrophic factor expression after lumbar ventral root avulsion and implantation. *Exp. Neurol.* **223**, 207–220 (2010).
15. Blits, B. *et al.* Rescue and sprouting of motoneurons following ventral root avulsion and reimplantation combined with intraspinal adeno-associated viral vector-mediated expression of glial cell line-derived neurotrophic factor or brain-derived neurotrophic factor. *Exp Neurol* **189**, 303–316 (2004).
16. Eggers, R. *et al.* Neuroregenerative effects of lentiviral vector-mediated GDNF expression in reimplanted ventral roots. *Mol. Cell. Neurosci.* **39**, 105–117 (2008).
17. Torres-Espín, A. *et al.* Neuroprotection and axonal regeneration after lumbar ventral root avulsion by re-implantation and mesenchymal stem cells transplant combined therapy. *Neurotherapeutics* **10**, 354–68 (2013).
18. Rodrigues Hell, R. C., Silva Costa, M. M., Goes, A. M. & Oliveira, A. L. R. Local injection of BDNF producing mesenchymal stem cells increases neuronal survival and synaptic stability following ventral root avulsion. *Neurobiol. Dis.* **33**, 290–300 (2009).
19. Pang, X. Y. *et al.* Lithium accelerates functional motor recovery by improving remyelination of regenerating axons following ventral root avulsion and reimplantation. *Neuroscience* **329**, 213–225 (2016).
20. Li, H. *et al.* Enhanced regeneration and functional recovery after spinal root avulsion by manipulation of the proteoglycan receptor PTP σ. *Nat. Publ. Gr.* 1–14, doi:10.1038/srep14923 (2015).

21. Herrando-Grabulosa, M. *et al.* Novel Neuroprotective Multicomponent Therapy for Amyotrophic Lateral Sclerosis Designed by Networked Systems. *PLoS One* **11**, e0147626 (2016).
22. Connor, E. A., McMahan, U. J. & Marshall, R. M. Cell accumulation in the junctional region of denervated muscle. *J. Cell Biol.* **104**, 109–120 (1987).
23. Isaacs, J. *et al.* Does partial muscle reinnervation preserve future re-innervation potential? *Muscle Nerve* 1–21, doi:10.1002/mus.25571 (2017).
24. Liu, K., Tedeschi, A., Park, K. K. & He, Z. Neuronal Intrinsic Mechanisms of Axon Regeneration. *Annu. Rev. Neurosci.* **34**, 131–152 (2011).
25. Sakuma, M. *et al.* Lack of motor recovery after prolonged denervation of the neuromuscular junction is not due to regenerative failure. *Eur. J. Neurosci.* **43**, 451–462 (2016).
26. Carlstedt, T., Misra, V. P., Papadaki, A., McRobbie, D. & Anand, P. Return of spinal reflex after spinal cord surgery for brachial plexus avulsion injury. *J. Neurosurg.* **116**, 414–417 (2012).
27. Udina, E., Ceballos, D., Verdú, E., Gold, B. G. & Navarro, X. Bimodal dose-dependence of FK506 on the rate of axonal regeneration in mouse peripheral nerve. *Muscle Nerve* **26**, 348–55 (2002).
28. Al-Majed, A. A., Neumann, C. M., Brushart, T. M. & Gordon, T. Brief electrical stimulation promotes the speed and accuracy of motor axonal regeneration. *J. Neurosci.* **20**, 2602–2608 (2000).
29. Elzinga, K. *et al.* Brief electrical stimulation improves nerve regeneration after delayed repair in Sprague Dawley rats. *Exp. Neurol.* **269**, 142–153 (2015).
30. Sun, H. H. *et al.* Geldanamycin accelerated peripheral nerve regeneration in comparison to FK-506 *in vivo*. *Neuroscience* **223**, 114–123 (2012).
31. Gordon, T., Sulaiman, O. A. R. & Ladak, A. Chapter 24: Electrical stimulation for improving nerve regeneration: where do we stand? *Int. Rev. Neurobiol.* **87**, 433–44 (2009).
32. Stefancic, M., Vidmar, G. & Blagus, R. Long-term recovery of muscle strength after denervation in the fibular division of the sciatic nerve. *Muscle and Nerve* **54**, 702–708 (2016).
33. Fischer, D. & Leibinger, M. Promoting optic nerve regeneration. *Prog. Retin. Eye Res.* **31**, 688–701 (2012).
34. Jones, D. M., Tucker, B. A., Rahimtula, M. & Mearow, K. M. The synergistic effects of NGF and IGF-1 on neurite growth in adult sensory neurons: convergence on the PI 3-kinase signaling pathway. *J. Neurochem.* **86**, 1116–28 (2003).
35. Park, K. K. *et al.* Promoting Axon Regeneration in the Adult CNS by Modulation of the PTEN/mTOR Pathway. *Science (80-.).* **322**, 963–966 (2008).
36. Liu, K. *et al.* PTEN deletion enhances the regenerative ability of adult corticospinal neurons. *Nat. Neurosci.* **13**, 1075–1081 (2010).
37. Park, K. K. *et al.* Promoting axon regeneration in the adult CNS by modulation of the PTEN/mTOR pathway. *Science* **322**, 963–6 (2008).
38. Dankort, D. *et al.* Braf (V600E) cooperates with Pten loss to induce metastatic melanoma. *Nat. Genet.* **41**, 544–52 (2009).
39. Glass, D. J. Skeletal muscle hypertrophy and atrophy signaling pathways. *Int. J. Biochem. Cell Biol.* **37**, 1974–1984 (2005).
40. Lai, K. V *et al.* Conditional Activation of Akt in Adult Skeletal Muscle Induces Rapid Hypertrophy Conditional Activation of Akt in Adult Skeletal Muscle Induces Rapid Hypertrophy. **24**, 9295–9304 (2004).
41. Tang, H. *et al.* mTORC1 promotes denervation-induced muscle atrophy through a mechanism involving the activation of FoxO and E3 ubiquitin ligases. *Sci. Signal.* **7**, ra18 (2014).
42. Yeung, F. *et al.* Modulation of NF-kappaB-dependent transcription and cell survival by the SIRT1 deacetylase. *EMBO J.* **23**, 2369–80 (2004).
43. Lee, D. & Goldberg, A. L. SIRT1 Protein, by Blocking the Activities of Transcription Factors FoxO1 and FoxO3, Inhibits Muscle Atrophy and Promotes Muscle Growth*. **288**, 30515–30526 (2013).
44. Chalkiadaki, A., Igarashi, M., Nasamu, A. S., Knezevic, J. & Guarente, L. Muscle-Specific SIRT1 Gain-of-Function Increases Slow-Twitch Fibers and Ameliorates Pathophysiology in a Mouse Model of Duchenne Muscular Dystrophy. **10**, 1–12 (2014).
45. Arbat-Plana, A., Torres-Espín, A., Navarro, X. & Udina, E. Activity dependent therapies modulate the spinal changes that motoneurons suffer after a peripheral nerve injury. *Exp. Neurol.* **263**, 293–305 (2015).
46. Gundersen, H. Stereology of arbitrary particles. A review of unbiased number and size estimators and the presentation of some new ones, in memory of William R. Thompson. *J. Microsc.* **143**, 3–45 (1986).

Acknowledgements

This work was mainly supported by the Ministerio de Economía y Competitividad of Spain (#SAF 2014-59701). We are also grateful for support from CIBERNED and TERCEL. The RT97, CSPG, and SYT1 antibodies were obtained from the Developmental Studies Hybridoma Bank developed under the auspices of the NICHD and maintained by the University of Iowa, Department of Biology.

Author Contributions

D.R.G. performed the experiments, analyzed the results, and wrote part of the paper. J.F. performed the surgeries. X.N. helped with electrophysiological analyses and contributed to writing of the paper. C.C. conceived, designed, supervised, and analyzed all the experiments and wrote the paper.

Additional Information

Competing Interests: The authors declare that they have no competing interests.

Publisher's note: Springer Nature remains neutral with regard to jurisdictional claims in published maps and institutional affiliations.

GENERAL DISCUSSION

General Discussion

The results presented in this thesis demonstrated that the use of system biology holistic point of view can be useful to discover new neuroprotectants to treat different type of PNL. The repurposing of Acamprosate, a drug used for alcohol dependence, combined with Ribavirin, a nucleoside used for treating viral infections such as Hepatitis, exerted neuroprotective effects in models of MN death, enhanced SIRT1 activity and improved functional recovery after PNL. This drug combination, termed as NeuroHeal (NH), also reduces the apoptotic and the ER-stress death of MNs, increases the presence of motor-transport proteins and induces a pro-survival autophagic flux. With the data from this work, we conclude that NH refurnishes the molecular subroutines that are triggered by MNs after nerve injuries at different stages of development, shifting their molecular maps to those that favor their survival and enhance their axonal regrowth. Therefore, NH is a feasible drug therapy for human PNL.

Aiming to find neuroprotectants to sustain MN survival, we discovered the NH as a new drug therapy for PNL using a novel bioinformatic tool that is based on systems biology approach and ANN. With this tool, we used and treated the whole protein network that characterizes MN demise after RA, instead of directly modulate a single protein or molecular axis. Currently, in biomedicine areas this point of view has become mandatory because the human pathologies are not provoked by a single cellular or genetic event and the discover of new-targets for drugs therapy has reached its limits (Lindsay, 2005). Therefore, Systems biology combined with ANN for drug discovery allow to focus on the alteration of entire pathways rather than single proteins, allowing the discovery of new therapies (Pujol et al., 2010). Moreover, systems biology is also useful to determine efficacy and safety of new drug therapies (Bai and Abernethy, 2013; Schneider and Klabunde, 2013). We add our drug therapy to the successful list of therapeutic discoveries obtained through systems biology approaches (Azmi et al., 2010; Sigurdsson et al., 2012).

We found that TPMS predicted at least two drug combinations with a demonstrated neuroprotective effect in our model of RA. The rationale behind our study is similar to one reported previously (Herrando-Grabulosa et al., 2016), where

TPMS discovered neuroprotective drugs for ALS. In both cases, the starting material of pathological and desired conditions was accurate. In this scenario, TPMS is able to discover effective therapies. In other study, this tool reported a drug therapy that exacerbated the AD pathology instead of alleviate it (Badiola et al., 2013). In this case, the "healthy" or "desired" condition was not well defined, and TPMS elucidated ineffective therapies (Badiola et al., 2013). So, the starting material must be very precise to effectively discover new therapies.

Systems biology holistic view allows to the discovery of therapies that treat whole pathologic network instead of a particular hallmark or protein (Berger and Iyengar, 2009; Jaeger and Aloy, 2012). In some complex pathologies such cancer, thee modulation of a particular protein like p53 can provoke undesired effects (Jaeger and Aloy, 2012). In our case, we need to modulate the whole network that characterizes MNs death because it involves the crosstalk of several pro-death mechanisms (Casas et al., 2015). Otherwise, for those monogenic pathologies, systems biology cannot be so useful, so other approaches such as gene therapy can be performed. Nevertheless, the clinical studies based of viral gene therapy are arising undesired effects such as immune system reaction and possibility of causing a tumor, among others (Yla-Herttuala, 2003; Naldini, 2015), so its clinical application has to be highly controlled. In fact, the number viral-based therapies that arrive at phase IV is very incipient (Ginn et al., 2013). Perhaps, the future treatment of monogenic disease are novel biotechnological techniques such as CRISPR/cas9, which allows the genome editing of different type of cells (Sander and Joung, 2014; Lander, 2016) avoiding undesired genome modifications. This tool yield promising effects on cancer field (Platt et al., 2014) and neurodegenerative diseases such as ALS (Batra et al., 2017).

NH is composed by Acamprosate and Ribavirin, two repurposed drugs that are used for human healthcare. In fact, they are used for health conditions that need long-lasting treatment. The reposition of drugs drastically reduces the time-lines from bench to bedside (Ashburn and Thor, 2004). Drug repurposing has advantages, because the behavior and the safety of the drugs within the human organism are well-described. Nowadays, no undesired effects are described regarding both drugs, so the clinical translation of NH can be performed within years. It is also important

to remark that we administered both drugs at less concentration that this used in other experimental procedures in murine models (Daoust et al., 1992; Solbrig et al., 2002; Lavrnja et al., 2012). Rats received NH treatment during 6 months and we did not observed detrimental effects on its behavior. Initially, we performed an *in vitro* pre-screening to determine the best ratio between both drugs and the concentration to achieve a supra-additive effect for an optimal neuroprotective effect. It is important to notice that the discovered drugs combinations reduce MN cell death after ER-stress, and that NH also do it in the SOCs model, which represents better the natural-conditions of MN demise (Guzmán-Lenis et al., 2009). Therefore, the discovered drug combinations may be useful to treat those neurodegenerative diseases in which ER-stress is related with pathology progression (Taylor et al., 2002), although deeply studies are needed to check their exact mechanisms.

Recently, it was described that Acamprosate combined with the anti-spasticity drug baclofen reduce AD and PD pathology (Chumakov et al., 2015; Hajj et al., 2015). Indeed, this drug combination is in phase II of clinical studies for AD and in phase I for ALS. The drug-repurposed combination PXT3003, which is based on systems biology and it is composed by baclofen, naltrexone and sorbitol, has passed preclinical phase II for Charcot-Marie-Tooth Disease Type 1A without remarkable undesired effects (Mandel et al., 2015) and it is currently in phase III. PXT3003 also increases nerve regeneration and muscle reinnervation after nerve injury in mice, and it is a feasible therapy for those pathologies characterized by myelin disturbances (Chumakov et al., 2014)

In some cases and although the therapy is effective, their bioinformatical-predicted mechanisms do not fit with the results obtained in the experimental model, which represents the “real life”. Therefore, the predicted information is not always ascertained and it has to be taken with caution. In this way, several *in silico* studies reported false negatives (Li and Jones, 2012). To ensure that the elucidated information is valuable and reliable, several quality-control tools are described to ensure a correct drug screening (Parker and Bajorath, 2006). Therefore, the verifications of the *in silico*-predicted mechanisms of action (MoA) are essential to perform further studies. MoA of newly-discovered drugs refers to the direct modulated target, or to the understanding of the biological processes that treatment

modifies. Therefore, it is mandatory to check the MoA of the *in silico*-designed therapies in the *in vivo*/*in vitro* context. MoA information is also useful for safety assessment, reducing to possibility of undesired molecular event or harmful effect due to the modulation of some secondary pathways (Berg, 2014). Moreover, check the MoA of a discovered drug therapy can open new windows for treating other related or un-related diseases.

MoA predicted for NH was ascertained at least for motor proteins (Kif5c and DCNT1), β-1 Integrin subunit, SIRT1 activity and PARP1. With the modulation of these specific proteins, we can hypothesize that NH can be beneficial for other neurodegenerative pathologies like ALS, in which kif5c and DNCT1 defects are present (LaMonte et al., 2002; Xia et al., 2003; Heiman-Patterson et al., 2015; De Vos and Hafezparast, 2017). Moreover, the increase on β-1 integrin can be yielding anti-anoikis effects to the MNs. In fact, the concomitant activation of AKT axis with an increase of β-1 integrin can be inhibiting anokis (Bouchard et al., 2007) or apoptosis (Kennedy et al., 1997) in our model.

SIRT1 activity depends on several factors like its post-translational modification state or cellular NAD^+ levels (Yang et al., 2007; Kang et al., 2009). Along this thesis, we have observed that SIRT1 presence is not always correlated with its deacetylase activity. SIRT1 nuclear presence is related with undifferentiated state of neurons (Hisahara et al., 2008; Liu et al., 2013; Rafalski et al., 2013). It has been described that neurons are more susceptible to death when they are immature (Kole et al., 2013). Hence, the injury can provoke the dedifferentiation of the MNs, which will lead to nuclear accumulation of SIRT1. Other plausible hypothesis is that other pro-death proteins such as PARP1 can consume the substrate of SIRT1 (NAD^+), leading to a dramatical fall of its activity within MNs. This can trigger SIRT1 overexpression to compensate the lack of its deacetylase activity.

Ribavirin inhibits S-adenosyl-L-homocysteine hydrolase and inosine-5'-monophosphate dehydrogenase 1 enzymes, which demand NAD^+ as a substrate to performs its activity (Cai et al., 2007; Koh et al., 2014). Therefore, Ribavirin can be the responsible of NH-mediated SIRT1 Gan-of-Function. Although we did not observe it in the MN death model used to discover NH, we found that NH modifies the levels of PARP1. SIRT1 activity represses the expression of PARP1 promoter

(Senthilkumar et al., 2009), so NH can be reducing PARP1 expression and therefore its levels.

Strikingly, we also found that NH induces a slight autophagic flux. mTOR, which is one of the main inhibitors of autophagy and it is activated by the PI3K/AKT, directly phosphorylates p70s6k at the residue that we analyzed. NH-treated MNs exhibited an increased PI3K/AKT axis in two different models, which correlates with an increased mTOR activity. Controversially, this pathway has been related with autophagic initiation. Moreover, NH activates autophagy within MNs after nerve injury in PI3K/AKT-dependent way. PI3K activity induces the formation of the autophagosome, and the PI3K inhibitors such as 3-methyladenine or wortmannin are a potent blockers of autophagy (Noguchi et al., 2014; Klionsky et al., 2016). PI3K/AKT-promoted autophagy has been classified as a pro-survival effect. This autophagy is essential to reduce ischemia injury in neonatal rats (Balduini et al., 2012), although in other models this induction has detrimental effects (Wang et al., 2014).

Regarding SIRT1, its activity its deacetylase activity favor autophagy by the modulation of Atg or the inhibition of mTOR (Lee et al., 2008; Ghosh et al., 2010). Therefore, we found that NH activates AKT pathway and SIRT1, and this turns on A fine-tune modulation of autophagy and an increased axonal regeneration (Park et al., 2008). This results in the co-activation of mTOR and autophagy by NH, but these mechanisms have different roles regarding neuroprotection and axonal regeneration (Li et al., 2016a). PI3K/AKT and SIRT1 axis can converge in FOXOs, choosing an specific transcriptional layer from its repertoire (van der Horst and Burgering, 2007).

FOXO's were initially described as pro-death players because they induce apoptotic-mediators (Fu and Tindall, 2008; Farhan et al., 2017). However, recent studies showed that SIRT1/FOXO axis can block apoptosis and induce cell survival increasing autophagic clearance (Gu et al., 2016). Nowadays, their activity has demonstrated neuroprotection in HD or in death of MNs (Mojsilovic-Petrovic et al., 2009; Jiang et al., 2012) by autophagy induction (Xu et al., 2011). Although they are TF and their activity is mainly nuclear, it has been recently described that FOXO1 is

needed at cytosol to trigger autophagy (Zhao et al., 2010). We focus on FOXO3a, which is involved in neuronal response after traumatic injury (Wang et al., 2009; Zhang et al., 2013). We found that FOXO3a induce autophagy to sustain the viability of MNs. After TBI in humans or in rat experimental models, FOXO3a levels are increased, and its autophagy induction has detrimental role on functional outcome of those rats (Sun et al., 2017). Therefore, FOXO3a-mediated neuroprotection after trauma can depend of the sub-neuronal population and the developmental stage. Recent evidence also suggest that FOXO3a mediates P3IK/AKT activation, and this triggers FOXO1-induced autophagy, indicating that FOXOs can be modulated between them (Zhou et al., 2012).

It is important to validate the putative effect of NH in pure models of trauma to the nervous system which promote MNs death after axonal disconnection. They are a pure "clinical" models instead of the use genetically modified models. Although transgenic models of neurodegenerative diseases are useful for basic mechanistic studies, several issues regarding their limited utility as predictive models of human diseases have emerged, because normally they are gene-centric instead of network-centric. Therefore, those *in vivo* models of injury-provoked neuronal death yield valuable information about the "natural occurring process" (Lindsay, 2005). We demonstrated that NH sustains survival of MNs after nerve injury in two murine species and in different developmental stages. Therefore, the endogenous mechanisms trigger by MNs to survive are similar among different species and the molecular network modulated by NH include them. For example, MNs after DA axotomy trigger anti-apoptotic mechanisms (Perrelet et al., 2002, 2004; Kole et al., 2013; Casas et al., 2015), and it is feasible that NH treatment includes and induces them in neonatal MNs, in which under normal conditions they are not present.

Disconnection from their target organ after nerve injury will trigger cell-death mechanisms in the MNs. In this thesis, we shown evidences that not all the injuries equally affect MNs, and that these did not face up the injury with the same molecular subroutines. We validated the neuroprotective effect of NH in different *in vivo* models that can be used as pre-clinal models of brachial/lumbar plexus avulsion, injury to paired cranial nerves or nerve injury to newborns. Thus, NH activates in different pre-clinical models those endogenous neuroprotective

mechanisms that MNs have, so it can be a treatment for distinct clinical cases. We did not study if NH neuroprotective effect is gender-specific. Males have more Gastrocnemius-innervating spinal MNs than females (Mierzejewska-Krzyzowska et al., 2014), so the injuries towards L4-L5 nerve roots or sciatic crush can have different percentages of death, and the NH neuroprotective effect can be different. Regarding hypoglossal nuclei, it has never been described a comparison between genders. We suppose that males and females should have the same number of MNs, so NH will act similarly in both genders.

Under physiological conditions, MNs subpopulations are different regarding the developmental stage and excitability (Haenggeli and Kato, 2002; Tadros et al., 2016). The initial description englobed all types of death of MNs after a PNL as apoptotic (Martin et al., 1999; Martin and Liu, 2002; Terui et al., 2003; Kiryu-Seo et al., 2005) because MNs accumulate p53 and caspase 3 at their nuclei. Nevertheless, recent evidences show that not all MNs die through the same executive pathway (Penas et al., 2011; Casas et al., 2015). We observed nuclear accumulation of p53 within injured MNs in the used models. Indeed, we checked its acetylated form at k373, which is directly related with the induction of pro-apoptotic proteins and apoptosis initiation (Terui et al., 2003). Therefore, the injured MNs engaged apoptotic pathways (Casas et al., 2015) but the executive cleavage of caspase-3 was not observed (Penas et al., 2011). Although striking, NH promoted a reduction of the acetyl-p53, indicating that it can also act inhibiting p53-dependent apoptosis. In fact, HDAC inhibitors mediate apoptosis increasing this acetylation of p53 (Terui et al., 2003). We also observed that neonatal MNs trigger apoptotic executors after nerve injury such as caspase 3 and PARP1, and that NH blocks PARP1 cleavage. So NH treatment also contains anti-apoptotic features, and can be useful to treat other neurodegenerative pathologies in which apoptosis characterizes neuronal death.

We observed that the slope of death is different between neonates and adults, which indicates that their underling mechanisms are different. This fits with the hypothesis that the adult ones have matured machinery to fight death, which is called as anti-apoptotic endogenous mechanisms (Introduction 4.1.5) (Kole et al., 2013). On the other side, the distal axotomy of the Hypoglossal nerve in mice

triggered MNs death in a similar fashion that RA in rats, and we found that both models share molecular similarities between them (**Fig. 11**).

TBI and SCI, which are other models of trauma to the CNS, also provoke a massive death of MNs. Although the mechanisms of death are slightly different, NH can be a feasible therapy for them. It has been shown that SIRT1 activation reduces functional impairments after SCI (Chen et al., 2017). Moreover, SIRT1 may play some beneficial effect improving functional recovery after stroke or TBI. TBI reduces SIRT1 levels and it can has some protective activity (Wu et al., 2007). Moreover, SIRT1 role regarding brain stroke remains controversial, although is feasible that plays a protective role (Petegnief and Planas, 2013). Therefore, and although unexplored, NH can have some beneficial effect for other CNS traumas or insults.

We validated the therapeutic potential of NH in a pre-clinical model of root avulsion with delayed reimplantation, which recapitulates the 4 mandatory points needed for a good functional recovery described previously (Introduction 5). Initially, we need to set up this model because no one had never performed the delayed reimplantation of lumbar roots after its avulsion (Introduction 3.1). NH sustains MN viability during at least 6 months and reduces the production of inhibitory molecules of axonal regrowth at the CNS in this model. At the same time, NH increases GAP43 levels within the axonal tracks of MNs, a protein that is needed by mature neurons to reextend their axons (Udvadia et al., 2001). NH also activates the pro-regenerative pathway AKT under the PTEN level (Park et al., 2008). Found drug therapies that increase axonal regrowth by AKT activation without affect PTEN have raised interest, because they maintain PTEN tumor-suppressor activity (Tolkacheva and Chan, 2000).

GAP43 expression can be modulated by AKT axis (Liu et al., 2012), so an increased activation of PI3K/AKT axis can be the responsible of the GAP43 changes. The increase on the presence of this RAG is correlated with an enhanced nerve regeneration in our model of PNL, as described elsewhere (Afshari et al., 2009). Although not experimentally compared, we observed that NH ability to increase nerve regeneration is slightly higher than this described for FK506 (Udina et al.,

2002). Moreover, we tested the NH effect on axonal regeneration by fine electrophysiologic techniques that assess muscle reinnervation, obtaining more reliable results than those described for N-acetylcysteine and acetyl-L-carnitine (Welin et al., 2009; Farahpour and Ghayour, 2014).

Although we analyzed nerve regeneration in both models, they have slightly differences. In the crush model, we need to increase the regrowth of the peripheral zone of the axon of the MN. Moreover, in the RA+RE model, the MNs need to generate a new axon from its soma and it must cross the glial scar formed at the transition zone between CNS and PNS after RA. The glial scar is composed of CSPGs and ECM secreted by reactive astrocytes (Silver and Miller, 2004), so the described Ribavirin effects averting astrocyte reaction (Lavrnja et al., 2012) can be the mediator of this permissive environment. Interestingly, this new pre-clinical model yielded us proves that NH can partially blocks muscle atrophy that appears after long denervation.

A correct reconnection of MNs with muscle fiber is essential to warranty an optimal functional recovery after PNL. Thus, the re-extended axon needs to reach the denervated muscle. Moreover, although the NMJ is rebuilt, the machinery must be recruited to the synapsis. Mutant animals for a protein present in NMJ suffer electrophysiological abnormalities and reduced locomotor activity (MacDonald et al., 2017) which suggest that NMJ behavior is important for a correct motor system performance. In experimental models, an enhanced regeneration of motor fibers is not always correlated with an enhanced functional recovery (Cannoy et al., 2016). Therefore, once the axon re-attaches with the muscle, it is mandatory to build a functional NMJ.

Here, we observed that the amplitude of the CMAP is not well correlated with the percentage of NMJs reinnervated in muscles from animals that received the sciatic crush or root reimplantation, which indicates that reconnected axons need to stablish a functional NMJ. In clinical, although nerve regeneration is fully achieved, this does not correlate with a functional recovery. Among several factors, this can be due to an not functional NMJ (Sakuma et al., 2016) or an excessive muscle atrophy. Chronic muscle denervation is characterized by a drastic fall in the

proliferative capacity of satellite cells, an exacerbated muscle fibrosis and an atrophy that prevent any functional reconnection and recovery (Finkelstein et al., 1993; Stefancic et al., 2016)

Muscle atrophy is initially provoked by an excessive protein breakdown, followed by a reduction in the proteins synthesis. Two signaling axis orchestrates muscle atrophy: PI3K/AKT, which acts regulating mTOR and FOXOs, and NF-κb (Cai et al., 2004; Latres et al., 2005). AKT regulates the protein homeostasis and therefore muscle integrity by two synergic ways: by the inhibition of FOXOs (1 and 3a), which represses the expression of atrogenes, blocks protein degradation and inhibits FOXO-dependent autophagy (Sandri et al., 2004; Mammucari et al., 2007; Yamazaki et al., 2010; Schiaffino and Mammucari, 2011), and by the direct increase of protein synthesis through mTOR activation and p70s6k protein (Bodine et al., 2001; Rommel et al., 2001). Therefore, therapies have aiming to increase PI3K-AKT axis activity for treat muscle wasting are a good option, but their use is extremely hazardous due to the pro-oncogenic inclination of the axis (Cohen et al., 2014).

Other player in muscle atrophy, although it exact mechanism is partially clarified (Sriram et al., 2011), is the protein breakdown mediated by NF-κb. This evidence crosslinks those diseases with a marked inflammatory reaction (like a systemic release of cytokines or interleukins) with the subsequent muscle wasting (Yamaki et al., 2012). SIRT1 modulates both signaling pathways explained before (activates PI3K/AKT and inhibits NF-κB) (Sundaresan et l., 2011; Lee and Goldberg, 2015), and inhibits atrogenic transcriptome of FOXO at muscle (Lee and Goldberg, 2013). Moreover, SIRT1 protein levels dramatically fall during starvation in the fibers type II of skeletal muscle but not in type I (heart and soleus muscles). Therefore, NH-mediated SIRT1 Gain-of-Function can be a plausible therapeutic approximation for those diseases, clinical states or traumas that are characterized by a untreatable muscle atrophy (Cohen et al., 2014). In this thesis, we showed evidences that NH leads to SIRT1 and AKT activation, and therefore, NH-mediated anti-atrophy effect can be mediated by this dual activation. Regarding the data obtained for FOXO3a dual modulation, it is feasible that FOXO3a remains active but its transcriptome has anti-atrophic capabilities. So, the systemic treatment with NH

can be acting also at muscle level and can be a good therapy for muscle atrophy-related pathologies, but further studies are needed to depict its mechanisms.

Nowadays, we are analyzing the effect of NH in the rat model of cut and suture of the sciatic nerve, which is a pre-clinical model of nerve transection. In this model, we can elucidate the effect of NH on nerve regeneration and on muscle atrophy. To confirm the anti-atrophic effect of NH, we also will test the therapeutic effect of NH in a model of non-invasive hindlimb immobilization, which is a well-accepted model of disuse-provoked muscle atrophy. All these data will be helpful to get a more complete therapy to treat PNL. Although unexplored, NH also may be an effective treatment for those nervous compressive injuries such as hernia disc or Carpal tunnel, instead of the corticosteroids and nonsteroidal anti-inflammatory drugs currently used. These compounds only aim to reduce inflammation without enhance nerve regeneration (Deyo and Mirza, 2016; Padua et al., 2016), which leads to an impaired functional recovery. Corticosteroid treatment also slowed nerve regeneration after nerve injury in mice (Lieberman et al., 2011). Moreover, glucocorticoids as dexamethasone are an accelerators of muscle atrophy (Hasselgren et al., 2010), which have harmful effects on motor function recovery.

We observed that NH slightly reduced microgliosis and astrogliosis after RA and HA (data not shown). This inflammatory reaction is correlated with the neuropathic pain maintenance after RA (To et al. 2013). Moreover, SIRT1 activity at spinal level has been linked with a reduction of hyperalgesia and allodynia (Shao et al., 2014; Lv et al., 2015). Its effects can be mediated by an epigenetic mechanism (Zhou et al., 2017) or by its anti-inflammatory effects on spinal cord (H. Chen et al. 2017). In fact, resveratrol promoted algesic effects by inhibiting glial activation (Wang et al., 2016). SIRT1 deacetylates NF-Kb and blocks its pro-inflammatory capabilities (de Mingo et al., 2016; Wang et al., 2017). We observed that NH blocks the nuclear translocation of NF-κB to the nuclei of microglia *in vitro*, and this can reduce the production of pro-inflammatory cytokines. Therefore, NH can revert or partially reduce the neuropathic pain apparition that characterizes PNL by its anti-inflammatory abilities. On the other side, this inflammatory reaction is related with an exacerbation of the injury after stroke (Hernandez-Jimenez et al., 2013) and with progression of neurodegenerative diseases such as ALS (Lall and Baloh 2017).

Therefore, and although unexplored, NH can reduce NF-κB-dependent gene expression within microglial cells, delaying its pro-inflammatory response and reducing neurodegeneration or functional impairments after traumatic injuries (Grilli et al., 1996; Tan et al., 2008; Frakes et al., 2014; Li et al., 2016b; Wachholz et al., 2016).

In conclusion, PNL from different origins and throughout different development stages can lead to diverse types of MN death. Although the molecular mechanisms that drive the MNs to its degeneration seem to be different, the activation of the neuroprotective endogenous subroutines can sustain their survival. Therefore, force the molecular pathways that are present in other type of nervous traumas like SCI and TBI, or in neurodegenerative diseases like ALS, can achieve neuroprotection. NH can also be an effective treatment for those injuries that are characterized by an axonal degeneration, an exacerbated muscle atrophy or neuropathic pain apparition. Currently, NH is on PCT process and we want to validate its potential in other models non-related with neurological damage, aiming to elucidate other possible protective effects for it. From this thesis, we can extract two main conclusions: the usefulness of bioinformatic tools and systems biology to discover new therapies for complex pathologies, and the benefits that arises using the drug repurposing concept, which allows to hasten the process from bench-to-bedside.

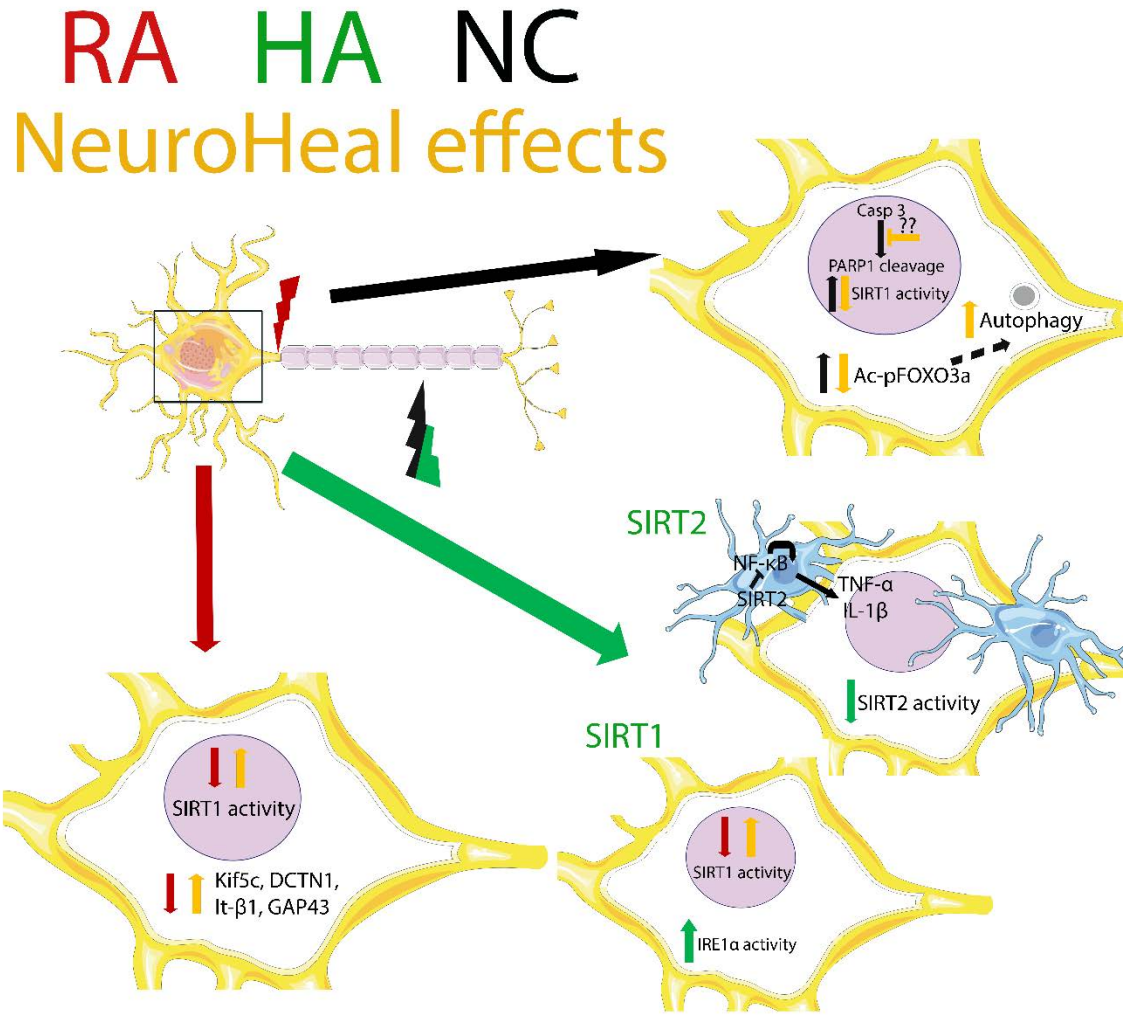

Figure 11: Representative draw showing the MN response after axonal injury and the protective effects of NeuroHeal. Root avulsion (RA) induces a blockage of SIRT1 activity and a reduction of kinesin 5c (kif5c), dynactin (DCTN1), subunit β-1 of integrins (It-β1) and Growth-associated protein 43 (GAP43). After hypoglossal axotomy (HA) SIRT1 and SIRT2 activities are affected. SIRT2 activity blocks the pro-inflammatory effects of NF-κB. Neonatal crush (NC) involves apoptosis hallmarks such as Caspase3 cleavage and PARP1 activation. NH avoids PARP1 processing and induces autophagy and autophagosomes formation.

CONCLUSIONS

CONCLUSIONS

Neuroprotection

Chapter 1: Neuroprotective Drug for Nerve Trauma Revealed Using Artificial Intelligence

- TPMS allowed the discovery of novel drug combinations with neuroprotective and proregenerative capability after peripheral nerve injury
- Elucidated drug combinations exert neuroprotection against Endoplasmic reticulum stress
- The oral treatment with NH reduces MN cell death after RA and increases functional recovery after nerve injury
- Mechanism of action predicted by TPMS was ascertained for the NH
- NeuroHeal neuroprotective effect is mediated through SIRT1 Gain of Function

Chapter 2: Neuroprotection of Disconnected Motoneurons requires Sirtuin 1 activation but Sirtuin 2 depletion or inhibition with AK-7 is detrimental

- SIRT1 and SIRT2 activities are modified after hypoglossal nerve injury
- SIRT1 activity is neuroprotective in different *in vitro* models of ER stress
- SIRT2 activity is detrimental for MN survival under ER stress
- SIRT2 activity reduces MN cell death *in vitro* and *in vivo* through the attenuation of the microglial cytotoxic activity

Chapter 3: NeuroHeal Confers Neonatal Neuroprotection Inducing SIRT1-Dependent Autophagy

- Death of MNs after neonatal nerve injury has apoptotic hallmarks, and NH blocks this death at PARP1 level.
- NH treatment increases MN survival *in vivo* and *in vitro* through SIRT1 Gain-of-function and the concominant PI3K/AKT axis activation

- Sciatic nerve injury increases the phosphorylation and acetylation of FOXO3, and NH increases it translocation to the MN nuclei.
- NH survival is mediated by autophagy increase *in vivo* and *in vitro*. These effects need SIRT1 and PI3K/AKT axis co-activation
- NH treatment during postnatal stages did not affect the normal peripheral nervous system development

Preclinical model of MN death and regeneration

Chapter 4: NH Boosts Regeneration and Reduced Denervated Muscle Atrophy

- NH enhances axonal regeneration, increases MN survival, reduces muscle atrophy and favors the formation of functional NMJs in a denervated muscle during a prolonged period in a pre-clinical model of root avulsion injury with delayed reimplantation
- NH treatment is a feasible therapeutic strategy for those injuries that affect the nervous system and where functional recovery is compromised due to a long distance-needed axonal regeneration and an exacerbated muscle atrophy

REFERENCES

References

Acosta-Alvear D, Zhou Y, Blais A, Tsikitis M, Lents NH, Arias C, Lennon CJ, Kluger Y, Dynlacht BD (2007) XBP1 Controls Diverse Cell Type- and Condition-Specific Transcriptional Regulatory Networks. Mol Cell 27:53–66.

Afshari FT, Kappagantula S, Fawcett JW (2009) Extrinsic and intrinsic factors controlling axonal regeneration after spinal cord injury. Expert Rev Mol Med 11:e37.

Aldskogius H, Liu L, Svensson M (1999) Glial responses to synaptic damage and plasticity. J Neurosci Res 58:33–41.

Allodi I, Guzmán-Lenis MS, Hernàndez J, Navarro X, Udina E (2011) In vitro comparison of motor and sensory neuron outgrowth in a 3D collagen matrix. J Neurosci Methods 198:53–61

Almeida-Souza L, Timmerman V, Janssens S (2011) Microtubule dynamics in the peripheral nervous system: A matter of balance. Bioarchitecture 1:267–270.

Ame J-C, Spenlehauer C, de Murcia G (2004) The PARP superfamily. Bioessays 26:882–893.

Andrabi SA, Kim NS, Yu S-W, Wang H, Koh DW, Sasaki M, Klaus JA, Otsuka T, Zhang Z, Koehler RC, Hurn PD, Poirier GG, Dawson VL, Dawson TM (2006) Poly(ADP-ribose) (PAR) polymer is a death signal. Proc Natl Acad Sci U S A 103:18308–18313

Andrade P, Visser-Vandewalle V, Hoffmann C, Steinbusch HWM, Daemen MA, Hoogland G (2011) Role of TNF-alpha during central sensitization in preclinical studies. Neurol Sci 32:757–771

Arce-Medina E, Paz-Paredes JI (2009) Artificial neural network modeling techniques applied to the hydrodesulfurization process. Math Comput Model 49:207–214

Ashburn TT, Thor KB (2004) Drug repositioning: identifying and developing new uses for existing drugs. Nat Rev Drug Discov 3:673–683

Aviles-Olmos I, Dickson J, Kefalopoulou Z, Djamshidian A, Ell P, Soderlund P, Whitton P, Wyse R, Isaacs T, Lees A, Limousin P, Foltynie T (2013) Exenatide and the treatment of patients with Parkinson's disease. J … 123:2370–2736

Azmi AS, Wang Z, Philip P a, Mohammad RM, Sarkar FH (2010) Proof of concept: network and systems biology approaches aid in the discovery of potent anticancer drug combinations. Mol Cancer Ther 9:3137–3144

Baas PW, Rao AN, Matamoros AJ, Leo L (2016) Stability properties of neuronal microtubules. Cytoskeleton (Hoboken) 73:442–460

Badea A, McCracken JM, Tillmaand EG, Kandel ME, Oraham AW, Mevis MB, Rubakhin SS, Popescu G,

Sweedler J V, Nuzzo RG (2017) 3D-Printed pHEMA Materials for Topographical and Biochemical Modulation of Dorsal Root Ganglion Cell Response. ACS Appl Mater Interfaces.

Badiola N, Alcalde V, Pujol A, Münter L-M, Multhaup G, Lleó A, Coma M, Soler-López M, Aloy P (2013) The proton-pump inhibitor lansoprazole enhances amyloid beta production. PLoS One 8:e58837

Baek M, Enriquez J, Mann RS (2013) Dual role for Hox genes and Hox co-factors in conferring leg motoneuron survival and identity in Drosophila. Development 140:2027–2038

Balduini W, Carloni S, Buonocore G (2012) Autophagy in hypoxia-ischemia induced brain injury. J Matern Fetal Neonatal Med 25 Suppl 1:30–34.

Barabási A-L (2007) Network medicine--from obesity to the "diseasome". N Engl J Med 357:404–407

Barabási A-L, Oltvai ZN (2004) Network biology: understanding the cell's functional organization. Nat Rev Genet 5:101–113

Barabási AL, Gulbahce N, Loscalzo J (2011) Network medicine: a network-based approach to human disease. Nat Rev 12:56–68

Baron R, Hans G, Dickenson AH (2013) Peripheral input and its importance for central sensitization. Ann Neurol 74:630–636.

Beirowski B, Gustin J, Armour SM, Yamamoto H, Viader A, North BJ (2011) myelination through polarity protein Par-3 / atypical protein kinase C (aPKC) signaling. October 2.

Bell RA V, Megeney LA (2017) Evolution of caspase-mediated cell death and differentiation: twins separated at birth. Cell Death Differ 24:1–10

Berger SI, Iyengar R (2009) Network analyses in systems pharmacology. Bioinformatics 25:2466–2472.

Bergerot A, Shortland PJ, Anand P, Hunt SP, Carlstedt T (2004) Co-treatment with riluzole and GDNF is necessary for functional recovery after ventral root avulsion injury. Exp Neurol 187:359–366.

Berry M, Ahmed Z, Morgan-Warren P, Fulton D, Logan A (2016) Prospects for mTOR-mediated functional repair after central nervous system trauma. Neurobiol Dis 85:99–110.

Bertolotti A, Zhang Y, Hendershot LM, Harding HP, Ron D (2000) Dynamic interaction of BiP and ER stress transducers in the unfolded-protein response. Nat Cell Biol 2:326–332.

Bi F, Huang C, Tong J, Qiu G, Huang B, Wu Q, Li F, Xu Z, Bowser R, Xia X-G, Zhou H (2013) Reactive astrocytes secrete lcn2 to promote neuron death. Proc Natl Acad Sci U S A 110:4069–4074.

Biermann J, Grieshaber P, Goebel U, Martin G, Thanos S, Di Giovanni S, Lagreze WA (2010) Valproic

acid-mediated neuroprotection and regeneration in injured retinal ganglion cells. Invest Ophthalmol Vis Sci 51:526–534.

Binker MG, Richards D, Gaisano HY, Cosen-Binker LI (2015) ER stress-associated CTRC mutants decrease stimulated pancreatic zymogen secretion through SIRT2-mediated microtubule dysregulation. Biochem Biophys Res Commun 463:329–335

Bisicchia E, Latini L, Cavallucci V, Sasso V, Nicolin V, Molinari M, D'Amelio M, Viscomi MT (2017) Autophagy Inhibition Favors Survival of Rubrospinal Neurons After Spinal Cord Hemisection. Mol Neurobiol 54:4896–4907.

Blenis XMM and J (2004) Molecular mechanisms of translational control. NatRevMolCell Biol 5:827–835

Blits B, Carlstedt TP, Ruitenberg MJ, de Winter F, Hermens WT, Dijkhuizen PA, Claasens JW, Eggers R, van der Sluis R, Tenenbaum L, Boer GJ, Verhaagen J (2004) Rescue and sprouting of motoneurons following ventral root avulsion and reimplantation combined with intraspinal adeno-associated viral vector-mediated expression of glial cell line-derived neurotrophic factor or brain-derived neurotrophic factor. Exp Neurol 189:303–316.

Bodine SC, Stitt TN, Gonzalez M, Kline WO, Stover GL, Bauerlein R, Zlotchenko E, Scrimgeour a, Lawrence JC, Glass DJ, Yancopoulos GD (2001) Akt/mTOR pathway is a crucial regulator of skeletal muscle hypertrophy and can prevent muscle atrophy in vivo. Nat Cell Biol 3:1014–1019.

Boland B, Kumar A, Lee S, Platt FM, Wegiel J, Yu WH, Nixon RA (2008) Autophagy induction and autophagosome clearance in neurons: relationship to autophagic pathology in Alzheimer's disease. J Neurosci 28:6926–6937.

Bollo M, Paredes RM, Holstein D, Zheleznova N, Camacho P, Lechleiter JD (2010) Calcineurin interacts with PERK and dephosphorylates calnexin to relieve ER stress in mammals and frogs. PLoS One 5:e11925.

Bonfoco E, Chen WS, Paul R, Cheresh DA, Cooper NR (2000) Beta-1 integrin antagonism on adherent, differentiated human neuroblastoma cells triggers an apoptotic signaling pathway. Neuroscience 101:1145–1152.

Bouchard V, Demers M-J, Thibodeau S, Laquerre V, Fujita N, Tsuruo T, Beaulieu J-F, Gauthier R, Vezina A, Villeneuve L, Vachon PH (2007) Fak/Src signaling in human intestinal epithelial cell survival and anoikis: differentiation state-specific uncoupling with the PI3-K/Akt-1 and MEK/Erk pathways. J Cell Physiol 212:717–728.

Bradke F, Fawcett JW, Spira ME (2012) Assembly of a new growth cone after axotomy: the precursor to axon regeneration. Nat Rev Neurosci 13:183–193

Brown GC, Vilalta A (2015) How microglia kill neurons. Brain Res:1–9

Brunet A, Bonni A, Zigmond MJ, Lin MZ, Juo P, Hu LS, Anderson MJ, Arden KC, Blenis J, Greenberg ME (1999) Akt Promotes Cell Survival by Phosphorylating and Inhibiting a Forkhead Transcription Factor. Cell 96:857–868.

Brunet A, Park J, Tran H, Hu LS, Hemmings BA, Greenberg ME (2001) Protein Kinase SGK Mediates Survival Signals by Phosphorylating the Forkhead Transcription Factor FKHRL1 (FOXO3a). Mol Cell Biol 21:952–965

Brunet A, Sweeney LB, Sturgill JF, Chua KF, Greer PL, Lin Y, Tran H, Ross SE, Mostoslavsky R, Cohen HY, Hu LS, Cheng H-L, Jedrychowski MP, Gygi SP, Sinclair DA, Alt FW, Greenberg ME (2004) Stress-dependent regulation of FOXO transcription factors by the SIRT1 deacetylase. Science 303:2011–2015

Buchheit CL, Weigel KJ, Schafer ZT (2014) Cancer cell survival during detachment from the ECM: multiple barriers to tumour progression. Nat Rev Cancer 14:632–641

Budayeva HG, Cristea IM (2016) Human sirtuin 2 localization, transient interactions, and impact on the proteome point to its role in intracellular trafficking.

Buitenhuis S, van Wijlen-Hempel RS, Pondaag W, Malessy MJA (2012) Obstetric brachial plexus lesions and central developmental disability. Early Hum Dev 88:731–734.

Byrne AB, Walradt T, Gardner KE, Hubbert A, Reinke V, Hammarlund M (2014) Insulin/IGF1 Signaling Inhibits Age-Dependent Axon Regeneration. Neuron 81:561–573

Cai D, Frantz JD, Tawa NE, Melendez PA, Oh BC, Lidov HGW, Hasselgren PO, Frontera WR, Lee J, Glass DJ, Shoelson SE (2004) IKKκ/NF-κB activation causes severe muscle wasting in mice. Cell 119:285–298.

Cai S, Li Q-S, Borchardt RT, Kuczera K, Schowen RL (2007) The antiviral drug ribavirin is a selective inhibitor of S-adenosyl-L-homocysteine hydrolase from Trypanosoma cruzi. Bioorg Med Chem 15:10.1016/j.bmc.2007.08.029

Calixto A, Jara JS, Court FA (2012) Diapause Formation and Downregulation of Insulin-Like Signaling via DAF-16/FOXO Delays Axonal Degeneration and Neuronal Loss. PLoS Genet 8.

Cannoy J, Crowley S, Jarratt A, Werts KL, Osborne K, Park S, English AW (2016) Upslope treadmill exercise enhances motor axon regeneration but not functional recovery following peripheral nerve injury. J Neurophysiol 116:jn.00129.2016

Canto C, Gerhart-Hines Z, Feige JN, Lagouge M, Noriega L, Milne JC, Elliott PJ, Puigserver P, Auwerx J (2009) AMPK regulates energy expenditure by modulating NAD+ metabolism and SIRT1 activity. Nature 458:1056–1060.

Caporali A, Sala-Newby GB, Meloni M, Graiani G, Pani E, Cristofaro B, Newby AC, Madeddu P, Emanueli C (2008) Identification of the prosurvival activity of nerve growth factor on cardiac myocytes. Cell Death Differ 15:299–311

Casas C, Isus L, Herrando-Grabulosa M, Mancuso FM, Borrás E, Sabidó E, Forés J, Aloy P (2015) Network-based proteomic approaches reveal the neurodegenerative, neuroprotective and pain-related mechanisms involved after retrograde axonal damage. Sci Rep 5:9185

Castri P, Lee Y ja, Ponzio T, Maric D, Spatz M, Bembry J, Hallenbeck J (2014) Poly(ADP-ribose) polymerase-1 and its cleavage products differentially modulate cellular protection through NF-kB-dependent signaling. Biochim Biophys Acta - Mol Cell Res 1843:640–651

Chaitanya GV, Babu PP (2009) Differential PARP cleavage: An indication of heterogeneous forms of cell death and involvement of multiple proteases in the infarct of focal cerebral ischemia in rat. Cell Mol Neurobiol 29:563–573.

Chaitanya G V, Steven AJ, Babu PP (2010) PARP-1 cleavage fragments: signatures of cell-death proteases in neurodegeneration. Cell Commun Signal 8:31

Chalkiadaki A, Guarente L (2015) The multifaceted functions of sirtuins in cancer. Nat Publ Gr 2:608–624

Chan YM, Wu W, Yip HK, So KF, Oppenheim RW (2001) Caspase inhibitors promote the survival of avulsed spinal motoneurons in neonatal rats. Neuroreport 12:541–545.

Chandran V et al. (2016) A Systems-Level Analysis of the Peripheral Nerve Intrinsic Axonal Growth Program. Neuron 89:956–970

Chen H, Ji H, Zhang M, Liu Z, Lao L, Deng C, Chen J, Zhong G (2017) An Agonist of the Protective Factor SIRT1 Improves Functional Recovery and Promotes Neuronal Survival by Attenuating Inflammation after Spinal Cord Injury. J Neurosci 37:2916–2930.

Chen J, Laramore C, Shifman MI (2016a) Differential expression of HDACs and KATs in high and low regeneration capacity neurons during spinal cord regeneration. Exp Neurol 280:50–59.

Chen L, Li Q, She T, Li H, Yue Y, Gao S, Yan T, Liu S, Ma J, Wang Y (2016b) IRE1α-XBP1 signaling pathway, a potential therapeutic target in multiple myeloma. Leuk Res 49:7–12

Chen X, Shen J, Prywes R (2002) The luminal domain of ATF6 senses endoplasmic reticulum (ER) stress and causes translocation of ATF6 from the er to the Golgi. J Biol Chem 277:13045–13052.

Chen X, Wales P, Quinti L, Zuo F, Moniot S, Herisson F, Rauf NA, Wang H, Silverman RB, Ayata C, Maxwell MM, Steegborn C, Schwarzschild MA, Outeiro TF, Kazantsev AG (2015) The sirtuin-2 inhibitor AK7 is neuroprotective in models of parkinson's disease but not amyotrophic lateral sclerosis and cerebral ischemia. PLoS One 10:1–15.

Chestnut B a, Chang Q, Price A, Lesuisse C, Wong M, Martin LJ (2011) Epigenetic regulation of motor neuron cell death through DNA methylation. J Neurosci 31:16619–16636

Chhabra A, Ahlawat S, Belzberg A, Andreseik G (2014) Peripheral nerve injury grading simplified on MR neurography: As referenced to Seddon and Sunderland classifications. Indian J Radiol Imaging 24:217–224

Chin TY, Kiat SS, F HG (2017) The Effects of Minocycline on Spinal Root Avulsion Injury in Rat Model. 24:31–39.

Cho Y, Cavalli V (2012) HDAC5 is a novel injury-regulated tubulin deacetylase controlling axon regeneration. EMBO J 31:3063–3078

Cho Y, Sloutsky R, Naegle KM, Cavalli V (2013) Injury-induced HDAC5 nuclear export is essential for axon regeneration. Cell 155:894–908.

Chopra V, Quinti L, Kim J, Vollor L, Narayanan KL, Edgerly C, Cipicchio PM, Lauver MA, Choi SH, Silverman RB, Ferrante RJ, Hersch S, Kazantsev AG (2012) The Sirtuin 2 Inhibitor AK-7 Is Neuroprotective in Huntington's Disease Mouse Models. Cell Rep 2:1492–1497

Clement AM, Nguyen MD, Roberts EA, Garcia ML, Boillee S, Rule M, McMahon AP, Doucette W, Siwek D, Ferrante RJ, Brown RHJ, Julien J-P, Goldstein LSB, Cleveland DW (2003) Wild-type nonneuronal cells extend survival of SOD1 mutant motor neurons in ALS mice. Science 302:113–117.

Cobianchi S, Arbat-Plana A, Lopez-Alvarez VM, Navarro X (2017) Neuroprotective Effects of Exercise Treatments After Injury: The Dual Role of Neurotrophic Factors. Curr Neuropharmacol 15:495–518.

Cohen S, Nathan J a., Goldberg AL (2014) Muscle wasting in disease: molecular mechanisms and promising therapies. Nat Rev Drug Discov 14:58–74

Cohen SP, Mao J (2014) Neuropathic pain: mechanisms and their clinical implications. BMJ 348:f7656–f7656

Colloca L, Ludman T, Bouhassira D, Baron R, Dickenson AH, Yarnitsky D, Freeman R, Truini A, Attal N, Finnerup NB, Eccleston C, Kalso E, Bennett DL, Dworkin RH, Raja SN (2017) Neuropathic pain. Nat Rev Dis Prim 3:17002 A

Colonna M, Butovsky O (2017) Microglia Function in the Central Nervous System During Health and Neurodegeneration. :441–468.

Compagnucci C, Piemonte F, Sferra A, Piermarini E, Bertini E (2016) The cytoskeletal arrangements necessary to neurogenesis. Oncotarget 5

Conforti L, Dell'Agnello C, Calvaresi N, Tortarolo M, Giorgini A, Coleman MP, Bendotti C (2003) Kif1Bbeta isoform is enriched in motor neurons but does not change in a mouse model of amyotrophic lateral sclerosis. J Neurosci Res 71:732–739

Consonni S, Leone S, Becchetti A, Amadeo A (2009) Developmental and neurochemical features of cholinergic neurons in the murine cerebral cortex. BMC Neurosci 10:18

Cooper EC, Jan LY (1999) Ion channel genes and human neurological disease: Recent progress, prospects, and challenges. Proc Natl Acad Sci U S A 96:4759–4766

Crain SM, Peter ER (1967) No Title. 6:750–762.

Daly CA, Payne SH, Seiler JG (2016) Severe Brachial Plexus Injuries in American Football. Orthopedics 39:e1188–e1192.

Datan E, Shirazian A, Benjamin S, Matassov D, Tinari A, Malorni W, Lockshin RA, Garcia-Sastre A, Zakeri Z (2014) mTOR/p70S6K signaling distinguishes routine, maintenance-level autophagy from autophagic cell death during influenza A infection. Virology 0:175–190

de Mingo A, de Gregorio E, Moles A, Tarrats N, Tutusaus A, Colell A, Fernandez-Checa JC, Morales A, Mari M (2016) Cysteine cathepsins control hepatic NF-kappaB-dependent inflammation via sirtuin-1 regulation. Cell Death Dis 7:e2464.

De Vos KJ, Hafezparast M (2017) Neurobiology of axonal transport defects in motor neuron diseases: Opportunities for translational research? Neurobiol Dis

Deckwerth TL, Elliott JL, Knudson CM, Johnson EM, Snider WD, Korsmeyer SJ (1996) BAX is required for neuronal death after trophic factor deprivation and during development. Neuron 17:401–411

Deumens R, Bozkurt A, Meek MF, Marcus MAE, Joosten EAJ, Weis J, Brook GA (2010) Repairing injured peripheral nerves: Bridging the gap. Prog Neurobiol 92:245–276

Dijkers PF, Medema RH, Lammers JW, Koenderman L, Coffer PJ (2000) Expression of the pro-apoptotic Bcl-2 family member Bim is regulated by the forkhead transcription factor FKHR-L1. Curr Biol 10:1201–1204.

Diodato D, Tasca G, Verrigni D, D'Amico A, Rizza T, Tozzi G, Martinelli D, Verardo M, Invernizzi F, Nasca A, Bellacchio E, Ghezzi D, Piemonte F, Dionisi-Vici C, Carrozzo R, Bertini E (2016) A novel AIFM1 mutation expands the phenotype to an infantile motor neuron disease. Eur J Hum Genet 24:463–466

Donmez G, Outeiro TF (2013) SIRT1 and SIRT2 : emerging targets in neurodegeneration. :344–352.

Duan X, Qiao M, He Z, Duan X, Qiao M, Bei F, Kim I, He Z, Sanes JR (2015) Subtype-Specific

Regeneration of Retinal Ganglion Cells following Axotomy : Effects of Osteopontin and mTOR Signaling Article Subtype-Specific Regeneration of Retinal Ganglion Cells following Axotomy : Effects of Osteopontin and mTOR Signaling. Neuron:1–13

Dubey J, Ratnakaran N, Koushika SP (2015) Neurodegeneration and microtubule dynamics: death by a thousand cuts. Front Cell Neurosci 9:343

Eggers R, Tannemaat MR, Ehlert EM, Verhaagen J (2010) A spatio-temporal analysis of motoneuron survival , axonal regeneration and neurotrophic factor expression after lumbar ventral root avulsion and implantation. 223:207–220.

Eira J, Santos C, Mendes M, Almeida M (2016) Progress in Neurobiology The cytoskeleton as a novel therapeutic target for old neurodegenerative disorders. Prog Neurobiol 141:61–82

England JD, Asbury AK (2004) Peripheral neuropathy. Lancet 363:2151–2161.

Erlanger J, Gasser HS (1930) THE ACTION POTENTIAL IN FIBERS OF SLOW CONDUCTION IN SPINAL ROOTS AND SOMATIC NERVES. Am J Physiol -- Leg Content 92:43 LP-82

Fagoe ND, van Heest J, Verhaagen J (2014) Spinal Cord Injury and the Neuron-Intrinsic Regeneration-Associated Gene Program. NeuroMolecular Med 16:799–813.

Fan J, Dawson TM, Dawson VL (2017) Cell Death Mechanisms of Neurodegeneration. Adv Neurobiol 15:403–425.

Fang XY, Zhang WM, Zhang CF, Wong WM, Li W, Wu W, Lin JH (2016) Lithium accelerates functional motor recovery by improving remyelination of regenerating axons following ventral root avulsion and reimplantation. Neuroscience 329:213–225.

Fankhauser C, Friedlander RM, Gagliardini V (2000) Prevention of nuclear localization of activated caspases correlates with inhibition of apoptosis. Apoptosis 5:117–132.

Farahpour MR, Ghayour SJ (2014) Effect of in situ delivery of acetyl-L-carnitine on peripheral nerve regeneration and functional recovery in transected sciatic nerve in rat. Int J Surg 12:1409–1415

Farhan M, Wang H, Gaur U, Little PJ, Xu J, Zheng W (2017) FOXO Signaling Pathways as Therapeutic Targets in Cancer. Int J Biol Sci 13:815–827.

Faris M, Kokot N, Latinis K, Kasibhatla S, Green DR, Koretzky GA, Nel A, Faris M, Kokot N, Latinis K, Kasibhatla S, Green DR, Koretzky GA, Nel A (2016) The c-Jun N-Terminal Kinase Cascade Plays a Role in Stress-Induced Apoptosis in Jurkat Cells by Up-Regulating Fas Ligand Expression.

Faulkner JR (2004) Reactive Astrocytes Protect Tissue and Preserve Function after Spinal Cord Injury. J Neurosci 24:2143–2155

Fels DR, Koumenis C (2006) The PERK/eIF2α/ATF4 module of the UPR in hypoxia resistance and

tumor growth. Cancer Biol Ther 5:723–728.

Figueroa-Romero C, Hur J, Bender DE, Delaney CE, Cataldo MD, Smith AL, Yung R, Ruden DM, Callaghan BC, Feldman EL (2012) Identification of Epigenetically Altered Genes in Sporadic Amyotrophic Lateral Sclerosis. PLoS One 7.

Finkbeiner S (2000) CREB Couples Neurotrophin Signals to Survival Messages. Neuron 25:11–14

Finkelstein DL, Dooley PC, Luff AR (1993) Recovery of muscle after different periods of denervation and treatments. 16:769–777.

Fossati S, Cipriani G, Moroni F, Chiarugi A (2007) Neither energy collapse nor transcription underlie in vitro neurotoxicity of poly(ADP-ribose) polymerase hyper-activation. Neurochem Int 50:203–210.

Frakes AE, Ferraiuolo L, Haidet-Phillips AM, Schmelzer L, Braun L, Miranda CJ, Ladner KJ, Bevan AK, Foust KD, Godbout JP, Popovich PG, Guttridge DC, Kaspar BK (2014) Microglia induce motor neuron death via the classical NF-kappaB pathway in amyotrophic lateral sclerosis. Neuron 81:1009–1023.

Francelle L, Lotz C, Outeiro T, Brouillet E, Merienne K (2017) Contribution of Neuroepigenetics to Huntington's Disease. Front Hum Neurosci 11:17

Francos-Quijorna I, Amo-Aparicio J, Martinez-Muriana A, Lopez-Vales R (2016) IL-4 drives microglia and macrophages toward a phenotype conducive for tissue repair and functional recovery after spinal cord injury. Glia 64:2079–2092.

Fridman JS, Lowe SW (2003) Control of apoptosis by p53. Oncogene 22:9030–9040

Frisch SM, Screaton RA (2001) Anoikis mechanisms. Curr Opin Cell Biol 13:555–562.

Frye RA (1999) Characterization of Five Human cDNAs with Homology to the Yeast SIR2 Gene : Sir2-like Proteins (Sirtuins) Metabolize NAD and May Have Protein ADP-Ribosyltransferase Activity. 279:273–279.

Fu Z, Tindall DJ (2008) FOXOs, cancer and regulation of apoptosis. Oncogene 27:2312–2319

hi Y, Hayashi Y, Minamoto T, Nakada M (2017) Biological basis and clinical study of glycogen synthase kinase- 3β-targeted therapy by drug repositioning for glioblastoma. Oncotarget 8:22811–22824.

Galluzzi L et al. (2017) Molecular definitions of autophagy and related processes. EMBO J 36:1811–1836

Galluzzi L, Pedro JMB-S, Blomgren K, Kroemer G (2016) Autophagy in acute brain injury. Nat Rev Neurosci 17:467–484

Gan L, Zheng W, Chabot JG, Unterman TG, Quirion R (2005) Nuclear/cytoplasmic shuttling of the transcription factor FoxO1 is regulated by neurotrophic factors. J Neurochem 93:1209–1219.

Gaub P, Joshi Y, Wuttke A, Naumann U, Schnichels S, Heiduschka P, Di Giovanni S (2011) The histone acetyltransferase p300 promotes intrinsic axonal regeneration. Brain 134:2134–2148.

Georgiou M, Golding JP, Loughlin AJ, Kingham PJ, Phillips JB (2015) Engineered neural tissue with aligned, differentiated adipose-derived stem cells promotes peripheral nerve regeneration across a critical sized defect in rat sciatic nerve. Biomaterials 37:242–251.

Gerace E, Pellegrini-Giampietro DE, Mannaioni FM and G (2015) Poly(ADP-Ribose)Polymerase 1 (PARP-1) Activation and Ca^{2+} Permeable α-Amino-3-Hydroxy-5-Methyl-4-Isoxazolepropionic Acid (AMPA) Channels in Post-Ischemic Brain Damage: New Therapeutic Opportunities? CNS Neurol Disord - Drug Targets 14:636–646

Geuna S, Raimondo S, Fregnan F, Haastert-Talini K, Grothe C (2016) In vitro models for peripheral nerve regeneration. Eur J Neurosci 43:287–296.

Ghavami S, Shojaei S, Yeganeh B, Ande SR, Jangamreddy JR, Mehrpour M, Christoffersson J, Chaabane W, Rezaei A, Kashani HH, Hashemi M, Owji AA, Łos MJ (2014) Progress in Neurobiology Autophagy and apoptosis dysfunction in neurodegenerative disorders. Prog Neurobiol 112:24–49

Ghosh-Roy A, Wu Z, Goncharov A, Jin Y, Chisholm AD (2010) Calcium and cyclic AMP promote axonal regeneration in Caenorhabditis elegans and require DLK-1 kinase. J Neurosci 30:3175–3183.

Ghosh AP, Klocke BJ, Ballestas ME, Roth KA (2012) CHOP potentially co-operates with FOXO3a in neuronal cells to regulate PUMA and BIM expression in response to ER stress. PLoS One 7.

Glaus SW, Johnson PJ, Mackinnon SE (2011) Clinical Strategies to Enhance Nerve Regeneration in Composite Tissue Allotransplantation. Hand Clin 27:495–509

Gobeil S, Boucher CC, Nadeau D, Poirier GG (2001) Characterization of the necrotic cleavage of poly(ADP-ribose) polymerase (PARP-1): implication of lysosomal proteases. Cell Death Differ 8:588–594

Goldie BS, Coates CJ (1992) Brachial plexus injury: a survey of incidence and referral pattern. J Hand Surg Br 17:86–88.

Gomes P, Fleming Outeiro T, Cavadas C (2015) Emerging Role of Sirtuin 2 in the Regulation of Mammalian Metabolism. Trends Pharmacol Sci 36:756–768.

González-Forero D, Moreno-López B (2014) Retrograde response in axotomized motoneurons: Nitric oxide as a key player in triggering reversion toward a dedifferentiated phenotype. Neuroscience 283:138–165.

Gottlieb TM, Leal JFM, Seger R, Taya Y, Oren M (2002) Cross-talk between Akt, p53 and Mdm2: possible implications for the regulation of apoptosis. Oncogene 21:1299–1303

Greenhalgh AD, David S (2014) Differences in the Phagocytic Response of Microglia and Peripheral Macrophages after Spinal Cord Injury and Its Effects on Cell Death. 34:6316–6322.

Grilli M, Pizzi M, Memo M, Spano P (1996) Neuroprotection by aspirin and sodium salicylate through blockade of NF-kappaB activation. Science 274:1383–1385.

Grinsell D, Keating CP (2014) Peripheral Nerve Reconstruction after Injury: A Review of Clinical and Experimental Therapies. Biomed Res Int 2014.

Gu H-Y, Chai H, Zhang J-Y, Yao Z-B, Zhou L-H, Wong W-M, Bruce IC, Wu W-T (2005) Survival, regeneration and functional recovery of motoneurons after delayed reimplantation of avulsed spinal root in adult rat. Exp Neurol 192:89–99

Gu X, Han D, Chen W, Zhang L, Lin Q, Gao J, Fanning S, Han B (2016) SIRT1-mediated FoxOs pathways protect against apoptosis by promoting autophagy in osteoblast-like MC3T3-E1 cells exposed to sodium fluoride. Oncotarget 7:1–13

Guan Z, Kuhn JA, Wang X, Colquitt B, Solorzano C, Vaman S, Guan AK, Evans-Reinsch Z, Braz J, Devor M, Abboud-Werner SL, Lanier LL, Lomvardas S, Basbaum AI (2015) Injured sensory neuron–derived CSF1 induces microglial proliferation and DAP12-dependent pain. Nat Neurosci 19:1–10

Guo W, Qian L, Zhang J, Zhang W, Morrison A, Hayes P, Wilson S, Chen T, Zhao J (2011) Sirt1 overexpression in neurons promotes neurite outgrowth and cell survival through inhibition of the mTOR signaling. J Neurosci Res 89:1723–1736.

Guzmán-Lenis M-S, Navarro X, Casas C (2009a) Selective sigma receptor agonist 2-(4-morpholinethyl)1-phenylcyclohexanecarboxylate (PRE084) promotes neuroprotection and neurite elongation through protein kinase C (PKC) signaling on motoneurons. Neuroscience 162:31–38

Guzmán-Lenis MS, Navarro X, Casas C (2009b) Drug screening of neuroprotective agents on an organotypic-based model of spinal cord excitotoxic damage. Restor Neurol Neurosci 27:335–349.

Haastert K, Grosskreutz J, Jaeckel M, Laderer C, Bufler J, Grothe C, Claus P (2005) Rat embryonic motoneurons in long-term co-culture with Schwann cells--a system to investigate motoneuron diseases on a cellular level in vitro. J Neurosci Methods 142:275–284.

Haastert K, Mauritz C, Chaturvedi S, Grothe C (2007) Human and rat adult Schwann cell cultures: fast and efficient enrichment and highly effective non-viral transfection protocol. Nat Protoc 2:99–

104.

Haberland M, Montgomery RL, Olson EN (2009) The many roles of histone deacetylases in development and physiology: implications for disease and therapy. Nat Rev Genet 10:32–42

Haenggeli C, Kato AC (2002) Differential vulnerability of cranial motoneurons in mouse models with motor neuron degeneration. Neurosci Lett 335:39–43.

Hall L, Borke R (1988) A morphometric analysis of the somata and organelles of regenerating hypoglossal motoneurons from the rat. J Neurocytol 17:835–844

HAMBURGER V, LEVI-MONTALCINI R (1949) Proliferation, differentiation and degeneration in the spinal ganglia of the chick embryo under normal and experimental conditions. J Exp Zool 111:457–501.

Haninec P, Houšťava L, Stejskal L, Dubový P (2003) Rescue of rat spinal motoneurons from avulsion-induced cell death by intrathecal administration of IGF-I and Cerebrolysin. Ann Anat 185:233–238.

Harding HP, Novoa I, Zhang Y, Zeng H, Wek R, Schapira M, Ron D (2000a) Regulated Translation Initiation Controls Stress-Induced Gene Expression in Mammalian Cells. Mol Cell 6:1099–1108.

Harding HP, Zhang Y, Bertolotti A, Zeng H, Ron D (2000b) Perk is essential for translational regulation and cell survival during the unfolded protein response. Mol Cell 5:897–904.

Harding HP, Zhang Y, Zeng H, Novoa I, Lu PD, Calfon M, Sadri N, Yun C, Popko B, Paules R, Stojdl DF, Bell JC, Hettmann T, Leiden JM, Ron D (2003) An integrated stress response regulates amino acid metabolism and resistance to oxidative stress. Mol Cell 11:619–633.

Hasegawa K, Yoshikawa K (2008) Necdin regulates p53 acetylation via Sirtuin1 to modulate DNA damage response in cortical neurons. J Neurosci 28:8772–8784

Hayashi A, Kasahara T, Iwamoto K, Ishiwata M, Kametani M, Kakiuchi C, Furuichi T, Kato T (2007) The role of brain-derived neurotrophic factor (BDNF)-induced XBP1 splicing during brain development. J Biol Chem 282:34525–34534.

He M, Ding Y, Chu C, Tang J, Xiao Q, Luo Z-G (2016) Autophagy induction stabilizes microtubules and promotes axon regeneration after spinal cord injury. Proc Natl Acad Sci 113:11324–11329

Heiman-Patterson TD, Blankenhorn EP, Sher RB, Jiang J, Welsh P, Dixon MC, Jeffrey JI, Wong P, Cox GA, Alexander GM (2015) Genetic background effects on disease onset and lifespan of the mutant dynactin p150glued mouse model of motor neuron disease. PLoS One 10:e0117848

Hernandez-Jimenez M, Hurtado O, Cuartero MI, Ballesteros I, Moraga A, Pradillo JM, McBurney MW, Lizasoain I, Moro MA (2013) Silent information regulator 1 protects the brain against cerebral

ischemic damage. Stroke 44:2333–2337.

Herrando-Grabulosa M, Mulet R, Pujol A, Mas JM, Navarro X, Aloy P, Coma M, Casas C (2016) Novel Neuroprotective Multicomponent Therapy for Amyotrophic Lateral Sclerosis Designed by Networked Systems. PLoS One 11:e0147626.

Hettich MM, Matthes F, Ryan DP, Griesche N, Schröder S, Dorn S, Krauβ S, Ehninger D (2014) The Anti-Diabetic Drug Metformin Reduces BACE1 Protein Level by Interfering with the MID1 Complex. PLoS One 9:e102420

Hetz C, Mollereau B (2014) Disturbance of endoplasmic reticulum proteostasis in neurodegenerative diseases. Nat Rev Neurosci 15:233–249

Hisahara S, Chiba S, Matsumoto H, Tanno M, Yagi H, Shimohama S, Sato M, Horio Y (2008) Histone deacetylase SIRT1 modulates neuronal differentiation by its nuclear translocation. Proc Natl Acad Sci U S A 105:15599–15604.

Hite E, Callaway TR, Davies J, Katz ME, Ruzin A, Ross HF, Kurepina N, Novick RP, Lindsay J, Novick RP, Ubeda C, Adhikari RP, Penades JR, Novick RP, Weisberg RA, Gottesman ME (2009) References and Notes 1. 323:141–144.

Hong SJ, Dawson TM, Dawson VL (2006) PARP and the Release of Apoptosis-Inducing Factor from Mitochondria BT - Poly(ADP-Ribosyl)ation. In (Bürkle A, ed), pp 103–117. Boston, MA: Springer US.

Hoshida S, Hatano M, Furukawa M, Ito M (2009) Neuroprotective effects of vitamin E on adult rat motor neurones following facial nerve avulsion. Acta Otolaryngol 129:330–336

Houtkooper RH, Pirinen E, Auwerx J (2012) Sirtuins as regulators of metabolism and healthspan. Nat Rev Mol Cell Biol 13:225–238

Htut M, Misra VP, Anand P, Birch R, Carlstedt T (2007) Motor recovery and the breathing arm after brachial plexus surgical repairs, including re-implantation of avulsed spinal roots into the spinal cord. J Hand Surg Am 32:170–178

Hu Y (2016) Axon injury induced endoplasmic reticulum stress and neurodegeneration. Neural Regen Res 11:1557–1559.

Hu Y, Park KK, Yang L, Wei X, Yang Q, Cho K-S, Thielen P, Lee A-H, Cartoni R, Glimcher LH, Chen DF, He Z (2012) Differential effects of unfolded protein response pathways on axon injury-induced death of retinal ganglion cells. Neuron 73:445–452

Ichim, Gabriel; Tait SWG (2016) A fate worse than death: apoptosis as an oncogenic process. Nat Rev Cancer 16:539–548

Ikeda K, Sakamoto T, Marubuchi S, Kawazoe Y, Terashima N, Iwasaki Y, Kinoshita M, Ono S, Nakagawa M, Watabe K (2003) Oral administration of a neuroprotective compound T-588 prevents motoneuron degeneration after facial nerve avulsion in adult rats. Amyotroph Lateral Scler Other Motor Neuron Disord 4:74–80.

Imai S, Armstrong CM, Kaeberlein M, Guarente L (2000) Transcriptional silencing and longevity protein Sir2 is an NAD-dependent histone deacetylase. Nature 403:795–800.

Isaacs J, Mallu S, Shall M, Patel G, Shah P, Shah S, Feger MA, Graham G, Pasula N (2017) Does partial muscle reinnervation preserve future re-innervation potential? Muscle Nerve:1–21

J. F. R. KERR AHWAARCurrie (1972) Apoptosis: a Basic Biological Phenomenon With Wide- Ranging Implications in Tissue Kinetics. J Intern Med 258:479–517.

Jacquier A, Delorme C, Belotti E, Juntas-Morales R, Sole G, Dubourg O, Giroux M, Maurage C-A, Castellani V, Rebelo A, Abrams A, Zuchner S, Stojkovic T, Schaeffer L, Latour P (2017) Cryptic amyloidogenic elements in mutant NEFH causing Charcot-Marie-Tooth 2 trigger aggresome formation and neuronal death. Acta Neuropathol Commun 5:55.

Jaeger S, Aloy P (2012) From protein interaction networks to novel therapeutic strategies. IUBMB Life 64:529–537

Jain P, Vig S, Datta M, Jindel D, Mathur AK, Mathur K, Sharma A (2013) Systems Biology Approach Reveals Genome to Phenome Correlation in Type 2 Diabetes. 8.

Janjic JM, Gorantla VS (2017) Peripheral Nerve Nanoimaging: Monitoring Treatment and Regeneration. AAPS J 19:1304–1316

Jeong H, Cohen DE, Cui L, Supinski a, Savas JN, Mazzulli JR, Yates 3rd JR, Bordone L, Guarente L, Krainc D (2012) Sirt1 mediates neuroprotection from mutant huntingtin by activation of the TORC1 and CREB transcriptional pathway. Nat Med 18:159–165

Jeong H, Mason SP, Barabási a L, Oltvai ZN (2001) Lethality and centrality in protein networks. Nature 411:41–42.

Jiang M et al. (2012) Neuroprotective role of Sirt1 in mammalian models of Huntington's disease through activation of multiple Sirt1 targets. Nat Med 18:153–158

Jin H, Kanthasamy A, Harischandra DS, Kondru N, Ghosh A, Panicker N, Anantharam V, Rana A, Kanthasamy AG (2014a) Histone hyperacetylation up-regulates protein kinase Cδ in dopaminergic neurons to induce cell death: Relevance to epigenetic mechanisms of neurodegeneration in Parkinson disease. J Biol Chem 289:34743–34767.

Jin H, Mimura N, Kashio M, Koseki H, Aoe T (2014b) Late-onset of spinal neurodegeneration in knock-in mice expressing a mutant BIP. PLoS One 9.

Joshi S, Ryan KM (2014) Autophagy chews Fap to promote apoptosis. Nat Cell Biol 16:23–25 .

Joza N et al. (2001) Essential role of the mitochondrial apoptosis-inducing factor in programmed cell death. Nature 410:549–554.

Jung HY, Yoo DY, Kim JW, Kim DW, Choi JH (2016) Sirtuin-2 inhibition affects hippocampal functions and sodium butyrate ameliorates the reduction in novel object memory , cell proliferation , and neuroblast differentiation. 6055:224–230.

Kachramanoglou C, Carlstedt T, Koltzenburg M, Choi D (2017) Long-Term Outcome of Brachial Plexus Reimplantation After Complete Brachial Plexus Avulsion Injury. World Neurosurg 103:28–36

Kanai Y, Okada Y, Tanaka Y, Harada a, Terada S, Hirokawa N (2000) KIF5C, a novel neuronal kinesin enriched in motor neurons. J Neurosci 20:6374–6384.

Kang H, Jung JW, Kim MK, Chung JH (2009) CK2 is the regulator of SIRT1 substrate-binding affinity, deacetylase activity and cellular response to DNA-damage. PLoS One 4:1–9.

Kang R, Zeh HJ, Lotze MT, Tang D (2011) The Beclin 1 network regulates autophagy and apoptosis. Cell Death Differ 18:571–580

Kapitein LC, Hoogenraad CC (2015) Building the Neuronal Microtubule Cytoskeleton. Neuron 87:492–506

Karalija A, Novikova LN, Orädd G, Wiberg M, Novikov LN (2016) Differentiation of Pre- and Postganglionic Nerve Injury Using MRI of the Spinal Cord. PLoS One 11:e0168807

Kaur J, Debnath J (2015) Autophagy at the crossroads of catabolism and anabolism. Nat Rev Mol Cell Biol 16:461–472

Kennedy SG, Wagner AJ, Conzen SD, Jordán J, Bellacosa A, Tsichlis PN, Hay N (1997) The PI 3-kinase/Akt signaling pathway delivers an anti-apoptotic signal. Genes Dev 11:701–713.

Kenyon C, Chang J, Gensch E, Rudner A, Tabtiang R (1993) A C. elegans mutant that lives twice as long as wild type. Nature 366:461–464.

Kharbanda S, Saxena S, Yoshida K, Pandey P, Kaneki M, Wang Q, Cheng K, Chen Y, Campbell A, Sudha T, Yuan Z, Narula J, Weichselbaum R, Nalin C, Kufe D (2000) Translocation of SAPK / JNK to Mitochondria and Interaction with Bcl-xl in Response to DNA Damage. J Biol Chem 275:322–327.

Kim D, Nguyen MD, Dobbin MM, Fischer A, Sananbenesi F, Rodgers JT, Delalle I, Baur JA, Sui G, Armour SM, Puigserver P, Sinclair DA, Tsai L-H (2007) SIRT1 deacetylase protects against neurodegeneration in models for Alzheimer's disease and amyotrophic lateral sclerosis. EMBO J 26:3169–3179

Kim MJ, Kim DW, Park JH, Kim SJ, Lee CH, Yong JI, Ryu EJ, Cho S Bin, Yeo HJ, Hyeon J, Cho S-W, Kim D-S, Son O, Park J, Han KH, Cho YS, Eum WS, Choi SY (2013) PEP-1-SIRT2 inhibits inflammatory response and oxidative stress-induced cell death via expression of antioxidant enzymes in murine macrophages. Free Radic Biol Med 63:432–445

Kiryu-Seo S, Hirayama T, Kato R, Kiyama H (2005) Noxa is a critical mediator of p53-dependent motor neuron death after nerve injury in adult mouse. J Neurosci 25:1442–1447.

Kitano H (2002) Computational systems biology. Nature 420:206–210

Klar AJ, Fogel S, Macleod K (1979) MAR1-a Regulator of the HMa and HMalpha Loci in SACCHAROMYCES CEREVISIAE. Genetics 93:37–50

Klein JA, Longo-Guess CM, Rossmann MP, Seburn KL, Hurd RE, Frankel WN, Bronson RT, Ackerman SL (2002) The harlequin mouse mutation downregulates apoptosis-inducing factor. Nature 419:367–374

Klionsky DJ et al. (2016) Guidelines for the use and interpretation of assays for monitoring autophagy (3rd edition). Autophagy 12:1–222.

Kobayashi M, Konishi H, Takai T, Kiyama H (2015) A DAP12-dependent signal promotes pro-inflammatory polarization in microglia following nerve injury and exacerbates degeneration of injured neurons. Glia 63:1073–1082.

Koike M, Shibata M, Tadakoshi M, Gotoh K, Komatsu M, Waguri S, Kawahara N, Kuida K, Nagata S, Kominami E, Tanaka K, Uchiyama Y (2008) Inhibition of autophagy prevents hippocampal pyramidal neuron death after hypoxic-ischemic injury. Am J Pathol 172:454–469.

Kole AJ, Annis RP, Deshmukh M (2013) Mature neurons: equipped for survival. Cell Death Dis 4:e689

Koliatsos VE, Price WL, Pardo CA, Price DL (1994) Ventral root avulsion: an experimental model of death of adult motor neurons. J Comp Neurol 342:35–44

Komatsu M, Waguri S, Chiba T, Murata S, Iwata J, Tanida I, Ueno T, Koike M, Uchiyama Y, Kominami E, Tanaka K (2006) Loss of autophagy in the central nervous system causes neurodegeneration in mice. Nature 441:880–884.

Kostereva N V., Wang Y, Fletcher DR, Unadkat J V., Schnider JT, Komatsu C, Yang Y, Stolz DB, Davis MR, Plock JA, Gorantla VS (2016) IGF-1 and chondroitinase ABC augment nerve regeneration after vascularized composite limb allotransplantation. PLoS One 11:1–17.

Kuang E, Wan Q, Li X, Xu H, Liu Q, Qi Y (2005) ER Ca2+ depletion triggers apoptotic signals for endoplasmic reticulum (ER) overload response induced by overexpressed reticulon 3 (RTN3/HAP). J Cell Physiol 204:549–559.

Lago N, Navarro X (2006) Correlation between Target Reinnervation and Distribution. 23:227–240.

Laing NG (2012) Genetics of neuromuscular disorders. Crit Rev Clin Lab Sci 49:33–48

Lall D, Baloh RH (2017) Microglia and C9orf72 in neuroinflammation and ALS and frontotemporal dementia. J Clin Invest 127:3250–3258.

LaMonte BH, Wallace KE, Holloway BA, Shelly SS, Ascaño J, Tokito M, Van Winkle T, Howland DS, Holzbaur ELF (2002) Disruption of dynein/dynactin inhibits axonal transport in motor neurons causing late-onset progressive degeneration. Neuron 34:715–727.

Lan X, Han X, Li Q, Yang Q, Wang J (2017) Modulators of microglial activation and polarization after intracerebral haemorrhage. Nat Rev | Neurol 13

Lance-Jones C (1982) Motoneuron cell death in the developing lumbar spinal cord of the mouse. Brain Res 256:473–479.

Latres E, Amini AR, Amini AA, Griffiths J, Martin FJ, Wei Y, Hsin CL, Yancopoulos GD, Glass DJ (2005) Insulin-like growth factor-1 (IGF-1) inversely regulates atrophy-induced genes via the phosphatidylinositol 3-kinase/Akt/mammalian target of rapamycin (PI3K/Akt/mTOR) pathway. J Biol Chem 280:2737–2744.

Lazo-Gómez R, Ramírez-Jarquín UN, Tovar-Y-Romo LB, Tapia R (2013) Histone deacetylases and their role in motor neuron degeneration. Front Cell Neurosci 7:243

Lebeaupin C, Proics E, de Bieville CHD, Rousseau D, Bonnafous S, Patouraux S, Adam G, Lavallard VJ, Rovere C, Le Thuc O, Saint-Paul MC, Anty R, Schneck AS, Iannelli A, Gugenheim J, Tran A, Gual P, Bailly-Maitre B (2015) ER stress induces NLRP3 inflammasome activation and hepatocyte death. Cell Death Dis 6:e1879

Lee D, Goldberg AL (2013) SIRT1 Protein , by Blocking the Activities of Transcription Factors FoxO1 and FoxO3 , Inhibits Muscle Atrophy and Promotes Muscle Growth *. 288:30515–30526.

Lee D, Goldberg AL (2015) Muscle wasting in fasting requires activation of NF-κB and inhibition of AKT/Mechanistic target of rapamycin (mTOR) by the protein acetylase, GCN5. J Biol Chem 290:30269–30279.

Lee MK, Xu Z, Wong PC, Cleveland DW (1993) Neurofilaments are obligate heteropolymers in vivo. J Cell Biol 122:1337–1350.

Leibinger M, Andreadaki A, Fischer D (2012) Role of mTOR in neuroprotection and axon regeneration after inflammatory stimulation. Neurobiol Dis 46:314–324

Levi-Montalcini R, Booker B (1960) DESTRUCTION OF THE SYMPATHETIC GANGLIA IN MAMMALS BY AN ANTISERUM TO A NERVE-GROWTH PROTEIN. Proc Natl Acad Sci U S A 46:384–391.

Li H, Wong C, Li W, Ruven C, He L, Wu X, Lang BT (2015) Enhanced regeneration and functional recovery after spinal root avulsion by manipulation of the proteoglycan receptor PTP σ. Nat Publ Gr:1–14

Li L, Houenou LJ, Wu W, Lei M, Prevette DM, Oppenheim RW (1998) Characterization of spinal motoneuron degeneration following different types of peripheral nerve injury in neonatal and adult mice. J Comp Neurol 396:158–168.

Li S, Yang L, Selzer ME, Hu Y (2013a) Neuronal endoplasmic reticulum stress in axon injury and neurodegeneration. Ann Neurol 74:768–777.

Li S, Yang L, Selzer ME, Hu Y (2013b) Neuronal endoplasmic reticulum stress in axon injury and neurodegeneration. Ann Neurol 74:768–777

Li X, Chen C, Tu Y, Sun H (2013c) Sirt1 Promotes Axonogenesis by Deacetylation of Akt and Inactivation of GSK3. 3:490–499.

Li Y-H, Fu H-L, Tian M-L, Wang Y-Q, Chen W, Cai L-L, Zhou X-H, Yuan H-B (2016) Neuron-derived FGF10 ameliorates cerebral ischemia injury via inhibiting NF-κB-dependent neuroinflammation and activating PI3K/Akt survival signaling pathway in mice. Sci Rep 6:19869

Li YY, Jones SJ (2012) Drug repositioning for personalized medicine. Genome Med 4:27

Liddelow SA et al. (2017) Neurotoxic reactive astrocytes are induced by activated microglia. Nature 541:481–487.

Lin A, Yao J, Zhuang L, Wang D, Han J, Lam EW-F, Gan B (2014) The FoxO-BNIP3 axis exerts a unique regulation of mTORC1 and cell survival under energy stress. Oncogene 33:3183–3194.

Lin J, Sun B, Jiang C, Hong H, Zheng Y (2013) Sirt2 suppresses inflammatory responses in collagen-induced arthritis. Biochem Biophys Res Commun 441:897–903

Lindholm D, Wootz H, Korhonen L (2006) ER stress and neurodegenerative diseases. Cell Death Differ 13:385–392

Liu CM, Wang RY, Saijilafu, Jiao ZX, Zhang BY, Zhou FQ (2013a) MicroRNA-138 and SIRT1 form a mutual negative feedback loop to regulate mammalian axon regeneration. Genes Dev 27:1473–1483.

Liu D, Zhang M, Yin H (2013b) Signaling pathways involved in endoplasmic reticulum stress-induced neuronal apoptosis. Int J Neurosci 123:155–162

Liu G, Su L, Hao X, Zhong N, Zhong D, Singhal S, Liu X (2012a) Salermide up-regulates death receptor 5 expression through the ATF4-ATF3-CHOP axis and leads to apoptosis in human cancer cells.

J Cell Mol Med 16:1618–1628.

Liu Z, Cai H, Zhang P, Li H, Liu H, Li Z (2012b) Activation of ERK1/2 and PI3K/Akt by IGF-1 on GAP-43 expression in DRG neurons with excitotoxicity induced by glutamate in vitro. Cell Mol Neurobiol 32:191–200.

Loane DJ, Byrnes KR (2010) Role of Microglia in Neurotrauma. Neurotherapeutics 7:366–377.

Lock R, Debnath J (2008) Extracellular matrix regulation of autophagy. Curr Opin Cell Biol 20:583–588

Loos B, du Toit A, Hofmeyr J-HS (2014) Defining and measuring autophagosome flux-concept and reality. Autophagy 10:2087–2096.

Louessard M, Bardou I, Lemarchand E, Thiebaut AM, Parcq J, Leprince J, Terrisse A, Carraro V, Fafournoux P, Bruhat A, Orset C, Vivien D, Ali C, Roussel BD (2017) Activation of cell surface GRP78 decreases endoplasmic reticulum stress and neuronal death. Cell Death Differ 24:1518–1529

Lowrie MB, Lavalette D, Davies CE (1994) Time Course of Motoneurone Death after Neonatal Sciatic Nerve Crush in the Rat. Dev Neurosci 16:279–284

Lowry K, Quach H, Wreford N, Cheema SS (2001) There is no loss of motor neurons in the rat spinal cord during postnatal maturation. J Anat 198:473–479

Lu P, Kamboj A, Gibson SB, Anderson CM (2014) Poly(ADP-Ribose) Polymerase-1 Causes Mitochondrial Damage and Neuron Death Mediated by Bnip3. J Neurosci 34:15975–15987

Luchting B, Rachinger-Adam B, Heyn J, Hinske LC, Kreth S, Azad SC (2015) Anti-inflammatory T-cell shift in neuropathic pain. J Neuroinflammation 12:12

Luo C, Ouyang M, Fang Y, Li S, Zhou Q, Fan J (2017) Dexmedetomidine Protects Mouse Brain from Ischemia-Reperfusion Injury via Inhibiting Neuronal Autophagy through Up-Regulating HIF-1 α. 11:1–13.

Luo J, Nikolaev AY, Imai S, Chen D, Su F, Shiloh A, Guarente L, Gu W (2001a) Negative control of p53 by Sir2alpha promotes cell survival under stress. Cell 107:137–148

Luo J, Nikolaev AY, Imai S, Chen D, Su F, Shiloh A, Guarente L, Gu W (2001b) Negative control of p53 by Sir2alpha promotes cell survival under stress. Cell 107:137–148.

Luo L (2002) Actin Cytoskeleton Regulation in Neuronal Morphogenesis and Structural Plasticity. Annu Rev Cell Dev Biol 18:601–635.

Lv C, Hu H-Y, Zhao L, Zheng H, Luo X-Z, Zhang J (2015) Intrathecal SRT1720, a SIRT1 agonist, exerts anti-hyperalgesic and anti-inflammatory effects on chronic constriction injury-induced

neuropathic pain in rats. Int J Clin Exp Med 8:7152–7159.

M. Gingras, M. Beaulieu, V. Gagnon, H, D. Durham and FB (2009) In Vitro Study of Axonal Migration and Myelination of Motor Neurons in a Three-Dimensional Tissue-Engineered Model. Glia 56:354–364.

Ma Y, Hendershot LM (2003) Delineation of a negative feedback regulatory loop that controls protein translation during endoplasmic reticulum stress. J Biol Chem 278:34864–34873.

MacDonald R, Barbat-Artigas S, Cho C, Peng H, Shang J, Moustaine A, Carbonetto S, Robitaille R, Chalifour LE, Paudel H (2017) A Novel Egr-1-Agrin Pathway and Potential Implications for Regulation of Synaptic Physiology and Homeostasis at the Neuromuscular Junction. Front Aging Neurosci 9:1–18

Magnuson B, Ekim B, Fingar DC (2012) Regulation and function of ribosomal protein S6 kinase (S6K) within mTOR signalling networks. Biochem J 441:1–21

Maiuri MC, Zalckvar E, Kimchi A, Kroemer G (2007) Self-eating and self-killing: crosstalk between autophagy and apoptosis. Nat Rev Mol Cell Biol 8:741–752

Mammucari C, Milan G, Romanello V, Masiero E, Rudolf R, Del Piccolo P, Burden SJ, Di Lisi R, Sandri C, Zhao J, Goldberg AL, Schiaffino S, Sandri M (2007) FoxO3 Controls Autophagy in Skeletal Muscle In Vivo. Cell Metab 6:458–471.

Man SM, Kanneganti T-D (2016) Converging roles of caspases in inflammasome activation, cell death and innate immunity TL - 16. Nat Rev Immunol 16 VN-r:7–21

Mancuso R, Santos-Nogueira E, Osta R, Navarro X (2011) Electrophysiological analysis of a murine model of motoneuron disease. Clin Neurophysiol 122:1660–1670.

Mandolesi G, Madeddu F, Bozzi Y, Maffei L, Ratto GM (2004) Acute physiological response of mammalian central neurons to axotomy: ionic regulation and electrical activity. FASEB J 18:1934–1936.

Maria E. Giannakou and Linda Partridge (2004) The interaction between FOXO and SIRT1: tipping the balance towards survival. Trends Cell Biol 14:408–412.

Marinelli S, Nazio F, Tinari A, Ciarlo L, D'Amelio M, Pieroni L, Vacca V, Urbani A, Cecconi F, Malorni W, Pavone F (2014) Schwann cell autophagy counteracts the onset and chronification of neuropathic pain. Pain 155:93–107.

Marino G, Niso-Santano M, Baehrecke EH, Kroemer G (2014) Self-consumption: the interplay of autophagy and apoptosis. Nat Rev Mol Cell Biol 15:81–94

Martin LJ, Kaiser A, Price AC (1999) Motor neuron degeneration after sciatic nerve avulsion in adult

rat evolves with oxidative stress and is apoptosis. J Neurobiol 40:185–201.

Martin LJ, Liu Z (2002) Injury-induced spinal motor neuron apoptosis is preceded by DNA single-strand breaks and is p53- and Bax-dependent. J Neurobiol 50:181–197.

Martinez FO, Gordon S (2014) The M1 and M2 paradigm of macrophage activation: time for reassessment. F1000Prime Rep 6:13

Masiero E, Agatea L, Mammucari C, Blaauw B, Loro E, Komatsu M, Metzger D, Reggiani C, Schiaffino S, Sandri M (2009) Autophagy Is Required to Maintain Muscle Mass. Cell Metab 10:507–515

Mattson MP, Meffert MK (2006) Roles for NF-κB in nerve cell survival, plasticity, and disease. Cell Death Differ 13:852–860

Maxwell MM, Tomkinson EM, Nobles J, Wizeman JW, Amore AM, Quinti L, Chopra V, Hersch SM, Kazantsev AG (2011) The Sirtuin 2 microtubule deacetylase is an abundant neuronal protein that accumulates in the aging CNS. Hum Mol Genet 20:3986–3996.

Mayr B, Montminy M (2001) Transcriptional regulation by the phosphorylation-dependent factor CREB. Nat Rev Mol Cell Biol 2:599–609

McCarty KS, McCarty Kenneth S. J (1974) Protein Modification, Metabolic Controls, and Their Significance in Transformation in Eukaryotic Cells1. JNCI J Natl Cancer Inst 53:1509–1514

Menu P, Mayor A, Zhou R, Tardivel A, Ichijo H, Mori K, Tschopp J (2012) ER stress activates the NLRP3 inflammasome via an UPR-independent pathway. Cell Death Dis 3:e261

Menzies FM, Fleming A, Rubinsztein DC (2015) Compromised autophagy and neurodegenerative diseases. Nat Rev Neurosci 16:345–357

Mestres J, Gregori-Puigjané E, Valverde S, Solé R V (2009) The topology of drug-target interaction networks: implicit dependence on drug properties and target families. Mol Biosyst 5:1051–1057.

Meusser B, Hirsch C, Jarosch E, Sommer T (2005) ERAD: The long road to destruction. Nat Cell Biol 7:766–772

Meyer C, Stenberg L, Gonzalez-Perez F, Wrobel S, Ronchi G, Udina E, Suganuma S, Geuna S, Navarro X, Dahlin LB, Grothe C, Haastert-Talini K (2016) Chitosan-film enhanced chitosan nerve guides for long-distance regeneration of peripheral nerves. Biomaterials 76:33–51.

Michaelevski I, Segal-Ruder Y, Rozenbaum M, Medzihradszky KF, Shalem O, Coppola G, Horn-Saban S, Ben-Yaakov K, Dagan SY, Rishal I, Geschwind DH, Pilpel Y, Burlingame AL, Fainzilber M (2010) Signaling to Transcription Networks in the Neuronal Retrograde Injury Response. Sci Signal 3

Michaelidis TM, Sendtner M, Cooper JD, Airaksinen MS, Holtmann B, Meyer M, Thoenen H (1996) Inactivation of bcl-2 results in progressive degeneration of motoneurons, sympathetic and sensory neurons during early postnatal development. Neuron 17:75–89.

Michishita E, Park JY, Burneskis JM, Barrett JC, Horikawa I (2005) Evolutionarily conserved and nonconserved cellular localizations and functions of human SIRT proteins. Mol Biol Cell 16:4623–4635.

Millecamps S, Julien J-P (2013) Axonal transport deficits and neurodegenerative diseases. Nat Rev Neurosci 14:161–176

Mills C, Makwana M, Wallace A, Benn S, Schmidt H, Tegeder I, Costigan M, Brown RH, Raivich G, Woolf CJ (2008) Ro5-4864 promotes neonatal motor neuron survival and nerve regeneration in adult rats. Eur J Neurosci 27:937–946.

Misawa T, Takahama M, Kozaki T, Lee H, Zou J, Saitoh T, Akira S (2013) Microtubule-driven spatial arrangement of mitochondria promotes activation of the NLRP3 inflammasome. Nat Immunol 14:454–460

Miura M (2011) Apoptotic and non-apoptotic caspase functions in neural development. Neurochem Res 36:1253–1260.

Mojsilovic-Petrovic J, Nedelsky N, Boccitto M, Mano I, Georgiades SN, Zhou W, Liu Y, Neve RL, Taylor JP, Driscoll M, Clardy J, Merry D, Kalb RG (2009) FOXO3a Is Broadly Neuroprotective In Vitro and In Vivo against Insults Implicated in Motor Neuron Diseases. J Neurosci 29:8236–8247

Moon J-H, Lee J-H, Nazim UM, Lee Y-J, Seol J-W, Eo S-K, Lee J-H, Park S-Y (2016) Human prion protein-induced autophagy flux governs neuron cell damage in primary neuron cells. Oncotarget 7:29989–30002.

Morales FR, Boxer PA, Fung SJ, Chase MH (1987) Basic electrophysiological properties of spinal cord motoneurons during old age in the cat. J Neurophysiol 58:180 LP-194

Moriya S, Hasegawa M, Inamasu J, Kogame H, Hirose Y, Higashi R, Ito M, Imai F (2017) Neuroprotective effects of pregabalin in a rat model of intracisternal facial nerve avulsion. J Neurosurg Sci 61:495–503.

Motta MC, Divecha N, Lemieux M, Kamel C, Chen D, Gu W, Bultsma Y, McBurney M, Guarente L (2004) Mammalian SIRT1 Represses Forkhead Transcription Factors. Cell 116:551–563.

Mouchiroud L, Houtkooper RH, Moullan N, Katsyuba E, Ryu D, Cantó C, Mottis A, Jo YS, Viswanathan M, Schoonjans K, Guarente L, Auwerx J (2013) XThe NAD+/sirtuin pathway modulates longevity through activation of mitochondrial UPR and FOXO signaling. Cell 154.

Mueller BKL et al. (2016) Inflammatory neuroprotection following traumatic brain injury. Sci Press

353:168–175.

Nahm M, Lee M-J, Parkinson W, Lee M, Kim H, Kim Y-J, Kim S, Cho YS, Min B-M, Bae YC, Broadie K, Lee S (2013) Spartin Regulates Synaptic Growth and Neuronal Survival by Inhibiting BMP-Mediated Microtubule Stabilization. Neuron 77:10.1016/j.neuron.2012.12.015

Najafi A, Masoudi-nejad A, Ghanei M, Nourani M, Moeini A (2014) Pathway Reconstruction of Airway Remodeling in Chronic Lung Diseases : A Systems Biology Approach. 9:1–10.

Naranjo JR, Zhang H, Villar D, Gonzalez P, Dopazo XM, Moron-Oset J, Higueras E, Oliveros JC, Arrabal MD, Prieto A, Cercos P, Gonzalez T, De la Cruz A, Casado-Vela J, Rabano A, Valenzuela C, Gutierrez-Rodriguez M, Li J-Y, Mellstrom B (2016) Activating transcription factor 6 derepression mediates neuroprotection in Huntington disease. J Clin Invest 126:627–638.

Naser P V, Kuner R (2017) Molecular, cellular and circuit basis of cholinergic modulation of pain. Neuroscience

Navarro X (2016) Functional evaluation of peripheral nerve regeneration and target reinnervation in animal models : a critical overview. 43:271–286.

Navarro X, Udina E, Ceballos D, Gold BG (2001) Effects of FK506 on nerve regeneration and reinnervation after graft or tube repair of long nerve gaps. Muscle Nerve 24:905–915.

Navarro X, Vivó M, Valero-Cabré A (2007) Neural plasticity after peripheral nerve injury and regeneration. Prog Neurobiol 82:163–201.

Nelson AD, Jenkins PM (2017) Axonal Membranes and Their Domains: Assembly and Function of the Axon Initial Segment and Node of Ranvier. Front Cell Neurosci 11:136

Nimmagadda VK, Bever CT, Vattikunta NR, Talat S, Ahmad V, Nagalla NK, Trisler D, Judge SI V, Royal W 3rd, Chandrasekaran K, Russell JW, Makar TK (2013) Overexpression of SIRT1 protein in neurons protects against experimental autoimmune encephalomyelitis through activation of multiple SIRT1 targets. J Immunol 190:4595–4607.

Nishitoh H, Matsuzawa A, Tobiume K, Saegusa K, Takeda K, Inoue K, Hori S, Kakizuka A, Ichijo H (2002) ASK1 is essential for endoplasmic reticulum stress-induced neuronal cell death triggered by expanded polyglutamine repeats. Genes Dev 16:1345–1355.

Noble J, Munro CA, Prasad VS, Midha R (1998) Analysis of upper and lower extremity peripheral nerve injuries in a population of patients with multiple injuries. J Trauma 45:116–122

Nogradi A, Vrbova G (2001) The effect of riluzole treatment in rats on the survival of injured adult and grafted embryonic motoneurons. Eur J Neurosci 13:113–118.

Noguchi M, Hirata N, Suizu F (2014) The links between AKT and two intracellular proteolytic

cascades: Ubiquitination and autophagy. Biochim Biophys Acta - Rev Cancer 1846:342–352.

Noguchi T, Ohta S, Kakinoki R, Ikeguchi R, Kaizawa Y, Oda H, Matsuda S (2015) The neuroprotective effect of erythropoietin on spinal motor neurons after nerve root avulsion injury in rats. Restor Neurol Neurosci 33:461–470.

North BJ, Marshall BL, Borra MT, Denu JM, Verdin E, Francisco S (2003) The Human Sir2 Ortholog, SIRT2, Is an NAD+-Dependent Tubulin Deacetylase Brian. Mol Cell 11:437–444.

Nozaki S, Sledge Jr GW, Nakshatri H (2001) Repression of GADD153/CHOP by NF-kappaB: a possible cellular defense against endoplasmic reticulum stress-induced cell death. Oncogene 20:2178–2185

Ohtake Y, Park D, Abdul-Muneer PM, Li H, Xu B, Sharma K, Smith GM, Selzer ME, Li S (2014) The effect of systemic PTEN antagonist peptides on axon growth and functional recovery after spinal cord injury. Biomaterials 35:4610–4626

Okada S, Nakamura M, Katoh H, Miyao T, Shimazaki T, Ishii K, Yamane J, Yoshimura A, Iwamoto Y, Toyama Y, Okano H (2006) Conditional ablation of Stat3 or Socs3 discloses a dual role for reactive astrocytes after spinal cord injury. Nat Med 12:829–834.

Oliveira a. LR, Langone F (2000) GM-1 ganglioside treatment reduces motoneuron death after ventral root avulsion in adult rats. Neurosci Lett 293:131–134.

Oliveira AL, Risling M, Deckner M, Lindholm T, Langone F, Cullheim S (1997) Neonatal sciatic nerve transection induces TUNEL labeling of neurons in the rat spinal cord and DRG. Neuroreport 8:2837–2840.

Olmos-Alonso A, Schetters STT, Sri S, Askew K, Mancuso R, Vargas-Caballero M, Holscher C, Perry VH, Gomez-Nicola D (2016) Pharmacological targeting of CSF1R inhibits microglial proliferation and prevents the progression of Alzheimer's-like pathology. Brain 139:891–907

Olsson T, Piehl F, Swanberg M, Lidman O (2005) Genetic dissection of neurodegeneration and CNS inflammation. J Neurol Sci 233:99–108.

Oñate M, Catenaccio A, Martínez G, Armentano D, Parsons G, Kerr B, Hetz C, Court FA (2016) Activation of the unfolded protein response promotes axonal regeneration after peripheral nerve injury. Sci Rep 6:21709

Oppenheim RW (1996) Neurotrophic survival molecules for motoneurons: An embarrassment of riches. Neuron 17:195–197.

Outeiro TF, Kontopoulos E, Altmann SM, Kufareva I, Strathearn KE, Amore AM, Volk CB, Maxwell MM, Rochet J-C, McLean PJ, Young AB, Abagyan R, Feany MB, Hyman BT, Kazantsev AG (2007) Sirtuin 2 inhibitors rescue alpha-synuclein-mediated toxicity in models of Parkinson's disease.

Science 317:516–519.

Pais TF, Marques O, Miller-fleming L, Antas P, Oliveira RM De, Kasapoglu B, Outeiro TF (2013) The NAD-dependent deacetylase sirtuin 2 is a suppressor of microglial activation and brain. :2603–2616.

Pareyson D, Saveri P, Sagnelli A, Piscosquito G (2015) Mitochondrial dynamics and inherited peripheral nerve diseases. Neurosci Lett 596:66–77.

Park KK, Liu K, Hu Y, Smith PD, Wang C, Cai B, Xu B, Connolly L, Kramvis I, Sahin M, He Z (2008) Promoting axon regeneration in the adult CNS by modulation of the PTEN/mTOR pathway. Science 322:963–966

Park O, Lee KJ, Rhyu IJ, Geum D, Kim H, Buss R, Oppenheim RW, Sun W (2007) Bax-dependent and -independent death of motoneurons after facial nerve injury in adult mice. Eur J Neurosci 26:1421–1432

Penas C, Casas C, Robert I, Fores J, Navarro X (2009a) Cytoskeletal and activity-related changes in spinal motoneurons after root avulsion. J Neurotrauma 26:763–779.

Penas C, Font-Nieves M, Forés J, Petegnief V, Planas a, Navarro X, Casas C (2011a) Autophagy, and BiP level decrease are early key events in retrograde degeneration of motoneurons. Cell Death Differ 18:1617–1627

Penas C, Pascual-Font A, Mancuso R, Forés J, Casas C, Navarro X (2011b) Sigma receptor agonist 2-(4-morpholinethyl)1 phenylcyclohexanecarboxylate (Pre084) increases GDNF and BiP expression and promotes neuroprotection after root avulsion injury. J Neurotrauma 28:831–840

Perdan K, Lipnik-Štangelj M, Kržan M (2009) Chapter 8 The Impact of Astrocytes in the Clearance of Neurotransmitters by Uptake and Inactivation. Adv Planar Lipid Bilayers Liposomes 9:211–235.

Perera S, Artigas L, Mulet R, Mas JM, Sardón T (2014) Systems biology applied to non-alcoholic fatty liver disease (NAFLD): treatment selection based on the mechanism of action of nutraceuticals. Nutrafoods 13:61–68.

Perrelet D, Ferri A, Liston P, Muzzin P, Korneluk RG, Kato AC (2002) IAPs are essential for GDNF-mediated neuroprotective effects in injured motor neurons in vivo. Nat Cell Biol 4:175–179

Perrelet D, Perrin FE, Liston P, Korneluk RG, MacKenzie A, Ferrer-Alcon M, Kato AC (2004) Motoneuron resistance to apoptotic cell death in vivo correlates with the ratio between X-linked inhibitor of apoptosis proteins (XIAPs) and its inhibitor, XIAP-associated factor 1. J Neurosci 24:3777–3785.

Petegnief V, Planas AM (2013) SIRT1 regulation modulates stroke outcome. Transl Stroke Res 4:663–671.

Pfister JA, Ma C, Morrison BE, D'Mello SR (2008) Opposing effects of sirtuins on neuronal survival: SIRT1-mediated neuroprotection is independent of its deacetylase activity. PLoS One 3:1–8.

Pintér S, Gloviczki B, Szabó A, Márton G, Nógrádi A (2010) Increased survival and reinnervation of cervical motoneurons by riluzole after avulsion of the C7 ventral root. J Neurotrauma 27:2273–2282.

Pocock JM, Kettenmann H (2007) Neurotransmitter receptors on microglia. Trends Neurosci 30:527–535.

Pondaag W, A Malessy MJ, Gert van Dijk J, W M Thomeer RT (2004) Natural history of obstetric brachial plexus palsy: a systematic review. Dev Med Child Neurol 2004, 46:138–144

Portt L, Norman G, Clapp C, Greenwood M, Greenwood MT (2011) Anti-apoptosis and cell survival: A review. Biochim Biophys Acta - Mol Cell Res 1813:238–259

Prell T, Lautenschläger J, Weidemann L, Ruhmer J, Witte OW, Grosskreutz J (2014) Endoplasmic reticulum stress is accompanied by activation of NF-κB in amyotrophic lateral sclerosis. J Neuroimmunol 270:29–36

Presnell SR, Cohen FE (1993) Artificial neural networks for pattern recognition in biochemical sequences. Structure:283–298.

Pujol A, Mosca R, Farrés J, Aloy P (2010) Unveiling the role of network and systems biology in drug discovery. Trends Pharmacol Sci 31:115–123.

Puttagunta R, Tedeschi A, Sória MG, Hervera A, Lindner R, Rathore KI, Gaub P, Joshi Y, Nguyen T, Schmandke A, Laskowski CJ, Boutillier A-L, Bradke F, Di Giovanni S (2014) PCAF-dependent epigenetic changes promote axonal regeneration in the central nervous system. Nat Commun 5:3527

Pyun K, Son JS, Kwon YB (2014) Chronic activation of sigma-1 receptor evokes nociceptive activation of trigeminal nucleus caudalis in rats. Pharmacol Biochem Behav 124C:278–283.

Qiao C, Zhang LX, Sun XY, Ding JH, Lu M, Hu G (2016) Caspase-1 Deficiency Alleviates Dopaminergic Neuronal Death via Inhibiting Caspase-7/AIF Pathway in MPTP/p Mouse Model of Parkinson's Disease. Mol Neurobiol:1–11.

Qu W, Tian D, Guo Z, Fang J, Zhang Q, Yu Z, Xie M, Zhang H, Lü J, Wang W (2012) Inhibition of EGFR/MAPK signaling reduces microglial inflammatory response and the associated secondary damage in rats after spinal cord injury. J Neuroinflammation 9:178

Rafalski VA, Ho PP, Brett JO, Ucar D, Dugas JC, Pollina EA, Chow LML, Ibrahim A, Baker SJ, Barres BA, Steinman L, Brunet A (2013) Expansion of oligodendrocyte progenitor cells following SIRT1 inactivation in the adult brain. Nat Cell Biol 15:614–624.

Raff MC, Barres BA, Burne JF, Coles HS, Ishizaki Y, Jacobson MD (1993) Programmed cell death and the control of cell survival: lessons from the nervous system. Science 262:695–700.

Rahman A, Haugh JM (2017) Kinetic Modeling and Analysis of the Akt/Mechanistic Target of Rapamycin Complex 1 (mTORC1) Signaling Axis Reveals Cooperative, Feedforward Regulation. J Biol Chem 292:jbc.M116.761205

Ramadori G, Coppari R (2010) Pharmacological Manipulations of CNS Sirtuins: Potential Effects on Metabolic Homeostasis. Pharmacol Res 62:48–54

Rami A, Bechmann I, Stehle JH (2008) Exploiting endogenous anti-apoptotic proteins for novel therapeutic strategies in cerebral ischemia. Prog Neurobiol 85:273–296.

Ransome MI, Turnley AM (2008) Erythropoietin promotes axonal growth in a model of neuronal polarization. Mol Cell Neurosci 38:537–547.

Ravikumar B, Acevedo-Arozena A, Imarisio S, Berger Z, Vacher C, O'Kane CJ, Brown SDM, Rubinsztein DC (2005) Dynein mutations impair autophagic clearance of aggregate-prone proteins. Nat Genet 37:771–776.

Ray Chaudhuri A, Nussenzweig A (2017) The multifaceted roles of PARP1 in DNA repair and chromatin remodelling. Nat Publ Gr

Rishal I, Fainzilber M (2014) Axon-soma communication in neuronal injury. Nat Rev Neurosci 15:32–42

Rivieccio MA, Brochier C, Willis DE, Walker BA, D'Annibale MA, McLaughlin K, Siddiq A, Kozikowski AP, Jaffrey SR, Twiss JL, Ratan RR, Langley B (2009) HDAC6 is a target for protection and regeneration following injury in the nervous system. Proc Natl Acad Sci U S A 106:19599–19604

Rizzo F, Ronchi D, Salani S, Nizzardo M, Fortunato F, Bordoni A, Stuppia G, Del Bo R, Piga D, Fato R, Bresolin N, Comi GP, Corti S (2016) Selective mitochondrial depletion, apoptosis resistance, and increased mitophagy in human Charcot-Marie-Tooth 2A motor neurons. Hum Mol Genet 25:4266–4281.

Robberecht W, Philips T (2013) The changing scene of amyotrophic lateral sclerosis. Nat Rev Neurosci 14:1–17

Roh D-H, Choi S-R, Yoon S-Y, Kang S-Y, Moon J-Y, Kwon S-G, Han H-J, Beitz AJ, Lee J-H (2011) Spinal nNOS activation mediates sigma-1 receptor-induced mechanical and thermal hypersensitivity

in mice: involvement of PKC-dependent NR1 phosphorylation. Br J Pharmacol.

Rokudai S, Fujita N, Hashimoto Y, Tsuruo T (2000) Cleavage and inactivation of antiapoptotic Akt/PKB by caspases during apoptosis. J Cell Physiol 182:290–296.

Rommel C, Bodine SC, Clarke B a, Rossman R, Nunez L, Stitt TN, Yancopoulos GD, Glass DJ (2001) Mediation of IGF-1-induced skeletal myotube hypertrophy by PI(3)K/Akt/mTOR and PI(3)K/Akt/GSK3 pathways. Nat Cell Biol 3:1009–1013.

Rothgiesser KM, Erener S, Waibel S, Lüscher B, Hottiger MO (2010) SIRT2 regulates NF-κB dependent gene expression through deacetylation of p65 Lys310. J Cell Sci 123:4251–4258

Ruschel J, Hellal F, Flynn KC, Dupraz S, Elliott DA, Tedeschi A, Bates M, Sliwinski C, Brook G, Dobrindt K, Peitz M, Brüstle O, Norenberg MD, Blesch A, Weidner N, Bunge MB, Bixby JL, Bradke F (2015) Systemic administration of epothilone B promotes axon regeneration after spinal cord injury. Science (80-) 348:347 LP-352

Russell RC, Tian Y, Yuan H, Park HW, Chang Y-Y, Kim J, Kim H, Neufeld TP, Dillin A, Guan K-L (2013) ULK1 induces autophagy by phosphorylating Beclin-1 and activating VPS34 lipid kinase. Nat Cell Biol 15:741–750

S. E. Mackinnon and A. L. Dellon (1988) “Nerve repair and grafts,.” Surg Peripher Nerve.

Saitoh Y, Fujikake N, Okamoto Y, Popiel HA, Hatanaka Y, Ueyama M, Suzuki M, Gaumer S, Murata M, Wada K, Nagai Y (2015) p62 plays a protective role in the autophagic degradation of polyglutamine protein oligomers in polyglutamine disease model flies. J Biol Chem 290:1442–1453.

Sakuma M, Gorski G, Sheu SH, Lee S, Barrett LB, Singh B, Omura T, Latremoliere A, Woolf CJ (2016) Lack of motor recovery after prolonged denervation of the neuromuscular junction is not due to regenerative failure. Eur J Neurosci 43:451–462.

Sandri M, Sandri C, Gilbert A, Skurk C, Calabria E, Picard A, Walsh K, Schiaffino S, Lecker SH, Goldberg AL (2004) Foxo transcription atrophy 2004 Sandri. 117:399–412.

Santos ARC, Corredor RG, Obeso BA, Trakhtenberg EF, Wang Y, Ponmattam J, Dvoriantchikova G, Ivanov D, Shestopalov VI, Goldberg JL, Fini ME, Bajenaru ML (2012) β1 Integrin-Focal Adhesion Kinase (FAK) Signaling Modulates Retinal Ganglion Cell (RGC) Survival. PLoS One 7.

Sarkar C, Zhao Z, Aungst S, Sabirzhanov B, Faden AI, Lipinski MM (2014) Impaired autophagy flux is associated with neuronal cell death after traumatic brain injury. Autophagy 10:2208–2222.

Schiaffino S, Mammucari C (2011) Regulation of skeletal muscle growth by the IGF1-Akt / PKB pathway : insights from genetic models. :1–14.

Schröder M, Kaufman RJ (2005) the Mammalian Unfolded Protein Response. Annu Rev Biochem 74:739–789

Scorisa JM, Zanon RG, Freria CM, Leite A, Oliveira R De (2009) Neuroscience Letters Glatiramer acetate positively influences spinal motoneuron survival and synaptic plasticity after ventral root avulsion. 451:34–39.

Seddon HJ (1943) THREE TYPES OF NERVE INJURY. Brain 66:237–288

Seltzer Z, Cohn S, Ginzburg R, Beilin B (1991) Modulation of neuropathic pain behavior in rats by spinal disinhibition and NMDA receptor blockade of injury discharge. Pain 45:69–75.

Senthilkumar , Rajamohan B, Pillai VB, Gupta M, Sundaresan NR, Birukov KG, Samant S, Hottiger MO, Gupta MP (2009) SIRT1 Promotes Cell Survival under Stress by Deacetylation-Dependent Deactivation of Poly(ADP-Ribose) Polymerase 1. Mol Cell Biol 29:4116–4129.

Severini C, Petrocchi Passeri P, Ciotti MT, Florenzano F, Petrella C, Malerba F, Bruni B, D'Onofrio M, Arisi I, Brandi R, Possenti R, Calissano P, Cattaneo A (2017) Nerve growth factor derivative NGF61/100 promotes outgrowth of primary sensory neurons with reduced signs of nociceptive sensitization. Neuropharmacology 117:134–148

Shahreza ML, Ghadiri N, Mousavi SR, Varshosaz J, Green JR (2017) A reviewof network-based approaches to drug repositioning. Brief Bioinform:1–15

Shamu CE, Walter P (1996) Oligomerization and phosphorylation of the Ire1p kinase during intracellular signaling from the endoplasmic reticulum to the nucleus. EMBO J 15:3028–3039.

Shao H, Xue Q, Zhang F, Luo Y, Zhu H, Zhang X, Zhang H, Ding W, Yu B (2014) Spinal SIRT1 activation attenuates neuropathic pain in mice. PLoS One 9.

Shih R-H, Wang C-Y, Yang C-M (2015) NF-kappaB Signaling Pathways in Neurological Inflammation: A Mini Review. Front Mol Neurosci 8:1–8

Shoichet MS, Tate CC, Baumann MD, LaPlaca MC (2008) Strategies for Regeneration and Repair in the Injured Central Nervous System. In (Reichert WM, ed). Boca Raton (FL).

Sidrauski C, Walter P (1997) The transmembrane kinase Ire1p is a site-specific endonuclease that initiates mRNA splicing in the unfolded protein response. Cell 90:1031–1039.

Silver J, Miller JH (2004) Regeneration beyond the glial scar. Nat Rev Neurosci 5:146–156

Silver J, Schwab ME, Popovich PG (2014) Central nervous system regenerative failure: role of oligodendrocytes, astrocytes, and microglia. Cold Spring Harb Perspect Biol 7:a020602.

Sim SK, Tan YC, Tee JH, Yusoff AA, Abdullah JM (2015) Paclitaxel inhibits expression of neuronal nitric oxide synthase and prevents mitochondrial dysfunction in spinal ventral horn in rats after C7

spinal root avulsion. Turk Neurosurg 25:617–624.

Sommer T, Jarosch E (2002) BiP binding keeps ATF6 at bay. Dev Cell 3:1–2.

Song G, Ouyang G, Bao S (2005) The activation of Akt/PKB signaling pathway and cell survival. J Cell Mol Med 9:59–71.

Song S, Kong X, Acosta S, Sava V, Borlongan C (2016) Granulocyte-colony stimulating factor promotes brain repair following traumatic brain injury by recruitment of microglia and increasing neurotrophic factor expression. 34:415–431.

Spilman P, Podlutskaya N, Hart MJ, Debnath J, Gorostiza O, Bredesen D, Richardson A, Strong R, Galvan V (2010) Inhibition of mTOR by rapamycin abolishes cognitive deficits and reduces amyloid-β levels in a mouse model of alzheimer's disease. PLoS One 5:1–8.

Sriram S, Subramanian S, Sathiakumar D, Venkatesh R, Salerno MS, Mcfarlane CD, Kambadur R, Sharma M (2011) Modulation of reactive oxygen species in skeletal muscle by myostatin is mediated through NF-κB. Aging Cell 10:931–948.

Stefancic M, Vidmar G, Blagus R (2016) Long-term recovery of muscle strength after denervation in the fibular division of the sciatic nerve. Muscle and Nerve 54:702–708.

Strosznajder JB, Czapski GA, Adamczyk A, Strosznajder RP (2012) Poly(ADP-ribose) polymerase-1 in amyloid beta toxicity and Alzheimer's disease. Mol Neurobiol 46:78–84.

Stünkel W, Peh BK, Tan YC, Nayagam VM, Wang X, Salto-Tellez M, Ni BH, Entzeroth M, Wood J (2007) Function of the SIRTI protein deacetylase in cancer. Biotechnol J 2:1360–1368.

Stupack DG, Cheresh DA (2002) Get a ligand, get a life: integrins, signaling and cell survival. J Cell Sci 115:3729–3738

Sugino T, Maruyama M, Tanno M, Kuno A, Houkin K, Horio Y (2010) Protein deacetylase SIRT1 in the cytoplasm promotes nerve growth factor-induced neurite outgrowth in PC12 cells. FEBS Lett 584:2821–2826

Sun HH, Saheb-Al-Zamani M, Yan Y, Hunter DA, MacKinnon SE, Johnson PJ (2012) Geldanamycin accelerated peripheral nerve regeneration in comparison to FK-506 in vivo. Neuroscience 223:114–123.

Sun L, Zhao M, Liu M, Su P, Zhang J, Li Y, Yang X, Wu Z (2017) Suppression of FoxO3a attenuates neurobehavioral deficits after traumatic brain injury through inhibiting neuronal autophagy. Behav Brain Res

Sun W, Oppenheim RW (2003) Response of motoneurons to neonatal sciatic nerve axotomy in Bax-knockout mice. Mol Cell Neurosci 24:875–886

Sunderland S (1951) A CLASSIFICATION OF PERIPHERAL NERVE INJURIES PRODUCING LOSS OF FUNCTION. Brain 74:491–516

Suzuki K, Koike T (2007) Mammalian Sir2-related protein (SIRT) 2-mediated modulation of resistance to axonal degeneration in slow Wallerian degeneration mice: A crucial role of tubulin deacetylation. Neuroscience 147:599–612.

Tadros MA, Fuglevand AJ, Brichta AM, Callister RJ (2016) Intrinsic excitability differs between murine hypoglossal and spinal motoneurons. J Neurophysiol:jn.01114.2015.

Tan L, Schedl P, Song H-J, Garza D, Konsolaki M (2008) The Toll NF-kappaB signaling pathway mediates the neuropathological effects of the human Alzheimer's Abeta42 polypeptide in Drosophila. PLoS One 3:e3966.

Tanaka H, Yokota H, Jover T, Cappuccio I, Calderone A, Simionescu M, Bennett MVL, Zukin RS (2004) Ischemic preconditioning: neuronal survival in the face of caspase-3 activation. J Neurosci 24:2750–2759.

Tang BL (2014) Class II HDACs and neuronal regeneration. J Cell Biochem 115:1225–1233.

Tang Y, Le W (2016) Differential Roles of M1 and M2 Microglia in Neurodegenerative Diseases. Mol Neurobiol 53:1181–1194.

Tannemaat MR, Eggers R, Hendriks WT, de Ruiter GCW, van Heerikhuize JJ, Pool CW, Malessy MJA, Boer GJ, Verhaagen J (2008) Differential effects of lentiviral vector-mediated overexpression of nerve growth factor and glial cell line-derived neurotrophic factor on regenerating sensory and motor axons in the transected peripheral nerve. Eur J Neurosci 28:1467–1479.

Tanny JC, Dowd GJ, Huang J, Hilz H, Moazed D (1999) An Enzymatic Activity in the Yeast Sir2 Protein that Is Essential for Gene Silencing. 99:735–745.

Taylor CA, Braza D, Rice JB, Dillingham T (2008a) The Incidence of Peripheral Nerve Injury in Extremity Trauma. Am J Phys Med Rehabil 87:381–385.

Taylor JP, Brown RH, Cleveland DW (2016) Decoding ALS: from genes to mechanism. Nature 539:197–206

Taylor JP, Hardy J, Fischbeck KH (2002) Toxic Proteins in Neurodegenerative Disease. Science (80-) 296:1991 LP-1995

Taylor RC, Cullen SP, Martin SJ (2008b) Apoptosis: controlled demolition at the cellular level. Nat Rev Mol Cell Biol 9:231–241.

Tedeschi A (2012) Tuning the orchestra: transcriptional pathways controlling axon regeneration. Front Mol Neurosci 4:1–12

Terui T, Murakami K, Takimoto R, Takahashi M, Takada K, Murakami T, Minami S, Matsunaga T, Takayama T, Kato J, Niitsu Y (2003) Induction of PIG3 and NOXA through acetylation of p53 at 320 and 373 lysine residues as a mechanism for apoptotic cell death by histone deacetylase inhibitors. Cancer Res 63:8948–8954.

Teyssou E, Takeda T, Lebon V, Boillee S, Doukoure B, Bataillon G, Sazdovitch V, Cazeneuve C, Meininger V, LeGuern E, Salachas F, Seilhean D, Millecamps S (2013) Mutations in SQSTM1 encoding p62 in amyotrophic lateral sclerosis: genetics and neuropathology. Acta Neuropathol 125:511–522.

Thal SE, Zhu C, Thal SC, Blomgren K, Plesnila N (2011) Role of apoptosis inducing factor (AIF) for hippocampal neuronal cell death following global cerebral ischemia in mice. Neurosci Lett 499:1–3.

Tintignac LA, Brenner H-R, Rüegg MA (2015) Mechanisms Regulating Neuromuscular Junction Development and Function and Causes of Muscle Wasting. Physiol Rev 95:809–852

To AM, Avulsion S, Pain I, Chew DJ, Murrell K, Carlstedt T, Shortland PJ (2013) Segmental Spinal Root Avulsion in the Adult Rat : 172:160–172.

Tolkacheva T, Chan a M (2000) Inhibition of H-Ras transformation by the PTEN/MMAC1/TEP1 tumor suppressor gene. Oncogene 19:680–689

Torres-Espín A, Corona-Quintanilla DL, Forés J, Allodi I, González F, Udina E, Navarro X (2013) Neuroprotection and axonal regeneration after lumbar ventral root avulsion by re-implantation and mesenchymal stem cells transplant combined therapy. Neurotherapeutics 10:354–368

Toruner M, Fernandez-Zapico M, Sha JJ, Pham L, Urrutia R, Egan LJ (2006) Antianoikis effect of nuclear factor-κB through up-regulated expression of osteoprotegerin, BCL-2, and IAP-1. J Biol Chem 281:8686–8696.

Tos P, Ronchi G, Papalia I, Sallen V, Legagneux J, Geuna S, Giacobini-Robecchi M (2009) Chapter 4 Methods and Protocols in Peripheral Nerve Regeneration Experimental Research: Part I-Experimental Models, 1st ed. Elsevier Inc.

Tournier C, Hess P, Yang DD, Xu J, Turner TK, Nimnual A, Bar-Sagi D, Jones SN, Flavell RA, Davis RJ (2000) Requirement of JNK for stress-induced activation of the cytochrome c-mediated death pathway. Science 288:870–874.

Tran H, Brunet A, Grenier JM, Datta SR, Fornace AJ, DiStefano PS, Chiang LW, Greenberg ME (2002) DNA Repair Pathway Stimulated by the Forkhead Transcription Factor FOXO3a Through the Gadd45 Protein. Science (80-) 296:530 LP-534

Tsang AHK, Lee Y-I, Ko HS, Savitt JM, Pletnikova O, Troncoso JC, Dawson VL, Dawson TM, Chung KKK (2009) S-nitrosylation of XIAP compromises neuronal survival in Parkinson's disease. Proc Natl Acad Sci U S A 106:4900–4905.

Tu H, Zhang D, Corrick RM, Muelleman RL, Wadman MC, Li YL (2017) Morphological regeneration and functional recovery of neuromuscular junctions after tourniquet-induced injuries in mouse hindlimb. Front Physiol 8:1–9.

Udvadia a J, Köster RW, Skene JH (2001) GAP-43 promoter elements in transgenic zebrafish reveal a difference in signals for axon growth during CNS development and regeneration. Development 128:1175–1182.

Vaccari I, Carbone A, Previtali SC, Mironova YA, Alberizzi V, Noseda R, Rivellini C, Bianchi F, Del Carro U, D'Antonio M, Lenk GM, Wrabetz L, Giger RJ, Meisler MH, Bolino A (2015) Loss of Fig4 in both Schwann cells and motor neurons contributes to CMT4J neuropathy. Hum Mol Genet 24:383–396.

Valenzuela V, Oñate M, Hetz C, Court FA (2016) Injury to the nervous system: A look into the ER. Brain Res 1648:617–625.

Valle C, Salvatori I, Gerbino V, Rossi S, Palamiuc L, René F, Carrì MT (2014) Tissue-specific deregulation of selected HDACs characterizes ALS progression in mouse models: pharmacological characterization of SIRT1 and SIRT2 pathways. Cell Death Dis 5:e1296

Valls R, Pujol A, Artigas L (2013) Anaxomics' methodologies: understanding the complexity of biological processes. white Pap.

Vanden Noven S, Wallace N, Muccio D, Turtz A, Pinter MJ (1993) Adult spinal motoneurons remain viable despite prolonged absence of functional synaptic contact with muscle. Exp Neurol 123:147–156.

Vaquero A (2009) The conserved role of sirtuins in chromatin regulation. Int J Dev Biol 53:303–322.

Vaquero A, Scher MB, Dong HL, Sutton A, Cheng HL, Alt FW, Serrano L, Sternglanz R, Reinberg D (2006) SirT2 is a histone deacetylase with preference for histone H4 Lys 16 during mitosis. Genes Dev 20:1256–1261.

Vaziri H, Dessain SK, Eaton EN, Imai SI, Frye R a., Pandita TK, Guarente L, Weinberg R a. (2001) hSIR2SIRT1 functions as an NAD-dependent p53 deacetylase. Cell 107:149–159.

Verma A, Ghosh S, Pradhan S, Basu A (2016) Microglial activation induces neuronal death in Chandipura virus infection. Sci Reports 6:22544

Villacampa N, Almolda B, Vilella A, Campbell IL, Gonzalez B, Castellano B (2015) Astrocyte-targeted production of IL-10 induces changes in microglial reactivity and reduces motor neuron death

after facial nerve axotomy. Glia 63:1166–1184.

Wachholz S, Esslinger M, Plumper J, Manitz M-P, Juckel G, Friebe A (2016) Microglia activation is associated with IFN-alpha induced depressive-like behavior. Brain Behav Immun 55:105–113.

Wang L-L, Shi D-L, Gu H-Y, Zheng M-Z, Hu J, Song X-H, Shen Y-L, Chen Y-Y (2016) Resveratrol attenuates inflammatory hyperalgesia by inhibiting glial activation in mice spinal cords. Mol Med Rep 13:4051–4057.

Wang P, Guan Y-F, Du H, Zhai Q-W, Su D-F, Miao C-Y (2012) Induction of autophagy contributes to the neuroprotection of nicotinamide phosphoribosyltransferase in cerebral ischemia. Autophagy 8:77–87.

Wang P, Lv C, Zhang T, Liu J, Yang J, Guan F, Hong T (2017) FOXQ1 regulates senescence-associated inflammation via activation of SIRT1 expression. Cell Death Dis 8:e2946

Wang X, Kong K, Qi W, Ye W, Song P (2005) Interleukin-1 beta induction of neuron apoptosis depends on p38 mitogen-activated protein kinase activity after spinal cord injury. Acta Pharmacol Sin 26:934–942

Wang XZ, Lawson B, Brewer JW, Zinszner H, Sanjay A, Mi LJ, Boorstein R, Kreibich G, Hendershot LM, Ron D (1996) Signals from the stressed endoplasmic reticulum induce C/EBP-homologous protein (CHOP/GADD153). Mol Cell Biol 16:4273–4280

Wang Y, Liu Y, Chen Y, Shi S, Qin J, Xiao F, Zhou D, Lu M, Lu Q, Shen A (2009) Peripheral nerve injury induces down-regulation of Foxo3a and p27kip1 in rat dorsal root ganglia. Neurochem Res 34:891–898.

Wang Y, Wang W, Li D, Li M, Wang P, Wen J, Liang M, Su B, Yin Y (2014) IGF-1 Alleviates NMDA-Induced Excitotoxicity in Cultured Hippocampal Neurons Against Autophagy via the NR2B/PI3K-AKT-mTOR Pathway. J Cell Physiol 229:1618–1629.

Watanabe S, Ageta-Ishihara N, Nagatsu S, Takao K, Komine O, Endo F, Miyakawa T, Misawa H, Takahashi R, Kinoshita M, Yamanaka K (2014) SIRT1 overexpression ameliorates a mouse model of SOD1-linked amyotrophic lateral sclerosis via HSF1/HSP70i chaperone system. Mol Brain 7:62

Welin D, Novikova LN, Wiberg M, Kellerth J-O, Novikov LN (2009) Effects of N-acetyl-cysteine on the survival and regeneration of sural sensory neurons in adult rats. Brain Res 1287:58–66.

Williams DW, Mukherjee A (2017) More alive than dead: non-apoptotic roles for caspases in neuronal development, plasticity and disease. Running title: Caspases in. 44:1–11

Winbush A, Weeks JC (2011) Steroid-triggered, cell-autonomous death of a Drosophila motoneuron during metamorphosis. Neural Dev 6:15

Wu A, Ying Z, Gomez-Pinilla F (2007) Omega-3 fatty acids supplementation restores mechanisms that maintain brain homeostasis in traumatic brain injury. J Neurotrauma 24:1587–1595.

Wu D, Li Q, Zhu X, Wu G, Cui S (2013) Valproic acid protection against the brachial plexus root avulsion-induced death of motoneurons in rats. Microsurgery

Wu W, Li L, Yick L, Chai H, Xie Y (2003) Spinal Root Avulsion in Adult Rats. 20:603–612.

Xia CH, Roberts EA, Her LS, Liu X, Williams DS, Cleveland DW, Goldstein LSB (2003) Abnormal neurofilament transport caused by targeted disruption of neuronal kinesin heavy chain KIF5A. J Cell Biol 161:55–66.

Xiang C, Wang Y, Zhang H, Han F (2016) The role of endoplasmic reticulum stress in neurodegenerative disease. Apoptosis 0:1–26.

Xu P, Das M, Reilly J, Davis RJ (2011) JNK regulates FoxO-dependent autophagy in neurons. Genes Dev 25:310–322

Yamaguchi Y, Miura M (2015) Programmed cell death in neurodevelopment. Dev Cell 32:478–490

Yamaki T, Wu C-L, Gustin M, Lim J, Jackman RW, Kandarian SC (2012) Rel A/p65 is required for cytokine-induced myotube atrophy. Am J Physiol Cell Physiol 303:C135-42

Yamazaki Y, Kamei Y, Sugita S, Akaike F, Kanai S, Miura S, Hirata Y, Troen BR, Kitamura T, Nishino I, Suganami T, Ezaki O, Ogawa Y (2010) The cathepsin L gene is a direct target of FOXO1 in skeletal muscle. Biochem J 427:171–178

Yang X, Cheng J, Gao Y, Ding J, Ni X (2017) Downregulation of Iduna is associated with AIF nuclear translocation in neonatal brain after hypoxia-ischemia. Neuroscience 346:74–80.

Yang Y, Fu W, Chen J, Olashaw N, Zhang X, Nicosia S V, Bhalla K, Bai W (2007) SIRT1 sumoylation regulates its deacetylase activity and cellular response to genotoxic stress. Nat Cell Biol 9:1253–1262

Ygge J (1989) Neuronal loss in lumbar dorsal root ganglia after proximal compared to distal sciatic nerve resection: a quantitative study in the rat. Brain Res 478:193–195.

Yonish-Rouach E, Resnitzky D, Lotem J, Sachs L, Kimchi A, Oren M (1991) Wild-type p53 induces apoptosis of myeloid leukaemic cells that is inhibited by interleukin-6. Nature 352:345–347.

Yoshida H, Matsui T, Yamamoto A, Okada T, Mori K (2001) XBP1 mRNA is induced by ATF6 and spliced by IRE1 in response to ER stress to produce a highly active transcription factor. Cell 107:881–891.

Yoshida H, Okada T, Haze K, Yanagi H, Yura T, Negishi M, Mori K (2000) ATF6 activated by proteolysis binds in the presence of NF-Y (CBF) directly to the cis-acting element responsible for the

mammalian unfolded protein response. Mol Cell Biol 20:6755–6767.

Yu Z, Sheng H, Liu S, Zhao S, Glembotski CC, Warner DS, Paschen W, Yang W (2017) Activation of the ATF6 branch of the unfolded protein response in neurons improves stroke outcome. J Cereb Blood Flow Metab 37:1069–1079.

Yuan F, Xu ZM, Lu LY, Nie H, Ding J, Ying WH, Tian HL (2016) SIRT2 inhibition exacerbates neuroinflammation and blood-brain barrier disruption in experimental traumatic brain injury by enhancing NF-κB p65 acetylation and activation. J Neurochem 136:581–593.

Zanzoni A, Soler-López M, Aloy P (2009) A network medicine approach to human disease. FEBS Lett 583:1759–1765

Zempel H, Mandelkow E-M (2015) Tau missorting and spastin-induced microtubule disruption in neurodegeneration: Alzheimer Disease and Hereditary Spastic Paraplegia. Mol Neurodegener 10:68

Zhang CG, Welin D, Novikov L, Kellerth JO, Wiberg M, Hart a. M (2005) Motorneuron protection by N-acetyl-cysteine after ventral root avulsion and ventral rhizotomy. Br J Plast Surg 58:765–773.

Zhang F, Su B, Wang C, Siedlak SL, Mondragon-Rodriguez S, Lee H-G, Wang X, Perry G, Zhu X (2015) Posttranslational modifications of α-tubulin in alzheimer disease. Transl Neurodegener 4:9

Zhang S, Huan W, Wei H, Shi J, Fan J, Zhao J, Shen A, Teng H (2013) FOXO3a/p27kip1 expression and essential role after acute spinal cord injury in adult rat. J Cell Biochem 114:354–365.

Zhao W, Xie W, Xiao Q, Beers DR, Appel SH (2006) Protective effects of an anti-inflammatory cytokine, interleukin-4, on motoneuron toxicity induced by activated microglia. J Neurochem 99:1176–1187.

Zhao XC, Wang LL, Wang YQ, Song FH, Li YQ, Fu R, Zheng WH, Wu W, Zhou LH (2012) Activation of phospholipase-Cδ and protein kinase C signal pathways helps the survival of spinal motoneurons injured by root avulsion. J Neurochem 121:362–372.

Zhao Y, Yang J, Liao W, Liu X, Zhang H, Wang S, Wang D, Feng J, Yu L, Zhu W-G (2010) Cytosolic FoxO1 is essential for the induction of autophagy and tumour suppressor activity. Nat Cell Biol 12:665–675.

Zhou B, Yu P, Lin MY, Sun T, Chen Y, Sheng ZH (2016) Facilitation of axon regeneration by enhancing mitochondrial transport and rescuing energy deficits. J Cell Biol 214:103–119.

Zhou C-H, Zhang M-X, Zhou S-S, Li H, Gao J, Du L, Yin X-X (2017) SIRT1 attenuates neuropathic pain by epigenetic regulation of mGluR1/5 expressions in type 2 diabetic rats. Pain 158:130–139.

Zhou J, Liao W, Yang J, Ma K, Li X, Wang Y, Wang D, Wang L, Zhang Y, Yin Y, Zhao Y, Zhu WG (2012)

FOXO3 induces FOXO1-dependent autophagy by activating the AKT1 signaling pathway. Autophagy 8:1712–1723.

Zhu P, Martinvalet D, Chowdhury D, Zhang D, Schlesinger A, Lieberman J (2009) The cytotoxic T lymphocyte protease granzyme A cleaves and inactivates poly (adenosine 5 J -diphosphate-ribose) polymerase-1. 114:1205–1216.

Ziv NE, Spira ME (1995) Axotomy induces a transient and localized elevation of the free intracellular calcium concentration to the millimolar range. J Neurophysiol 74:2625–2637.